Design of Ru(II)-NHC-Diamine Precatalysts Directed by Ligand Cooperation: Applications and Mechanistic Investigations for Asymmetric Hydrogenation

Wei Li, Tobias Wagener, Lars Hellmann, Constantin G. Daniliuc, Christian Mück-Lichtenfeld, Johannes Neugebauer,* and Frank Glorius**

Organisch-Chemisches Institut, Westfälische Wilhelms-Universität Münster, Corrensstraße 40, 48149 Münster, Germany

E-mail: glorius@uni-muenster.de

Supporting Information

CONTENTS:

(A) General

Unless otherwise noted, all reactions were carried out under an atmosphere of argon in oven-dried glassware. Reaction temperatures are reported as the temperature of the bath surrounding the vessel unless otherwise stated. The solvents used were purified by distillation over the drying agents indicated in parentheses and were transferred under argon: *n*-hexane (CaH_2), THF (Na-benzophenone), toluene (CaH_2), *i*-PrOH (molecular sieves).

All hydrogenation reactions were performed in Berghof High Pressure Reactors using hydrogen gas. Commercially available chemicals were bought from Acros Organics, Aldrich Chemical Co., Strem Chemicals, Alfa Aesar, ABCR, TCI Europe, Combi-Blocks and Chempur and used as received unless otherwise stated. NHC Ligands were synthesized following literature known procedures.[1] Chiral amines for the preparation of NHC ligands (*R,R*)-INpEt•Cl, (*R,R*)-SINpEt•HBF_4, (*S,S*)-SINpEt•HBF_4 were received from BASF SE. The chiral diamine ligands were purchased from Aldrich Chemical Co., Strem Chemicals, Alfa Aesar or prepared according to the literature.[2] All 3-substituted isocoumarin substrates **1** and benzothiophene 1,1-dioxides **3** were synthesized according to the literature.[3,4] All analytical data were in agreement with the reported data.

Analytical thin layer chromatography was performed on Polygram SIL G/UV_{254} plates and alox B. Visualization was accomplished with short wave UV light, and/or $KMnO_4$ staining solutions followed by heating. Flash chromatography was performed on Merck silica gel (40–63 mesh) by standard technique eluting with solvents as indicated.

^{1}H and ^{13}C-NMR spectra were recorded on a Bruker AV 300, AV 400, Varian 500 MHz INOVA or Varian Unity plus 600 in the indicated solvents. Chemical shifts (δ) are given in ppm relative to TMS. The residual solvent signals were used as references and the chemical shifts converted to the TMS scale ($CDCl_3$: δ_H = 7.26 ppm,

δ_C = 77.16 ppm; THF-d_8: δ_H = 1.72 ppm, δ_C = 25.31 ppm; toluene-d_8: δ_H = 2.08 ppm, δ_C = 20.43 ppm). ESI mass spectra were recorded on a Bruker Daltonics MicroTof. Specific rotation was measured on a Perkin Elmer 341 polarimeter at 22 °C using a quartz glass cell (100 mm path length).

(B) Preparation of Ru(II)-NHC-diamine complexes

a. Procedure 1

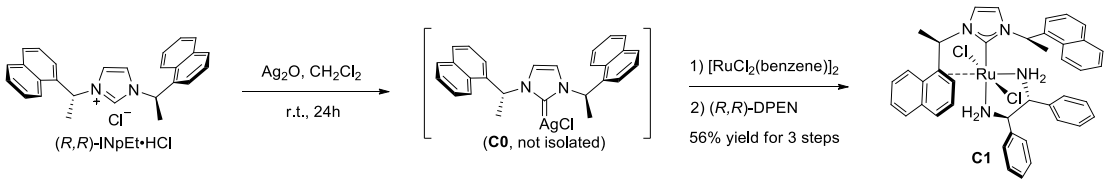

The silver carbene complex was synthesized following a literature procedure:[5] Ag_2O (0.55 mmol) was added to a solution of chloro-imidazolinium salt (*R*,*R*)-INpEt·HCl (1.0 mmol) in CH_2Cl_2 (15 mL). The mixture was stirred at room temperature for 24 h, filtered through celite and washed with CH_2Cl_2 (15 mL) to give a solution **C0** in CH_2Cl_2 (30 mL). Then $[RuCl_2(benzene)]_2$ (0.5 mmol) was added and the mixture was stirred at room temperature for 24 h. The mixture was filtered through celite and washed with CH_2Cl_2 (10 mL) to give the ruthenium-NHC complex in CH_2Cl_2 (40 mL). (*R*,*R*)-1,2-diphenylethylenediamine (DPEN) (1.0 mmol) was added to the solution and the mixture was stirred at room temperature for 16 h. The crude mixture was filtered through celite, washed with CH_2Cl_2, concentrated and purified by column chromatography on silica gel (pentane/ethylacetate = 20:1, later 10:1, 4 : 1) to yield the pure complex **C1** (56% yield over 3 steps).

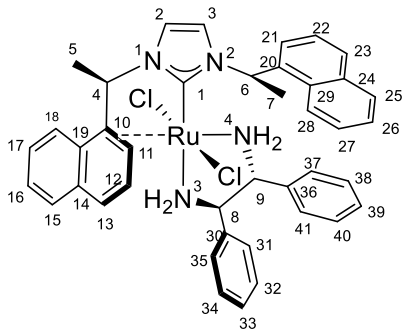

^{1}H NMR (500 MHz, $CDCl_3$, connectivities were confirmed by gCOSY, gHSQC, and gHMBC experiments) δ 8.18 – 8.08 (m, 2H, *H*C18, *H*C28), 7.49 – 7.41 (m, 3H, *H*C27, *H*C23, *H*C12), 7.42 – 7.33 (m, 3H, *H*C17, *H*C15, *H*C22), 7.35 – 7.28 (m, 1H, *H*C6), 7.29 (d, *J* = 2.2 Hz, 1H, *H*C3), 7.27 – 7.21 (m, 2H, *H*C16, *H*C25), 7.17 (d, *J* = 2.2 Hz, 1H, *H*C2), 7.08 – 7.01 (m, 1H, *H*C26), 6.99 – 6.90 (m, 5H, *H*C32, *H*C34, *H*C33, *H*C39, *H*C21), 6.90 (d, *J* = 9.0 Hz, 1H, *H*C13), 6.81 (t, *J* = 7.7 Hz, 2H, *H*C38, *H*C40), 6.59 – 6.54 (m, 2H, *H*C35, *H*C31), 6.22 – 6.13 (m, 2H, *H*C37, *H*C41), 5.79 (q, *J* = 6.5 Hz, 1H, *H*C4), 4.99 (d, *J* = 5.8 Hz, 1H, *H*C11), 3.74 (td, *J* = 11.7, 4.8 Hz, 1H, *H*C9), 3.66 (dd, *J* = 10.6, 5.0 Hz, 1H, H_2N4), 3.18 – 3.04 (m, 2H, *H*C8, H_2N4), 2.00 (d, *J* = 7.0 Hz, 3H, H_3C7), 1.69 (dd, *J* = 12.2, 10.4 Hz, 1H, H_2N3), 1.45 (d, *J* = 6.5 Hz, 3H, H_3C5), 0.34 (dd, *J* = 10.3, 4.9 Hz, 1H, H_2N3). **^{13}C NMR** (126 MHz, 26 ºC, $CDCl_3$, connectivities were confirmed by, gHSQC, gHMBC) δ 186.6 (C1), 140.3 (C20), 140.1 (C30), 138.8 (C19), 138.7 (C36), 136.5 (C12), 133.5 (C24), 131.1 (C14), 129.3 (C25), 128.8 (C29), 128.4 (C32, C34), 128.3 (C38, C40), 128.2 (C23), 127.6 (C40), 127.4 (C27), 127.3 (C39), 127.2 (C15), 126.8 (C31, C35), 126.5 (C37, C41), 126.1 (C18), 125.9 (C26), 125.8 (C16), 125.8 (C22), 125.6 (C17), 123.0 (C21), 122.4 (C13), 121.7 (C28), 118.6 (C3), 118.1 (C2), 92.0 (C10), 72.7 (C11), 65.5 (C9), 60.0 (C8), 57.1 (C4), 54.7 (C6), 22.0 (C7), 21.2 (C5).

ESI-MS: calculated $[C_{41}H_{40}Cl_2N_4Ru + Na]^+$: 783.1566, found: 783.1569**.**

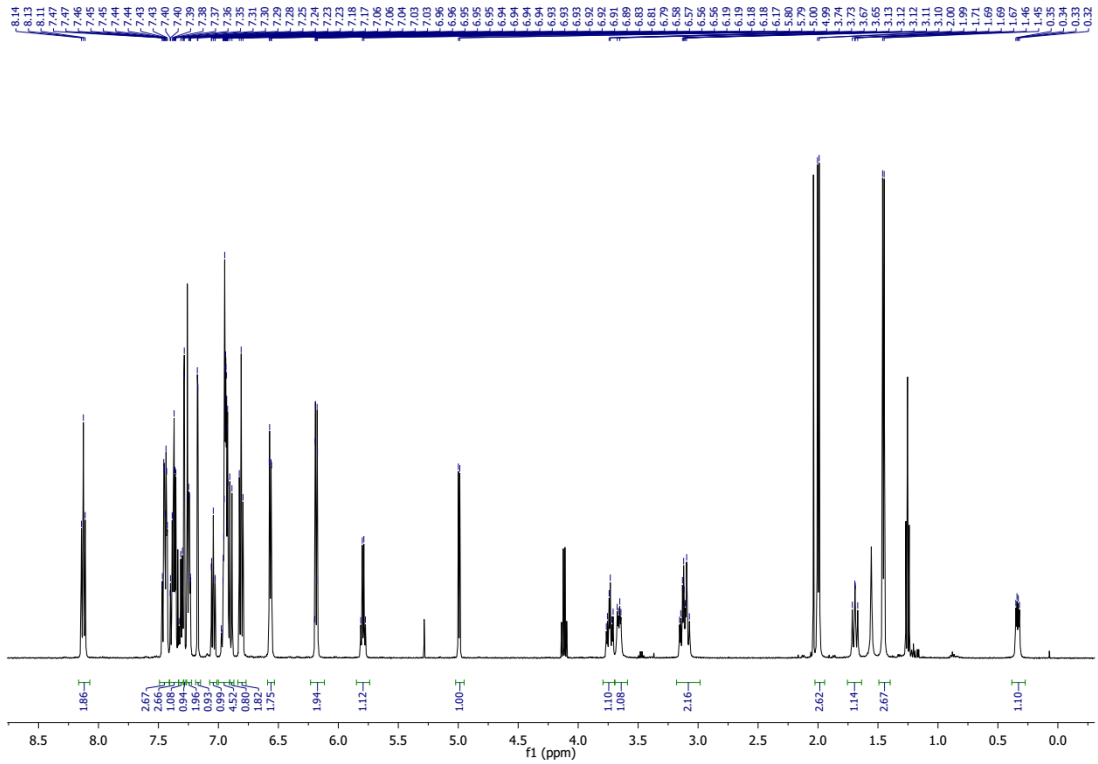
f1 (ppm)

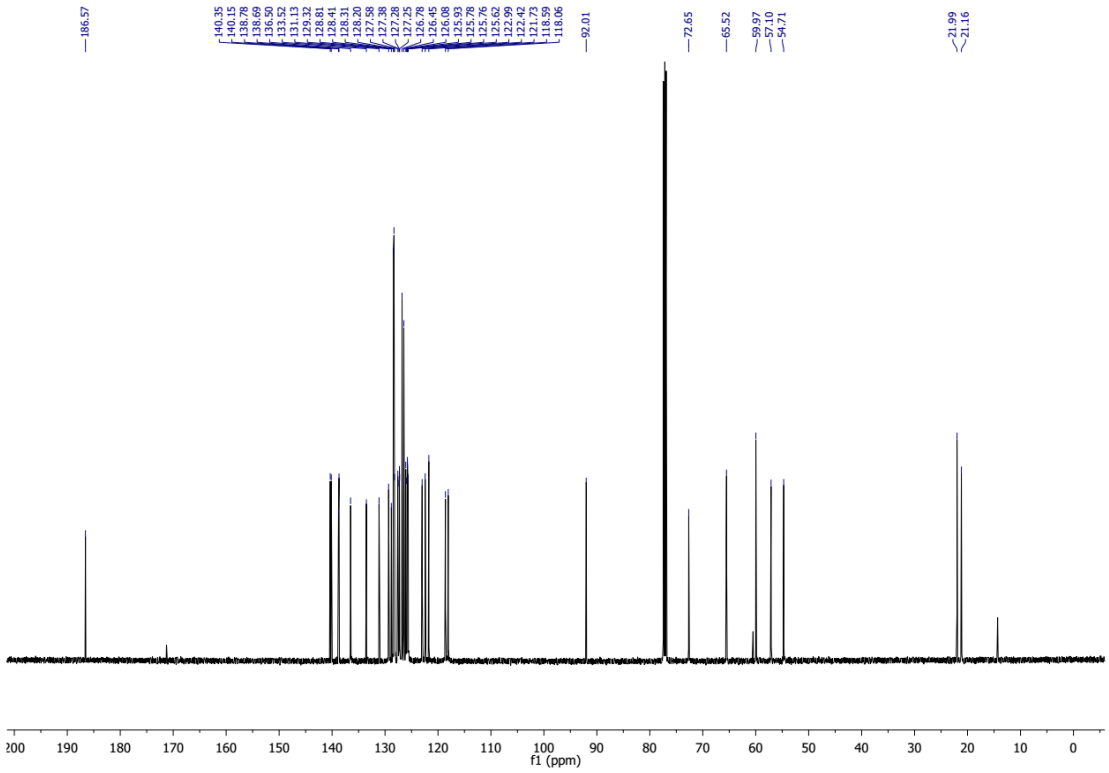
f1 (ppm)

gHSQC

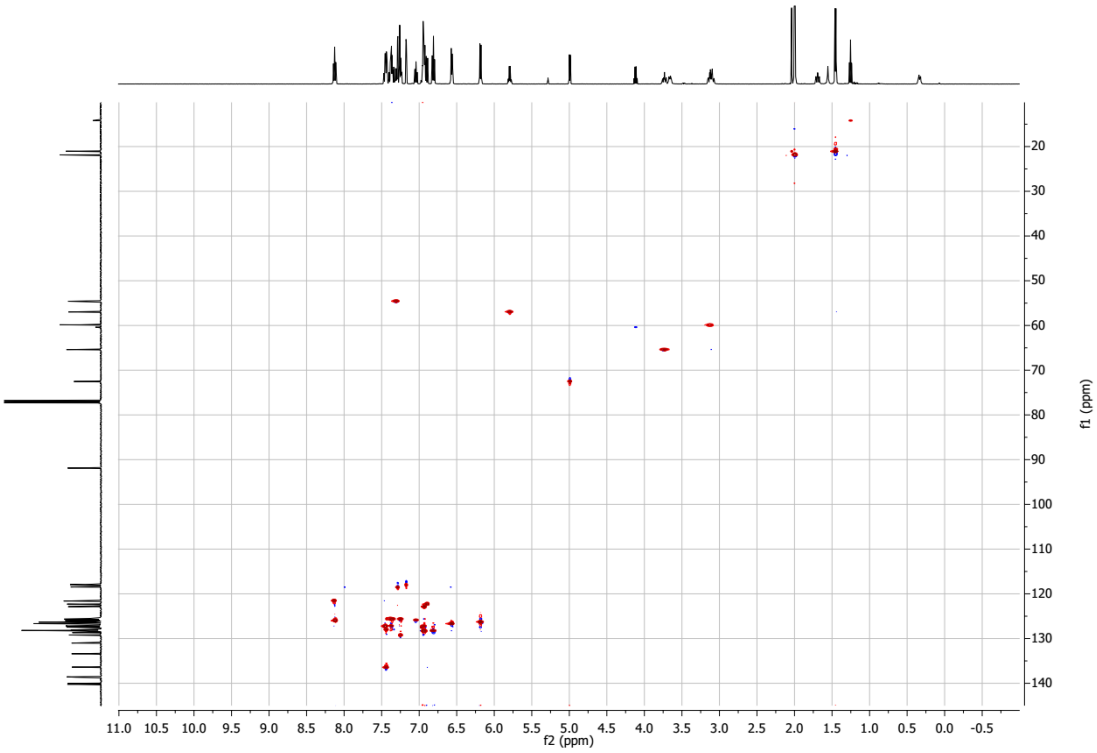

gCOSY

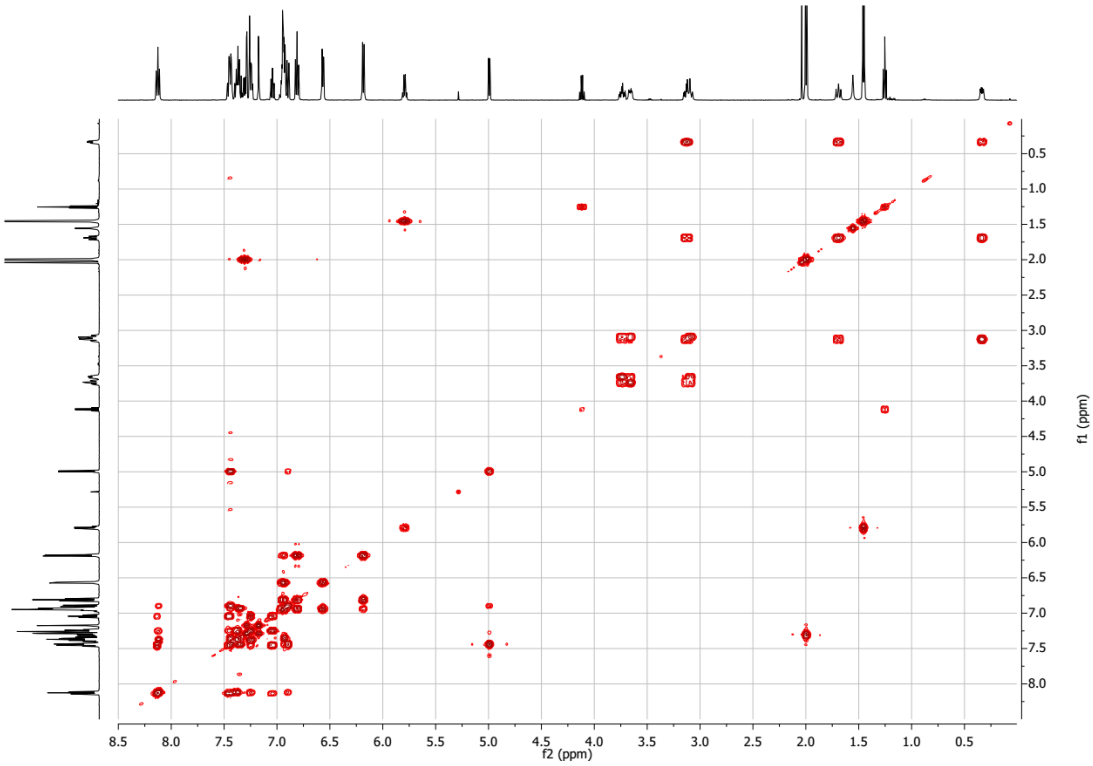

gHMBC

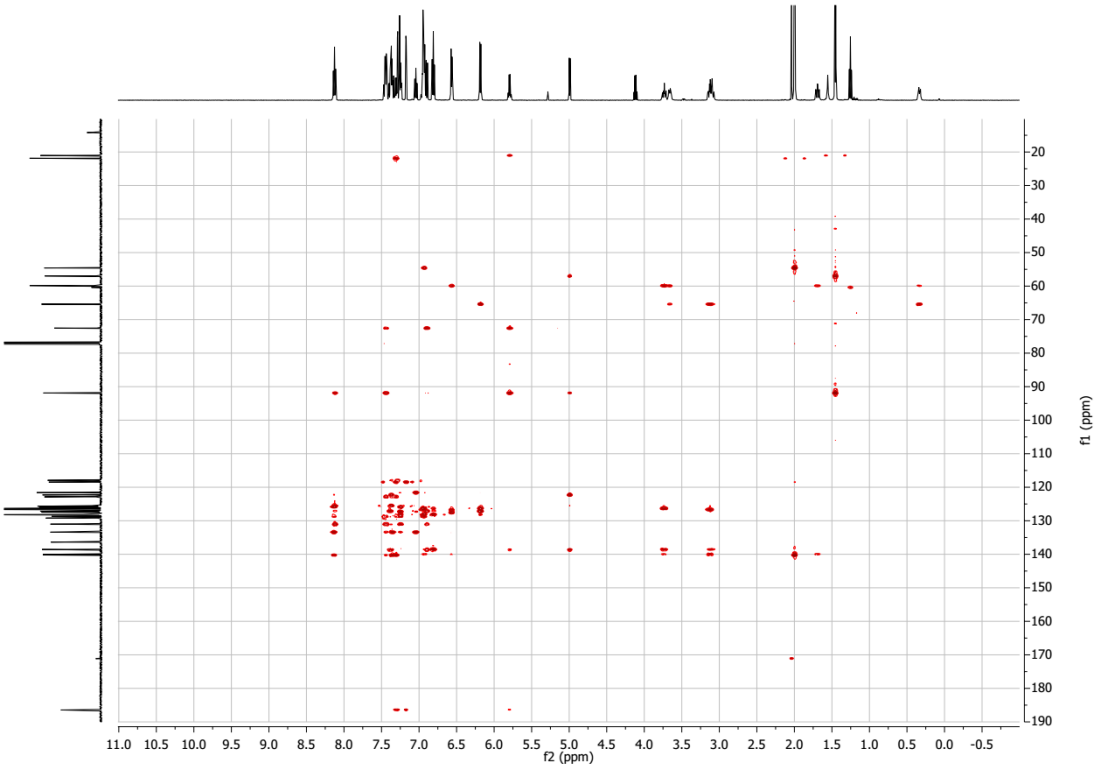

b. Procedure 2

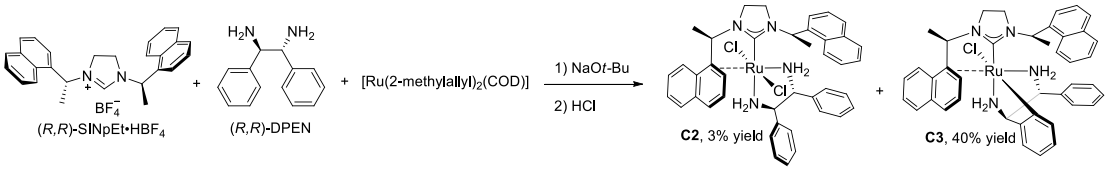

In a glove box, to a flame-dried screw-capped tube equipped with a magnetic stirring bar was added [Ru(2-methylallyl)$_2$(COD)] (1.5 mmol; COD = cyclooctadiene), (*R*,*R*)-SINpEt·HBF$_4$ (1.5 mmol), (*R*,*R*)-1,2-diphenylethylenediamine (1.5 mmol), and dry NaO*t*-Bu (1.8 mmol). The mixture was suspended in *n*-hexane (60 mL) and stirred at 40 °C for 4 days to give a black solution. HCl (4M in dioxane) (2.7 mmol) was then added to the reaction mixture at 0 ºC. After stirring for 30 min at 0 ºC, the mixture was concentrated and purified by column chromatography on silica gel (pentane/ethylacetate = 20:1, later 10:1, 4:1, 2:1) to yield the complexes **C2** (3% yield) and **C3** (40% yield).

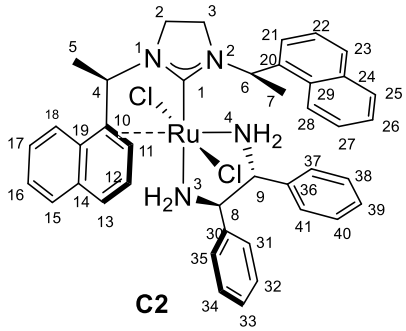

^{1}H NMR (600 MHz, 26 ºC, $CDCl_3$, connectivities were confirmed by gCOSY, gHSQC, and gHMBC experiments) δ 8.14 (d, *J* = 8.6 Hz, 1H, *H*C28), 8.11 (d, *J* = 8.2 Hz, 1H, *H*C18), 7.52 (d, *J* = 7.0 Hz, 1H, *H*C21), 7.48 (d, *J* = 8.1 Hz, 1H, *H*C23), 7.46 – 7.40 (m, 3H, *H*C27, *H*C22, *H*C12), 7.41 – 7.35 (m, 2H, *H*C17, *H*C15), 7.33 (d, *J* = 8.1 Hz, 1H, *H*C25), 7.24 (d, *J* = 7.4 Hz, 1H, *H*C16), 7.10 (t, *J* = 7.5 Hz, 1H, *H*C26), 6.99 – 6.85 (m, 6H, *H*C33, *H*C32, *H*C34, *H*C6, *H*C13, *H*C39), 6.76 (t, *J* = 7.6 Hz, 2H, *H*C40, *H*C38), 6.57 (d, *J* = 6.7 Hz, 2H, *H*C31, *H*C35), 6.17 (d, *J* = 7.6 Hz, 2H, *H*C37, *H*C41), 5.20 (d, *J* = 5.8 Hz, 1H, *H*C11), 5.07 (q, *J* = 6.4 Hz, 1H, *H*C4), 4.03 (dd, *J* = 11.5, 7.2 Hz, 2H, H_2C3), 3.87 (dt, *J* = 9.1, 7.2 Hz, 1H, H_2C2), 3.77 – 3.70 (m, 1H, *H*C9), 3.72 – 3.63 (m, 2H, *H2*C2, H_2N4), 3.19 (t, *J* = 11.0 Hz, 1H, H_2N4), 3.13 (td, *J* = 12.0, 4.8 Hz, 1H, *H*C8), 1.83 (d, *J* = 7.0 Hz, 3H, H_3C7), 1.77 (t, *J* = 11.4 Hz, 1H, H_2N3), 1.21 (d, *J* = 6.4 Hz, 3H, H_3C5), 0.43 (dd, *J* = 10.5, 4.9 Hz, 1H, H_2N3). **^{13}C NMR** (151 MHz, 26 ºC, $CDCl_3$, connectivities were confirmed by, gHSQC, gHMBC) δ 220.5 (C1), 140.2 (C30), 139.9 (C20), 139.0 (C19), 138.7 (C36), 136.5 (C12), 133.8 (C24), 131.2 (C14), 129.4 (C29), 129.4 (C25), 128.4 (C32, C34), 128.3 (C38, C40), 128.1 (C23), 127.6 (C33), 127.3 (C39), 127.2 (C15), 127.1 (C27), 126.8 (C31, C35), 126.5 (C18), 126.3 (C37, C41), 125.8 (C26), 125.8 (C16), 125.6 (C22), 125.5 (C17), 122.9 (C21), 122.7 (C13), 122.3 (C28), 93.1 (C10), 73.0 (C11), 65.6 (C9), 59.7 (C8), 56.9 (C4), 53.6 (C6), 47.1 (C3), 46.9 (C2), 20.9 (C7), 20.6 (C5). **ESI-MS**: calculated $[C_{41}H_{42}Cl_2N_4Ru - Cl]^+$: 727.2136, found: 727.2144.

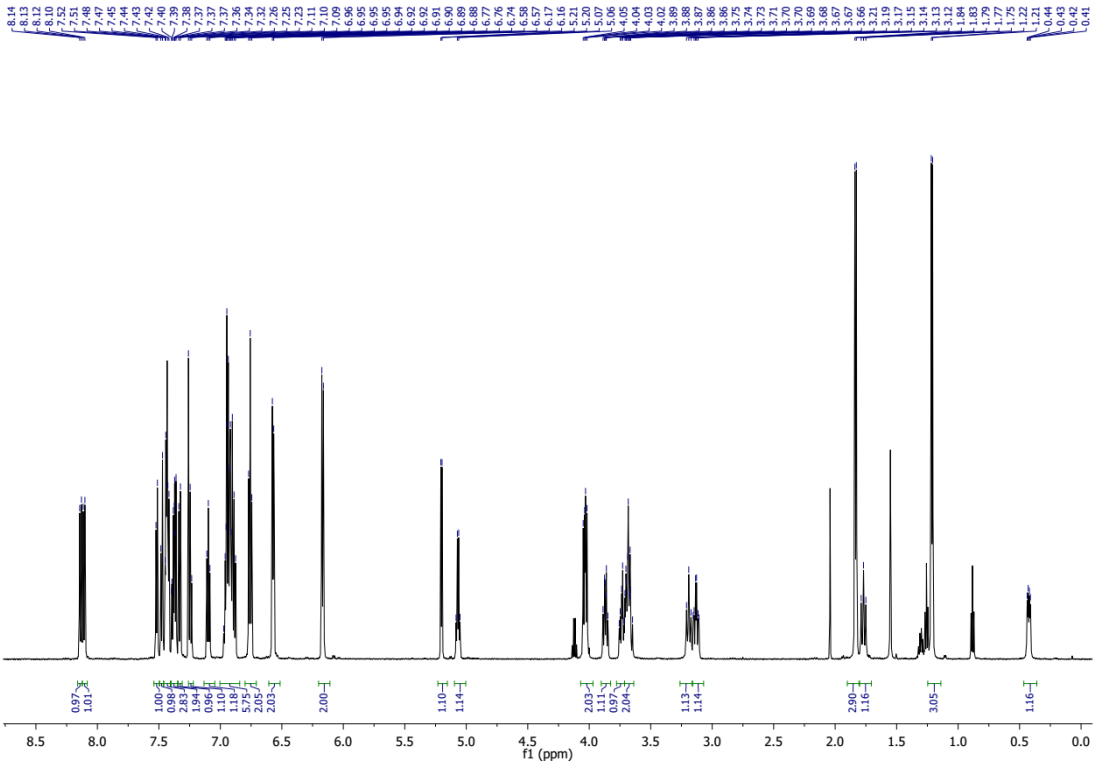
f1 (ppm)

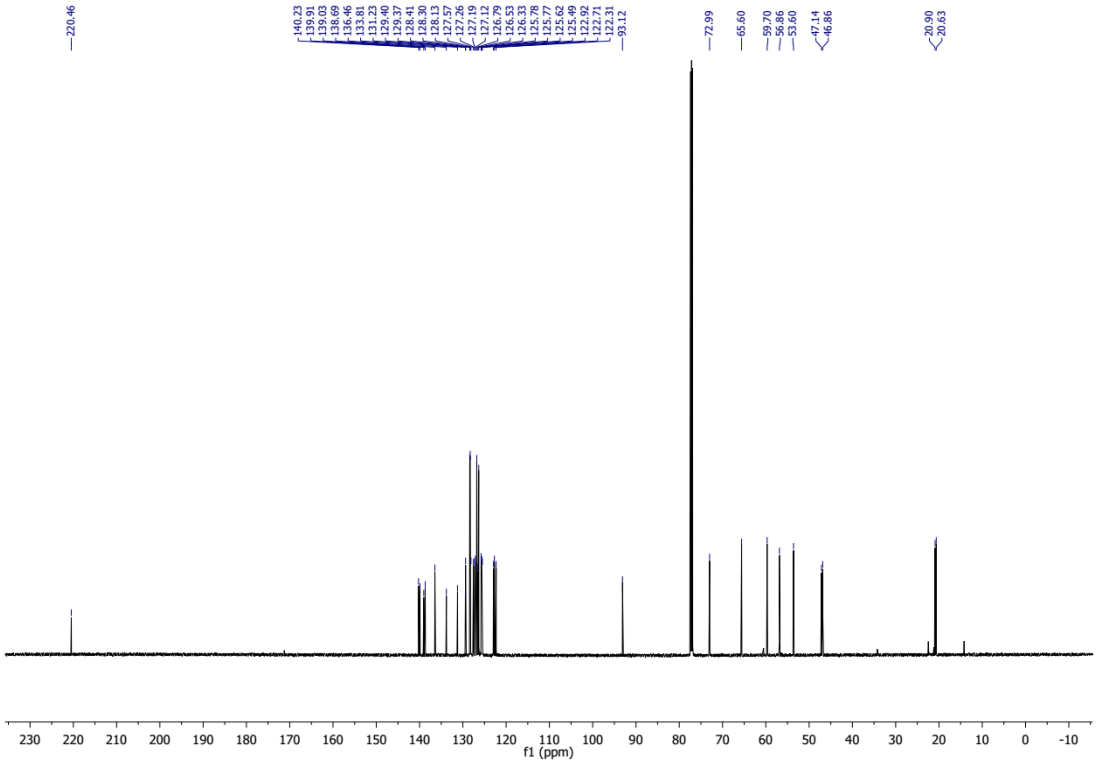
f1 (ppm)

gCOSY:

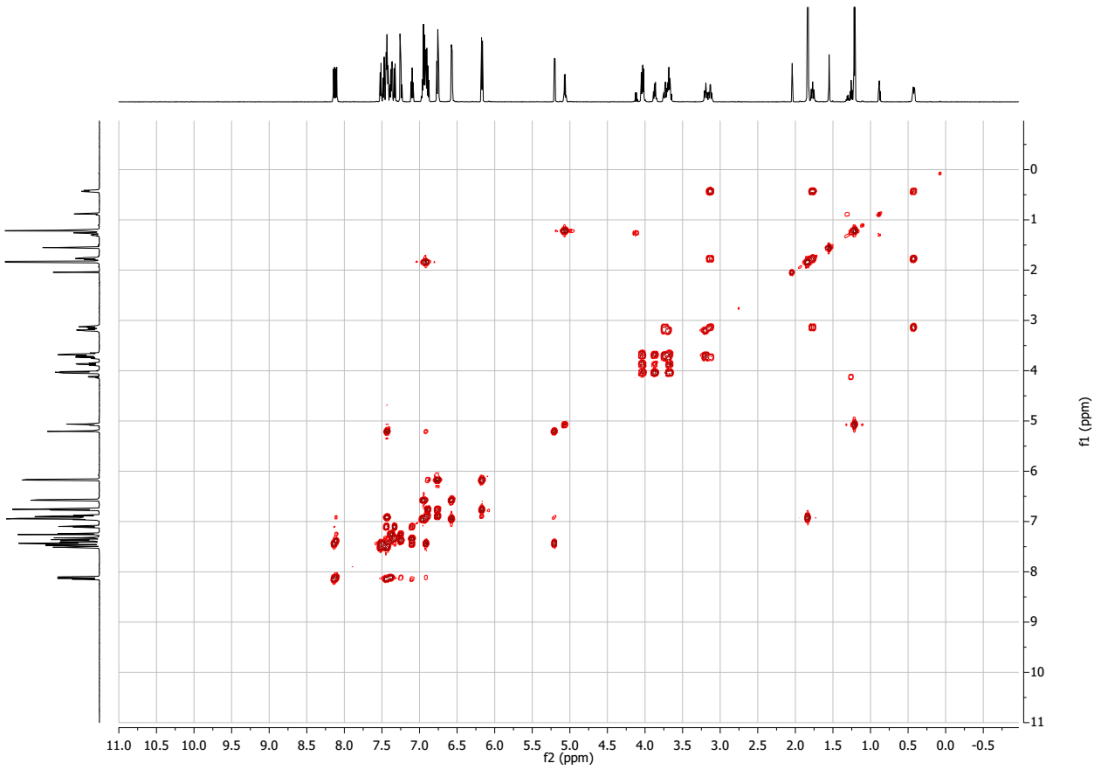

gHSQC:

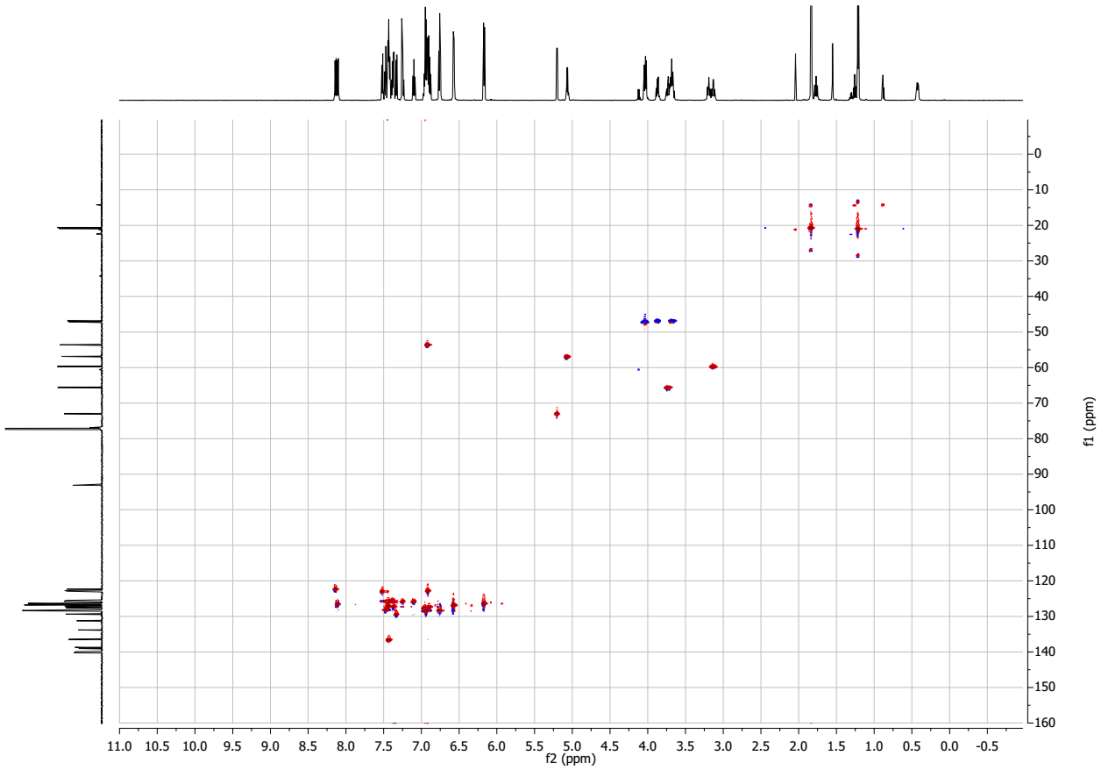

gHMBC:

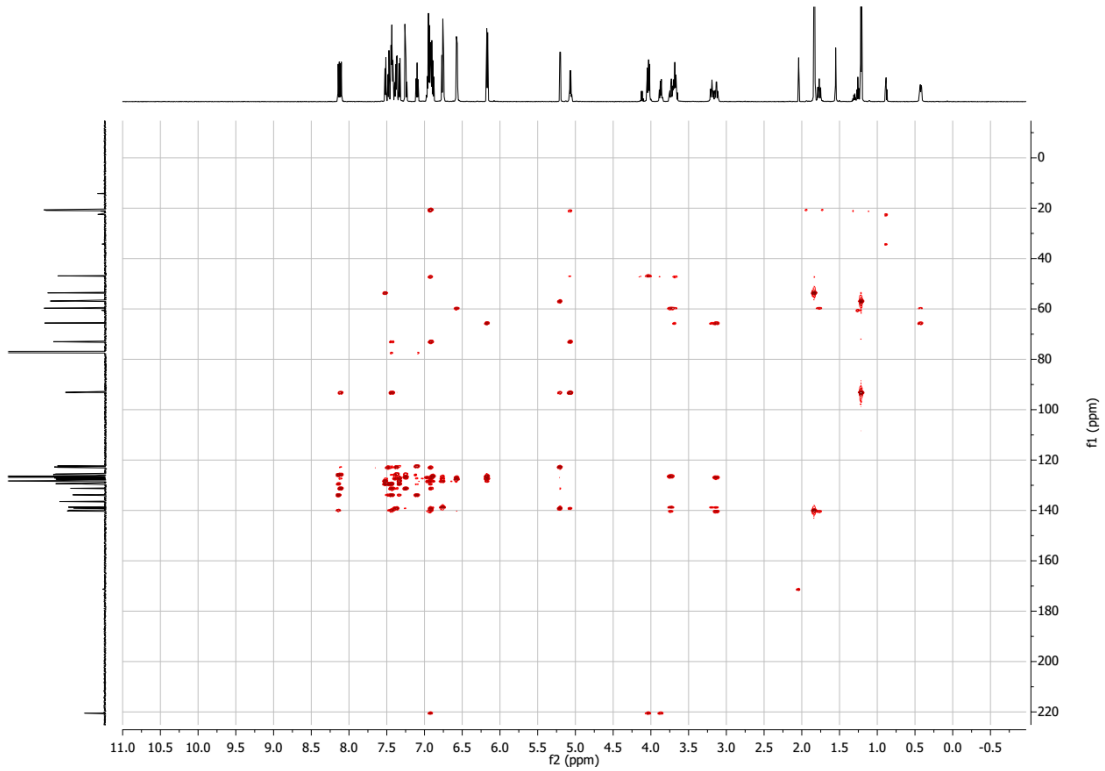

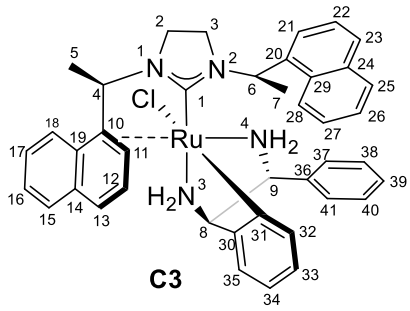

^{1}H NMR (600 MHz, 26 °C, Toluene-d_8, connectivities were confirmed by gCOSY, gHSQC, and gHMBC experiments) δ 8.70 (d, J = 8.2 Hz, 1H, *H*C18), 7.78 (d, J = 7.3 Hz, 1H, *H*C32), 7.50 – 7.40 (m, 2H, *H*C28, *H*C21), 7.38 – 7.34 (m, 2H, *H*C33, *H*C25), 7.32 (ddd, J = 8.3, 6.6, 1.8 Hz, 1H, *H*C17), 7.28 – 7.23 (m, 2H, *H*C23, *H*C27), 7.21 (t, J = 7.3 Hz, 1H, *H*C34), 7.18 (t, J = 7.7 Hz, 1H, *H*C22), 7.14 – 7.07 (m, 4H, *H*C15, *H*C16, *H*C37, *H*C41), 7.07 – 7.04 (m, 1H, *H*C26), 7.02 (d, J = 7.3 Hz, 1H, *H*C35), 6.72 – 6.67 (m, 2H, *H*C38, *H*C40), 6.67 – 6.63 (m, 1H, *H*C39), 6.48 – 6.37 (m, 2H, *H*C6, *H*C13), 6.27 (dd, J = 9.1, 5.7 Hz, 1H, *H*C12), 5.51 (q, J = 6.4 Hz, 1H *H*C4), 4.00 (dd, J = 10.8, 3.6 Hz, 1H, H_2N4), 3.76 (d, J = 5.7 Hz, 1H, *H*C11), 3.30 – 3.22 (m, 2H, H_2C3), 3.21 (s, 1H, *H*C8), 3.14 (td, J = 8.4, 4.9 Hz, 1H, H_2C2), 3.09 – 2.99 (m, 1H, H_2C2), 2.85 (t, J = 10.2 Hz, 1H, H_2N4), 2.75 (dd,

J = 9.8, 4.0 Hz, 1H, HC9), 1.43 (d, J = 7.0 Hz, 3H, H_3C7), 1.08 (d, J = 6.4 Hz, 3H, H_3C5), 1.04 (d, J = 9.4 Hz, 1H, H_2N3), -0.02 (d, J = 9.4 Hz, 1H, H_2N3). **^{13}C NMR** (151 MHz, 26 °C, Toluene-d_8, connectivities were confirmed by gHSQC and gHMBC experiments) δ 225.3 (C1), 176.5 (C31), 147.7 (C30), 142.1 (C19), 140.3 (C20), 140.2 (C32), 139.7 (C36), 137.0 (C12), 134.3 (C24), 131.3 (C14), 129.9 (C29), 129.6 (C25), 128.8 (C38, C40), 128.3 (C23), 127.8 (C18), 127.5 (C39), 127.1 (C27), 126.9 (C15), 126.6, (C37, C41) 126.3 (C22), 125.9 (C17), 125.8 (C33), 125.7 (C26), 124.6 (C16), 123.8 (C21), 122.6 (C28), 121.8 (C34), 121.4 (C13), 121.4 (C35), 83.4 (C10), 67.5 (C8), 66.8 (C11), 62.8 (C9), 57.8 (C4), 53.4 (C6), 46.8 (C2), 46.6 (C3), 20.3 (C5), 20.1 (C7). **ESI-MS**: calculated $[C_{41}H_{41}ClN_4Ru - Cl]^+$: 691.2369, found: 691.2374

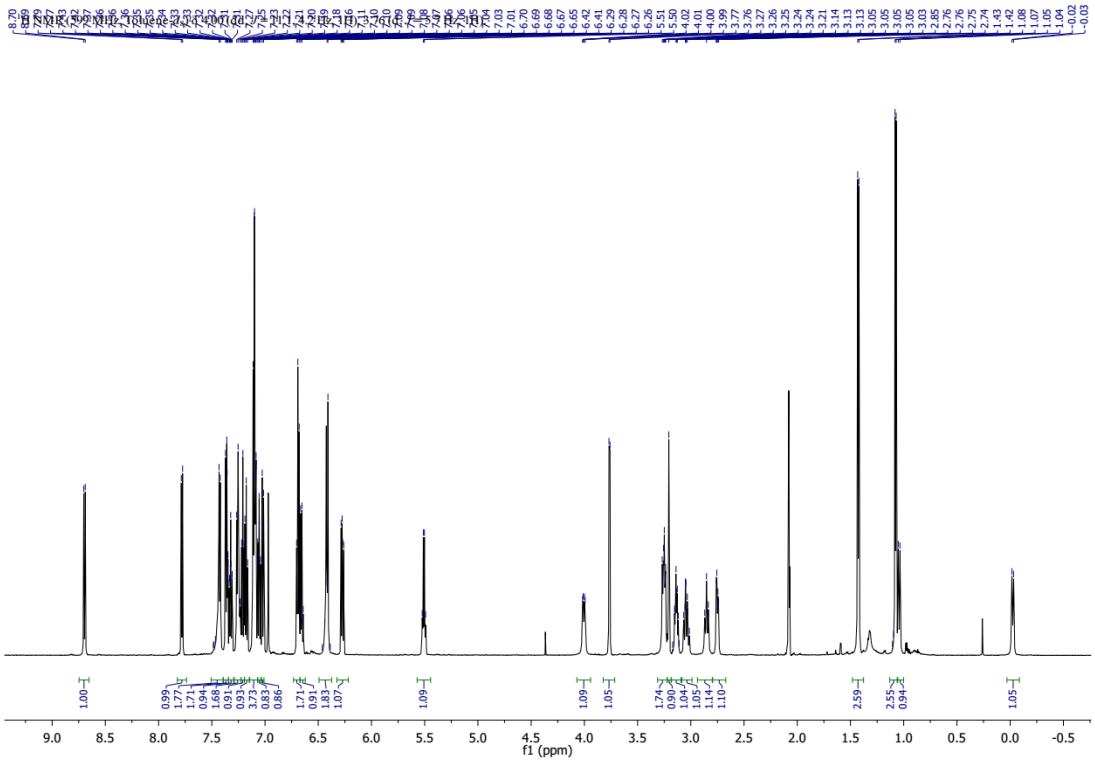

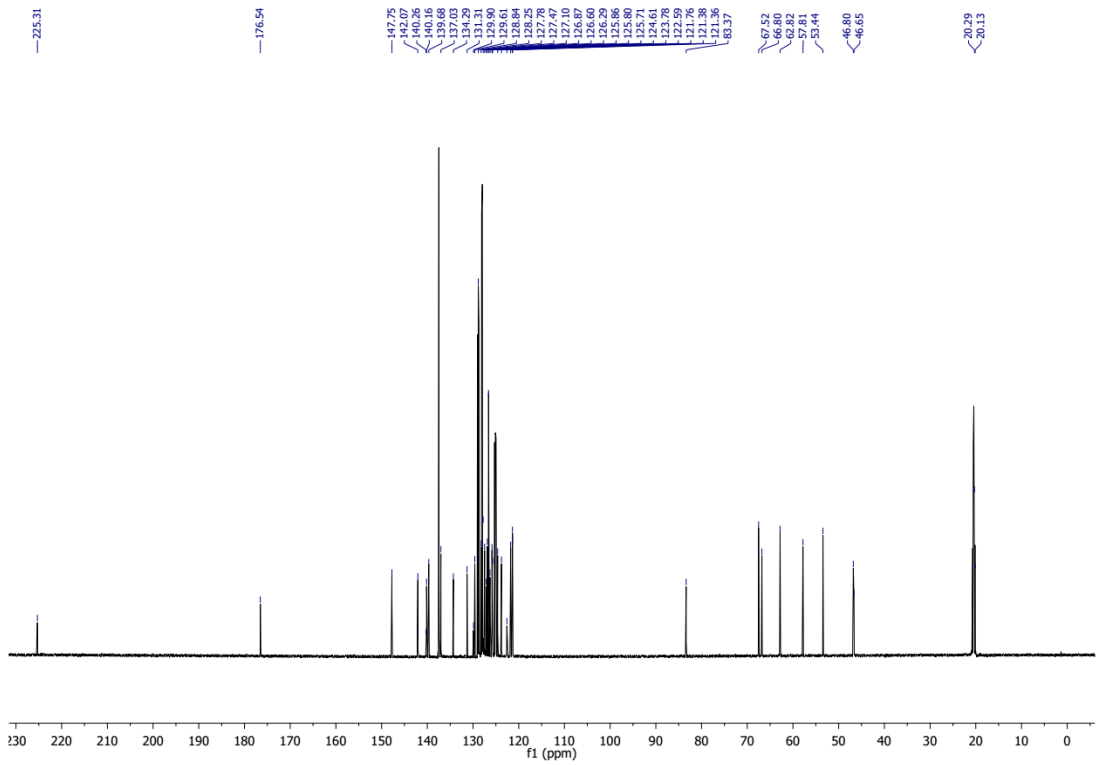
225.31
176.54
147.75
142.07
140.36
140.16
139.68
137.03
134.29
131.31
129.90
129.61
128.84
128.35
127.78
127.47
127.10
126.87
126.60
126.29
125.86
125.80
125.71
124.61
123.78
122.59
121.76
121.38
121.36
83.37
67.52
66.80
62.82
57.81
53.44
46.80
46.65
20.29
20.13
230 220 210 200 190 180 170 160 150 140 130 120 110 100 90 80 70 60 50 40 30 20 10 0
f1 (ppm)

gCOSY:

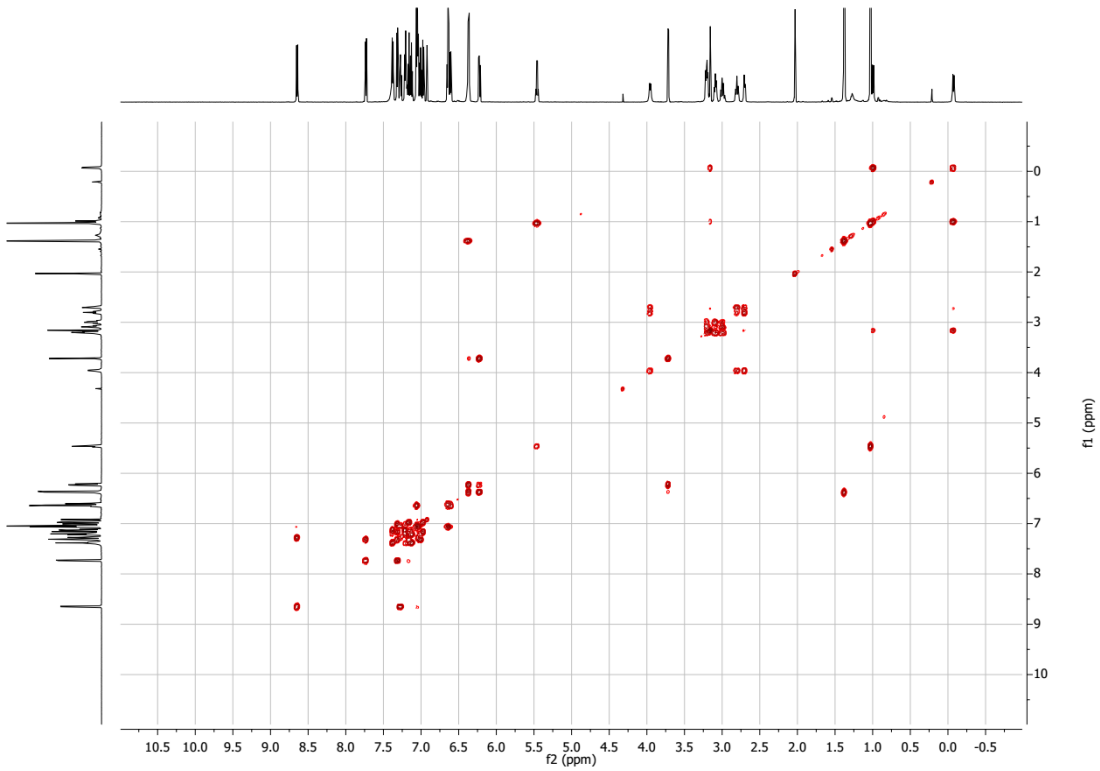
10.5 10.0 9.5 9.0 8.5 8.0 7.5 7.0 6.5 6.0 5.5 5.0 4.5 4.0 3.5 3.0 2.5 2.0 1.5 1.0 0.5 0.0 -0.5
f2 (ppm)
0 1 2 3 4 5 6 7 8 9 10
f1 (ppm)

gHSQC:

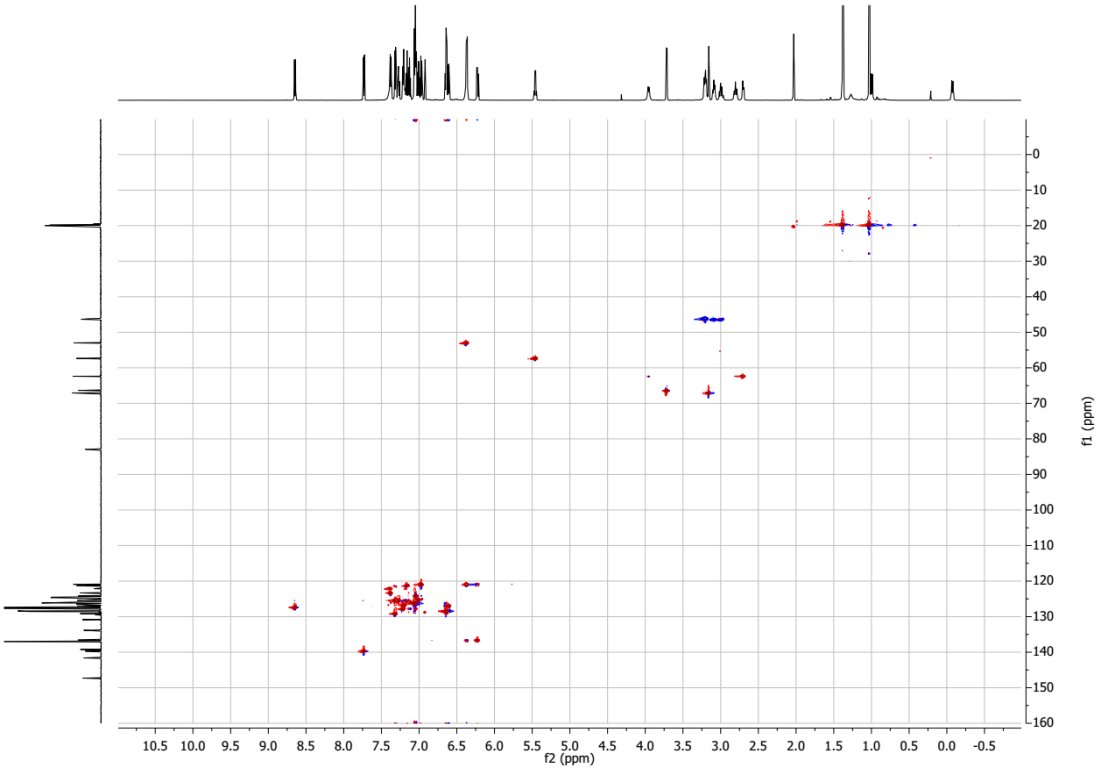

gHMBC:

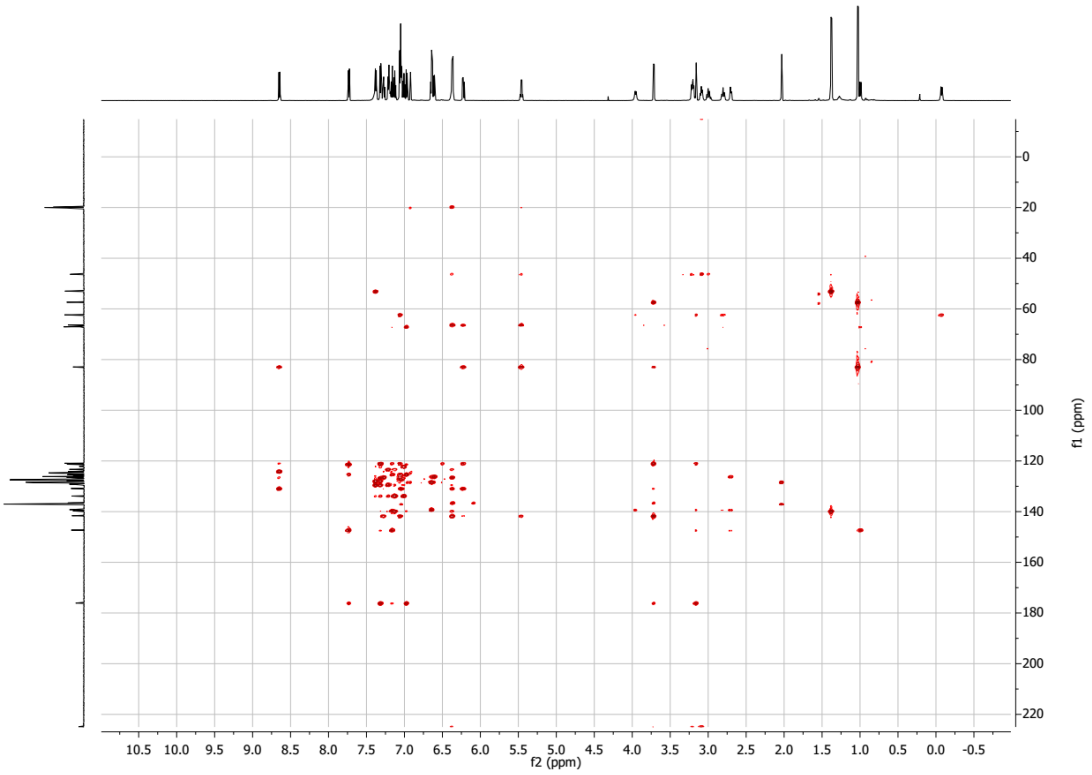

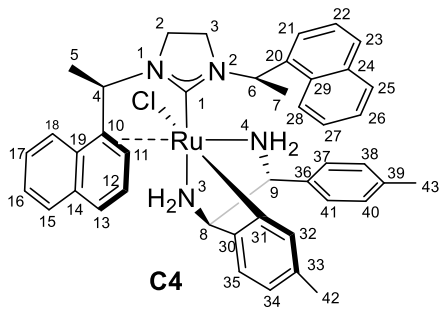

Complex **C4** was prepared in 38% yield according to the Procedure 2 using (1*R,*2*R*)-1,2-di-p-tolylethane-1,2-diamine.

^{1}H NMR (500 MHz, 26 ºC, THF-d_8, connectivities were confirmed by gCOSY, gHSQC and gHMBC experiments) δ 8.35 (d, *J* = 8.5 Hz, 1H, *H*C18), 7.81 – 7.76 (m, 1H, *H*C28), 7.75 (ddd, *J* = 8.2, 1.4, 0.7 Hz, 1H, *H*C25), 7.70 – 7.63 (m, 2H, *H*C23, *H*C32), 7.57 (dt, *J* = 7.2, 1.0 Hz, 1H, *H*C21), 7.50 – 7.44 (m, 1H, *H*C27), 7.40 (dd, *J* = 8.2, 7.2 Hz, 1H, *H*C22), 7.36 (ddd, *J* = 8.0, 6.8, 1.1 Hz, 1H, *H*C26), 7.24 – 7.20 (m, 2H, *H*C37, *H*C41), 7.20 – 7.17 (m, 1H, *H*C17), 7.07 (dd, *J* = 7.7, 1.7 Hz, 1H, *H*C15), 7.05 – 7.01 (m, 1H, *H*C16), 6.96 (d, *J* = 7.4 Hz, 1H, *H*C35), 6.88 – 6.84 (m, 2H, *H*C38, *H*C40), 6.81 (ddd, *J* = 7.4, 1.8, 0.7 Hz, 1H, *H*C34), 6.51 – 6.43 (m, 1H, *H*C13), 6.38 (q, *J* = 7.0 Hz, 1H, *H*C6), 6.05 (dd, *J* = 9.0, 5.7 Hz, 1H, *H*C12), 5.29 (q, *J* = 6.4 Hz, 1H, *H*C4), 4.10 – 4.04 (m, 1H, H_2N4), 3.85 – 3.74 (m, 1H, H_2C3), 3.70 (d, *J* = 5.7 Hz, 1H, *H*C11), 3.68 (s, 1H, *H*C8), 3.68 – 3.63 (m, 1H, H_2C2), 3.64 – 3.58 (m, 1H, H_2C3), 3.55 – 3.45 (m, 1H, H_2N4), 3.42 – 3.32 (m, 1H, H_2C2), 3.11 – 3.04 (m, 1H, *H*C9), 2.47 (s, 3H, H_3C42), 2.12 (s, 3H, H_3C43), 1.72 (d, *J* = 3.4 Hz, 3H, H_3C7), 1.16 – 1.10 (m, 4H, H_3C5, H_2N3), 0.10 (d, *J* = 9.4 Hz, 1H, H_2N3). **^{13}C NMR** (126 MHz, 26 ºC, THF-d_8, connectivities were confirmed by gHSQC and gHMBC experiments) δ 225.8 (C1), 176.8 (C31), 145.8 (C30), 142.7 (C19), 141.6 (C32), 140.4 (C20), 138.0 (C36), 137.7 (C12), 137.3 (C39), 134.9 (C24), 134.5 (C33), 131.9 (C14), 131.3 (C29), 129.8 (C38, C40), 129.6 (C25), 128.6 (C23), 128.1 (C18), 127.9 (C27), 127.3 (C37, C41), 126.9 (C15), 126.3 (C22), 126.3 (C26), 125.5 (C17), 124.5 (C21), 124.4 (C16), 124.3 (C28), 122.7 (C34), 121.4 (C13), 121.3 (C35), 82.9 (C10), 68.0 (C8), 67.1 (C11), 63.0 (C9), 58.5 (C4), 54.2, (C6) 47.8 (C2), 46.7 (C3), 21.7 (C42), 20.8 (C43), 20.5 (C5), 20.0 (C7). **ESI-MS**: calculated $[C_{43}H_{45}ClN_4Ru - Cl]^+$: 719.2682, found: 719.2692

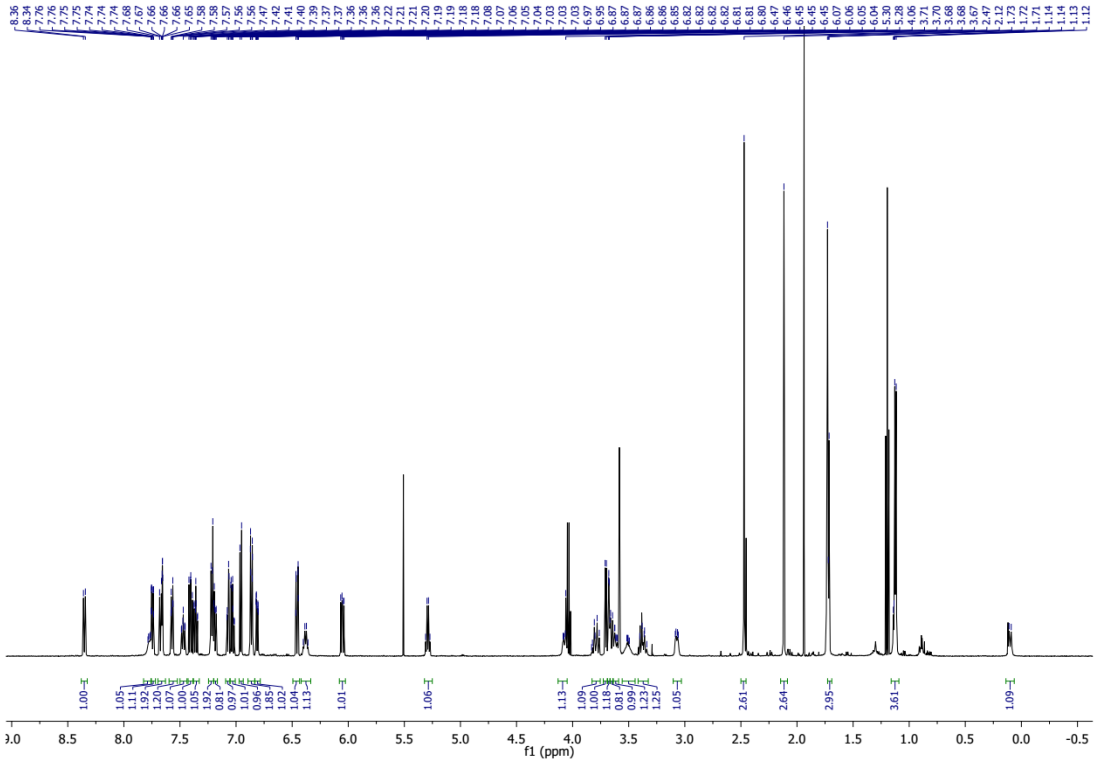
f1 (ppm)

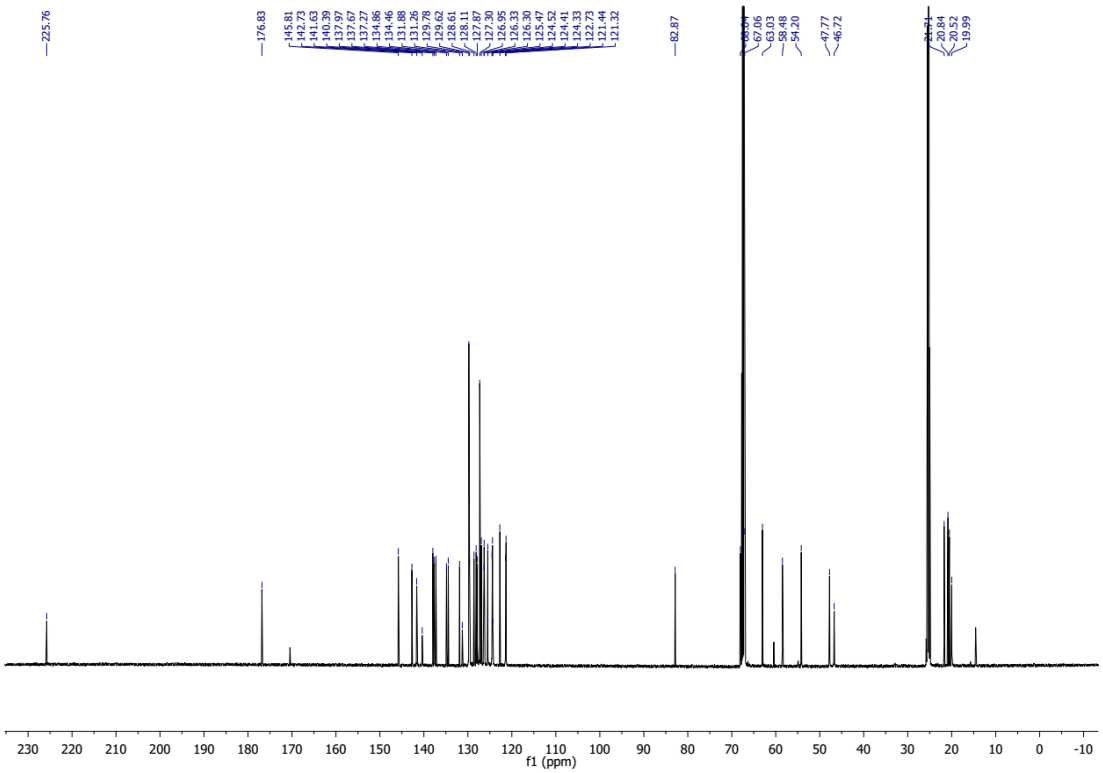
f1 (ppm)

gCOSY

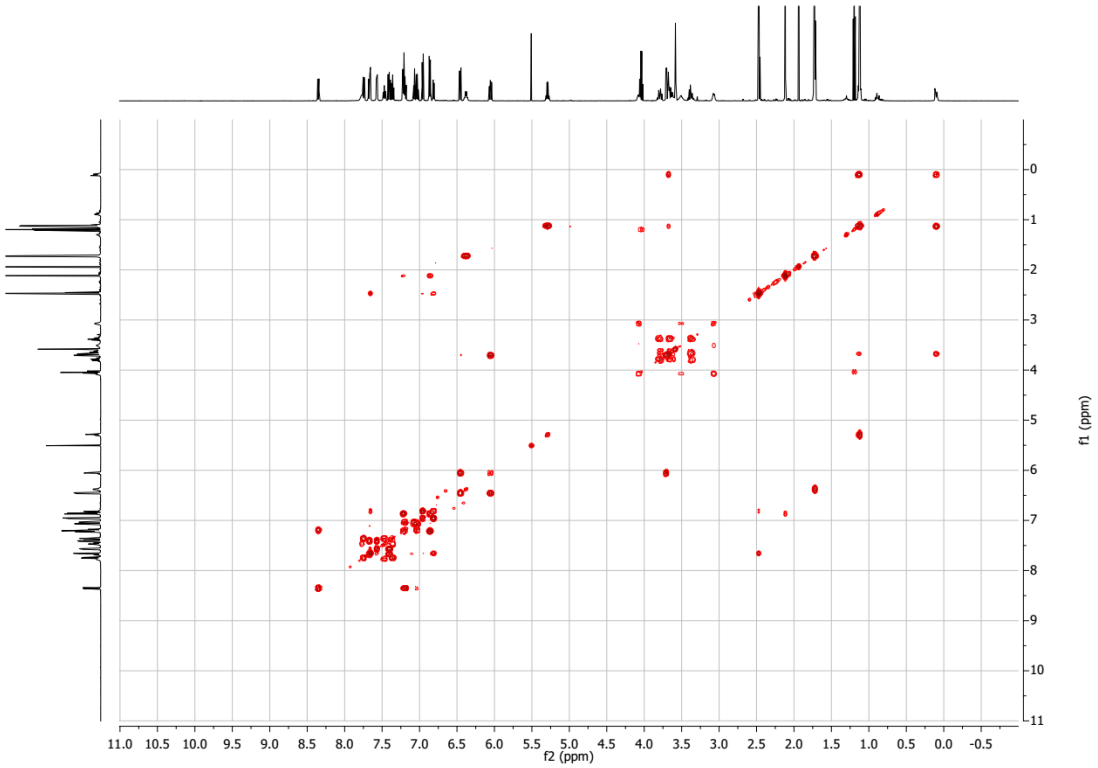

gHSQC

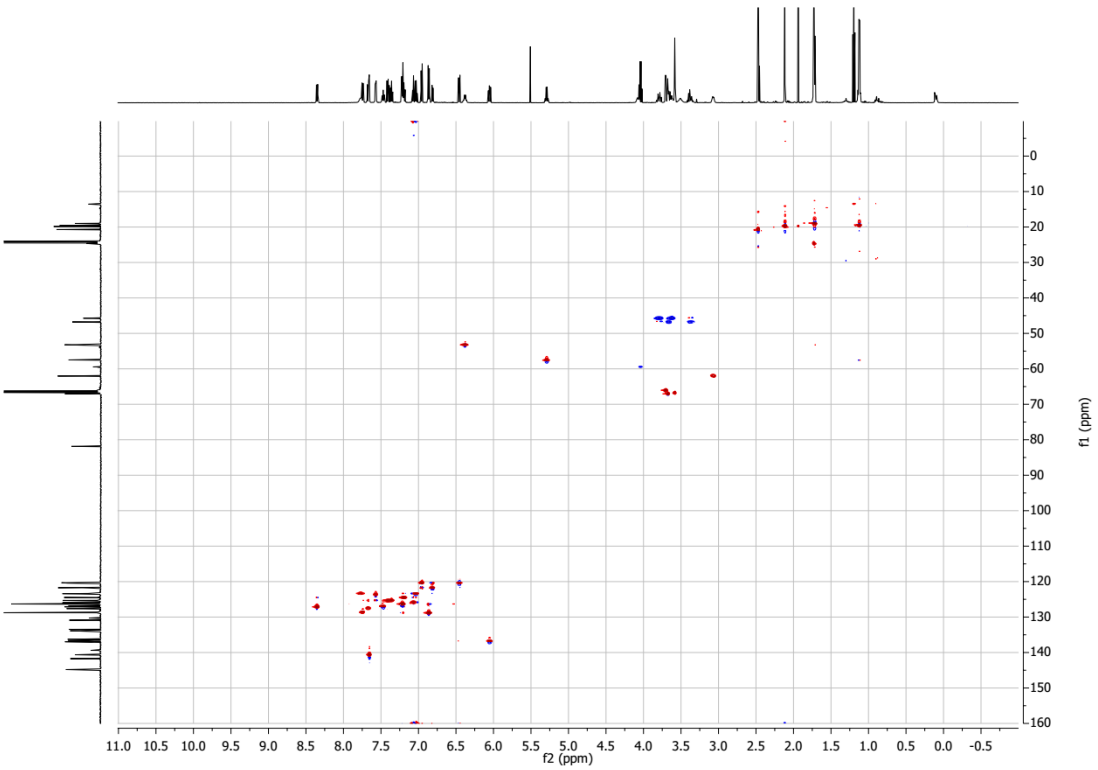

gHMBC

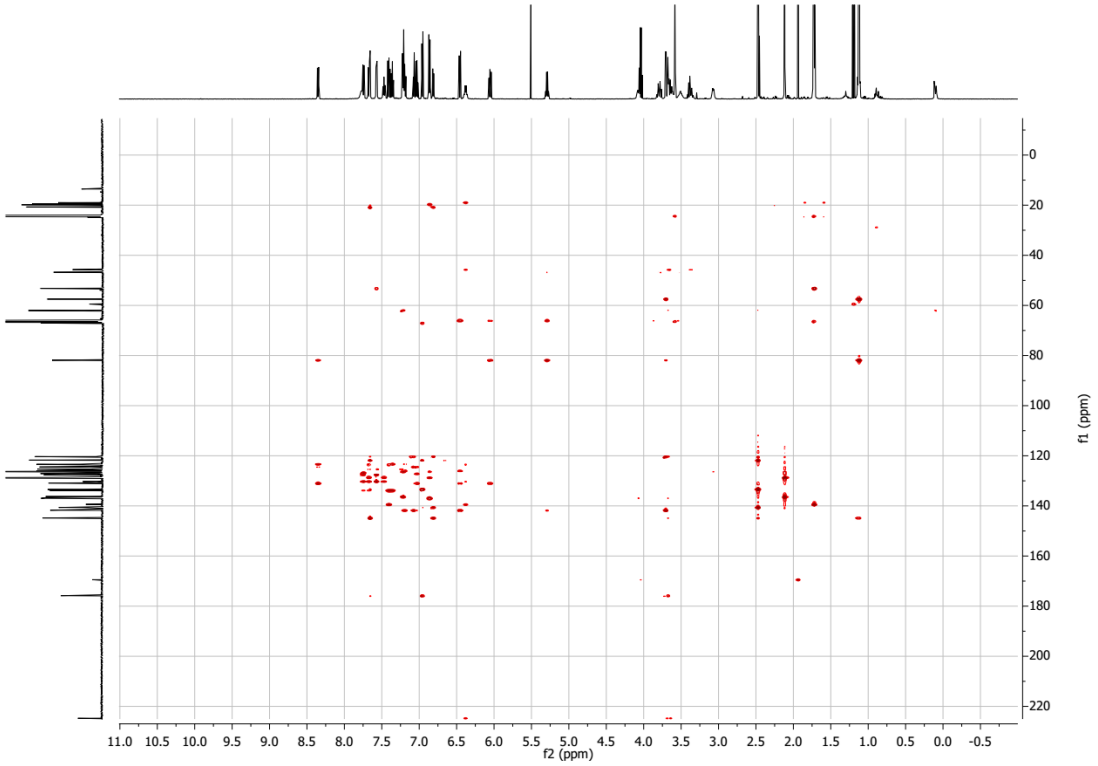

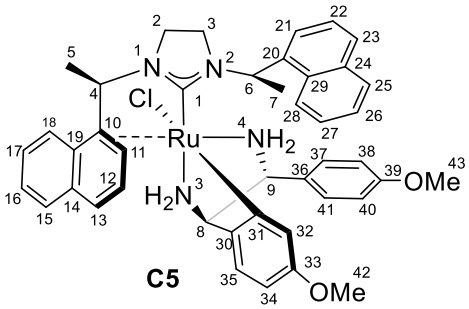

Complex **C5** was isolated in 34% yield according to the Procedure 2 using (1*R*,2*R*)-1,2-bis(4-methoxyphenyl)ethane-1,2-diamine.

^{1}H NMR (500 MHz, 26 °C, THF-d_8, connectivities were confirmed by gCOSY, gHSQC and gHMBC experiments) δ 8.34 (d, *J* = 8.1 Hz, 1H, *H*C18), 7.89 (d, *J* = 8.5 Hz, 1H, *H*C28), 7.78 – 7.71 (m, 1H, *H*C25), 7.67 (d, *J* = 8.2 Hz, 1H, *H*C23), 7.56 (d, *J* = 7.2 Hz, 1H, *H*C21), 7.49 (ddd, *J* = 8.5, 6.8, 1.4 Hz, 1H, *H*C27), 7.43 – 7.38 (m, 1H, *H*C22), 7.39 (d, *J* = 2.4 Hz, 1H, *H*C32), 7.36 (ddd, *J* = 7.9, 6.9, 0.9 Hz, 1H, *H*C26), 7.26 (d, *J* = 8.6 Hz, 2H, *H*C37, *H*C41), 7.19 (ddd, *J* = 8.3, 6.9, 1.6 Hz, 1H, *H*C17), 7.07 (dd, *J* = 7.6, 1.5 Hz, 1H, *H*C15), 7.03 (ddd, *J* = 7.7, 7.0, 1.1 Hz, 1H, *H*C16), 6.96 (d, *J* = 8.1 Hz, 1H, *H*C35), 6.63 – 6.57 (m, 2H, *H*C38, *H*C40), 6.55 (dd, *J* = 8.0, 2.5 Hz, 1H, *H*C34), 6.47 (d, *J* = 9.1 Hz, 1H, *H*C13), 6.33 (q, *J* = 6.9 Hz, 1H, *H*C6), 6.06 (dd, *J* = 9.0, 5.7 Hz, 1H, *H*C12), 5.26 (q, *J* = 6.4 Hz, 1H,

*H*C4), 3.96 (dd, *J* = 10.9, 3.4 Hz, 1H, H_2N4), 3.89 (s, 3H, H_3C42), 3.78 (dt, *J* = 11.7, 9.3 Hz, 1H, H_2C3), 3.73 (d, *J* = 5.7 Hz, 1H, *H*C11), 3.66 (dd, *J* = 9.0, 2.3 Hz, 1H, H_2C2), 3.62 (s, 1H, *H*C8), 3.58 (s, 3H, H_3C43), 3.58 – 3.54 (m, 2H, H_2N4, H_2C3), 3.39 – 3.29 (m, 1H, H_2C2), 3.08 (d, *J* = 9.1 Hz, 1H, *H*C9), 1.74 (d, *J* = 6.9 Hz, 3H, H_3C7), 1.13 – 1.08 (m, 4H, H_3C5, H_2N3), 0.06 (d, *J* = 9.5 Hz, 1H, H_2N3). **^{13}C NMR** (126 MHz, 26 ºC, THF-d_8, connectivities were confirmed by gHSQC and gHMBC experiments) δ 225.4 (C1), 178.5 (C31), 159.6 (C39), 158.3 (C33), 142.5 (C19), 141.1 (C30), 140.0 (C20), 137.4 (C12), 134.7 (C24), 132.6 (C36), 131.7 (C14), 131.1 (C29), 129.4 (C25), 128.5 (C23), 128.3 (C37, C41), 127.9 (C18), 127.7 (C27), 126.8 (C13), 126.1 (C22, C26), 125.7 (C32), 125.3 (C17), 124.4 (C21), 124.3 (C16, C28), 121.7 (C35), 121.4 (C13), 114.3 (C38, C40), 107.5 (C34), 82.9 (C10), 67.5 (C8), 67.4 (C11), 62.7 (C9), 58.4 (C4), 55.1 (C42), 55.0 (C43), 53.9 (C6), 47.7 (C2), 46.5 (C3), 20.4 (C5), 20.0 (C7). **ESI-MS**: calculated $[C_{43}H_{45}ClN_4O_2Ru - Cl]^+$: 751.2581, found: 751.2587.

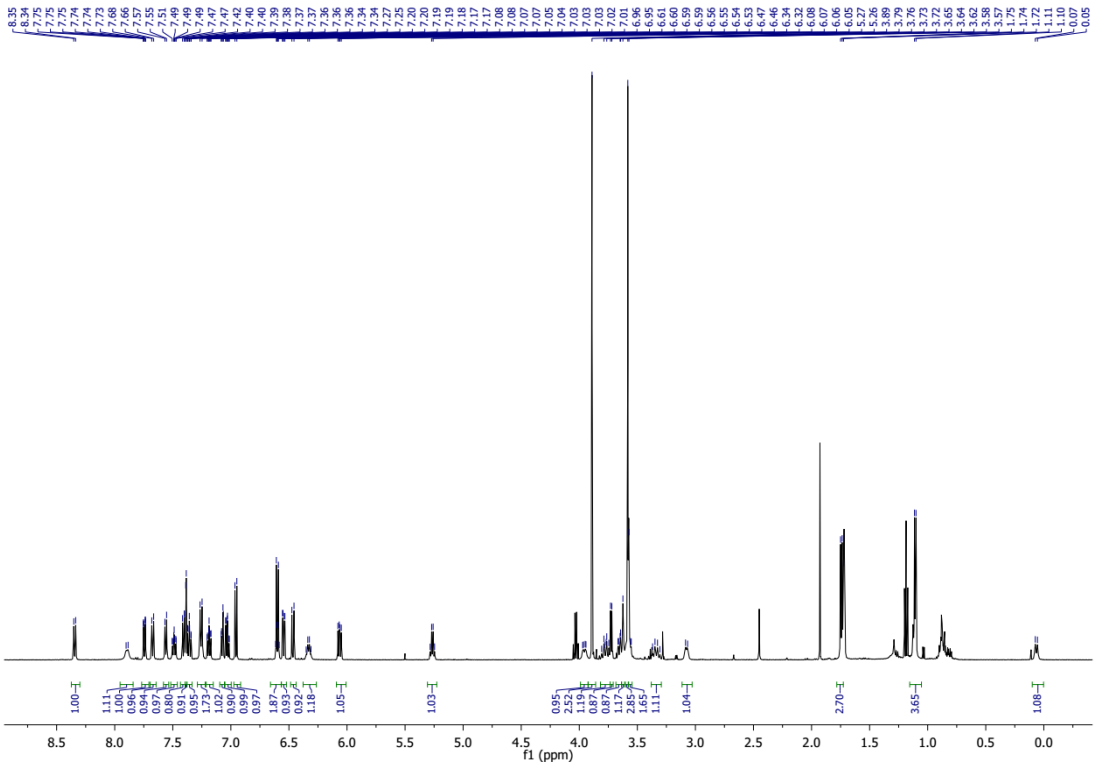

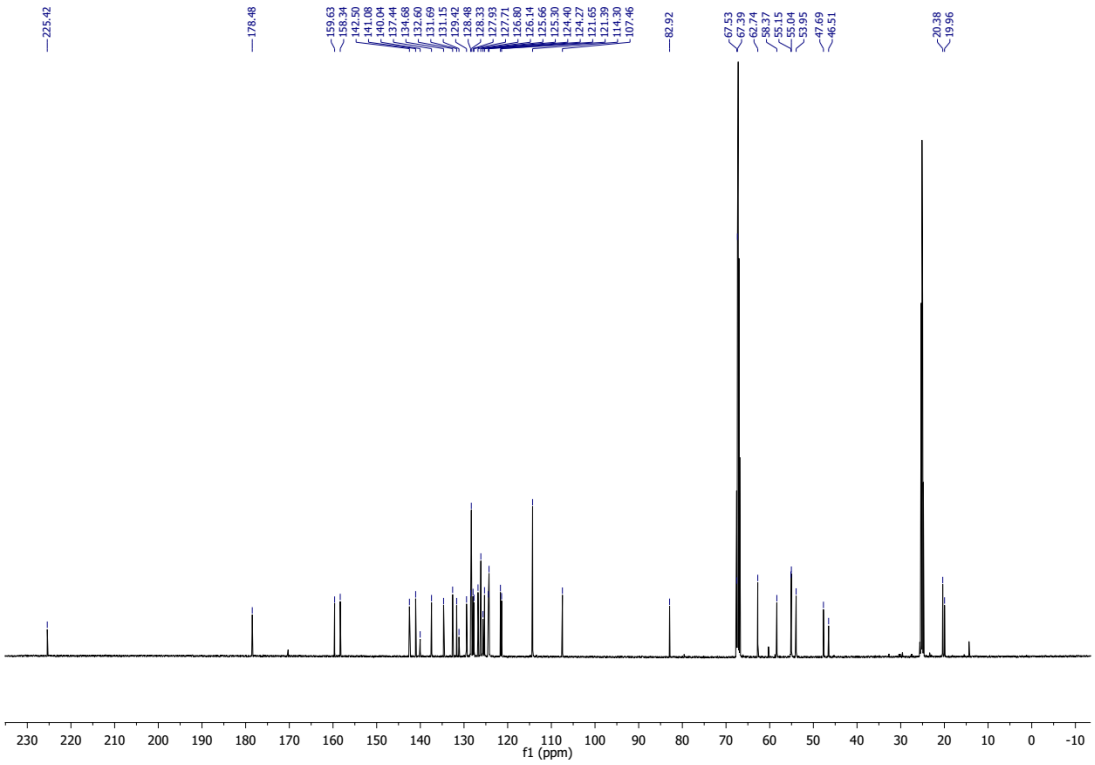
225.42
178.48
159.63
158.34
142.50
141.08
140.04
137.44
134.68
132.60
131.69
131.15
129.42
128.48
128.33
127.93
127.71
126.80
126.14
125.66
125.30
124.40
124.27
121.55
121.39
114.30
107.46
82.92
67.53
67.39
62.74
58.37
55.15
55.04
53.95
47.69
46.51
20.38
19.96
230 220 210 200 190 180 170 160 150 140 130 120 110 100 90 80 70 60 50 40 30 20 10 0 -10
f1 (ppm)

gCOSY:

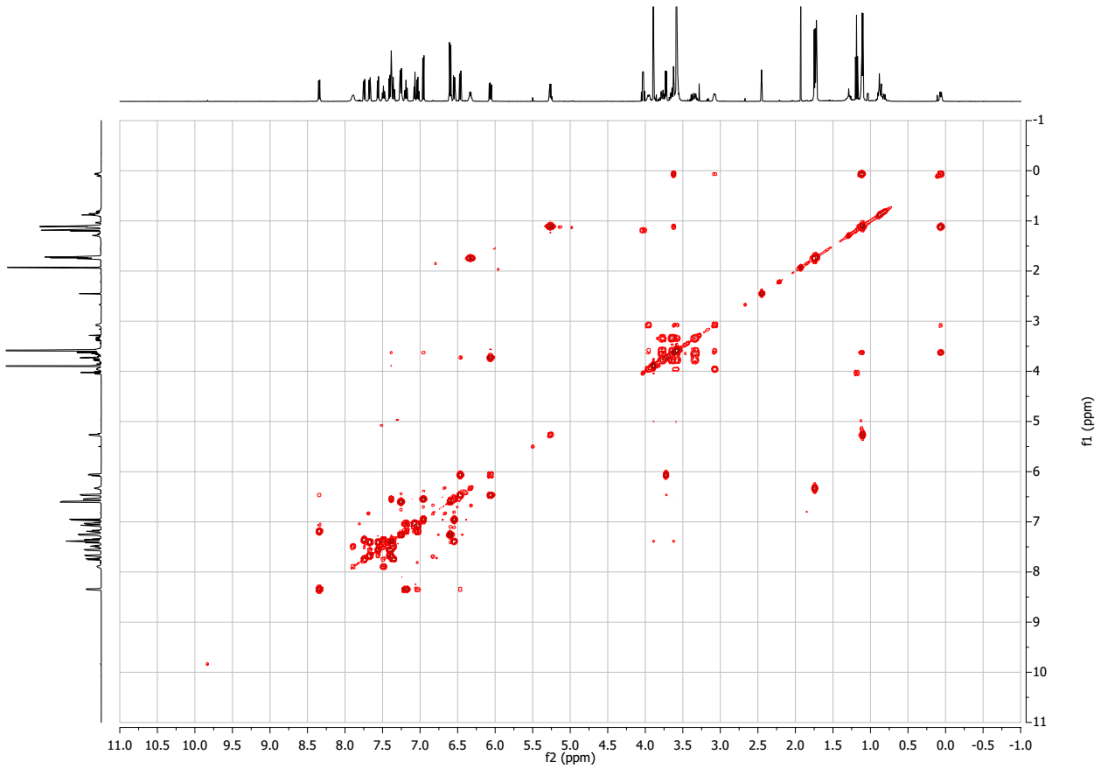
11.0 10.5 10.0 9.5 9.0 8.5 8.0 7.5 7.0 6.5 6.0 5.5 5.0 4.5 4.0 3.5 3.0 2.5 2.0 1.5 1.0 0.5 0.0 -0.5 -1.0
f2 (ppm)
-1 0 1 2 3 4 5 6 7 8 9 10 11
f1 (ppm)

gHSQC:

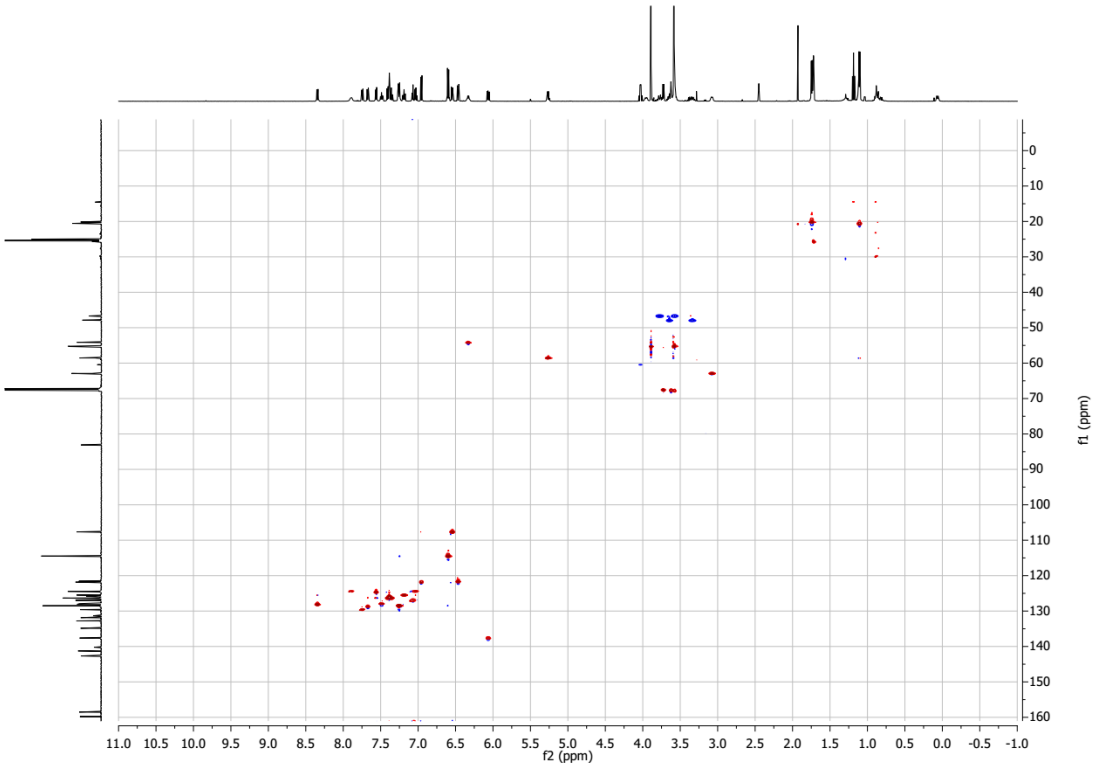

gHMBC

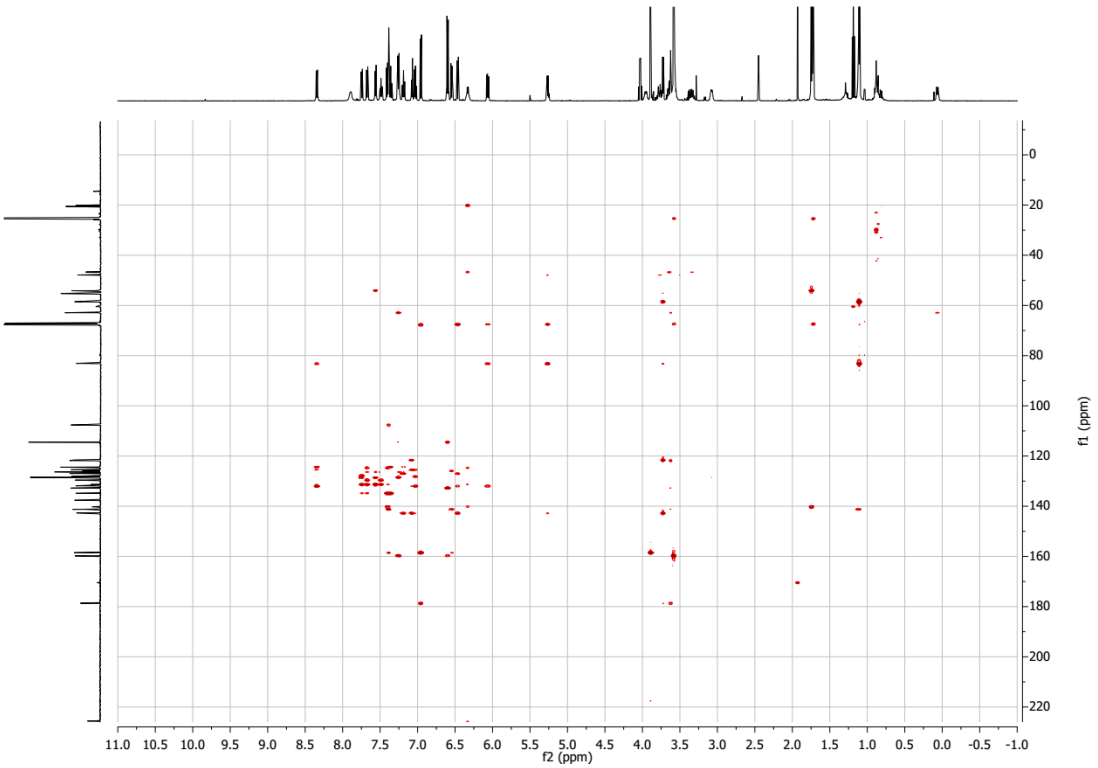

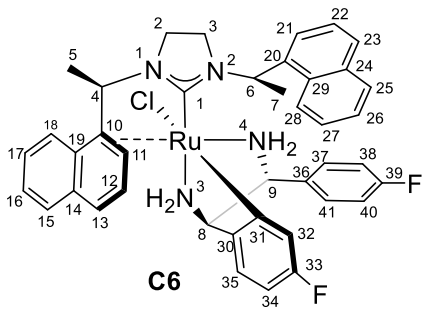

Complex **C6** was isolated in 32% yield according to the Procedure 2 using (1*R*,2*R*)-1,2-bis(4-fluorophenyl)ethane-1,2-diamine.

^{1}H NMR (600 MHz, 26 °C, $CDCl_3$, connectivities were confirmed by gCOSY, gHSQC and gHMBC experiments) δ 8.36 (d, *J* = 8.0 Hz, 1H, *H*C18), 7.75 – 7.73 (m, 1H, *H*C25), 7.65 (d, *J* = 8.2 Hz, 1H, *H*C23), 7.52 (d, *J* = 7.2 Hz, 1H, *H*C21), 7.49 – 7.44 (m, 2H, *H*C32, *H*C22), 7.39 (ddd, *J* = 8.4, 5.5, 3.1 Hz, 1H, *H*C17), 7.35 (ddd, *J* = 8.1, 6.9, 1.1 Hz, 1H, *H*C26), 7.31 (ddd, *J* = 8.3, 6.9, 1.5 Hz, 1H, *H*C27), 7.20 – 7.14 (m, 3H, *H*C28, *H*C15, *H*C16), 7.01 (dd, *J* = 8.2, 5.6 Hz, 1H, *H*C35), 6.95 (ddt, *J* = 8.3, 5.3, 2.6 Hz, 2H, *H*C38, *H*C40), 6.78 (ddd, *J* = 9.1, 8.1, 2.6 Hz, 1H, *H*C34), 6.76 – 6.72 (m, 2H, *H*C37, *H*C41), 6.57 (dt, *J* = 9.1, 0.7 Hz, 1H, *H*C13), 6.43 (q, *J* = 7.1 Hz, 1H, *H*C6), 6.17 (dd, *J* = 9.0, 5.7 Hz, 1H, *H*C12), 5.44 (q, *J* = 6.4 Hz, 1H, *H*C4), 4.08 – 4.01 (m, 1H, H_2C3), 4.02 – 3.96 (m, 1H, H_2C3), 3.84 – 3.78 (m, 1H, H_2C2), 3.73 (d, *J* = 5.5 Hz, 1H, *H*C11), 3.70 (dt, *J* = 10.8, 1.8 Hz, 1H, H_2C2), 3.67 (s, 1H, *H*C8), 3.44 – 3.38 (m, 1H, H_2N4), 2.84 – 2.74 (m, 2H, H_2N4, *H*C9), 1.68 (d, *J* = 7.1 Hz, 3H, H_3C7), 1.20 (d, *J* = 6.5 Hz, 3H, H_3C5), 1.10 (d, *J* = 9.5 Hz, 1H, H_2N3), 0.13 (d, *J* = 9.9 Hz, 1H, H_2N3). **^{13}C NMR** (151 MHz, 26 °C, $CDCl_3$, connectivities were confirmed by gHSQC and gHMBC experiments) δ 223.8 (C1), 179.74 (d, *J* = 2.9 Hz, C31), 162.03 (d, *J* = 247.0 Hz, C39), 161.41 (d, *J* = 247.1 Hz, C33), 142.85 (d, *J* = 1.9 Hz, C30), 141.1 (C19), 140.2 (C20), 136.1 (C12), 134.83 (d, *J* = 3.2 Hz, C36), 134.0 (C24), 130.8 (C14), 129.7 (C25), 129.0 (C29), 128.1 (C23), 128.04 (d, *J* = 8.0 Hz, C38, C40), 126.9 (C27), 126.9 (C15), 126.7 (C18), 126.6 (C22), 125.8 (C17), 125.7 (C26), 124.98 (d, *J* = 15.8 Hz, C32), 124.7 (C16), 123.4 (C21), 121.61 (d, *J* = 8.0 Hz, C35), 121.5 (C13), 121.4 (C28), 115.80 (d, *J* = 21.4 Hz, C37, C41), 108.34 (d, *J* = 22.4 Hz, C34), 85.3 (C10), 68.5 (C11), 66.2 (C8), 62.0 (C9), 57.0 (C4), 53.5 (C6), 47.3 (C3), 46.7 (C2), 20.7 (C7), 20.3 (C5). **^{19}F NMR** (564 MHz, $CDCl_3$) δ -114.6, -118.4. **ESI-MS**: calculated $[C_{41}H_{39}ClF_2N_4Ru – Cl]^+$: 727.2181, found: 727.2171.

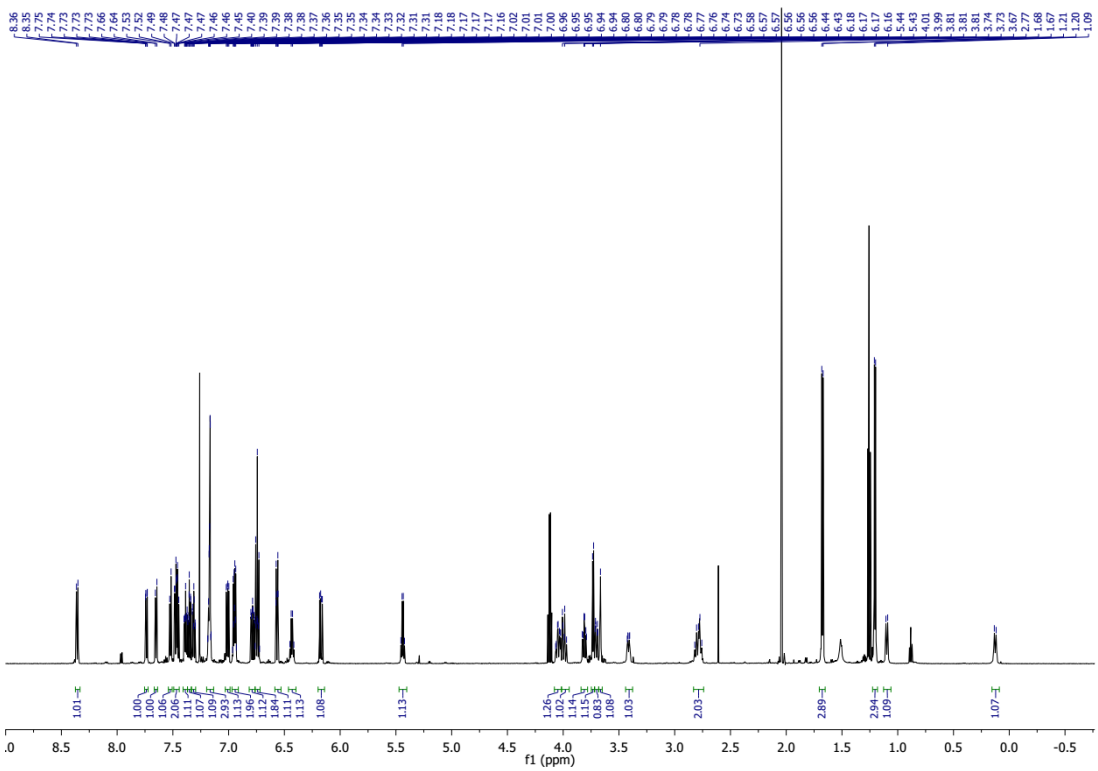
f1 (ppm)

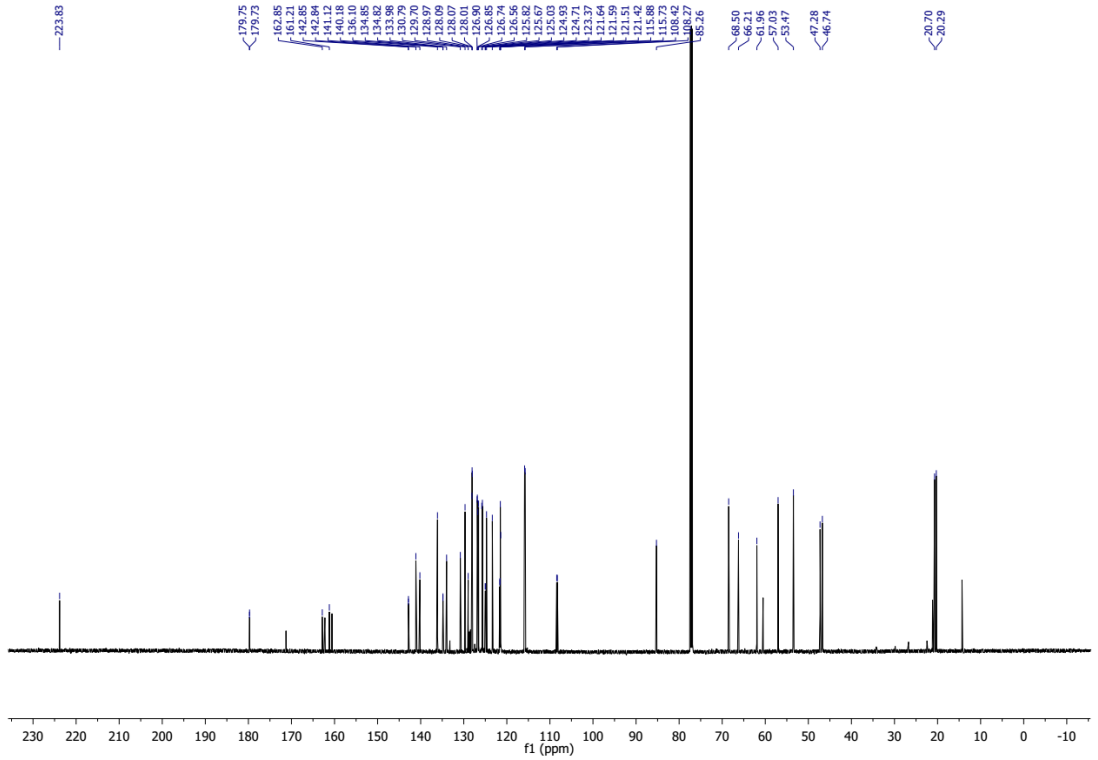
f1 (ppm)

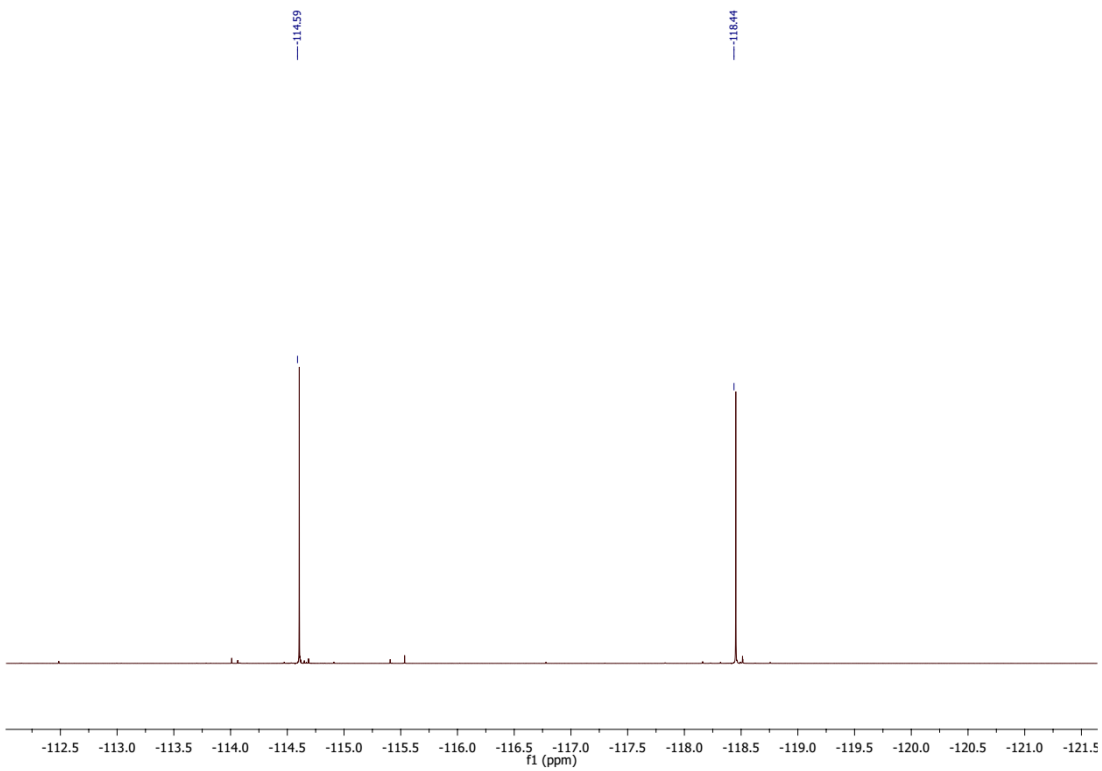
-114.59
-118.44
-112.5 -113.0 -113.5 -114.0 -114.5 -115.0 -115.5 -116.0 -116.5 -117.0 -117.5 -118.0 -118.5 -119.0 -119.5 -120.0 -120.5 -121.0 -121.5
f1 (ppm)

gCOSY:

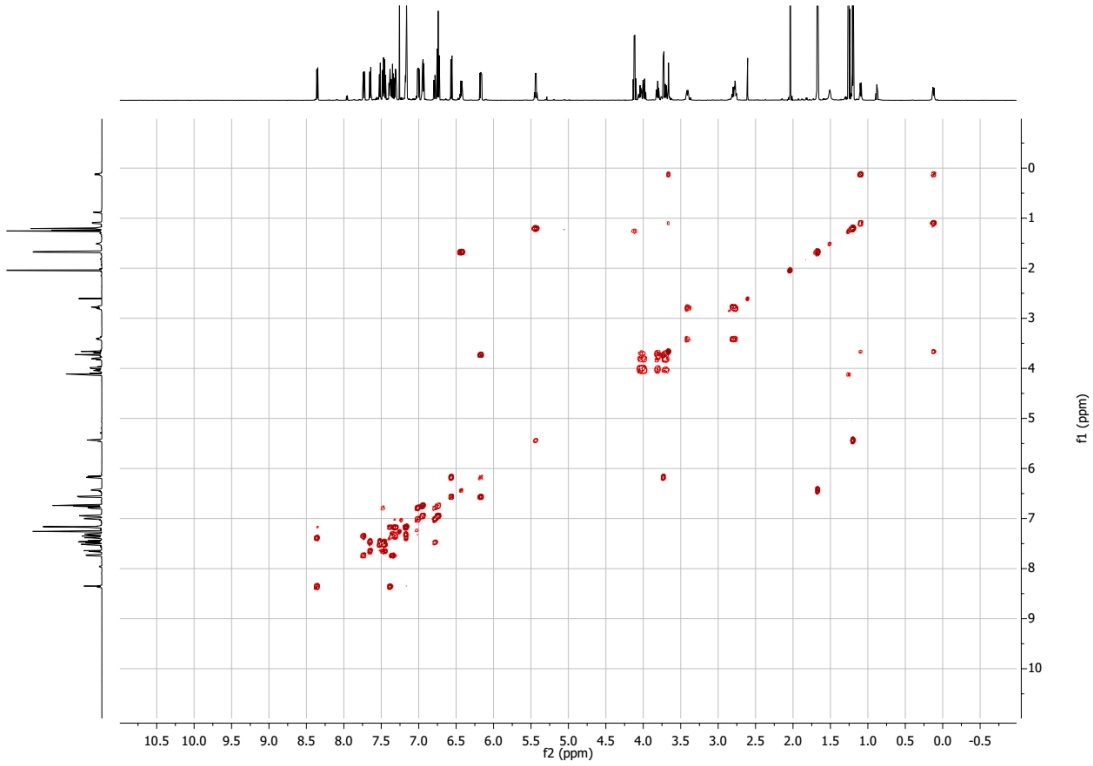
10.5 10.0 9.5 9.0 8.5 8.0 7.5 7.0 6.5 6.0 5.5 5.0 4.5 4.0 3.5 3.0 2.5 2.0 1.5 1.0 0.5 0.0 -0.5
f2 (ppm)
0 1 2 3 4 5 6 7 8 9 10
f1 (ppm)

gHSQC:

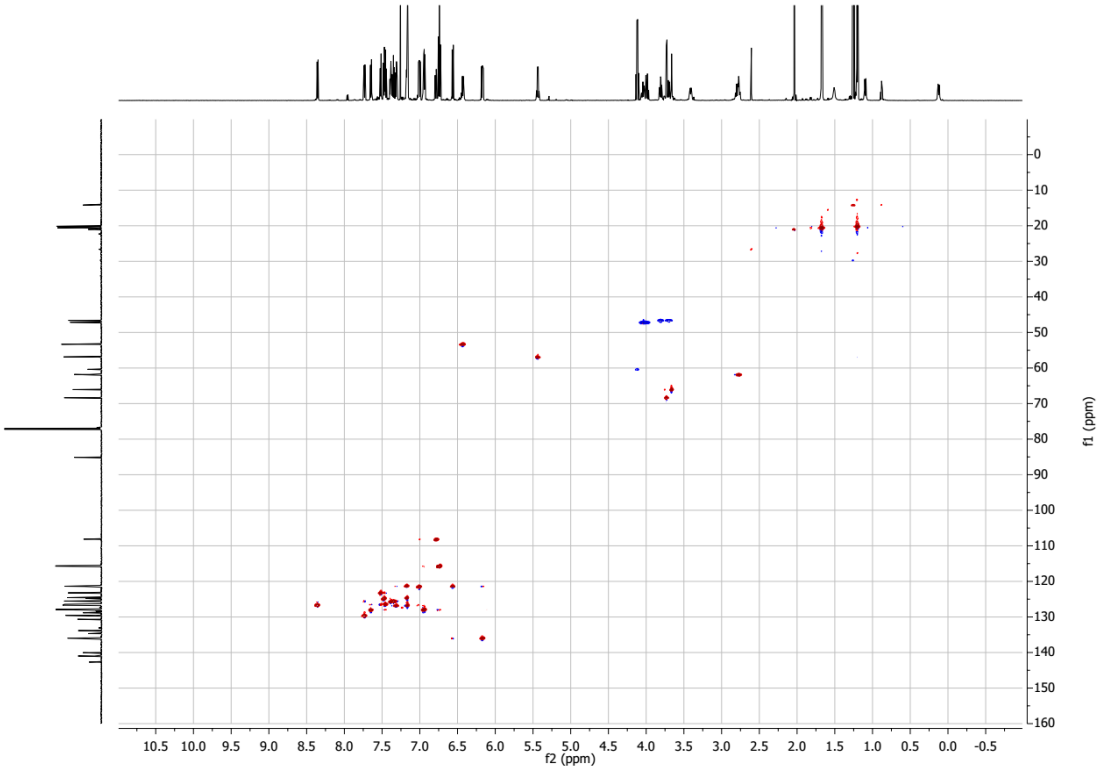

gHMBC:

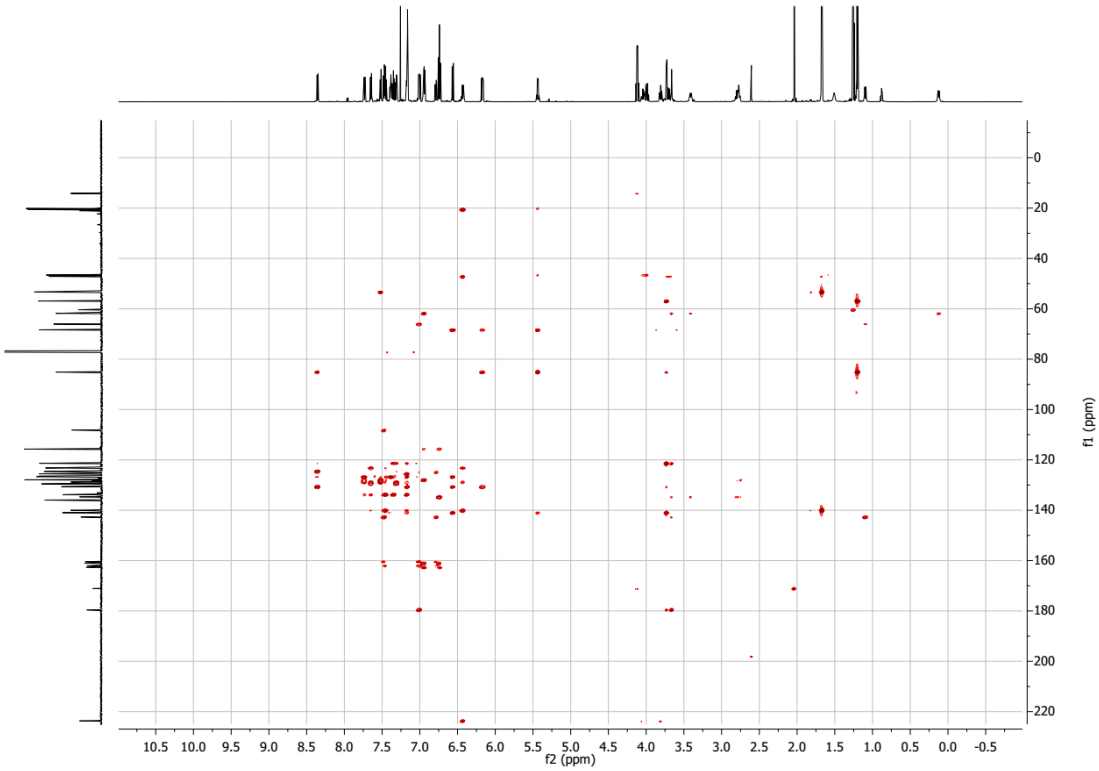

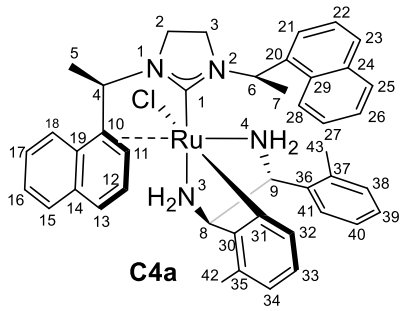

Complex **C4a** was isolated in 12% yield according to the Procedure 2 using (1*R*,2*R*)-1,2-bis(2-methylphenyl)ethane-1,2-diamine.

^{1}H NMR (600 MHz, 26 °C, Chloroform-*d*, connectivities were confirmed by gCOSY, gHSQC, and gHMBC experiments) δ 8.40 (d, *J* = 8.2 Hz, 1H, *H*C18), 7.72 (dd, *J* = 8.2, 1.3 Hz, 1H, *H*C28), 7.66 – 7.60 (m, 3H, *H*C22, *H*C32, *H*C41), 7.52 (d, *J* = 7.2 Hz, 1H, *H*C21), 7.43 – 7.38 (m, 2H, *H*C16, *H*C23), 7.34 (ddd, *J* = 8.0, 6.8, 1.1 Hz, 1H, *H*C26), 7.25 (ddd, *J* = 8.2, 6.9, 1.1 Hz, 1H, *H*C27), 7.20 (t, *J* = 7.4 Hz, 1H, *H*C33), 7.18 – 7.15 (m, 2H, *H*C15, *H*C17), 7.02 – 6.96 (m, 2H, *H*C25, *H*C39), 6.95 – 6.89 (m, 2H, *H*C34, *H*C40), 6.86 (d, *J* = 7.4 Hz, 1H, *H*C38), 6.70 (q, *J* = 7.0 Hz, 1H, *H*C6), 6.55 (d, *J* = 9.0 Hz, 1H, *H*C13), 6.22 (dd, *J* = 9.0, 5.7 Hz, 1H, *H*C12), 5.50 (q, *J* = 6.4 Hz, 1H, *H*C4), 4.03 (m, 1H, H_2C2), 3.99 – 3.92 (m, 2H, H_2C2, *H*C8), 3.82 – 3.79 (m, 1H, H_2C3), 3.78 (d, *J* = 5.7 Hz, 1H, *H*C11), 3.73 – 3.66 (m, 1H, H_2C3), 3.51 (dd, *J* = 11.2, 4.1 Hz, 1H, H_2N4), 3.02 – 2.97 (m, 1H, *H*C9), 2.89 (t, *J* = 10.5 Hz, 1H, H_2N4), 2.33 (s, 3H, H_3C42), 1.66 (s, 3H, H_3C43), 1.59 (d, *J* = 7.1 Hz, 3H, H_3C7), 1.22 (d, *J* = 6.5 Hz, 3H, H_3C5), 0.89 – 0.83 (m, 1H, H_2N3), 0.14 (d, *J* = 9.7 Hz, 1H, H_2N3). **^{13}C NMR** (151 MHz, 26 °C, Chloroform-*d*, connectivities were confirmed by gHSQC, and gHMBC experiments) δ 225.1 (C1), 176.0 (C31), 144.9 (C35), 141.5 (C14), 140.9 (C20), 138.2 (C36, C32), 136.8 (C12), 134.3 (C37), 134.1 (C24), 130.9 (C19), 130.6 (C38), 129.8 (C30), 129.6 (C28), 129.1 (C29), 127.9 (C22), 127.4 (C39), 127.3 (C40), 126.7 (C15, C18), 126.6 (C27), 126.5 (C23), 126.1 (C41), 125.7 (C16), 125.5 (C26), 125.4 (C33), 124.4 (C17), 123.4 (C34), 123.2 (C21), 122.0 (C25), 120.9 (C13), 84.8 (C10), 68.1 (C11), 61.2 (C8), 57.1 (C4), 56.8 (C9), 53.3 (C6), 47.3 (C3), 46.7 (C2), 21.0 (C7, C42), 20.3 (C5), 19.7 (C43). **ESI-MS**: calculated $[C_{43}H_{45}ClN_4Ru - Cl]^+$: 719.2694, found: 719.2690.

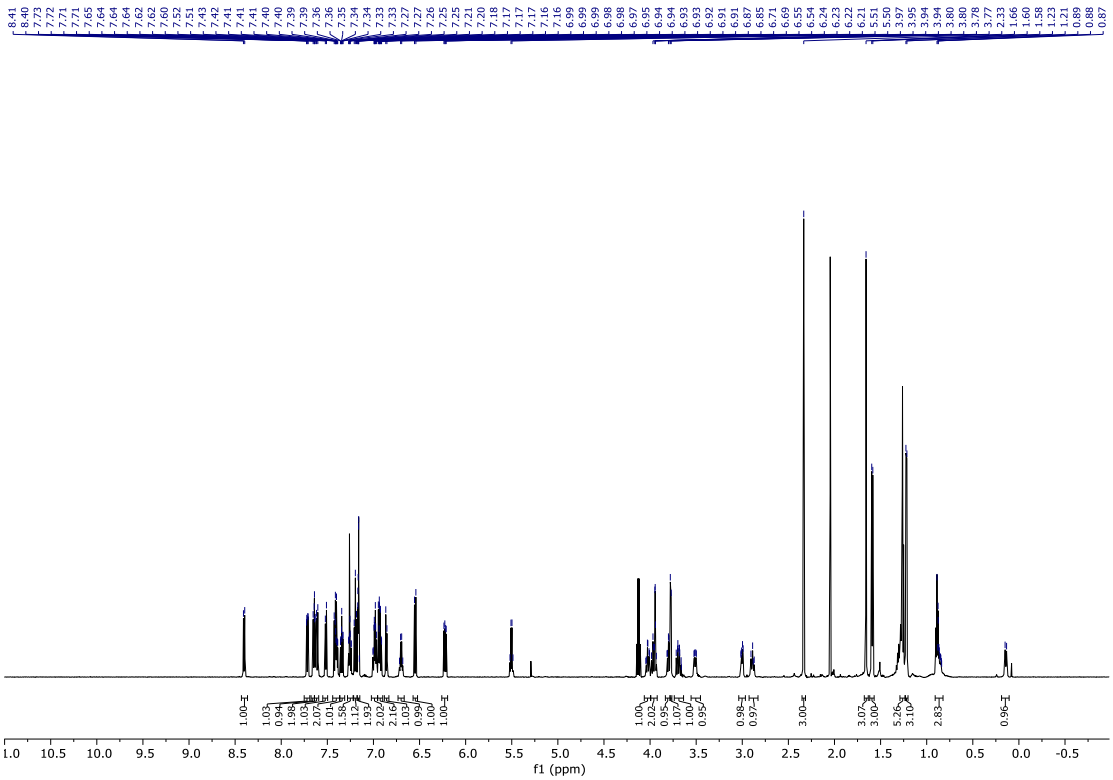
f1 (ppm)

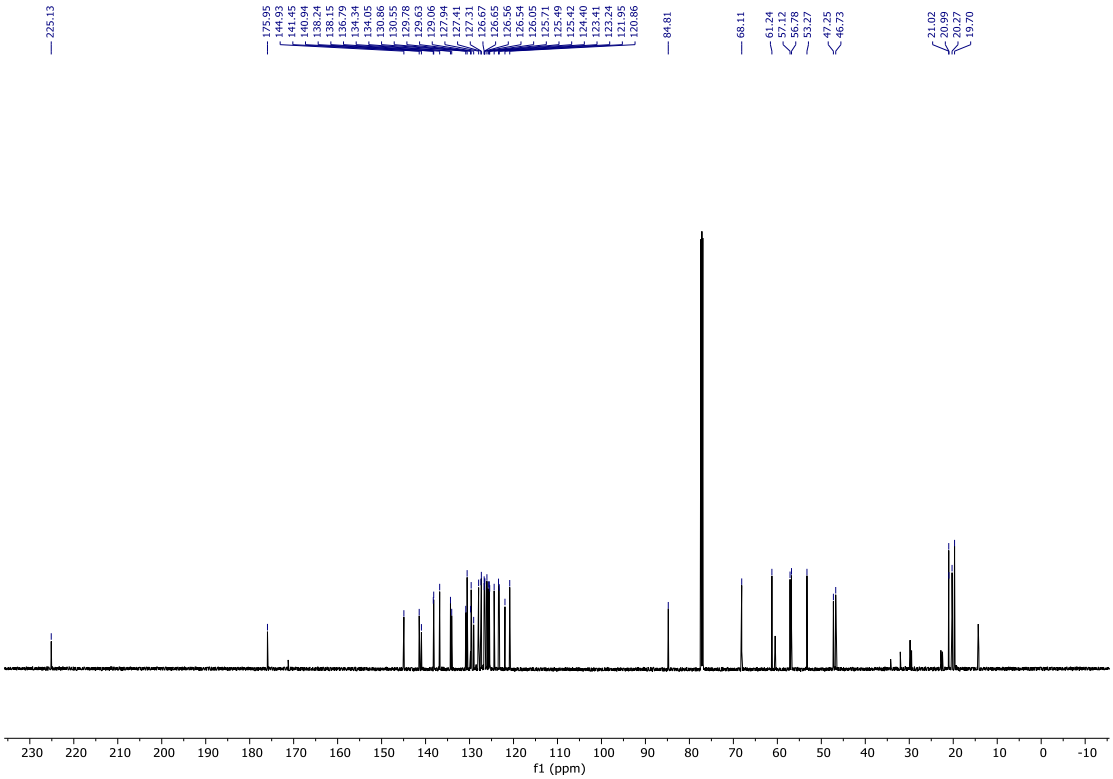
f1 (ppm)

gCOSY:

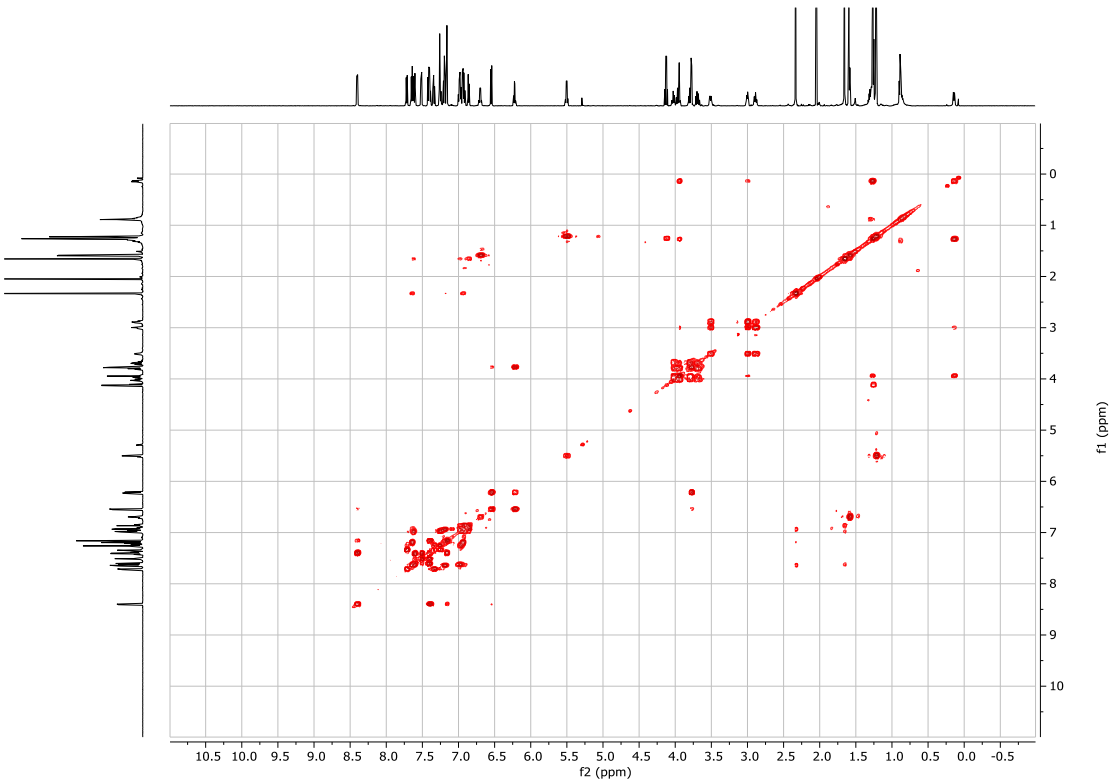

gHSQC:

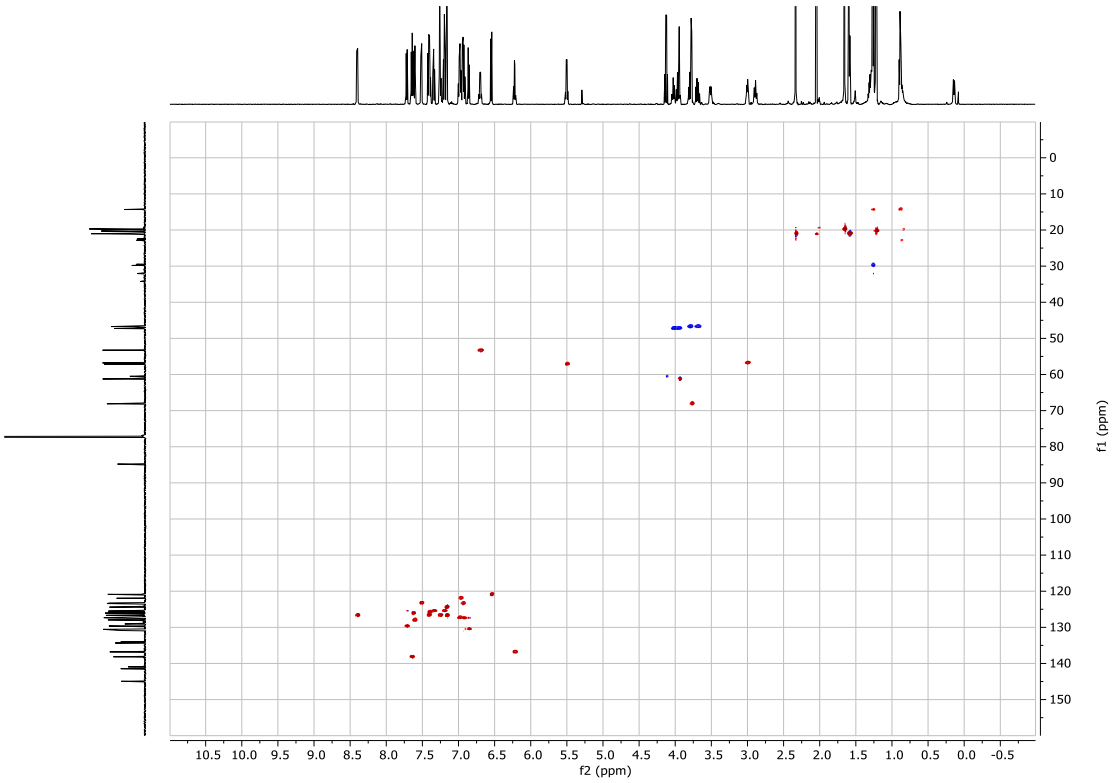

gHMBC:

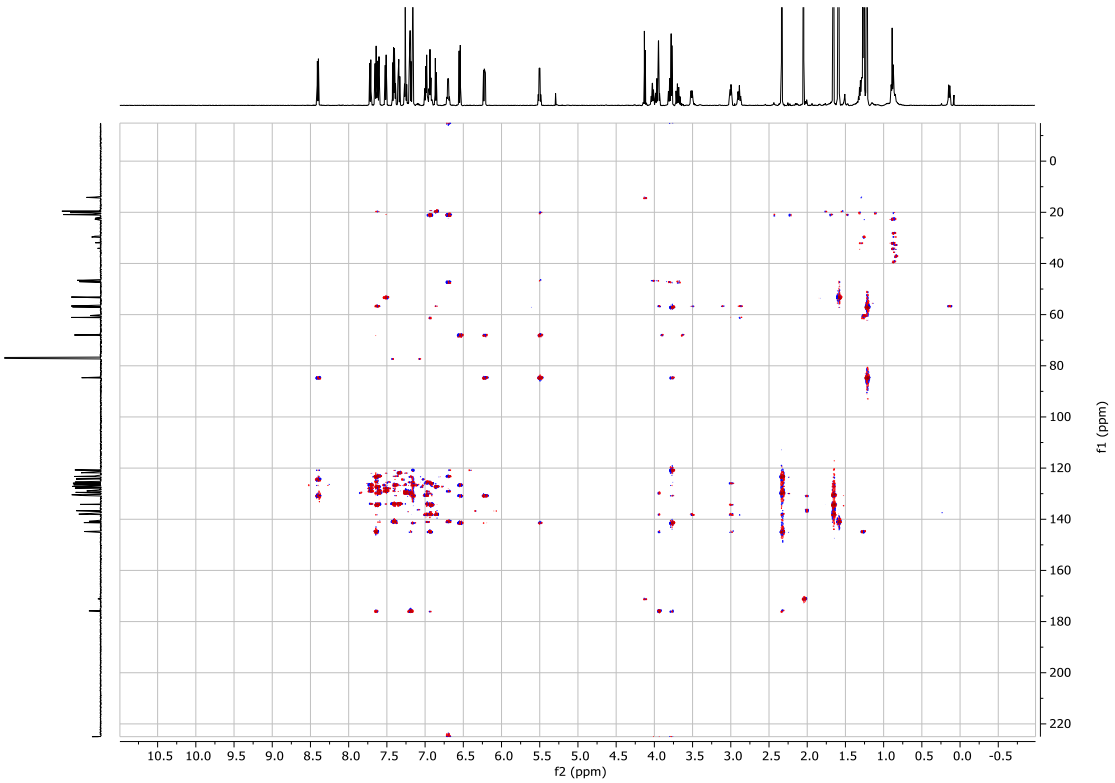

(C) X-Ray diffraction of complexes C1, C2, and C3

X-Ray diffraction: Data sets for compound **C1** were collected with a Nonius Kappa CCD diffractometer. Programs used: data collection, COLLECT (R. W. W. Hooft, Bruker AXS, **2008**, Delft, The Netherlands); data reduction Denzo-SMN (Z. Otwinowski, W. Minor, *Methods Enzymol.* **1997**, *276*, 307-326); absorption correction, Denzo (Z. Otwinowski, D. Borek, W. Majewski, W. Minor, *Acta Crystallogr*. **2003**, *A59*, 228-234); structure solution SHELXS-97 (G. M. Sheldrick, *Acta Crystallogr*. **1990**, *A46*, 467-473); structure refinement SHELXL-97 (G. M. Sheldrick, *Acta Crystallogr*. **2008**, *A64*, 112-122). Data sets for compounds **C2** and **C3** were collected with a D8 Venture CMOS diffractometer. Programs used: data collection: APEX3 V2016.1-0 (Bruker AXS Inc., **2016**); cell refinement: SAINT V8.37A (Bruker AXS Inc., **2015**); data reduction: SAINT V8.37A (Bruker AXS Inc., **2015**); absorption correction, SADABS V2014/7 (Bruker AXS Inc., **2014**); structure solution SHELXT-2015 (Sheldrick, **2015**); structure refinement SHELXL-2015 (Sheldrick, **2015**) and graphics, XP (Bruker AXS Inc., **2015**). *R*-values are given for observed reflections, and wR^2 values are given for all reflections.

Exceptions and special features: For compound **C1** one phenyl group and one naphthyl group and for compound **C3** one phenyl group were found disordered over two positions in the asymmetric unit. Several restraints (SADI, SAME, ISOR and SIMU) were used in order to improve refinement stability. For compound **C1** a badly disordered THF molecule and for compound **C3** four badly disordered THF molecules were found in the asymmetrical unit and could not be satisfactorily refined. The program SQUEEZE (Spek, A. L. (**2015**). *Acta Cryst. C71*, 9-18.) was therefore used to remove mathematically the effect of the solvent. The quoted formula and derived parameters are not included the squeezed solvent molecules.

X-ray crystal structure analysis of C1 (glo9197): formula $C_{41}H_{40}Cl_2N_4Ru$, M = 760.74, orange crystal, 0.38 x 0.04 x 0.02 mm, a = 22.9420(8) Å, b = 10.7497(5) Å, c = 17.5379(8) Å, β = 92.037(2)°, V = 4322.50(3) Å^3, ρ_{calc} = 1.169 gcm^{-3}, μ = 0.516 mm^{-1}, empirical absorption correction (0.828 ≤ T ≤ 0.990), Z = 4, monoclinic, space group $C2$ (No. 5), λ = 0.71073 Å, T = 173(2) K, ω and φ scans, 19941 reflections collected (±h, ±k, ±l), 7260 independent (R_{int} = 0.070) and 6371 observed reflections [I>2σI)], 575 refined parameters, R = 0.053, wR^2 = 0.124, max. (min.) residual electron density 0.69 (-0.50) e.Å^{-3}, the hydrogen atoms at N3 and N4 were refined freely, but with N-H distance restraint (DFIX and U-fixed value); others hydrogen atoms were calculated and refined as riding atoms. Flack parameter was refined to 0.04(4). CCDC Nr.: 1879259.

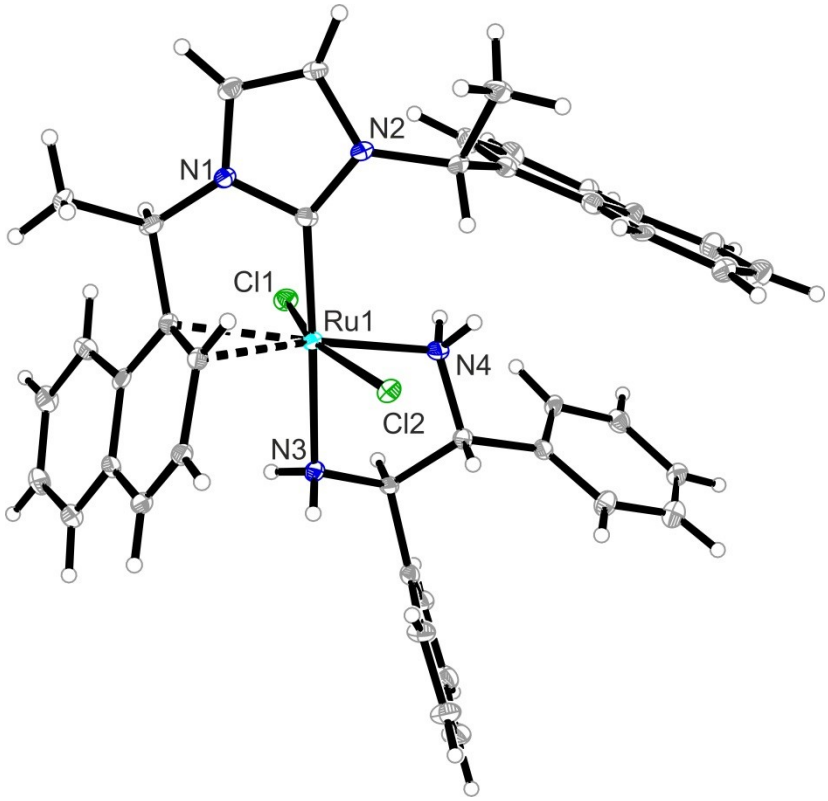

Figure S1. Crystal structure of compound **C1**. (Thermals ellipsoids are shown with 15% probability.)

X-ray crystal structure analysis of C2 (glo8770): A orange prism-like specimen of $C_{41}H_{42}Cl_2N_4Ru$, approximate dimensions 0.103 mm x 0.139 mm x 0.188 mm, was used for the X-ray crystallographic analysis. The X-ray intensity data were measured. A total of 1604 frames were collected. The total exposure time was 24.13 hours. The frames were integrated with the Bruker SAINT software package using a wide-frame algorithm. The integration of the data using a monoclinic unit cell yielded a total of 28574 reflections to a maximum θ angle of 72.07° (0.81 Å resolution), of which 6769 were independent (average redundancy 4.221, completeness = 98.8%, R_{int} = 3.63%, R_{sig} = 4.17%) and 6649 (98.23%) were greater than $2\sigma(F^2)$. The final cell constants of a = 12.4948(6) Å, b = 11.9927(5) Å, c = 13.5247(6) Å, β = 116.6000(10)°, volume = 1812.12(14) $Å^3$, are based upon the refinement of the XYZ-centroids of 9189 reflections above 20 σ(I) with 7.913° < 2θ < 144.1°. Data were corrected for absorption effects using the multi-scan method (SADABS). The ratio of minimum to maximum apparent transmission was 0.841. The calculated minimum and maximum transmission coefficients (based on crystal size) are 0.4460 and 0.6210. The structure was solved and refined using the Bruker SHELXTL Software Package, using the space group $P2_1$, with Z = 2 for the formula unit, $C_{41}H_{42}Cl_2N_4Ru$. The final anisotropic full-matrix least-squares refinement on F^2 with 455 variables converged at R1 = 2.18%, for the observed data and wR2 = 5.28% for all data. The goodness-of-fit was 1.041. The largest peak in the final difference electron density synthesis was 0.336 $e^-/Å^3$ and the largest hole was -0.591 $e^-/Å^3$ with an RMS deviation of 0.055 $e^-/Å^3$. On the basis of the final model, the calculated density was 1.398 g/cm^3 and F(000), 788 e^-. The hydrogens at N3, N4 and C12 atoms were refined freely. Flack parameter was refined to 0.06(1). CCDC Nr.: 1879260.

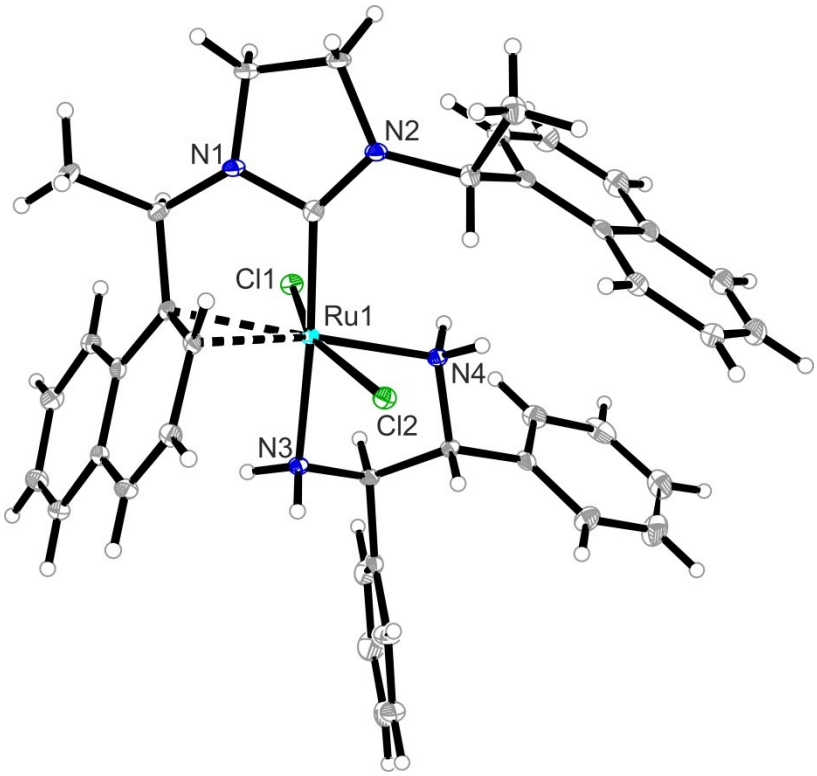

Figure S2. Crystal structure of compound **C2**. (Thermals ellipsoids are shown with 30% probability.)

X-ray crystal structure analysis of C3 (glo8794): A yellow needle-like specimen of $C_{41}H_{41}ClN_4Ru \cdot 0.5 \times C_4H_8O$, approximate dimensions 0.051 mm x 0.064 mm x 0.163 mm, was used for the X-ray crystallographic analysis. The X-ray intensity data were measured. A total of 1563 frames were collected. The total exposure time was 22.61 hours. The frames were integrated with the Bruker SAINT software package using a wide-frame algorithm. The integration of the data using a triclinic unit cell yielded a total of 45033 reflections to a maximum θ angle of 68.80° (0.83 Å resolution), of which 15014 were independent (average redundancy 2.999, completeness = 99.2%, R_{int} = 7.48%, R_{sig} = 7.39%) and 13253 (88.27%) were greater than $2\sigma(F^2)$. The final cell constants of a = 12.3170(4) Å, b = 13.9678(4) Å, c = 15.0411(5) Å, α = 63.519(2)°, β = 80.198(2)°, γ = 67.747(2)°, volume = 2143.69(13) $Å^3$, are based upon the refinement of the XYZ-centroids of 249 reflections above 20 σ(I) with 7.504° < 2θ < 103.1°. Data were corrected for absorption effects using the multi-scan method (SADABS). The

ratio of minimum to maximum apparent transmission was 0.820. The calculated minimum and maximum transmission coefficients (based on crystal size) are 0.5780 and 0.8310. The structure was solved and refined using the Bruker SHELXTL Software Package, using the space group *P*1, with Z = 2 for the formula unit, $C_{41}H_{41}ClN_4Ru \cdot 0.5$ x C_4H_8O. The final anisotropic full-matrix least-squares refinement on F^2 with 972 variables converged at R1 = 4.78%, for the observed data and wR2 = 10.55% for all data. The goodness-of-fit was 1.036. The largest peak in the final difference electron density synthesis was 0.695 $e^-/Å^3$ and the largest hole was -0.726 $e^-/Å^3$ with an RMS deviation of 0.066 $e^-/Å^3$. On the basis of the final model, the calculated density was 1.181 g/cm^3 and F(000), 792 e^-. The hydrogens at N3A, N4A, N3B, N4B, C12A and C12B atoms were refined freely, but with N-H and C-H distance restraints (DFIX and U-fixed value). Flack parameter was refined to -0.01(1). CCDC Nr.: 1879261.

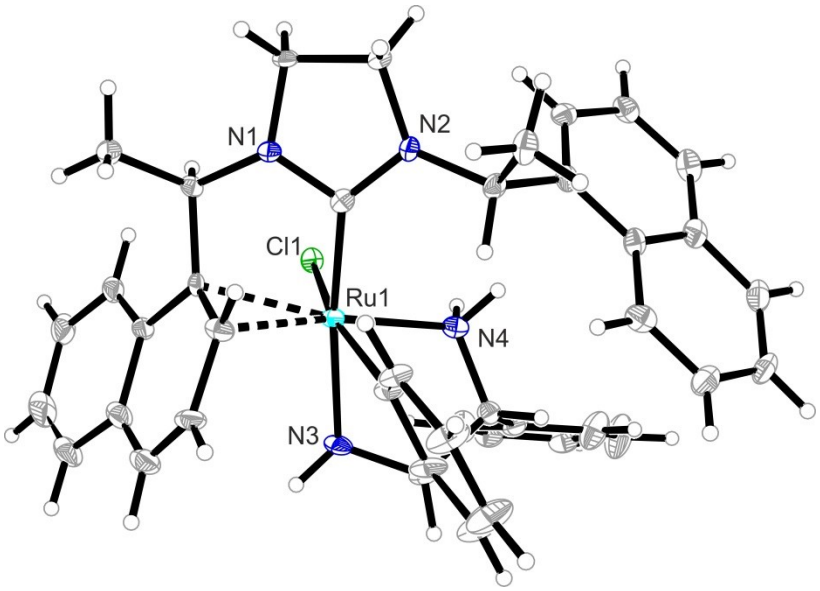

Figure S3. Crystal structure of compound **C3**. Only one molecule (molecule "A") of two found in the asymmetric unit is shown. (Thermals ellipsoids are shown with 30% probability.)

1. *APEX3* (**2016**), *SAINT* (**2015**) and *SADABS* (**2014**), Bruker AXS Inc., Madison, Wisconsin, USA.

2. *SHELX* software: Sheldrick, G. M. *Acta Cryst.,* **2015**, *A71*, 3-8.

(D) General procedure for the enantioselective hydrogenations

a. Ru(II)-catalyzed asymmetric hydrogenation of isocoumarins:

To a glass vial, complex **C4** (0.004 mmol, 2 mol%), NaO*t*-Bu (0.02 mmol, 10 mol%), isocoumarin **1** (0.20 mmol), and *n*-hexane (4 mL) were added under an argon atmosphere. The glass vial was placed in a 150 mL stainless steel autoclave under an argon atmosphere. The autoclave was pressurized and depressurized with hydrogen gas five times before the indicated pressure (50 bar or 80 bar) was set. The reaction mixture was stirred at 15–25 ºC for the indicated time. After the autoclave was carefully depressurized, the mixture was directly purified by flash column chromatography on silica gel (pentane/ethylacetate = 50:1, later 30:1, 20:1, 10:1) to afford the desired product **2**. The e.r. value of the product was determined by HPLC analysis using chiral column AS-H or AD-H.

Substrate Scope of the Ru(II)-Catalyzed Enantioselective Hydrogenation of Isocoumarins[a]

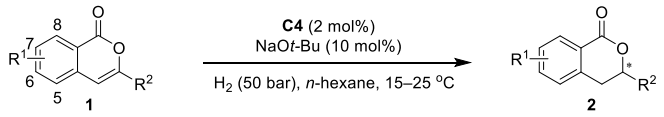

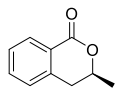

2a, 98.5:1.5 e.r.; 83% yield (98.5:1.5 e.r.; 82% yield)

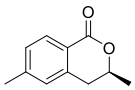

2b, 96:4 e.r.; 85% yield (96.5:3.5 e.r.; 86% yield)

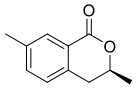

2c, 98:2 e.r.; 76% yield (98.5:1.5 e.r.; 80% yield)

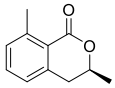

2d, 99:1 e.r.; 78% yield (99:1 e.r.; 80% yield)

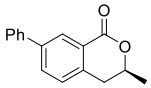

2e[b], 97.5:2.5 e.r.;72% yield (98.5:1.5 e.r.; 66% yield)

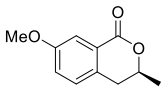

2f, 97:3 e.r.; 79% yield (98:2 e.r.; 78% yield)

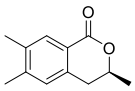

2g, 96:4 e.r.; 80% yield (97:3 e.r.; 88% yield)

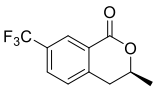

2h, 99.7:0.3 e.r.; 71% yield (99.5:0.5 e.r.; 71% yield)

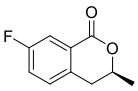

2i, 99:1 e.r.; 73% yield (99.5:0.5 e.r.; 78% yield)

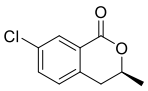

2j, 96:4 e.r.; 80% yield (98:2 e.r.; 81% yield)

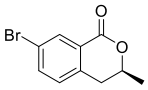

2k[b], 99:1 e.r.; 70% yield (99.5:0.5 e.r.; 68% yield)

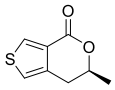

2l[b], 93:7 e.r.; 72% yield

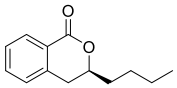

2m[c], 93.5:6.5 e.r.; 73% yield (97:3 e.r.; 62% yield)

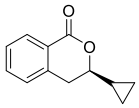

2n, 98:2 e.r.; 78% yield (99:1 e.r.; 75% yield)

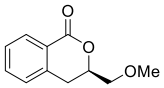

2o, 99:1 e.r.; 70% yield (95:5 e.r.; 73% yield)

[a]Unless otherwise noted, reactions were carried out with **1** (0.2 mmol), **C4** (0.004 mmol, 2 mol%), and NaO*t*-Bu (0.02 mmol, 10 mol%) under 50 bar H_2 in *n*-hexane (4.0 mL) at 15–25 °C for the indicated time. Isolated yields after column chromatography are reported. E.r. values were determined by HPLC analysis using a chiral stationary phase. Results in parentheses are our previously reported data (*J. Am. Chem. Soc.* **2017**, *139*, 2585) using in-situ prepared catalyst solution. [b]Using a solvent mixture of *n*-hexane : toluene (3 : 1). [c]Using 80 bar of H_2.

3-methylisochroman-1-one (2a)

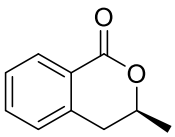

Colorless oil; H_2 (50 bar), 15 °C, 18 h, 83% yield, 98.5:1.5 e.r. $[\alpha]_D^{22}$ = +141.0 (c = 1.00 in $CHCl_3$). HPLC DAICEL CHIRALCEL AS-H, *n*-hexane/2-propanol = 80/20, flow rate = 1 mL/min, λ = 230 nm, retention time: 9.0 min (major), 10.9 min (minor). **^{1}H NMR** (500 MHz, $CDCl_3$) δ 8.15 – 8.02 (m, *J* = 7.8 Hz, 1H), 7.53 (td, *J* = 7.5, 1.3 Hz, 1H), 7.38 (t, *J* = 7.6 Hz, 1H), 7.23 (d, *J* = 7.6 Hz, 1H), 4.71 – 4.65 (m, 1H), 3.06 – 2.87 (m, 2H), 1.52 (d, *J* = 6.3 Hz, 3H).

Known compound, see: Li, W.; Wiesenfeldt. M. P.; Glorius, F. *J. Am. Chem. Soc.* **2017**, *139*, 2585.

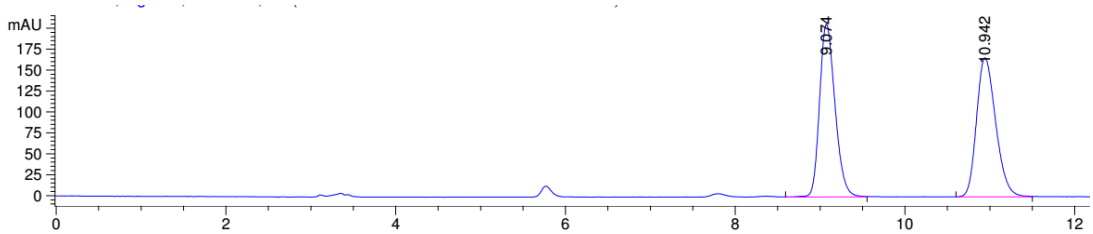

Peak #	RetTime [min]	Type	Width [min]	Area [mAU*s]	Height [mAU]	Area %
1	9.074	BB	0.1959	2614.89404	206.29051	50.1046
2	10.942	BB	0.2389	2603.97852	166.13945	49.8954

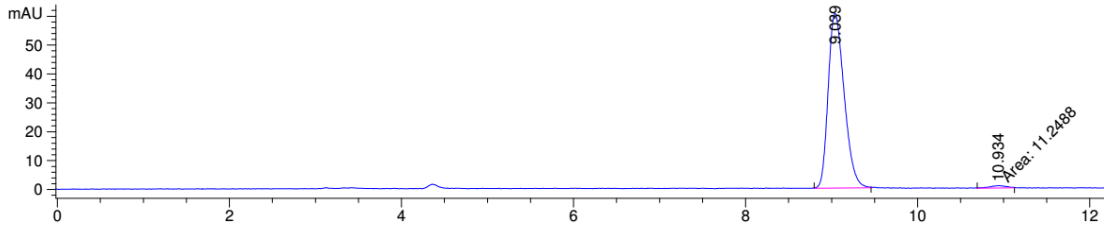

Peak #	RetTime [min]	Type	Width [min]	Area [mAU*s]	Height [mAU]	Area %
1	9.039	BB	0.1977	780.71332	60.43466	98.5796
2	10.934	MM	0.2323	11.24875	8.06984e-1	1.4204

3,6-dimethylisochroman-1-one (2b)

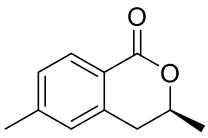

Colorless solid; H_2 (50 bar), 25 °C, 22 h, 85% yield, 96:4 e.r. $[\alpha]_D^{22}$ = +120.4 (c = 1.20 in $CHCl_3$). HPLC DAICEL CHIRALCEL AS-H, *n*-hexane/2-propanol = 80/20, flow rate = 1 mL/min, λ = 254 nm, retention time: 10.3 min (major), 12.8 min (minor). **^{1}H NMR** (400 MHz, $CDCl_3$) δ 7.96 (d, *J* = 7.9 Hz, 1H), 7.17 (d, *J* = 7.9 Hz, 1H), 7.02 (s, 1H), 4.64 (dqd, *J* = 10.1, 6.3, 3.8 Hz, 1H), 2.88 (qd, *J* = 16.2, 7.3 Hz, 2H), 2.39 (s, 3H), 1.50 (d, *J* = 6.3 Hz, 3H). Known compound see: Li, W.; Wiesenfeldt. M. P.; Glorius, F. *J. Am. Chem. Soc.* **2017**, *139*, 2585.

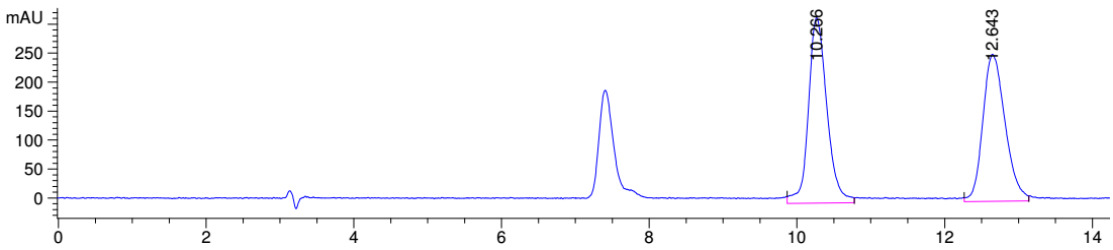

Peak #	RetTime [min]	Type	Width [min]	Area [mAU*s]	Height [mAU]	Area %
1	10.266	VV	0.2104	5584.63867	320.28476	51.1983
2	12.643	VV	0.2506	5323.21436	253.94463	48.8017

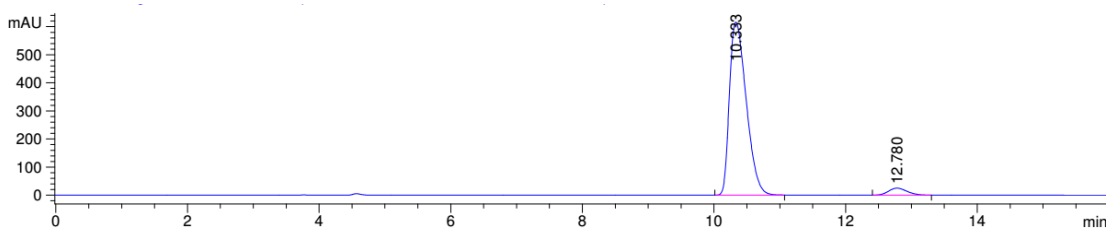

Peak #	RetTime [min]	Type	Width [min]	Area [mAU*s]	Height [mAU]	Area %
1	10.333	BB	0.2788	1.09250e4	616.23938	95.6688
2	12.780	BB	0.3079	494.61032	24.98822	4.3312

3,7-dimethylisochroman-1-one (2c)

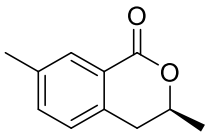

Colorless solid; H_2 (50 bar), 15 °C, 22 h, 76% yield, 98:2 e.r. $[\alpha]_D^{22}$ = +134.0 (c = 1.07 in $CHCl_3$). HPLC DAICEL CHIRALCEL AS-H, *n*-hexane/2-propanol = 80/20, flow rate = 1 mL/min, λ = 230 nm, retention time: 7.6 min (major), 11.3 min (minor). **^{1}H NMR** (500 MHz, $CDCl_3$) δ 7.89 (dd, *J* = 1.2, 0.5 Hz, 1H), 7.37 – 7.29 (m, 1H), 7.11 (d, *J* = 7.7 Hz, 1H), 4.64 (dqd, *J* = 10.0, 6.3, 4.7 Hz, 1H), 2.96 – 2.79 (m, 2H), 2.37 (s, 3H), 1.50 (d, *J* = 6.3 Hz, 3H). Known compound, see: Li, W.; Wiesenfeldt. M. P.; Glorius, F. *J. Am. Chem. Soc.* **2017**, *139*, 2585.

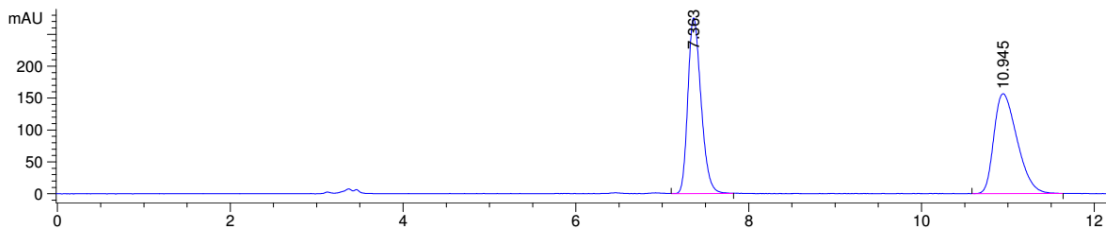

Peak #	RetTime [min]	Type	Width [min]	Area [mAU*s]	Height [mAU]	Area %
1	7.363	VV	0.1637	2919.13452	275.39487	49.9814
2	10.945	BB	0.2847	2921.30640	156.55716	50.0186

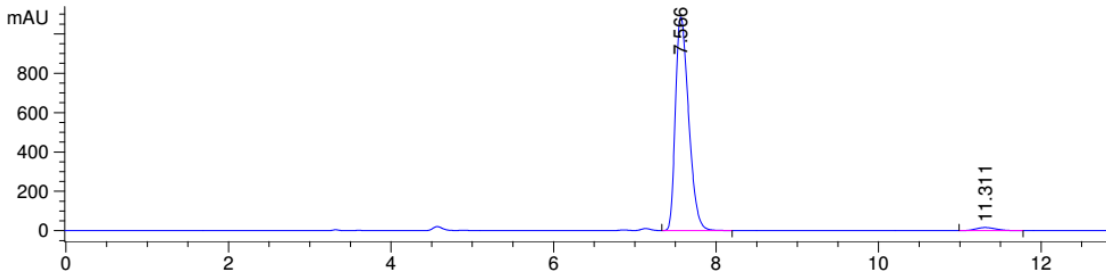

Peak #	RetTime [min]	Type	Width [min]	Area [mAU*s]	Height [mAU]	Area %
1	7.566	VB	0.1781	1.22850e4	1084.57336	97.7685
2	11.311	BB	0.2703	280.39001	16.00901	2.2315

3,8-dimethylisochroman-1-one (2d)

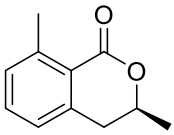

Colorless solid; H_2 (50 bar), 15 ºC, 16 h, 78% yield, 99:1 e.r. $[\alpha]_D^{22}$ = +160.7 (c = 0.37 in $CHCl_3$). HPLC DAICEL CHIRALCEL AS-H, *n*-hexane/2-propanol = 80/20, flow rate = 1 mL/min, λ = 254 nm, retention time: 5.9 min (major), 7.0 min (minor). **^{1}H NMR** (400 MHz, $CDCl_3$) δ 7.36 (t, *J* = 7.6 Hz, 1H), 7.19 (d, *J* = 7.7 Hz, 1H), 7.05 (d, *J* = 7.5 Hz, 1H), 4.62 – 4.51 (m, 1H), 2.99 – 2.83 (m, 2H), 2.67 (s, 3H), 1.49 (d, *J* = 6.3 Hz, 3H). Known compound see: Li, W.; Wiesenfeldt. M. P.; Glorius, F. *J. Am. Chem. Soc.* **2017**, *139*, 2585.

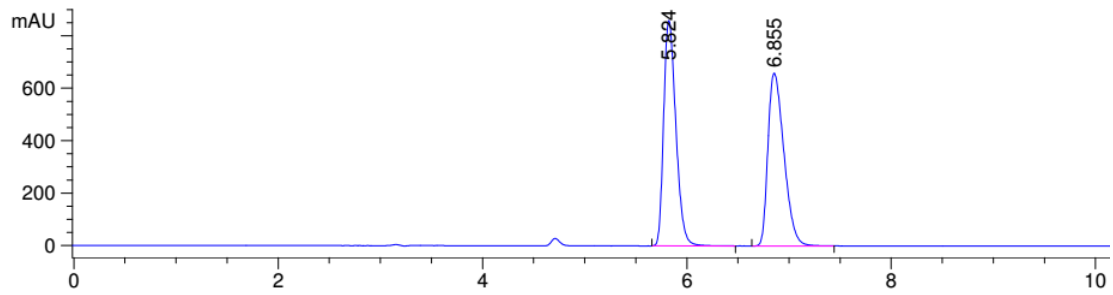

Peak #	RetTime [min]	Type	Width [min]	Area [mAU*s]	Height [mAU]	Area %
1	5.824	BB	0.1298	7133.03809	859.61871	49.9198
2	6.855	BV	0.1696	7155.96680	659.34052	50.0802

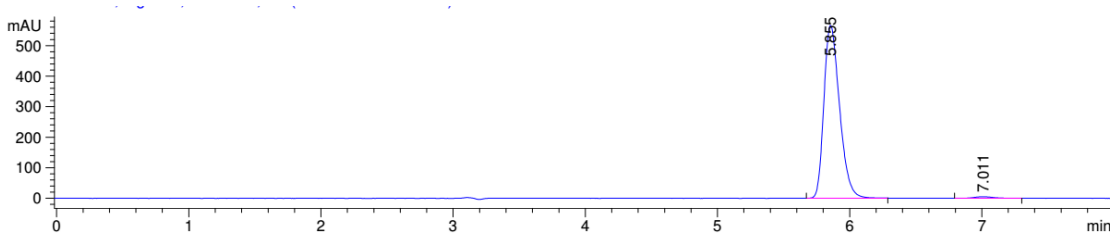

Peak #	RetTime [min]	Type	Width [min]	Area [mAU*s]	Height [mAU]	Area %
1	5.855	BB	0.1270	4658.04980	566.08173	98.9227
2	7.011	BB	0.1610	50.72565	5.01621	1.0773

3-methyl-7-phenylisochroman-1-one (2e)

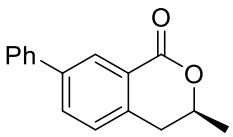

Colorless solid; H_2 (50 bar), 15 °C, 22 h, 72% yield, 97.5:2.5 e.r. $[\alpha]_D^{22}$ = +112.8 (c = 1.48 in $CHCl_3$). HPLC DAICEL CHIRALCEL AS-H, *n*-hexane/2-propanol = 80/20, flow rate = 1 mL/min, λ = 230 nm, retention time: 9.3 min (major), 15.9 min (minor). **^{1}H NMR** (500 MHz, $CDCl_3$) δ 8.34 (d, *J* = 1.8 Hz, 1H), 7.76 (dd, *J* = 7.9, 2.0 Hz, 1H), 7.62 (dd, *J* = 5.2, 3.3 Hz, 2H), 7.46 (dd, *J* = 10.4, 4.8 Hz, 2H), 7.38 (dd, *J* = 10.5, 4.3 Hz, 1H), 7.31 (d, *J* = 7.9 Hz, 1H), 4.76 – 4.62 (m, 1H), 3.04 – 2.89 (m, 2H), 1.55 (d, *J* = 6.3 Hz, 3H).

Known compound, see: Li, W.; Wiesenfeldt. M. P.; Glorius, F. *J. Am. Chem. Soc.* **2017**, *139*, 2585.

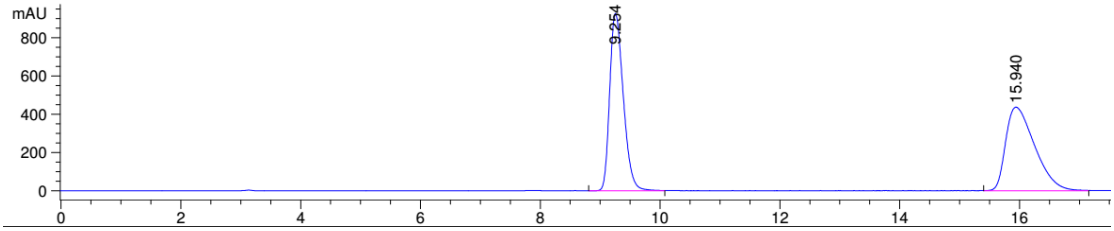

Peak #	RetTime [min]	Type	Width [min]	Area [mAU*s]	Height [mAU]	Area %
1	9.254	VV	0.2404	1.46653e4	927.78851	49.8481
2	15.940	VV	0.4034	1.47546e4	437.60928	50.1519

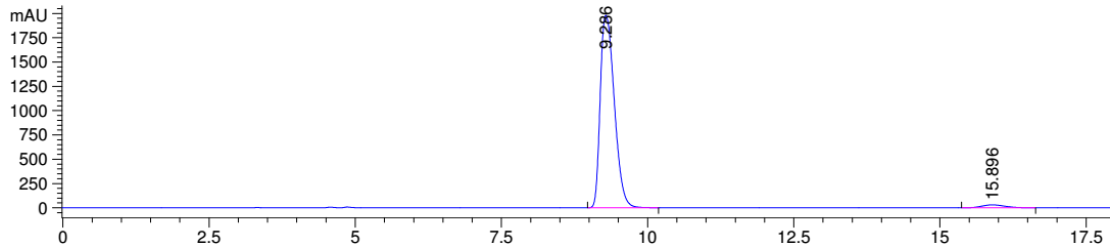

Peak #	RetTime [min]	Type	Width [min]	Area [mAU*s]	Height [mAU]	Area %
1	9.286	BB	0.2653	3.31687e4	1981.12402	97.4753
2	15.896	BB	0.4347	859.08551	30.67411	2.5247

7-methoxy-3-methylisochroman-1-one (2f)

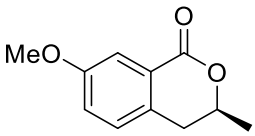

Colorless solid; H_2 (50 bar), 15 ºC, 22 h, 79% yield, 97:3 e.r. $[\alpha]_D^{22}$ = +130.0 (c = 1.35 in $CHCl_3$). HPLC DAICEL CHIRALCEL AS-H, *n*-hexane/2-propanol = 80/20, flow rate = 1 mL/min, λ = 230 nm, retention time: 8.4 min (major), 12.5 min (minor). **^{1}H NMR** (500 MHz, $CDCl_3$) δ 7.57 (d, *J* = 2.7 Hz, 1H), 7.13 (dd, *J* = 8.4, 0.4 Hz, 1H), 7.08 (dd, *J* = 8.4, 2.7 Hz, 1H), 4.65 (dqd, *J* = 9.8, 6.3, 5.0 Hz, 1H), 3.83 (s, 3H), 2.94 – 2.76 (m,

2H), 1.50 (d, J = 6.3 Hz, 3H). Known compound, see: Li, W.; Wiesenfeldt. M. P.; Glorius, F. *J. Am. Chem. Soc.* **2017**, *139*, 2585.

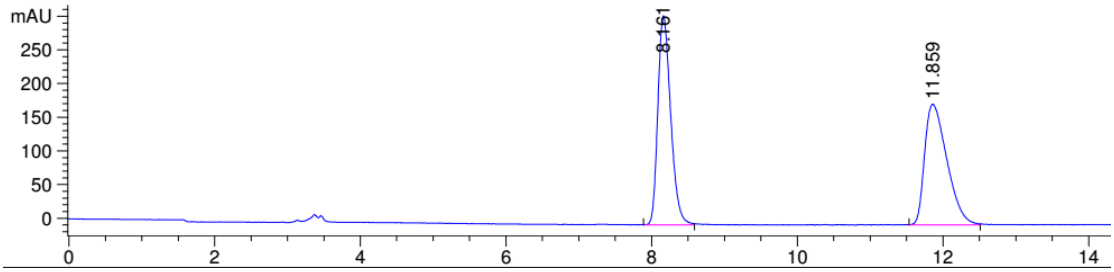

Peak #	RetTime [min]	Type	Width [min]	Area [mAU*s]	Height [mAU]	Area %
1	8.161	VV	0.1877	3796.99512	310.53513	49.8984
2	11.859	VV	0.3098	3812.45044	179.46191	50.1016

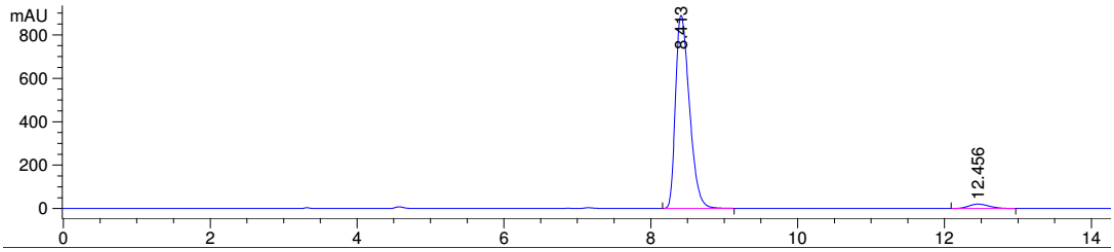

Peak #	RetTime [min]	Type	Width [min]	Area [mAU*s]	Height [mAU]	Area %
1	8.413	BB	0.2045	1.17069e4	889.80719	96.6830
2	12.456	BB	0.3037	401.64206	20.48893	3.3170

3,6,7-trimethylisochroman-1-one (2g)

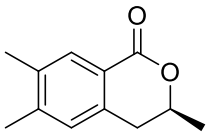

Colorless solid; H_2 (50 bar), 25 ºC, 21 h, 80% yield, 96:4 e.r. $[\alpha]_D^{22}$ = +119.9 (c = 1.25 in $CHCl_3$). HPLC DAICEL CHIRALCEL AS-H, *n*-hexane/2-propanol = 80/20, flow rate = 1 mL/min, λ = 254 nm, retention time: 7.9 min (major), 11.5 min (minor). **^{1}H NMR** (400 MHz, $CDCl_3$) δ 7.84 (s, 1H), 6.98 (s, 1H), 4.69 – 4.55 (m, 1H), 2.94 – 2.73 (m, 2H), 2.30 (s, 3H), 2.28 (s,

3H), 1.49 (d, J = 6.3 Hz, 3H). Known compound, see: Li, W.; Wiesenfeldt. M. P.; Glorius, F. *J. Am. Chem. Soc.* **2017**, *139*, 2585.

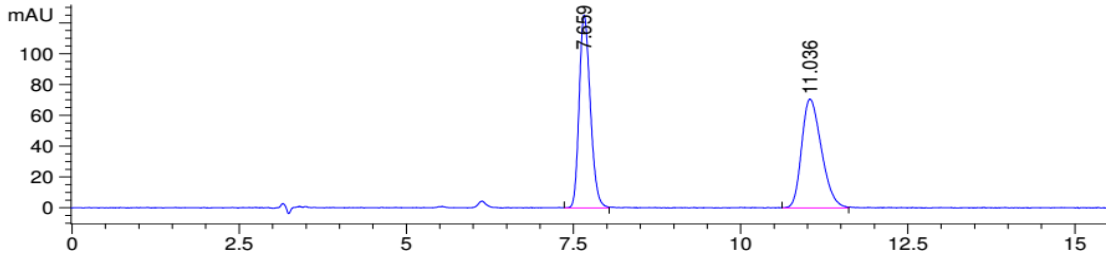

Peak #	RetTime [min]	Type	Width [min]	Area [mAU*s]	Height [mAU]	Area %
1	7.659	VV	0.1804	1454.23865	125.34120	49.9276
2	11.036	VV	0.2985	1458.45581	70.73730	50.0724

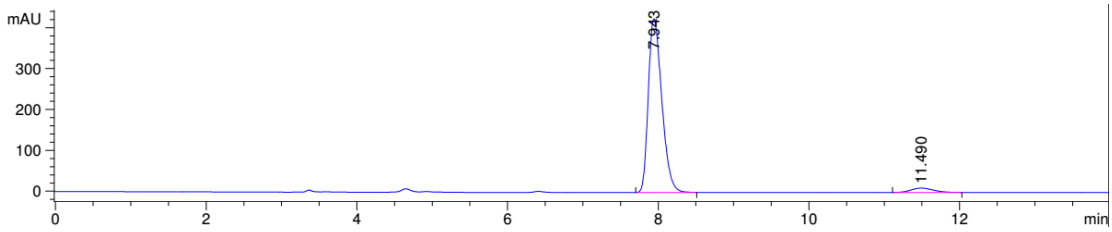

Peak #	RetTime [min]	Type	Width [min]	Area [mAU*s]	Height [mAU]	Area %
1	7.943	BB	0.1935	5301.68311	424.99863	96.0216
2	11.490	BB	0.3199	219.66232	10.59627	3.9784

3-methyl-7-(trifluoromethyl)isochroman-1-one (2h)

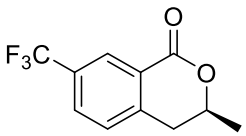

Colorless solid; H_2 (50 bar), 15 °C, 16 h, 70% yield, 99.7:0.3 e.r. $[\alpha]_D^{22}$ = +122.0 (c = 1.19 in $CHCl_3$). HPLC DAICEL CHIRALCEL AS-H, *n*-hexane/2-propanol = 80/20, flow rate = 1 mL/min, λ = 230 nm, retention time: 6.3 min (major), 9.4 min (minor). **^{1}H NMR** (400 MHz, $CDCl_3$) δ 8.37 (d, J = 0.7 Hz, 1H), 7.77 (dd, J = 8.0, 1.4 Hz, 1H), 7.39 (d, J = 8.0 Hz, 1H), 4.80 – 4.62 (m, 1H), 3.02 (d, J = 7.2 Hz, 2H), 1.54 (d, J = 6.3 Hz, 3H). Known

compound, see: Li, W.; Wiesenfeldt. M. P.; Glorius, F. *J. Am. Chem. Soc.* **2017**, *139*, 2585.

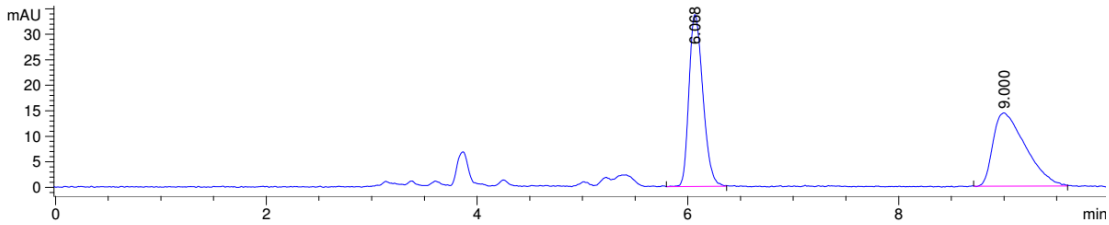

Peak #	RetTime [min]	Type	Width [min]	Area [mAU*s]	Height [mAU]	Area %
1	6.068	VB	0.1442	309.65964	33.69501	50.0850
2	9.000	BB	0.2920	308.60904	14.40240	49.9150

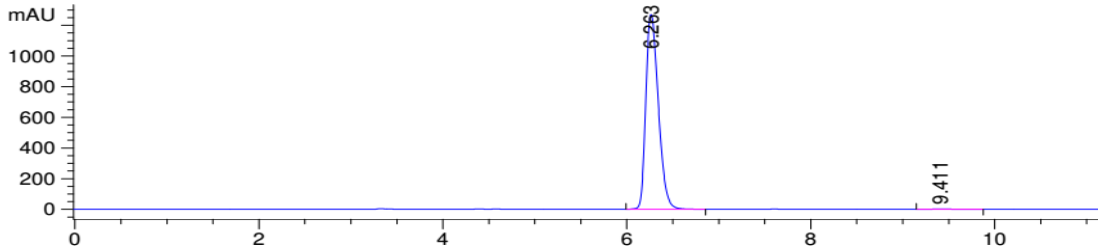

Peak #	RetTime [min]	Type	Width [min]	Area [mAU*s]	Height [mAU]	Area %
1	6.263	BB	0.1484	1.20311e4	1270.85559	99.6629
2	9.411	BB	0.2791	40.69621	1.85361	0.3371

7-fluoro-3-methylisochroman-1-one (2i)

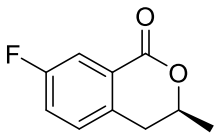

Colorless solid; H_2 (50 bar), 15 °C, 21 h, 73% yield, 99:1 e.r. $[\alpha]_D^{22}$ = +102.5 (c = 1.10 in $CHCl_3$). HPLC DAICEL CHIRALCEL AS-H, *n*-hexane/2-propanol = 80/20, flow rate = 1 mL/min, λ = 230 nm, retention time: 7.6 min (major), 9.8 min (minor). **^{1}H NMR** (400 MHz, $CDCl_3$) δ 7.80 – 7.69 (m, 1H), 7.25 – 7.19 (m, 2H), 4.76 – 4.51 (m, 1H), 2.91 (d, *J* = 6.5 Hz, 2H), 1.52 (d, *J* = 6.3 Hz, 3H). Known compound, see: Li, W.; Wiesenfeldt. M. P.; Glorius, F. *J. Am. Chem. Soc.* **2017**, *139*, 2585.

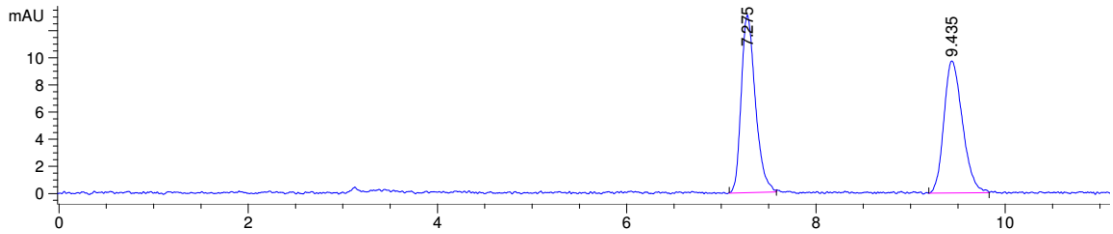

Peak #	RetTime [min]	Type	Width [min]	Area [mAU*s]	Height [mAU]	Area %
1	7.275	BB	0.1573	136.06046	13.08673	50.6472
2	9.435	BB	0.2060	132.58290	9.72609	49.3528

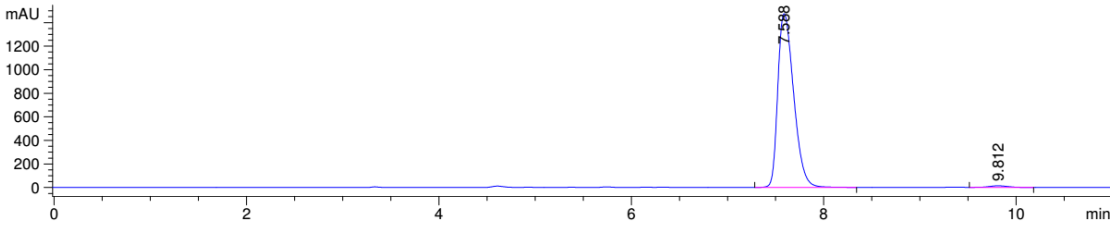

Peak #	RetTime [min]	Type	Width [min]	Area [mAU*s]	Height [mAU]	Area %
1	7.588	VB	0.1795	1.68801e4	1474.67920	98.8177
2	9.812	VB	0.2170	201.96916	14.11191	1.1823

7-chloro-3-methylisochroman-1-one (2j)

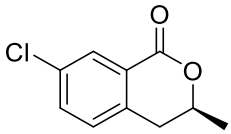

Colorless solid; H_2 (50 bar), 15 ºC, 16 h, 80% yield, 96:4 e.r. $[\alpha]_D^{22}$ = +119.0 (c = 0.95 in $CHCl_3$). HPLC DAICEL CHIRALCEL AS-H, *n*-hexane/2-propanol = 80/20, flow rate = 1 mL/min, λ = 254 nm, retention time: 10.9 min (major), 13.0 min (minor). **^{1}H NMR** (400 MHz, $CDCl_3$) δ 8.02 (d, *J* = 8.3 Hz, 1H), 7.40 – 7.32 (m, 1H), 7.27 – 7.18 (m, 1H), 4.67 (dqd, *J* = 10.5, 6.3, 4.2 Hz, 1H), 3.01 – 2.84 (m, 2H), 1.52 (d, *J* = 6.3 Hz, 3H). Known compound, see: Li, W.; Wiesenfeldt. M. P.; Glorius, F. *J. Am. Chem. Soc.* **2017**, *139*, 2585.

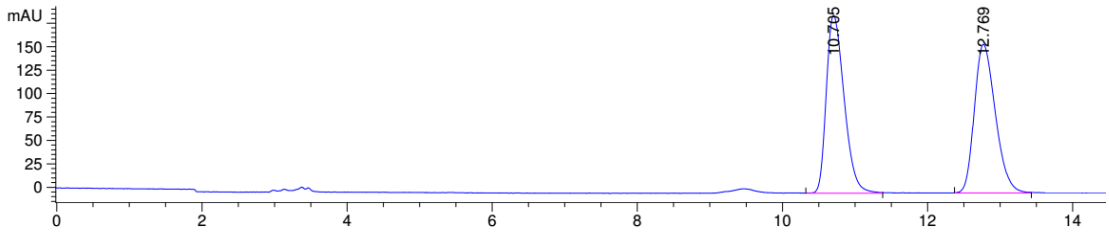

Peak #	RetTime [min]	Type	Width [min]	Area [mAU*s]	Height [mAU]	Area %
1	10.705	BB	0.2613	3225.45801	189.79683	50.1953
2	12.769	BB	0.3073	3200.35376	158.67160	49.8047

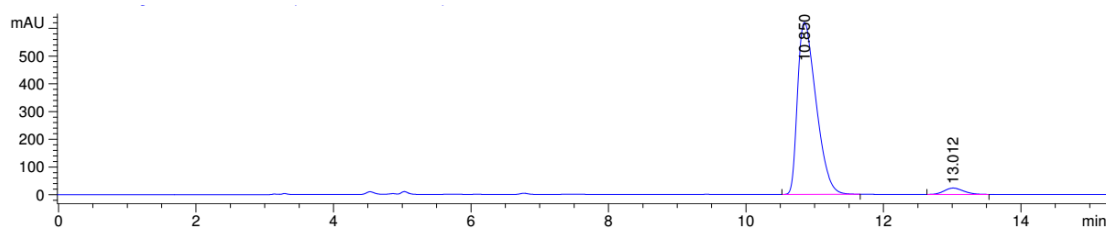

Peak #	RetTime [min]	Type	Width [min]	Area [mAU*s]	Height [mAU]	Area %
1	10.850	BB	0.2926	1.16185e4	620.04059	96.2747
2	13.012	BB	0.3067	449.57089	22.93270	3.7253

7-bromo-3-methylisochroman-1-one (2k)

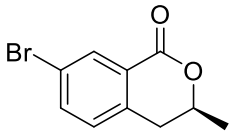

Colorless solid; H_2 (50 bar), 15 ºC, 22 h, 70% yield, 99:1 e.r. $[\alpha]_D^{22}$ = +111.4 (c = 1.45 in $CHCl_3$). HPLC DAICEL CHIRALCEL AS-H, *n*-hexane/2-propanol = 80/20, flow rate = 1 mL/min, λ = 230 nm, retention time: 8.8 min (major), 14.8 min (minor). **^{1}H NMR** (500 MHz, $CDCl_3$) δ 8.23 – 8.18 (m, 1H), 7.63 (dd, *J* = 8.1, 2.2 Hz, 1H), 7.17 – 7.10 (m, 1H), 4.76 – 4.52 (m, 1H), 2.95 – 2.85 (m, 2H), 1.51 (d, *J* = 6.3 Hz, 3H). Known compound, see: Li, W.; Wiesenfeldt. M. P.; Glorius, F. *J. Am. Chem. Soc.* **2017**, *139*, 2585.

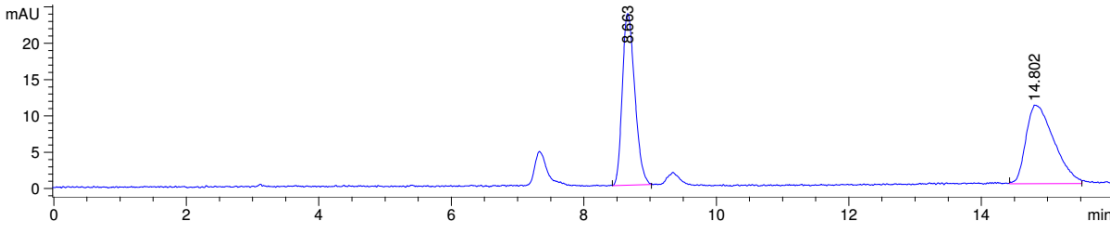

Peak #	RetTime [min]	Type	Width [min]	Area [mAU*s]	Height [mAU]	Area %
1	8.663	BB	0.1880	309.81393	23.61901	49.3941
2	14.802	BV	0.3483	317.41473	10.81930	50.6059

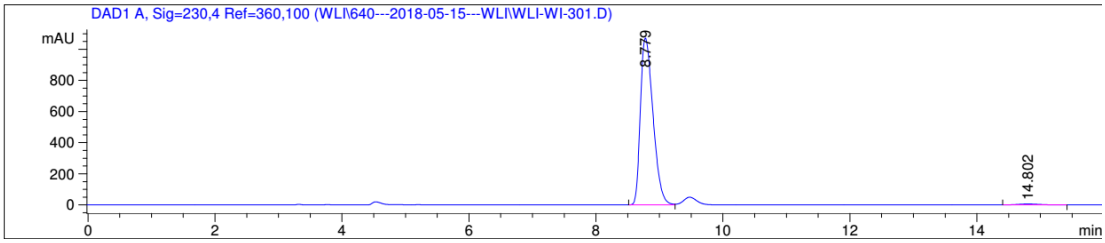

Peak #	RetTime [min]	Type	Width [min]	Area [mAU*s]	Height [mAU]	Area %
1	8.779	BV	0.2159	1.47936e4	1072.60889	99.0359
2	14.802	BB	0.3575	144.00781	6.01186	0.9641

6-methyl-6,7-dihydro-4H-thieno[3,4-c]pyran-4-one (2l)

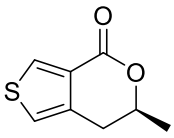

Colorless oil; H_2 (50 bar), 15 ºC, 45 h, 72% yield, 93:7 e.r. $[\alpha]_D^{22}$ = +33.2 (c = 0.35 in $CHCl_3$). HPLC DAICEL CHIRALCEL AD-H, *n*-hexane/2-propanol = 95/5, flow rate = 0.8 mL/min, λ = 230 nm, retention time: 19.9 min (minor), 21.0 min (major). **^{1}H NMR** (400 MHz, $CDCl_3$) δ 8.22 (d, *J* = 2.8 Hz, 1H), 7.05 (dd, *J* = 1.3, 0.8 Hz, 1H), 4.74 – 4.52 (m, 1H), 3.00 (dd, *J* = 16.0, 3.1 Hz, 1H), 2.89 – 2.65 (m, 1H), 1.50 (d, *J* = 6.3 Hz, 3H). **^{13}C NMR** (101 MHz, $CDCl_3$) δ 162.3, 137.3, 134.0, 128.2, 120.2, 76.4, 32.1, 20.8. ESI-MS: calculated $[C_8H_8O_2S + Na]^+$: 191.0137, found: 191.0141.

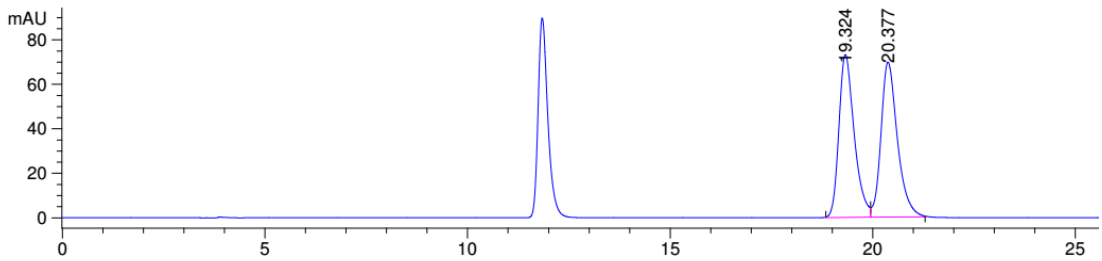

Peak #	RetTime [min]	Type	Width [min]	Area [mAU*s]	Height [mAU]	Area %
1	19.324	BV	0.3979	1920.60278	73.25793	49.5033
2	20.377	VB	0.4218	1959.14526	69.71868	50.4967

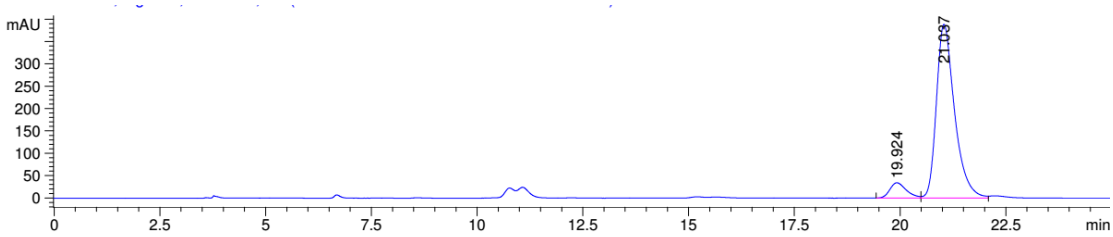

Peak #	RetTime [min]	Type	Width [min]	Area [mAU*s]	Height [mAU]	Area %
1	19.924	BV	0.4152	924.33405	34.21788	7.3912
2	21.037	VB	0.4498	1.15815e4	388.50464	92.6088

3-butylisochroman-1-one (2m)

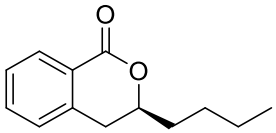

Colorless oil; H_2 (80 bar), 15 ºC, 40 h, 73% yield, 93.5:6.5 e.r.. $[\alpha]_D^{22}$ = +90.2 (c = 1.20 in $CHCl_3$). HPLC DAICEL CHIRALCEL AS-H, *n*-hexane/2-propanol = 90/10, flow rate = 1 mL/min, λ = 230 nm, retention time: 9.4 min (major), 10.7 min (minor). **^{1}H NMR** (300 MHz, $CDCl_3$) δ 8.08 (dd, *J* = 7.7, 0.9 Hz, 1H), 7.52 (td, *J* = 7.5, 1.4 Hz, 1H), 7.37 (t, *J* = 7.6 Hz, 1H), 7.23 (d, *J* = 7.6 Hz, 1H), 4.59 – 4.36 (m, 1H), 3.05 – 2.78 (m, 2H), 1.88 (dddd, *J* = 12.6, 10.0, 7.3, 5.2 Hz, 1H), 1.79 – 1.64 (m, 1H), 1.63 – 1.27 (m, 4H), 0.93 (t, *J* = 7.2 Hz, 3H). Known compound, see: Li, W.; Wiesenfeldt. M. P.; Glorius, F. *J. Am. Chem. Soc.* **2017**, *139*, 2585.

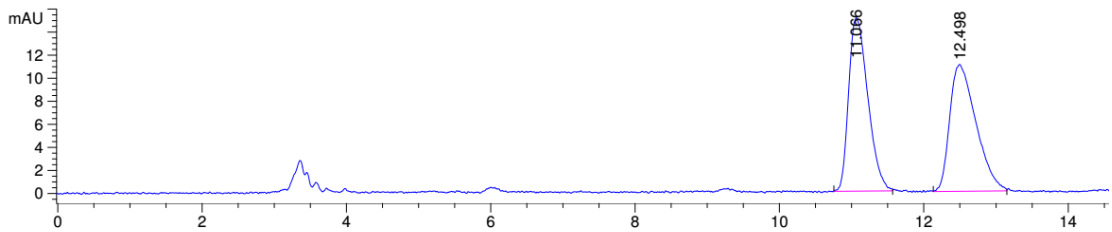

Peak #	RetTime [min]	Type	Width [min]	Area [mAU*s]	Height [mAU]	Area %
1	11.066	BB	0.2290	277.20535	15.04419	50.0040
2	12.498	BB	0.3038	277.16104	11.00654	49.9960

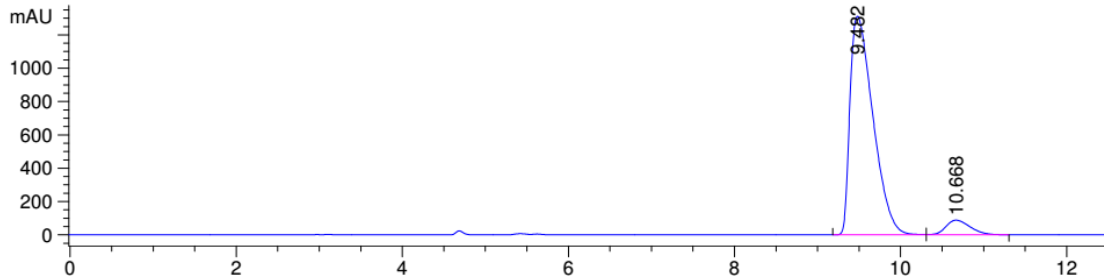

Peak #	RetTime [min]	Type	Width [min]	Area [mAU*s]	Height [mAU]	Area %
1	9.482	BV	0.2979	2.51688e4	1311.24036	93.4007
2	10.668	VB	0.3132	1778.31860	87.84839	6.5993

3-cyclopropylisochroman-1-one (2n)

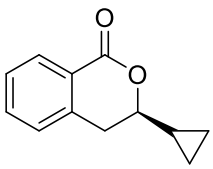

Colorless oil; H_2 (50 bar), 15 ºC, 40 h, 78% yield, 98:2 e.r. $[\alpha]_D^{22}$ = +92.8 (c = 1.06 in $CHCl_3$). HPLC DAICEL CHIRALCEL AS-H, *n*-hexane/2-propanol = 80/20, flow rate = 1 mL/min, λ = 230 nm, retention time: 9.4 min (major), 13.2 min (minor). **^{1}H NMR** (300 MHz, $CDCl_3$) δ 8.01 (dd, *J* = 7.7, 0.9 Hz, 1H), 7.46 (td, *J* = 7.5, 1.4 Hz, 1H), 7.31 (t, *J* = 7.6 Hz, 1H), 7.18 (d, *J* = 8.4 Hz, 1H), 3.74 (ddd, *J* = 10.4, 8.7, 3.9 Hz, 1H), 3.02 (qd, *J* = 16.3, 7.2 Hz, 2H), 1.27 – 1.03 (m, 1H), 0.71 – 0.43 (m, 3H), 0.35 – 0.16 (m, 1H). Known compound, see: Li, W.; Wiesenfeldt. M. P.; Glorius, F. *J. Am. Chem. Soc.* **2017**, *139*, 2585.

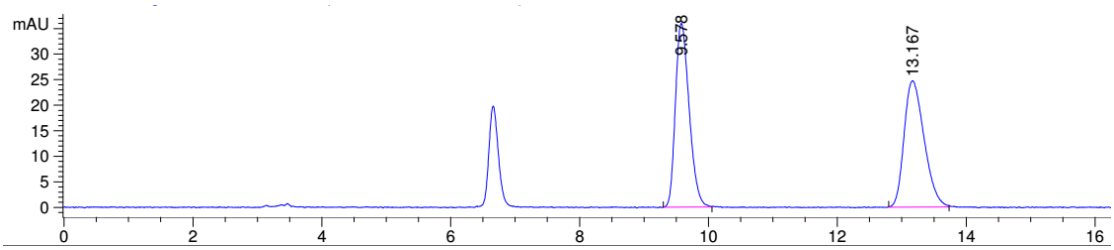

Peak #	RetTime [min]	Type	Width [min]	Area [mAU*s]	Height [mAU]	Area %
1	9.578	BB	0.2282	533.67529	35.95331	50.0017
2	13.167	BB	0.3191	533.63989	24.69434	49.9983

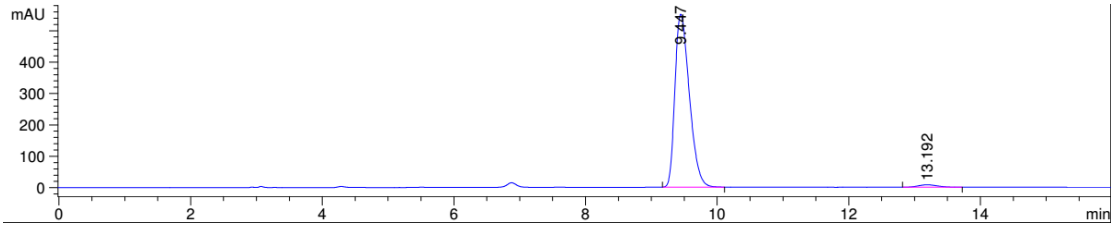

Peak #	RetTime [min]	Type	Width [min]	Area [mAU*s]	Height [mAU]	Area %
1	9.447	BB	0.2366	8392.84863	551.22333	98.0955
2	13.192	BB	0.3062	162.94420	7.87996	1.9045

3-(methoxymethyl)isochroman-1-one (2o)

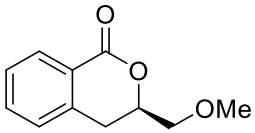

Colorless oil; H_2 (50 bar), 15 ºC, 22 h, 70% yield, 99:1 e.r. $[\alpha]_D^{22}$ = +123.4 (c = 1.07 in $CHCl_3$). HPLC DAICEL CHIRALCEL AS-H, *n*-hexane/2-propanol = 70/30, flow rate = 1 mL/min, λ = 230 nm, retention time: 8.5 min (major), 11.0 min (minor). **^{1}H NMR** (300 MHz, $CDCl_3$) δ 8.08 (dd, *J* = 7.7, 1.0 Hz, 1H), 7.53 (td, *J* = 7.5, 1.4 Hz, 1H), 7.38 (t, *J* = 7.6 Hz, 1H), 7.26 (d, *J* = 7.6 Hz, 1H), 4.67 (dtd, *J* = 11.6, 4.9, 3.4 Hz, 1H), 3.68 (qd, *J* = 10.4, 4.9 Hz, 2H), 3.44 (s, 3H), 3.15 (dd, *J* = 16.4, 11.6 Hz, 1H), 2.95 (dd, *J* = 16.4, 3.4 Hz, 1H). Known compound, see: Li, W.; Wiesenfeldt. M. P.; Glorius, F. *J. Am. Chem. Soc.* **2017**, *139*, 2585.

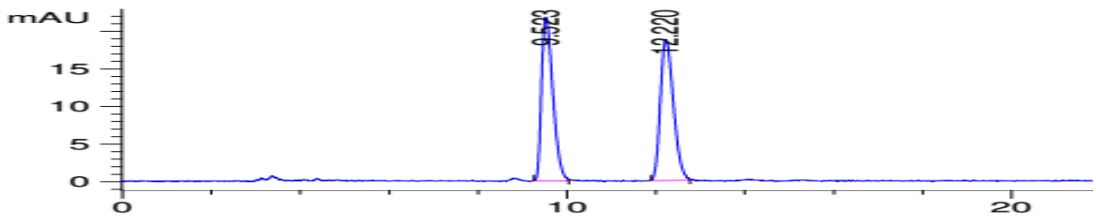

Peak #	RetTime [min]	Type	Width [min]	Area [mAU*s]	Height [mAU]	Area %
1	9.523	BB	0.2554	384.59167	21.73944	50.1569
2	12.220	BB	0.2909	382.18521	18.73958	49.8431

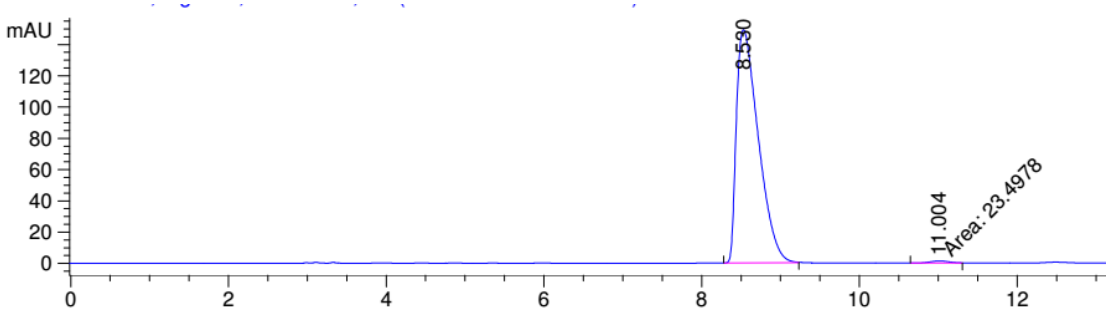

Peak #	RetTime [min]	Type	Width [min]	Area [mAU*s]	Height [mAU]	Area %
1	8.530	BB	0.2990	2875.91528	149.14720	99.1896
2	11.004	MM	0.2907	23.49785	1.34735	0.8104

b. Ruthenium-catalyzed asymmetric hydrogenation of benzothiophene 1,1-dioxides:

To a glass vial, complex **C3** (0.0015 mmol, 0.5 mol%), NaO*t*-Bu (0.02 mmol, 6.7 mol%), benzothiophene 1,1-dioxide **3** (0.3 mmol), and toluene (2.0 mL) were added under an argon atmosphere. The glass vial was placed in a 150 mL stainless steel autoclave under an argon atmosphere. The autoclave was pressurized and depressurized with hydrogen gas five times before the indicated pressure (5 bar or 30 bar) was set. The reaction mixture was stirred at 25 or 0 ºC for 24 h. After the autoclave was carefully depressurized, the mixture was directly purified by flash column chromatography on silica gel (pentane/ethylacetate = 20:1 to 4:1) to afford the desired product **4**.

2-methyl-2,3-dihydrobenzo[*b*]thiophene 1,1-dioxide (4a)

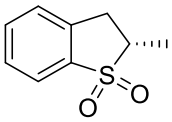

Colorless solid; H_2 (5 bar), 25 °C, 24 h, 99% yield, 97:3 e.r. $[\alpha]_D^{22}$ = +18.5 (c = 1.00 in $CHCl_3$). HPLC DAICEL CHIRALCEL AS-H, *n*-hexane/2-propanol = 70/30, flow rate = 1 mL/min, λ = 230 nm, retention time: 14.4 min (major), 21.6 min (minor). **^{1}H NMR** (300 MHz, $CDCl_3$) δ 7.74 (d, *J* = 7.7 Hz, 1H), 7.56 (dd, *J* = 10.7, 4.2 Hz, 1H), 7.45 (t, *J* = 7.4 Hz, 1H), 7.34 (d, *J* = 7.6 Hz, 1H), 3.61 – 3.37 (m, 2H), 2.95 (dd, *J* = 15.5, 7.1 Hz, 1H), 1.52 (d, *J* = 6.7 Hz, 3H). Known compound, see: Tosatti, P.; Pfaltz, A. *Angew. Chem., Int. Ed.* **2017**, *56*, 4579.

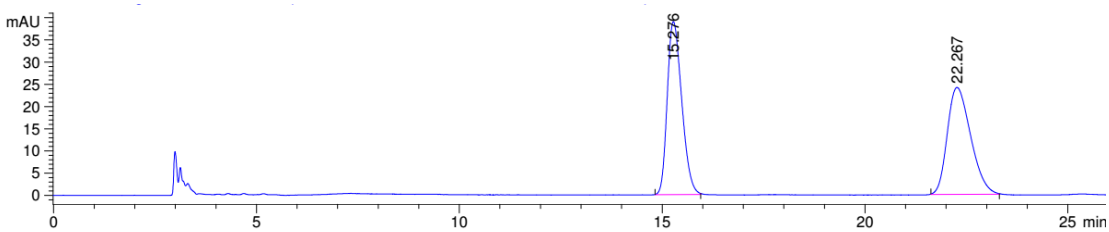

Peak #	RetTime [min]	Type	Width [min]	Area [mAU*s]	Height [mAU]	Area %
1	15.276	BB	0.3790	964.36456	38.93037	50.0064
2	22.267	BB	0.5302	964.11829	24.07430	49.9936

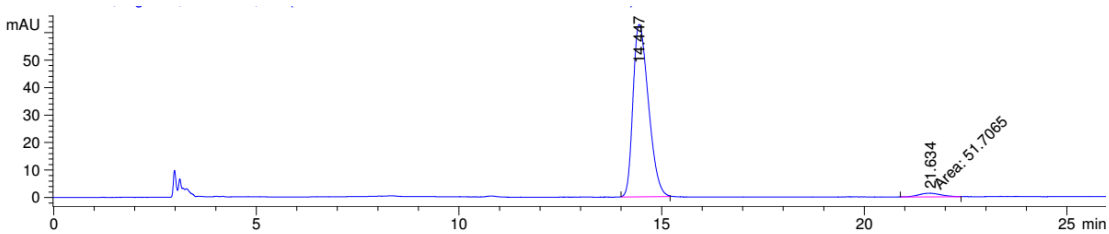

Peak #	RetTime [min]	Type	Width [min]	Area [mAU*s]	Height [mAU]	Area %
1	14.447	BB	0.4086	1658.98535	62.71007	96.9774
2	21.634	MM	0.6417	51.70653	1.34300	3.0226

2,5-dimethyl-2,3-dihydrobenzo[*b*]thiophene 1,1-dioxide (4b)

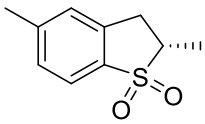

Colorless oil; H_2 (5 bar), 25 °C, 24 h, 94% yield, 93:7 e.r. $[\alpha]_D^{22}$ = +13.1 (c = 0.90 in $CHCl_3$). HPLC DAICEL CHIRALCEL AS-H, *n*-

hexane/2-propanol = 70/30, flow rate = 0.8 mL/min, λ = 230 nm, retention time: 25.7 min (major), 45.74 min (minor). **^{1}H NMR** (400 MHz, $CDCl_3$) δ 7.63 (d, *J* = 7.9 Hz, 1H), 7.26 (d, *J* = 7.9 Hz, 1H), 7.15 (s, 1H), 3.53 (dt, *J* = 13.6, 6.8 Hz, 1H), 3.42 (dd, *J* = 16.0, 7.5 Hz, 1H), 2.91 (dd, *J* = 15.9, 7.4 Hz, 1H), 2.43 (s, 3H), 1.52 (dd, *J* = 6.8, 0.9 Hz, 3H). **^{13}C NMR** (101 MHz, $CDCl_3$) δ 144.3, 136.9, 135.9, 129.7, 127.6, 121.8, 56.9, 33.9, 21.8, 12.5. **ESI-MS**: calculated $[C_{10}H_{12}O_2S + Na]^+$: 219.0450, found: 219.0456.

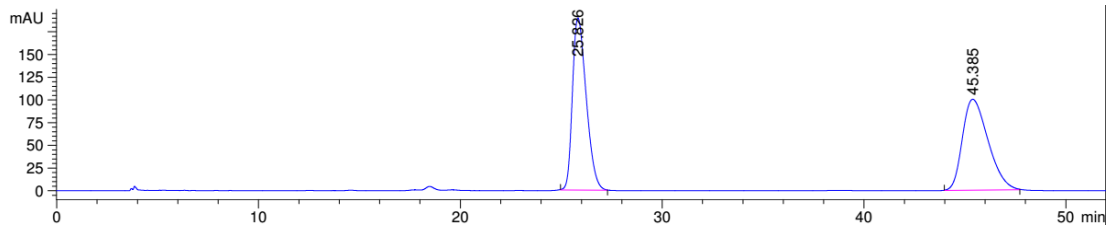

Peak #	RetTime [min]	Type	Width [min]	Area [mAU*s]	Height [mAU]	Area %
1	25.826	BB	0.7330	8986.42773	189.57390	50.4247
2	45.385	BB	1.2580	8835.05078	100.07108	49.5753

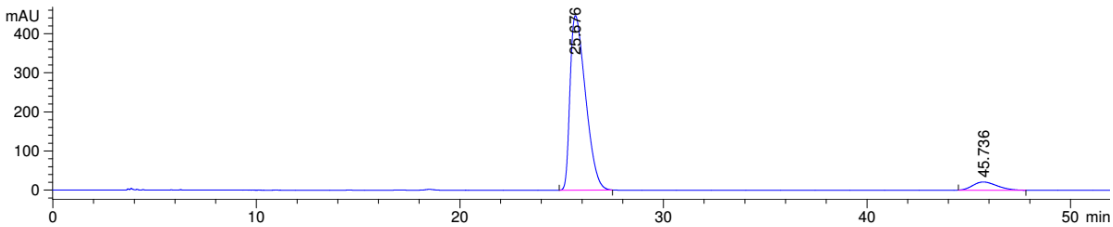

Peak #	RetTime [min]	Type	Width [min]	Area [mAU*s]	Height [mAU]	Area %
1	25.676	BB	0.8195	2.35684e4	446.00381	93.1016
2	45.736	BB	0.9722	1746.30798	21.13016	6.8984

5-methoxy-2-methyl-2,3-dihydrobenzo[*b*]thiophene 1,1-dioxide (4c)

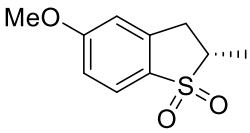

Colorless solid; H_2 (5 bar), 25 °C, 24 h, 92% yield, 95:5 e.r. $[\alpha]_D^{22}$ = +12.9 (c = 0.65 in $CHCl_3$). HPLC DAICEL CHIRALCEL AS-H, *n*-hexane/2-propanol = 70/30, flow rate = 1.0 mL/min, λ = 230

nm, retention time: 42.1 min (major), 68.1 min (minor). **^{1}H NMR** (300 MHz, $CDCl_3$) δ 7.65 (d, *J* = 8.6 Hz, 1H), 6.95 (dd, *J* = 8.6, 2.3 Hz, 1H), 6.82 – 6.71 (m, 1H), 3.85 (s, 3H), 3.53 (dt, *J* = 14.2, 7.1 Hz, 1H), 3.40 (dd, *J* = 16.0, 7.6 Hz, 1H), 2.90 (dd, *J* = 16.0, 7.5 Hz, 1H), 1.50 (d, *J* = 6.8 Hz, 3H). **^{13}C NMR** (75 MHz, $CDCl_3$) δ 163.7, 139.1, 130.6, 123.5, 115.4, 111.2, 56.9, 55.8, 34.0, 12.5. **ESI-MS**: calculated $[C_{10}H_{12}O_3S + Na]^+$: 235.0399, found: 235.0395.

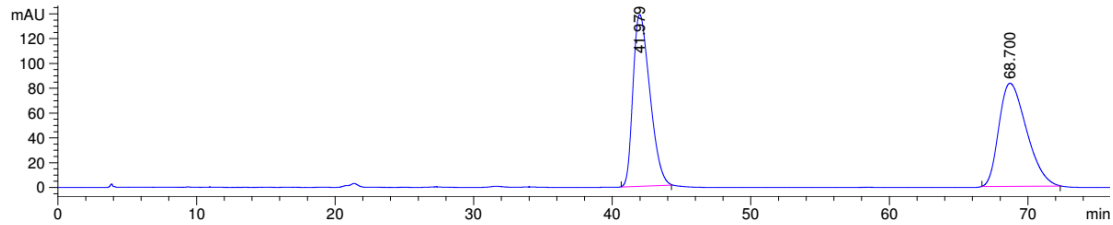

Peak #	RetTime [min]	Type	Width [min]	Area [mAU*s]	Height [mAU]	Area %
1	41.979	BB	1.1223	1.17282e4	138.59518	50.3843
2	68.700	BB	1.6253	1.15492e4	83.21100	49.6157

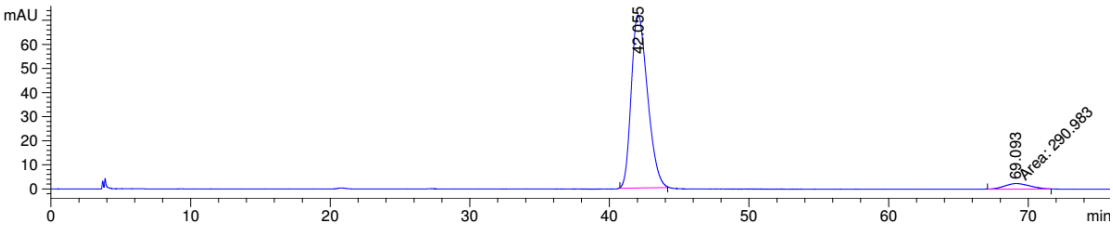

Peak #	RetTime [min]	Type	Width [min]	Area [mAU*s]	Height [mAU]	Area %
1	42.055	BB	1.1605	5801.98779	71.89574	95.2243
2	69.093	MM	2.1001	290.98282	2.30926	4.7757

2-methyl-5-(trifluoromethyl)-2,3-dihydrobenzo[*b*]thiophene 1,1-dioxide (4d)

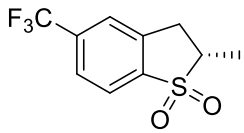

Colorless oil; H_2 (5 bar), 25 °C, 24 h, 86% yield, 99:1 e.r. $[\alpha]_D^{22}$ = +13.4 (c = 0.75 in $CHCl_3$). HPLC DAICEL CHIRALCEL AS-H, *n*-hexane/2-propanol = 70/30, flow rate = 0.8 mL/min, λ = 230

nm, retention time: 12.9 min (major), 19.2 min (minor). **^{1}H NMR** (400 MHz, $CDCl_3$) δ 7.88 (d, *J* = 8.0 Hz, 1H), 7.73 (d, *J* = 8.1 Hz, 1H), 7.63 (s, 1H), 3.69 – 3.40 (m, 2H), 3.02 (dd, *J* = 15.9, 7.2 Hz, 1H), 1.55 (dd, *J* = 6.7, 0.9 Hz, 3H). **^{13}C NMR** (101 MHz, $CDCl_3$) δ 142.1, 137.6, 135.4 (q, *J* = 32.8 Hz), 126.2 (q, *J* = 3.6 Hz), 124.6 (dd, *J* = 7.7, 3.9 Hz), 123.0, 121.9, 57.0, 34.0, 12.4. **^{19}F NMR** (282 MHz, $CDCl_3$) δ –62.94. **ESI-MS**: calculated $[C_{10}H_9F_3O_2S + Na]^+$: 273.0168, found: 273.0165.

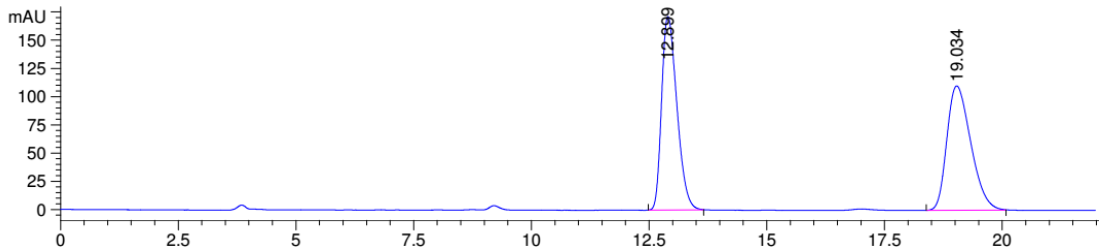

Peak #	RetTime [min]	Type	Width [min]	Area [mAU*s]	Height [mAU]	Area %
1	12.899	BB	0.3518	3865.50781	171.59088	49.8313
2	19.034	BB	0.5391	3891.67334	110.17706	50.1687

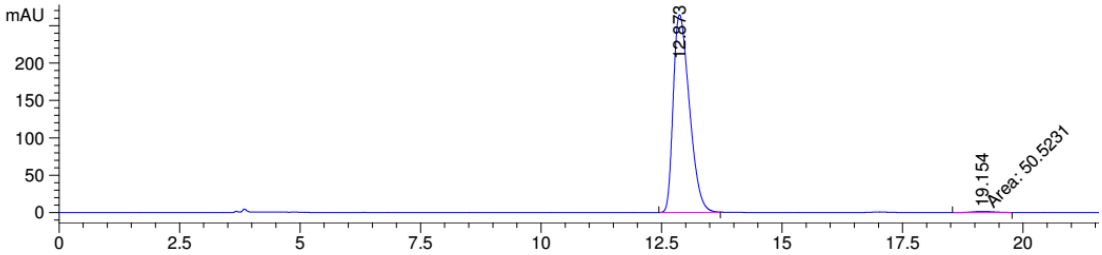

Peak #	RetTime [min]	Type	Width [min]	Area [mAU*s]	Height [mAU]	Area %
1	12.873	BB	0.3656	6152.85449	264.32779	99.1856
2	19.154	MM	0.5445	50.52309	1.54648	0.8144

5-fluoro-2-methyl-2,3-dihydrobenzo[*b*]thiophene 1,1-dioxide (4e)

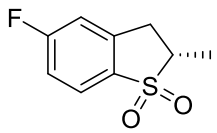

Colorless oil; H_2 (5 bar), 25 °C, 24 h, 88% yield, 97.5:2.5 e.r. $[\alpha]_D^{22}$ = +18.0 (c = 1.0 in $CHCl_3$). HPLC DAICEL CHIRALCEL AS-H, *n*-hexane/2-propanol = 70/30, flow rate = 0.8 mL/min, λ = 230 nm,

retention time: 21.5 min (major), 33.6 min (minor). **^{1}H NMR** (400 MHz, $CDCl_3$) δ 7.74 (dd, *J* = 8.5, 5.0 Hz, 1H), 7.15 (td, *J* = 8.5, 2.1 Hz, 1H), 7.03 (dd, *J* = 8.3, 0.9 Hz, 1H), 3.65 – 3.51 (m, 1H), 3.44 (dd, *J* = 16.2, 7.6 Hz, 1H), 2.94 (dd, *J* = 16.3, 7.6 Hz, 1H), 1.52 (d, *J* = 6.9 Hz, 3H). **^{13}C NMR** (101 MHz, $CDCl_3$) δ 165.7 (d, *J* = 254.7 Hz), 139.9 (d, *J* = 9.6 Hz), 134.7 (d, *J* = 2.8 Hz), 124.5 (d, *J* = 10.0 Hz), 116.8 (d, *J* = 23.8 Hz), 114.2 (d, *J* = 23.1 Hz), 57.1, 33.9 (d, *J* = 1.7 Hz, 14H), 12.5. **^{19}F NMR** (282 MHz, $CDCl_3$) δ -104.45. **ESI-MS**: calculated $[C_9H_9FO_2S + Na]^+$: 223.0199, found: 223.0208.

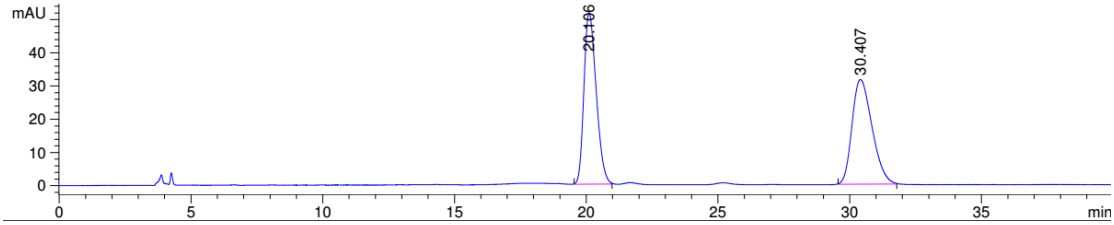

Peak #	RetTime [min]	Type	Width [min]	Area [mAU*s]	Height [mAU]	Area %
1	20.106	BB	0.4827	1660.84741	51.57866	50.0351
2	30.407	BB	0.6367	1658.51978	31.47949	49.9649

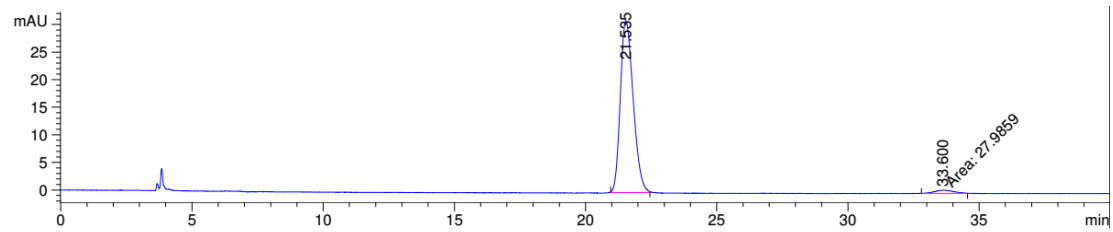

Peak #	RetTime [min]	Type	Width [min]	Area [mAU*s]	Height [mAU]	Area %
1	21.535	BB	0.5344	1059.18347	31.17280	97.4258
2	33.600	MM	0.8257	27.98594	5.64924e-1	2.5742

5-chloro-2-methyl-2,3-dihydrobenzo[*b*]thiophene 1,1-dioxide (4f)

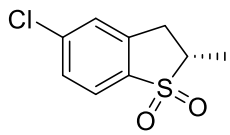

Colorless solid; H_2 (5 bar), 25 °C, 24 h, 92% yield, 98:2 e.r. $[\alpha]_D^{22}$ = +13.0 (c = 1.0 in $CHCl_3$). HPLC DAICEL CHIRALCEL AS-H, *n*-hexane/2-propanol = 70/30, flow rate = 0.8 mL/min, λ = 230 nm, retention time: 21.6 min (major), 35.1 min (minor). **^{1}H NMR** (400 MHz, $CDCl_3$) δ 7.67

(d, J = 8.2 Hz, 1H), 7.42 (d, J = 8.2 Hz, 1H), 7.34 (s, 1H), 3.68 – 3.50 (m, 1H), 3.43 (dd, J = 16.2, 7.5 Hz, 1H), 2.93 (dd, J = 16.2, 7.6 Hz, 1H), 1.51 (dd, J = 6.8, 0.8 Hz, 3H). **^{13}C NMR** (101 MHz, $CDCl_3$) δ 139.7, 138.6, 137.2, 129.4, 127.4, 123.4, 56.9, 33.7, 12.4. **ESI-MS**: calculated $[C_9H_9ClO_2S + Na]^+$: 238.9904, found: 238.9913.

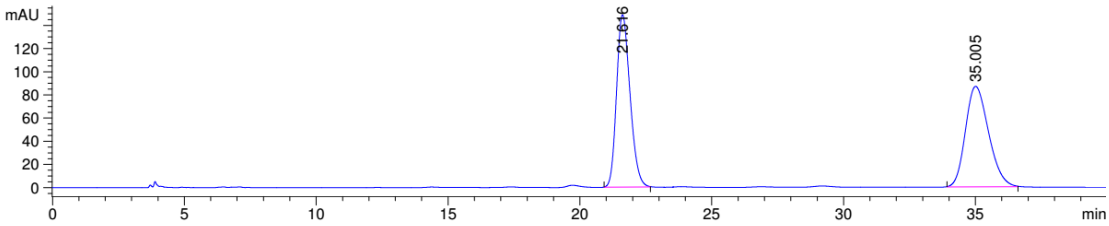

Peak #	RetTime [min]	Type	Width [min]	Area [mAU*s]	Height [mAU]	Area %
1	21.616	BB	0.5470	5282.60010	148.85904	50.0017
2	35.005	BB	0.8637	5282.23828	86.71546	49.9983

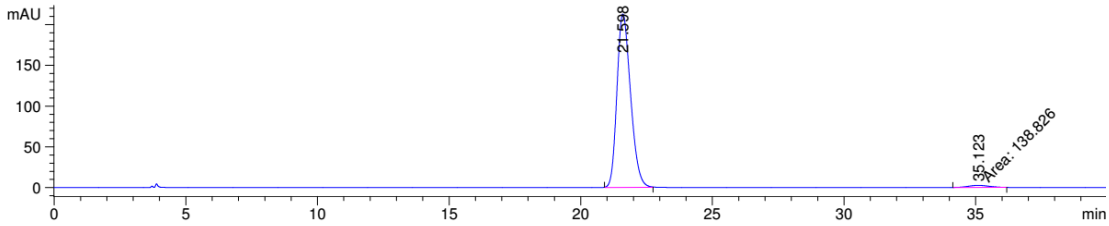

Peak #	RetTime [min]	Type	Width [min]	Area [mAU*s]	Height [mAU]	Area %
1	21.598	BB	0.5567	7634.73535	212.73131	98.2141
2	35.123	MM	0.9302	138.82573	2.48732	1.7859

5-bromo-2-methyl-2,3-dihydrobenzo[*b*]thiophene 1,1-dioxide (4g)

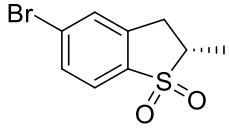

Colorless solid; H_2 (5 bar), 25 °C, 24 h, 93% yield, 98.5:1.5 e.r. $[\alpha]_D^{22}$ = +9.3 (c = 1.0 in $CHCl_3$). HPLC DAICEL CHIRALCEL AS-H, *n*-hexane/2-propanol = 70/30, flow rate = 0.8 mL/min, λ = 230 nm, retention time: 23.3 min (major), 37.7 min (minor). **^{1}H NMR** (400 MHz,

$CDCl_3$) δ 7.67 – 7.56 (m, 2H), 7.51 (s, 1H), 3.62 – 3.50 (m, 1H), 3.43 (dd, J = 16.1, 7.5 Hz, 1H), 2.93 (dd, J = 16.1, 7.5 Hz, 1H), 1.51 (dd, J = 6.8, 1.0 Hz, 3H). **^{13}C NMR** (101 MHz, $CDCl_3$) δ 138.6, 137.6, 132.2, 130.3, 128.0, 123.4, 56.8, 33.6, 12.3. **ESI-MS**: calculated $[C_9H_9BrO_2S + Na]^+$: 282.9399, 284.9385, found: 282.9404, 284.9385.

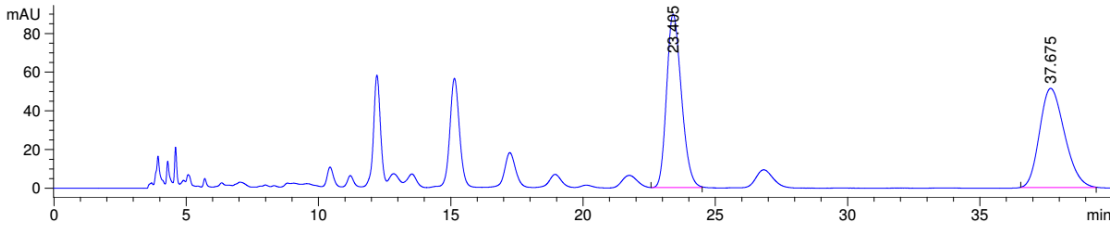

Peak #	RetTime [min]	Type	Width [min]	Area [mAU*s]	Height [mAU]	Area %
1	23.405	VB	0.6047	3496.27319	89.69832	50.8816
2	37.675	BB	0.9369	3375.12280	51.34334	49.1184

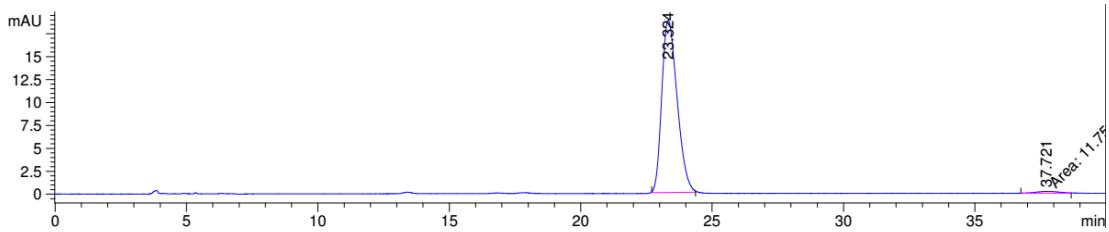

Peak #	RetTime [min]	Type	Width [min]	Area [mAU*s]	Height [mAU]	Area %
1	23.324	BB	0.5800	760.99164	18.77039	98.4789
2	37.721	MM	0.9771	11.75435	2.00492e-1	1.5211

2-propyl-2,3-dihydrobenzo[*b*]thiophene 1,1-dioxide (4h)

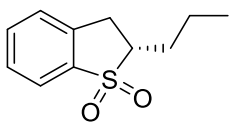

Colorless solid; H_2 (30 bar), 0 °C, 24 h, 96% yield, 94:6 e.r. $[\alpha]_D^{22}$ = +17.7 (c = 1.0 in $CHCl_3$). HPLC DAICEL CHIRALCEL AS-H, *n*-hexane/2-propanol = 70/30, flow rate = 1.0 mL/min, λ = 230 nm, retention time: 12.9 min (major), 20.8 min (minor). **^{1}H NMR** (400 MHz, $CDCl_3$) δ 7.73 (d, J = 7.7 Hz, 1H), 7.54 (td, J = 7.5, 1.1 Hz, 1H), 7.44 (t, J = 7.5 Hz, 1H), 7.33 (d, J =

7.7 Hz, 1H), 3.43 (tt, J = 21.1, 7.6 Hz, 2H), 3.05 – 2.84 (m, 1H), 2.20 – 1.99 (m, 1H), 1.82 – 1.48 (m, 3H), 1.02 (t, J = 7.2 Hz, 3H). **^{13}C NMR** (101 MHz, $CDCl_3$) δ 139.2, 136.5, 133.3, 128.7, 127.0, 121.8, 61.3, 32.5, 29.6, 20.3, 13.9. **ESI-MS**: calculated $[C_{11}H_{14}O_2S + Na]^+$: 233.0607, found: 233.0611.

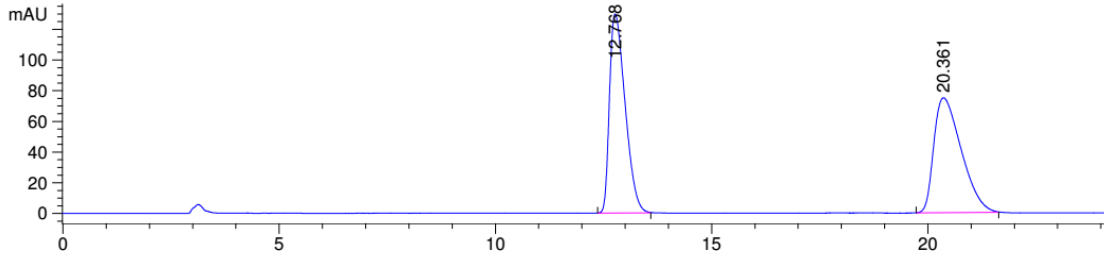

Peak #	RetTime [min]	Type	Width [min]	Area [mAU*s]	Height [mAU]	Area %
1	12.768	BB	0.3859	3256.17920	129.68271	49.6090
2	20.361	BB	0.6364	3307.50391	74.87461	50.3910

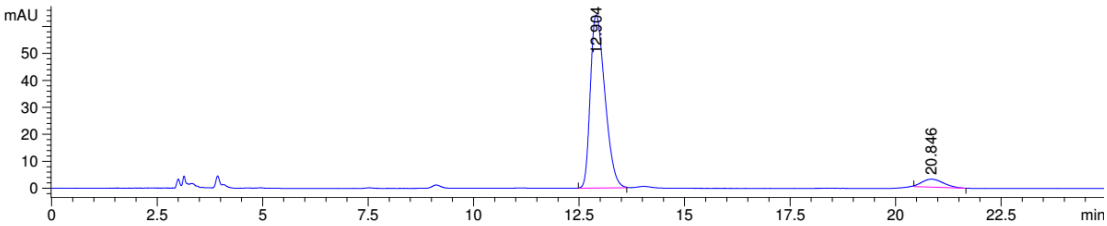

Peak #	RetTime [min]	Type	Width [min]	Area [mAU*s]	Height [mAU]	Area %
1	12.904	BB	0.3702	1536.30469	64.18867	93.6180
2	20.846	BB	0.4291	104.73110	2.96525	6.3820

2-(methoxymethyl)-2,3-dihydrobenzo[*b*]thiophene 1,1-dioxide (4i)

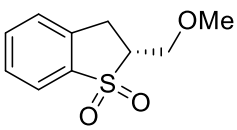

Colorless solid; H_2 (30 bar), 0 ºC, 24 h, 90% yield, 96.5:3.5 e.r. $[\alpha]_D^{22}$ = +14.1 (c = 1.0 in $CHCl_3$). HPLC DAICEL CHIRALCEL AS-H, *n*-hexane/2-propanol = 70/30, flow rate = 0.8 mL/min, λ = 210 nm, retention time: 31.2 min (major), 39.7 min (minor). **^{1}H NMR** (300 MHz, $CDCl_3$) δ 7.74 (d, J = 7.7 Hz, 1H), 7.56 (t, J = 7.5 Hz, 1H), 7.45 (t, J = 7.5 Hz, 1H),

7.35 (d, J = 7.7 Hz, 1H), 3.97 (ddd, J = 10.7, 6.7, 3.6 Hz, 1H), 3.82 – 3.64 (m, 2H), 3.51 – 3.34 (m, 4H), 3.11 (dd, J = 16.4, 6.8 Hz, 1H). **^{13}C NMR** (75 MHz, $CDCl_3$) δ 139.1, 136.1, 133.6, 128.9, 127.3, 121.9, 69.3, 60.5, 59.5, 29.5. **ESI-MS**: calculated $[C_{10}H_{12}O_3S + Na]^+$: 235.0399, found: 235.0407.

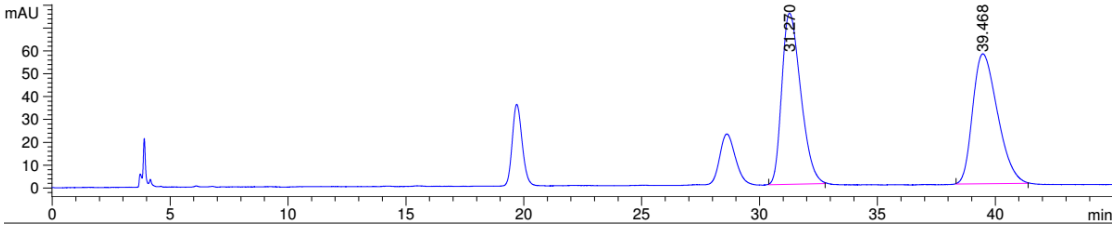

Peak #	RetTime [min]	Type	Width [min]	Area [mAU*s]	Height [mAU]	Area %
1	31.270	BB	0.7256	4175.89160	74.87778	50.0910
2	39.468	BB	0.9138	4160.72607	56.85415	49.9090

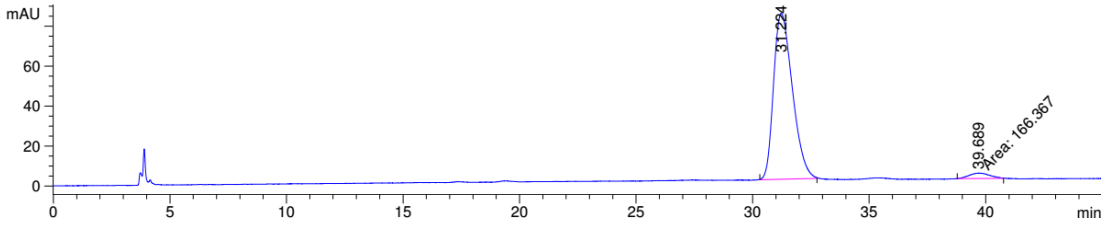

Peak #	RetTime [min]	Type	Width [min]	Area [mAU*s]	Height [mAU]	Area %
1	31.224	BB	0.8213	4663.67188	83.03462	96.5556
2	39.689	MM	1.0149	166.36746	2.73208	3.4444

2-(4-chlorobutyl)-2,3-dihydrobenzo[*b*]thiophene 1,1-dioxide (4j)

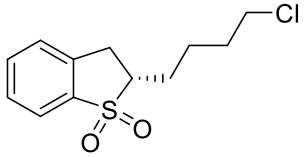

Colorless oil; H_2 (30 bar), 0 ºC, 24 h, 98% yield, 94:6 e.r. $[\alpha]_D^{22}$ = +9.6 (c = 1.0 in $CHCl_3$). HPLC DAICEL CHIRALCEL AS-H, *n*-hexane/2-propanol = 70/30, flow rate = 1.0 mL/min, λ = 210 nm, retention time: 23.7 min (major), 36.3 min (minor). **^{1}H**

NMR (300 MHz, $CDCl_3$) δ 7.74 (d, J = 7.7 Hz, 1H), 7.56 (t, J = 7.5 Hz, 1H), 7.45 (t, J = 7.5 Hz, 1H), 7.34 (d, J = 7.6 Hz, 1H), 3.58 (t, J = 6.4 Hz, 2H), 3.52 – 3.34 (m, 2H), 3.11 – 2.89 (m, 1H), 2.26 – 2.03 (m, 1H), 2.03 – 1.64 (m, 5H). **^{13}C NMR** (75 MHz, $CDCl_3$) δ 139.1, 136.4, 133.5, 128.9, 127.2, 122.0, 61.4, 44.6, 32.5, 32.3, 27.1, 24.4. **ESI-MS**: calculated $[C_{12}H_{15}ClO_2S + Na]^+$: 281.0373, found: 281.0383.

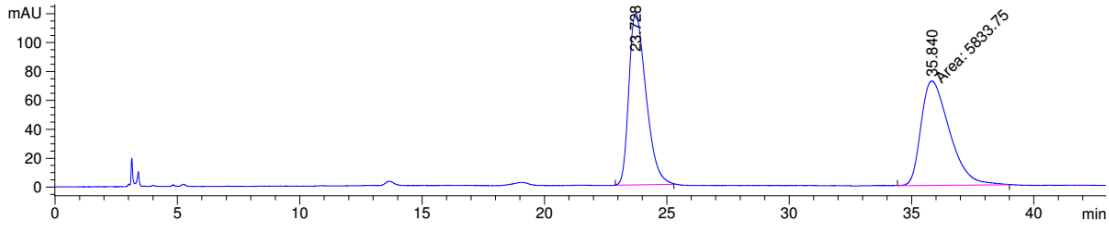

Peak #	RetTime [min]	Type	Width [min]	Area [mAU*s]	Height [mAU]	Area %
1	23.728	BB	0.5839	5806.90039	118.88425	49.8847
2	35.840	MM	1.3455	5833.75293	72.26392	50.1153

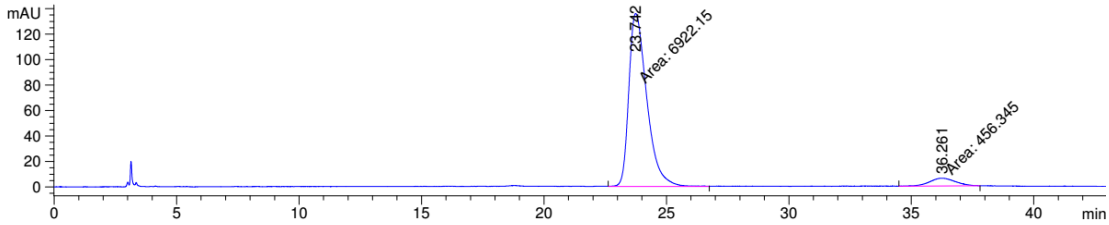

Peak #	RetTime [min]	Type	Width [min]	Area [mAU*s]	Height [mAU]	Area %
1	23.742	MM	0.8494	6922.15039	135.82114	93.8152
2	36.261	MM	1.2375	456.34485	6.14608	6.1848

c. Enantioselective hydrogenation of ketones catalyzed by Ru(II)-NHC-diamine complexes:

For an easier handling, a stock solution of complex of **C4** (0.006 mmol, 4.7 mg) in THF (4.0 mL) was prepared. To a glass vial, 200 μL of the **C4** solution was added, and the solvent was removed under vacuum. To this vial, NaO*t*-Bu (0.02 mmol, 6.7 mol%),

ketone **5** (1.0 mmol), and *i*-PrOH (1.0 mL) were added under an argon atmosphere. The glass vial was placed in a 150 mL stainless steel autoclave under an argon atmosphere. The autoclave was pressurized and depressurized with hydrogen gas five times before the indicated pressure (5 bar or 10 bar) was set. The reaction mixture was stirred at 22 °C for 24 h. After the autoclave was carefully depressurized, the mixture was directly purified by flash column chromatography on silica gel (pentane/ethylacetate = 20:1 to 4:1) to afford the desired product **6**. All the obtained products **6** have been reported previously.

1-phenylethan-1-ol (6a)

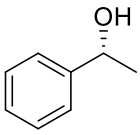

Colorless oil; H_2 (5 bar), 22 °C, 24 h, 99% yield, 93:7 e.r. $[\alpha]_D^{22}$ = +48.0 (c = 0.85 in $CHCl_3$). HPLC DAICEL CHIRALCEL OJ-H, *n*-hexane/2-propanol = 98/2, flow rate = 0.8 mL/min, λ = 254 nm, retention time: 25.9 min (minor), 28.7 min (major). **^{1}H NMR** (300 MHz, $CDCl_3$) δ 7.45 – 7.25 (m, 5H), 4.92 (q, *J* = 6.4 Hz, 1H), 2.01 (s, 1H), 1.53 (d, *J* = 6.5 Hz, 3H).

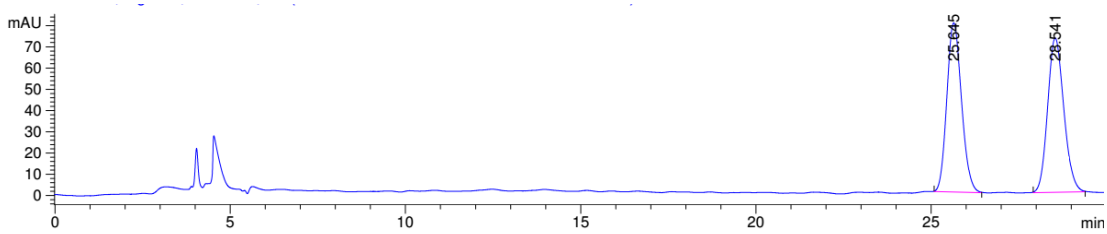

Peak #	RetTime [min]	Type	Width [min]	Area [mAU*s]	Height [mAU]	Area %
1	25.645	BB	0.4529	2314.05835	79.66157	49.8290
2	28.541	BB	0.4892	2329.94116	72.64352	50.1710

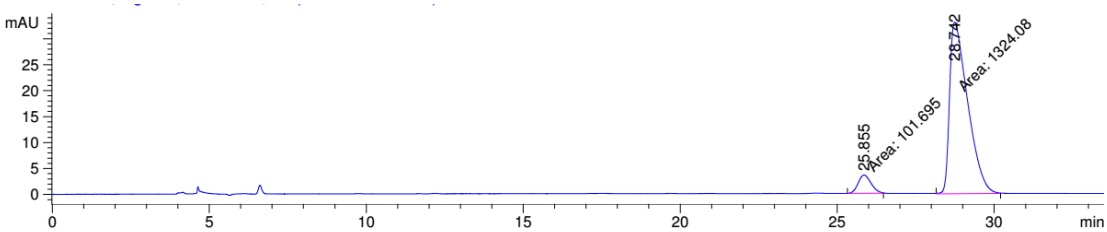

Peak #	RetTime [min]	Type	Width [min]	Area [mAU*s]	Height [mAU]	Area %
1	25.855	MM	0.4778	101.69521	3.54747	7.1326
2	28.742	MM	0.6680	1324.07715	33.03671	92.8674

1-(benzo[d][1,3]dioxol-5-yl)ethan-1-ol (6b)

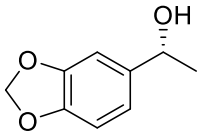

Colorless oil; H_2 (10 bar), 22 ºC, 24 h, 99% yield, 92:8 e.r. $[\alpha]_D^{22}$ = +40.3 (c = 0.90 in $CHCl_3$). HPLC DAICEL CHIRALCEL AD-H, *n*-hexane/2-propanol = 95/5, flow rate = 0.8 mL/min, λ = 254 nm, retention time: 20.8 min (major), 23.3 min (minor). **^{1}H NMR** (300 MHz, $CDCl_3$) δ 6.88 (d, *J* = 1.1 Hz, 1H), 6.79 (dt, *J* = 14.1, 4.6 Hz, 2H), 5.94 (s, 2H), 4.81 (q, *J* = 6.4 Hz, 1H), 1.92 (s, 1H), 1.45 (d, *J* = 6.4 Hz, 3H).

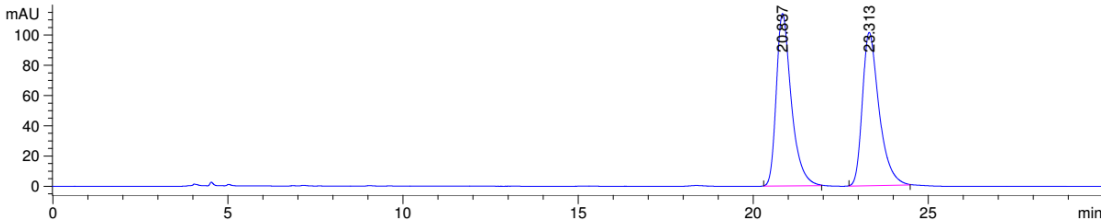

Peak #	RetTime [min]	Type	Width [min]	Area [mAU*s]	Height [mAU]	Area %
1	20.837	BB	0.4467	3400.38940	114.10450	50.2551
2	23.313	BB	0.5001	3365.86499	101.44231	49.7449

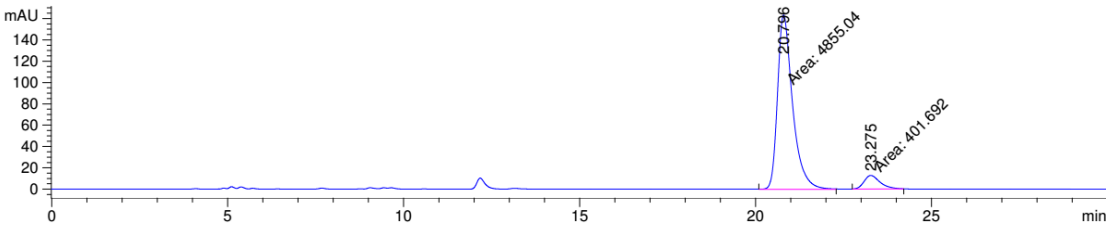

Peak #	RetTime [min]	Type	Width [min]	Area [mAU*s]	Height [mAU]	Area %
1	20.796	MM	0.4950	4855.04248	163.46036	92.3585
2	23.275	MM	0.5263	401.69156	12.72034	7.6415

1-(thiophen-3-yl)ethan-1-ol (6c)

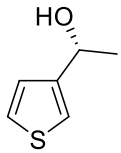

Colorless oil; H_2 (10 bar), 22 °C, 24 h, 99% yield, 91:9 e.r. $[\alpha]_D^{22}$ = +25.5 (c = 1.40 in $CHCl_3$). HPLC DAICEL CHIRALCEL OJ-H, *n*-hexane/2-propanol = 95/5, flow rate = 1.0 mL/min, λ = 230 nm, retention time: 12.2 min (minor), 14.5 min (major). **^{1}H NMR** (300 MHz, $CDCl_3$) δ 7.30 (dd, *J* = 5.0, 3.0 Hz, 1H), 7.24 – 7.17 (m, 1H), 7.10 (dd, *J* = 5.0, 1.3 Hz, 1H), 4.97 (q, *J* = 6.4 Hz, 1H), 1.90 (s, 1H), 1.53 (d, *J* = 6.5 Hz, 3H).

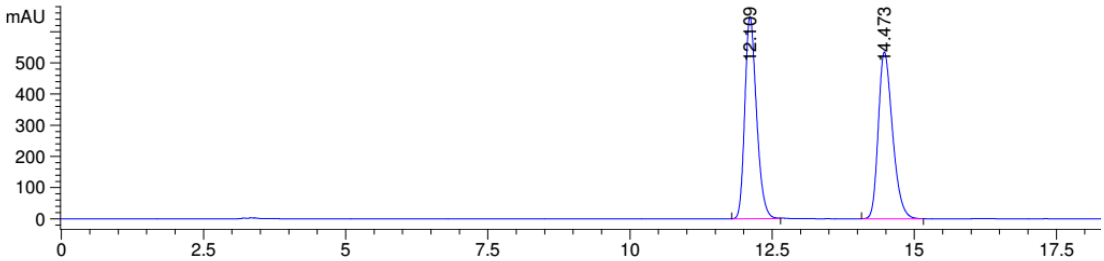

Peak #	RetTime [min]	Type	Width [min]	Area [mAU*s]	Height [mAU]	Area %
1	12.109	BB	0.2186	9263.92969	648.73163	49.9108
2	14.473	BB	0.2667	9297.04590	535.08679	50.0892

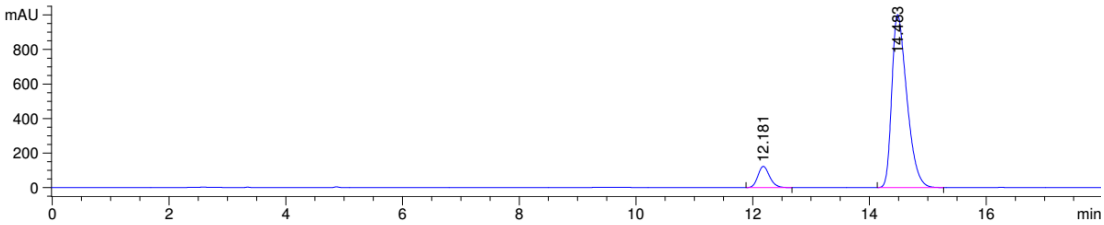

Peak #	RetTime [min]	Type	Width [min]	Area [mAU*s]	Height [mAU]	Area %
1	12.181	BB	0.2152	1723.94714	123.24348	8.7658
2	14.483	BB	0.2749	1.79429e4	1002.17914	91.2342

1,2,3,4-tetrahydronaphthalen-1-ol (6d)

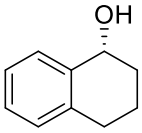

Colorless oil; H_2 (10 bar), 22 ºC, 24 h, 99% yield, 97:3 e.r. $[\alpha]_D^{22} = -28.5$ (c = 1.02 in $CHCl_3$). HPLC DAICEL CHIRALCEL AD-H, *n*-hexane/2-propanol = 95/5, flow rate = 0.8 mL/min, λ = 230 nm, retention time: 11.9 min (minor), 12.9 min (major). **^{1}H NMR** (300 MHz, $CDCl_3$) δ 7.49 – 7.35 (m, 1H), 7.25 – 7.16 (m, 2H), 7.11 (dd, *J* = 5.5, 3.5 Hz, 1H), 4.78 (s, 1H), 2.94 – 2.61 (m, 2H), 2.08 – 1.71 (m, 5H).

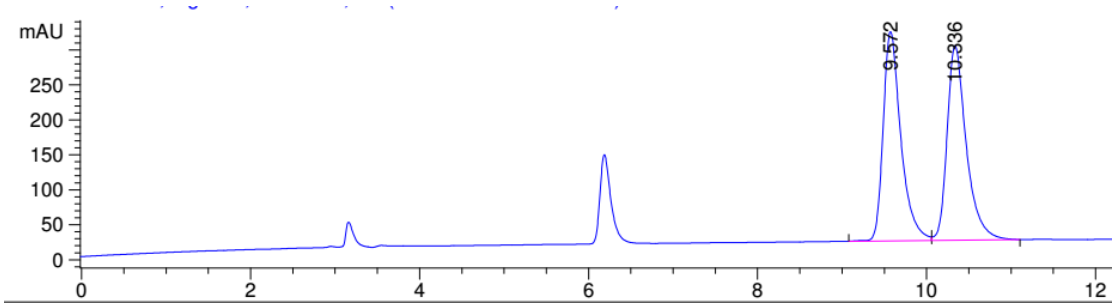

Peak #	RetTime [min]	Type	Width [min]	Area [mAU*s]	Height [mAU]	Area %
1	9.572	BV	0.2192	4362.45752	299.08920	49.8007
2	10.336	VB	0.2366	4397.37744	277.90781	50.1993

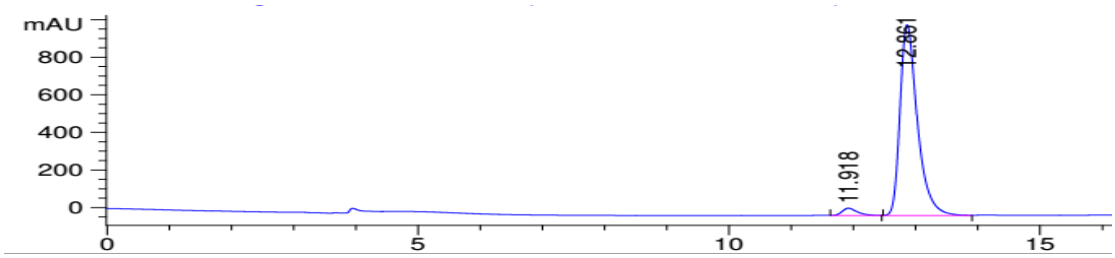

Peak #	RetTime [min]	Type	Width [min]	Area [mAU*s]	Height [mAU]	Area %
1	11.918	VB	0.2593	679.98999	39.21931	3.3219
2	12.861	BB	0.2935	1.97897e4	1014.93079	96.6781

6-methoxy-1,2,3,4-tetrahydronaphthalen-1-ol (6e)

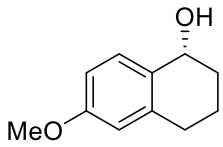

Colorless oil; H_2 (10 bar), 22 ºC, 24 h, 96% yield, 93:7 e.r. $[\alpha]_D^{22}$ = −20.9 (c = 1.0 in $CHCl_3$). HPLC DAICEL CHIRALCEL OD-H, *n*-hexane/2-propanol = 95/5, flow rate = 0.8 mL/min, λ = 230 nm, retention time: 14.3 min (minor), 15.3 min (major). **^{1}H NMR** (400 MHz, $CDCl_3$) δ 7.32 (d, *J* = 8.5 Hz, 1H), 6.76 (dd, *J* = 8.5, 2.4 Hz, 1H), 6.62 (d, *J* = 1.7 Hz, 1H), 4.72 (d, *J* = 4.8 Hz, 1H), 3.78 (s, 3H), 2.84 – 2.63 (m, 2H), 2.06 (s, 1H), 2.01 – 1.84 (m, 3H), 1.79 – 1.71 (m, 1H).

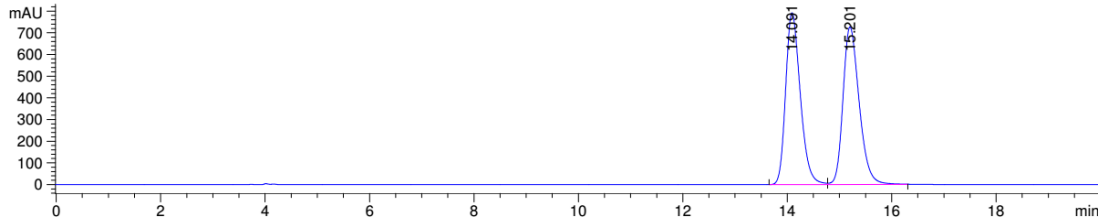

Peak #	RetTime [min]	Type	Width [min]	Area [mAU*s]	Height [mAU]	Area %
1	14.091	BV	0.2999	1.54204e4	792.81757	49.7185
2	15.201	VB	0.3303	1.55951e4	726.84210	50.2815

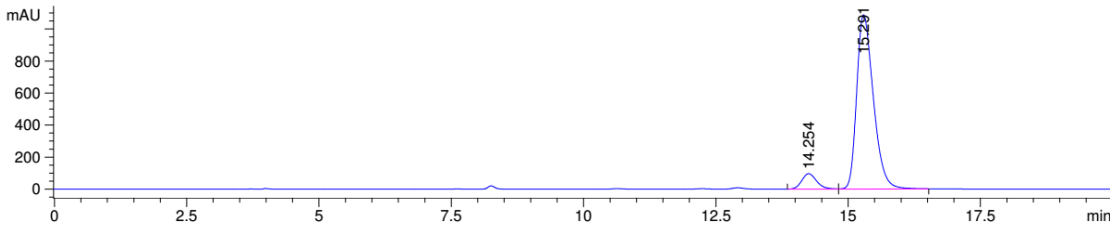

Peak #	RetTime [min]	Type	Width [min]	Area [mAU*s]	Height [mAU]	Area %
1	14.254	BV	0.2998	1882.32837	96.41793	7.3292
2	15.291	VB	0.3362	2.38004e4	1087.85364	92.6708

5,7-dimethyl-1,2,3,4-tetrahydronaphthalen-1-ol (6f)

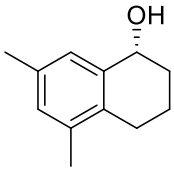

Colorless oil; H_2 (10 bar), 22 °C, 24 h, 96% yield, 91:9 e.r. $[\alpha]_D^{22}$ = − 28.4 (c = 1.0 in $CHCl_3$). HPLC DAICEL CHIRALCEL OD-H, *n*-hexane/2-propanol = 95/5, flow rate = 1.0 mL/min, λ = 230 nm, retention time: 7.0 min (minor), 8.4 min (major). **^{1}H NMR** (300 MHz, $CDCl_3$) δ 7.13 (s, 1H), 6.94 (s, 1H), 4.75 (s, 1H), 2.76 – 2.59 (m, 1H), 2.59 – 2.42 (m, 1H), 2.31 (s, 3H), 2.21 (s, 3H), 2.07 – 1.68 (m, 5H).

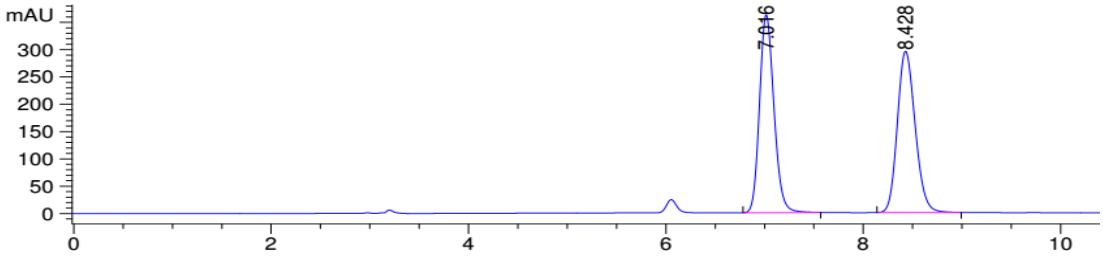

Peak #	RetTime [min]	Type	Width [min]	Area [mAU*s]	Height [mAU]	Area %
1	7.016	BB	0.1587	3682.90210	361.93198	49.8203
2	8.428	BB	0.1956	3709.46362	295.30344	50.1797

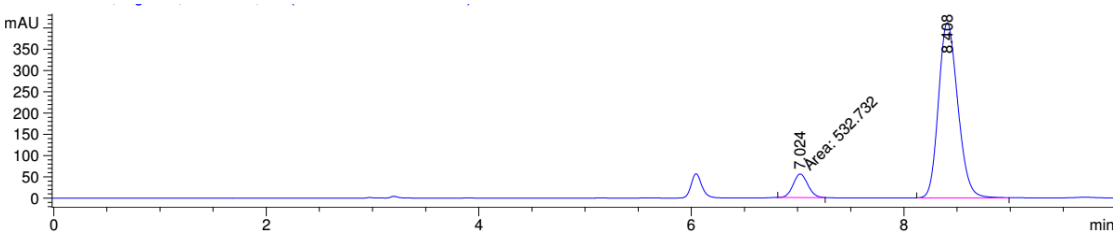

Peak #	RetTime [min]	Type	Width [min]	Area [mAU*s]	Height [mAU]	Area %
1	7.024	MM	0.1603	532.73236	55.40173	9.2960
2	8.408	BB	0.1962	5198.03857	412.01373	90.7040

7-fluoro-1,2,3,4-tetrahydronaphthalen-1-ol (6g)

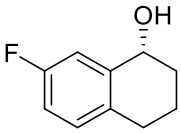

Colorless oil; H_2 (10 bar), 22 ºC, 24 h, 99% yield, 96:4 e.r. $[\alpha]_D^{22} = -36.8$ (c = 1.0 in $CHCl_3$). HPLC DAICEL CHIRALCEL AD-H, *n*-hexane/2-propanol = 95/5, flow rate = 1.0 mL/min, λ = 254 nm, retention time: 9.8 min (minor), 10.9 min (major). **^{1}H NMR** (300 MHz, $CDCl_3$) δ 7.15 (dd, *J* = 9.6, 2.7 Hz, 1H), 7.05 (dd, *J* = 8.4, 5.8 Hz, 1H), 6.89 (td, *J* = 8.4, 2.7 Hz, 1H), 4.74 (s, 1H), 2.87 – 2.54 (m, 2H), 2.13 – 1.66 (m, 5H).

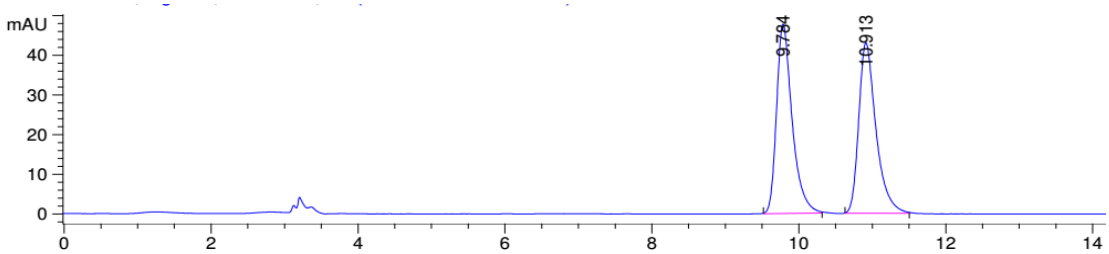

Peak #	RetTime [min]	Type	Width [min]	Area [mAU*s]	Height [mAU]	Area %
1	9.784	BB	0.2208	703.43280	47.76301	50.0953
2	10.913	BB	0.2452	700.75696	42.97340	49.9047

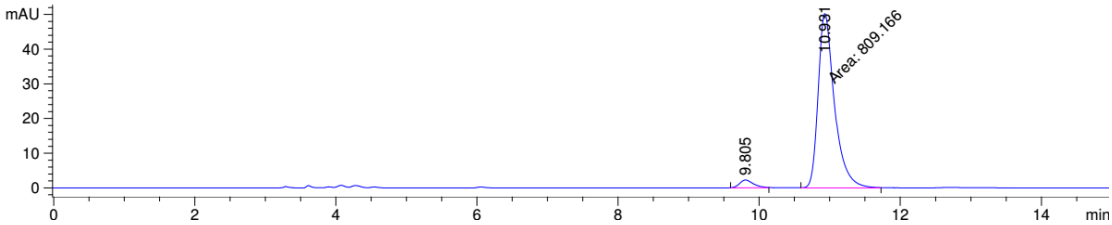

Peak #	RetTime [min]	Type	Width [min]	Area [mAU*s]	Height [mAU]	Area %
1	9.805	BB	0.2023	30.88971	2.24880	3.6771
2	10.931	MM	0.2684	809.16602	50.24074	96.3229

7-bromo-1,2,3,4-tetrahydronaphthalen-1-ol (6h)

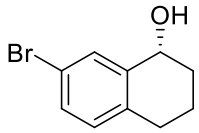

Colorless oil; H_2 (10 bar), 22 ºC, 24 h, 98% yield, 95:5 e.r. $[\alpha]_D^{22} = -60.2$ (c = 1.0 in $CHCl_3$). HPLC DAICEL CHIRALCEL AD-H, *n*-hexane/2-propanol = 95/5, flow rate = 1.0 mL/min, λ = 230 nm, retention time: 9.7 min (minor), 12.1 min (major). **^{1}H NMR** (400 MHz, $CDCl_3$) δ 7.59 (s, 1H), 7.29 (d, *J* = 8.2 Hz, 1H), 6.97 (d, *J* = 8.2 Hz, 1H), 4.73 (s, 1H), 2.93 – 2.58 (m, 2H), 2.05 – 1.72 (m, 5H).

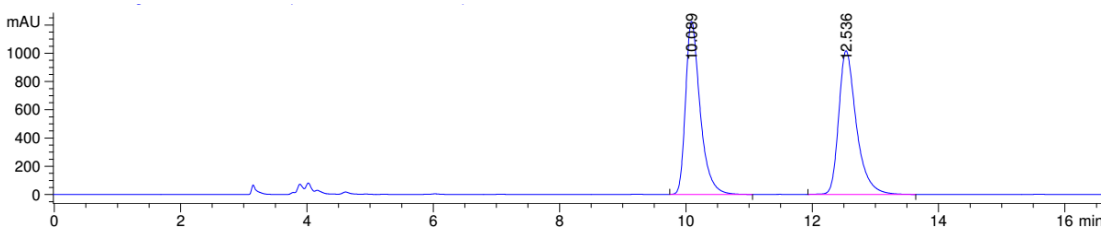

Peak #	RetTime [min]	Type	Width [min]	Area [mAU*s]	Height [mAU]	Area %
1	10.089	BB	0.2420	1.96133e4	1223.95227	49.8387
2	12.536	BB	0.2926	1.97403e4	1016.28198	50.1613

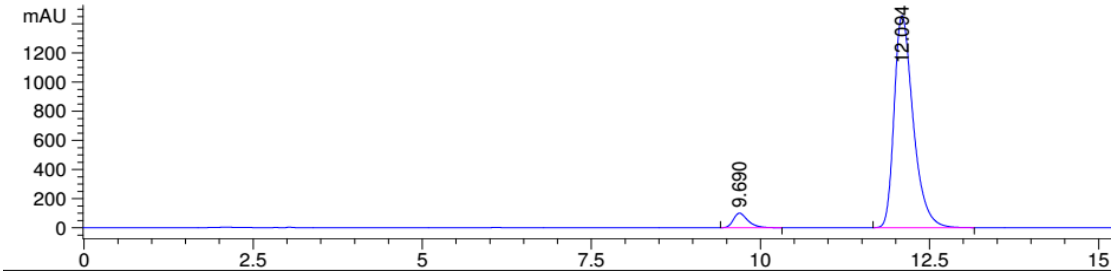

Peak #	RetTime [min]	Type	Width [min]	Area [mAU*s]	Height [mAU]	Area %
1	9.690	BB	0.2246	1503.73853	100.50675	5.0088
2	12.094	BB	0.2987	2.85183e4	1454.51062	94.9912

chroman-4-ol (6i)

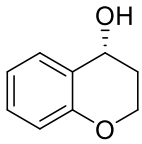

Colorless oil; H_2 (10 bar), 22 °C, 24 h, 95% yield, 96.5:3.5 e.r. $[\alpha]_D^{22} = -67.5$ (c = 1.0 in $CHCl_3$). HPLC DAICEL CHIRALCEL AS-H, *n*-hexane/2-propanol = 95/5, flow rate = 1.0 mL/min, λ = 230 nm, retention time: 9.3 min (minor), 11.7 min (major). **^{1}H NMR** (300 MHz, $CDCl_3$) δ 7.30 (dd, *J* = 7.6, 1.6 Hz, 1H), 7.21 (ddd, *J* = 8.8, 7.5, 1.7 Hz, 1H), 6.92 (td, *J* = 7.5, 1.2 Hz, 1H), 6.84 (dd, *J* = 8.2, 1.0 Hz, 1H), 4.76 (d, *J* = 3.8 Hz, 1H), 4.31 – 4.16 (m, 2H), 2.19 – 1.94 (m, 3H).

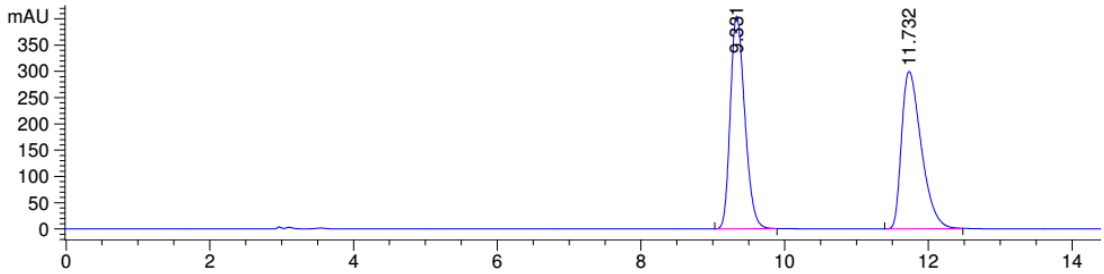

Peak #	RetTime [min]	Type	Width [min]	Area [mAU*s]	Height [mAU]	Area %
1	9.331	BB	0.2187	5680.36182	404.87570	49.8531
2	11.732	BB	0.2946	5713.84277	299.50082	50.1469

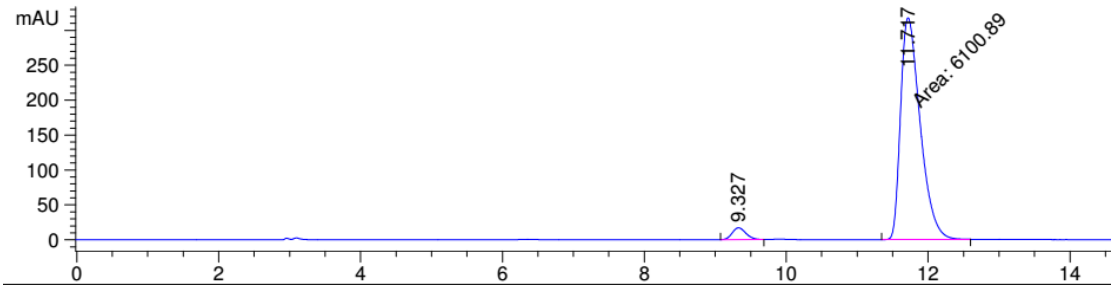

Peak #	RetTime [min]	Type	Width [min]	Area [mAU*s]	Height [mAU]	Area %
1	9.327	BB	0.2050	226.59337	16.95139	3.5811
2	11.717	MM	0.3201	6100.88818	317.66943	96.4189

6,7,8,9-tetrahydro-5H-benzo[7]annulen-5-ol (6j)

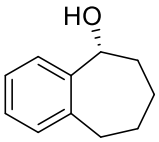

Colorless oil; H_2 (10 bar), 22 ºC, 24 h, 99% yield, 95.5:4.5 e.r. $[\alpha]_D^{22}$ = −67.5 (c = 1.0 in $CHCl_3$). HPLC DAICEL CHIRALCEL AD-H, *n*-hexane/2-propanol = 95/5, flow rate = 0.8 mL/min, λ = 254 nm, retention time: 12.1 min (major), 13.5 min (minor). **^{1}H NMR** (300 MHz, $CDCl_3$) δ 7.44 (d, *J* = 7.2 Hz, 1H), 7.25 – 7.05 (m, 3H), 4.93 (d, *J* = 7.7 Hz, 1H), 2.93 (dd, *J* = 14.0, 8.3 Hz, 1H), 2.73 (dd, *J* = 17.6, 7.1 Hz, 1H), 2.18 – 1.89 (m, 3H), 1.81 (ddd, *J* = 9.7, 7.4, 4.7 Hz, 3H), 1.58 – 1.37 (m, 1H).

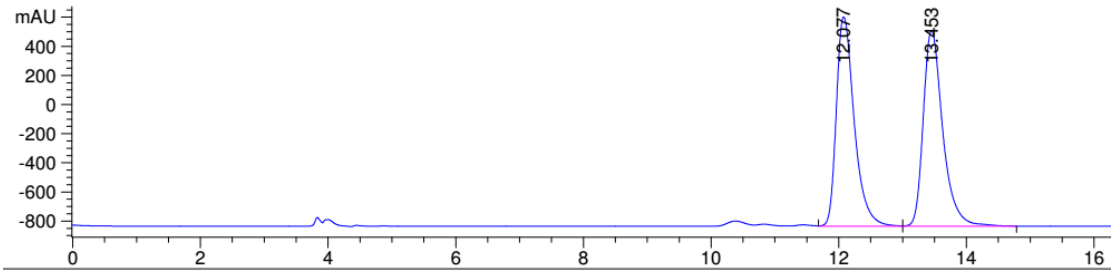

Peak #	RetTime [min]	Type	Width [min]	Area [mAU*s]	Height [mAU]	Area %
1	12.077	VV	0.2963	2.79977e4	1436.88989	49.5901
2	13.453	VB	0.3212	2.84606e4	1343.46021	50.4099

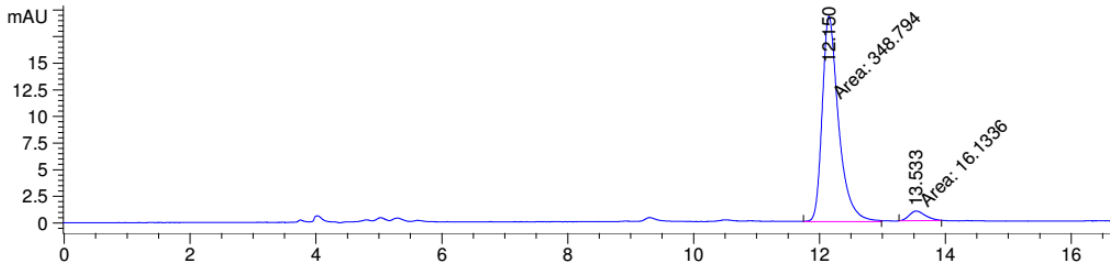

Peak #	RetTime [min]	Type	Width [min]	Area [mAU*s]	Height [mAU]	Area %
1	12.150	MM	0.3012	348.79391	19.29943	95.5790
2	13.533	MM	0.2968	16.13357	9.05896e-1	4.4210

(E) Stoichiometric reactions for mechanistic investigations

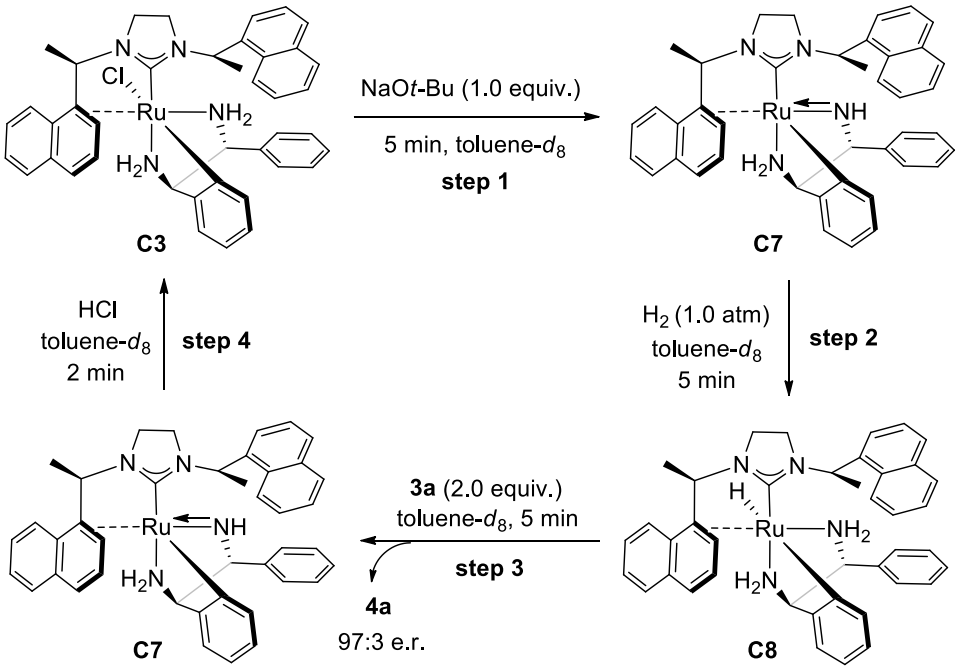

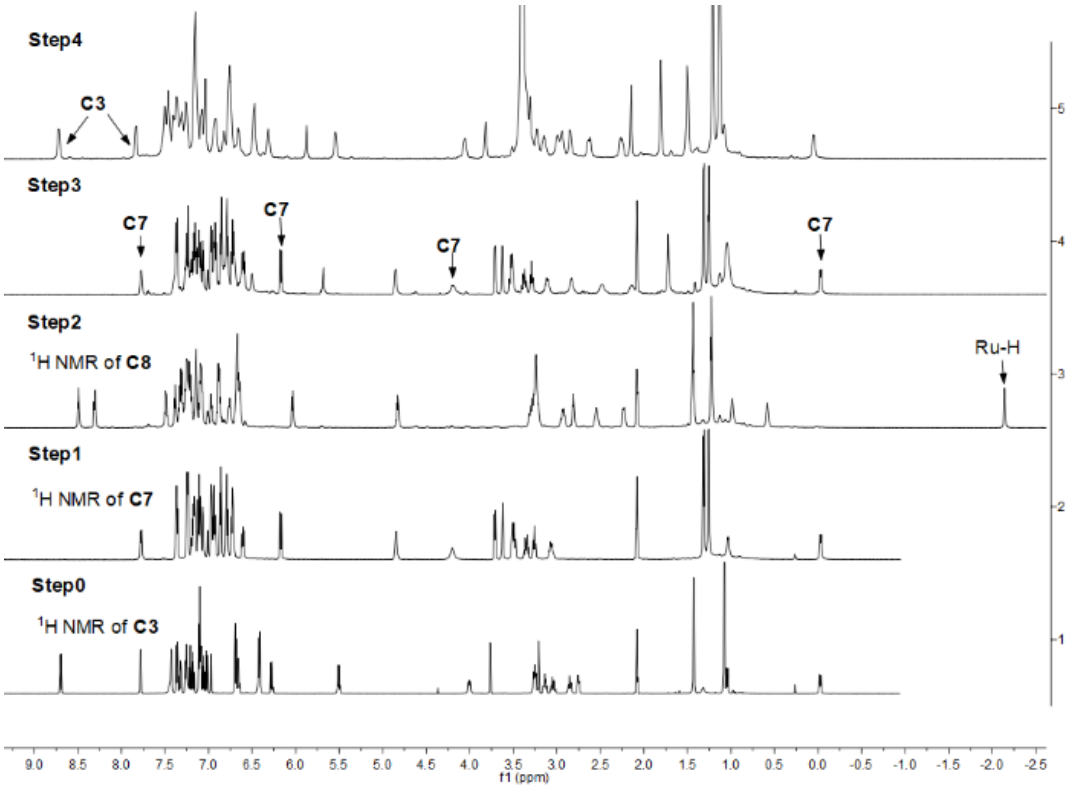

C3 (0.1 mmol, 73mg) and toluene-d_8 (0.7 mL) were added to a Young NMR tube in the glove box, and ^{1}H NMR was measured. NaO*t*-Bu (0.1 mmol, 1 equiv.) was then added to the mixture in the glove box. The dehydrochlorination reaction immediately occured visuliazed by a color change from yellow to dark red. After 5 minutes, the solvent and the byproduct *t*-BuOH were remove under vaccum. Toluene-d_8 (0.7 mL) was again added to the mixture, and NMR spectra were measured (**step1**). After quickly removing the gas of the NMR tube in vacumm, H_2 was added to reach 1 atm. After shaking the NMR tube several times, the reaction completed within 5 min. ^{1}H NMR of **step2** was measured immediately at 26 ºC. The full NMR spectra of **C8** (^{1}H, ^{13}C, gCOSY, gHSQC, and gHMBC) were measured at -30 ºC because **C8** is not stable in solution at room temperature. After releasing the H_2 gas from the NMR tube, substrate **3a** (0.2 mmol, 2 equiv.) was added to the solution of **C8**. The reaction was completed within 5 mins, and ^{1}H NMR was measured (**step3**). Finally, 1.0 equiv. of HCl solution (4M in dioxane) was added to the reaction, and ^{1}H NMR was measured (**step4**). The product **4a** and **C3** were recovered by column chromatography on silica gel (pentane/ethylacetate = 20:1, 10:1, 4:1, 2:1). The e.r. value of **4a** was also measured.

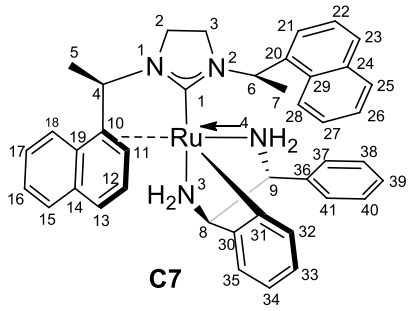

^{1}H NMR (600 MHz, 26 ºC, Toluene-d_8, connectivities were confirmed by gCOSY, gHSQC, gHMBC, 1D-NOESY and 1D-TOCSY experiments) δ 7.78 (d, *J* = 8.0 Hz, 1H, *H*C18), 7.37 (t, *J* = 6.9 Hz, 2H, *H*C32, *H*C25), 7.27 – 7.22 (m, 3H, *H*C33, *H*C21, *H*C23), 7.21 – 7.13 (m, 3H, *H*C34, *H*C17, *H*C27), 7.13 – 7.08 (m, 2H, *H*C22, *H*C26), 7.06 (d, *J* = 7.1 Hz, 1H, *H*C35), 6.99 – 6.90 (m, 3H, *H*C15, *H*C16, *H*C28), 6.86 (d, *J* = 7.5 Hz, 2H, *H*C37, *H*C41), 6.79 (t, *J* = 7.4 Hz, 2H, *H*C38, *H*C40), 6.72 (q, *J* = 6.7 Hz, 2H, *H*C39, *H*C6), 6.60 (dd, *J* = 9.0, 6.0 Hz, 1H, *H*C12), 6.17 (d, *J* = 8.9 Hz, 1H, *H*C13), 4.85 (q, *J* = 5.6 Hz, 1H, *H*C4), 4.20 (s, 1H, *H*N4), 3.71 (d, *J* = 6.0 Hz, 1H, *H*C11), 3.62 (s, 1H, *H*C8), 3.54 – 3.45 (m, 2H, *H*C9, H_2C3), 3.35 (dt, *J* = 13.0, 9.5 Hz, 1H, H_2C3), 3.26 (t, *J* = 8.9 Hz, 1H, H_2C2), 3.06 (q, *J* = 10.2 Hz, 1H, H_2C2), 1.31 (d, *J* = 7.1 Hz, 3H, H_3C7), 1.26 (d, *J* = 6.2 Hz, 3H, H_3C5), 1.03 (d, *J* = 8.6 Hz, 1H, H_2N3), -0.03 (d, *J* = 8.1 Hz, 1H, H_2N3). **^{13}C NMR** (151 MHz, 26 ºC, Toluene-d_8, connectivities were confirmed by gHSQC and gHMBC experiments) δ 228.2 (C1), 165.8 (C31), 146.4 (C30), 145.5 (C36), 143.7 (C20), 140.4 (C12), 140.4 (C32), 140.1 (C19), 134.4 (C24), 132.3 (C14), 129.9 (C29), 129.0 (C25), 128.0 (C38, C40), 127.6 (C23), 127.1 (C15), 126.7 (C37, C41), 126.3 (C39), 126.2 (C27), 126.0 (C17), 125.5 (C22), 125.5 (C26), 125.5 (C33), 123.6 (C28), 123.1 (C16), 122.5 (C18), 121.6 (C21), 121.3 (C35, C34), 116.7 (C13), 85.5 (C10), 71.9 (C9), 71.1 (C8), 65.3 (C11), 57.8 (C4), 53.4 (C6), 47.5 (C3), 46.8 (C2), 20.9 (C7), 20.9 (C5). **ESI-MS:** calculated $[C_{41}H_{40}N_4Ru + H^+]^+$: 691.2369, found: 691.2378.

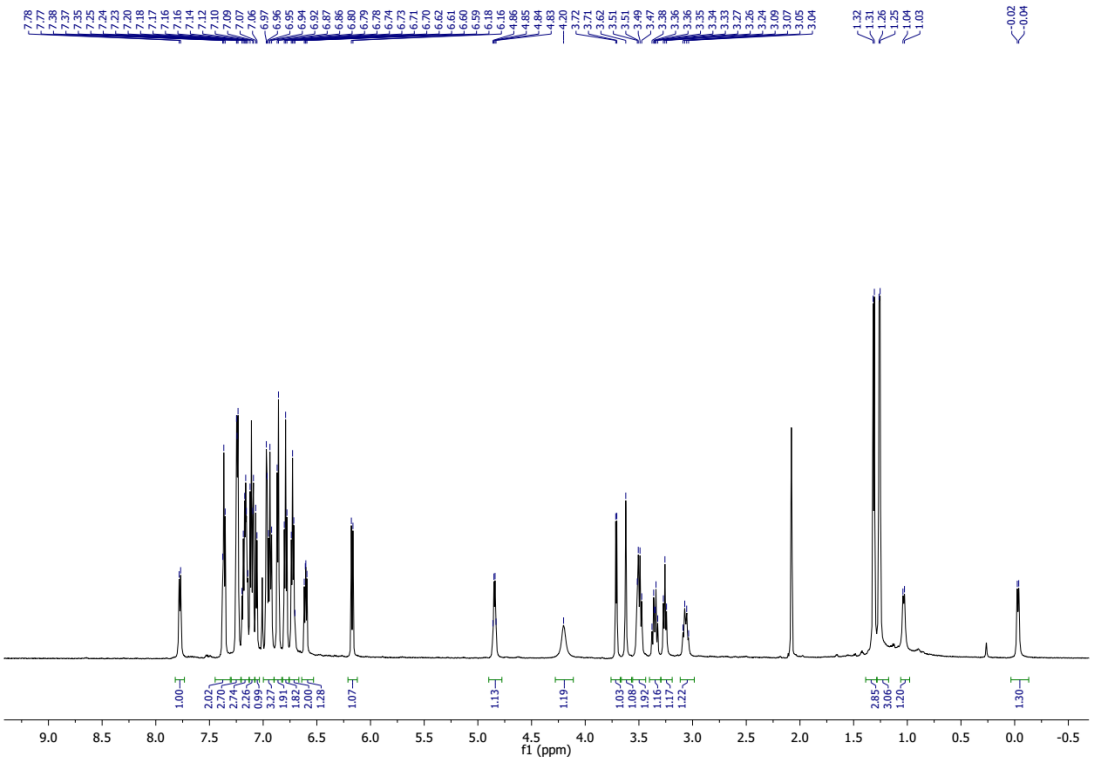

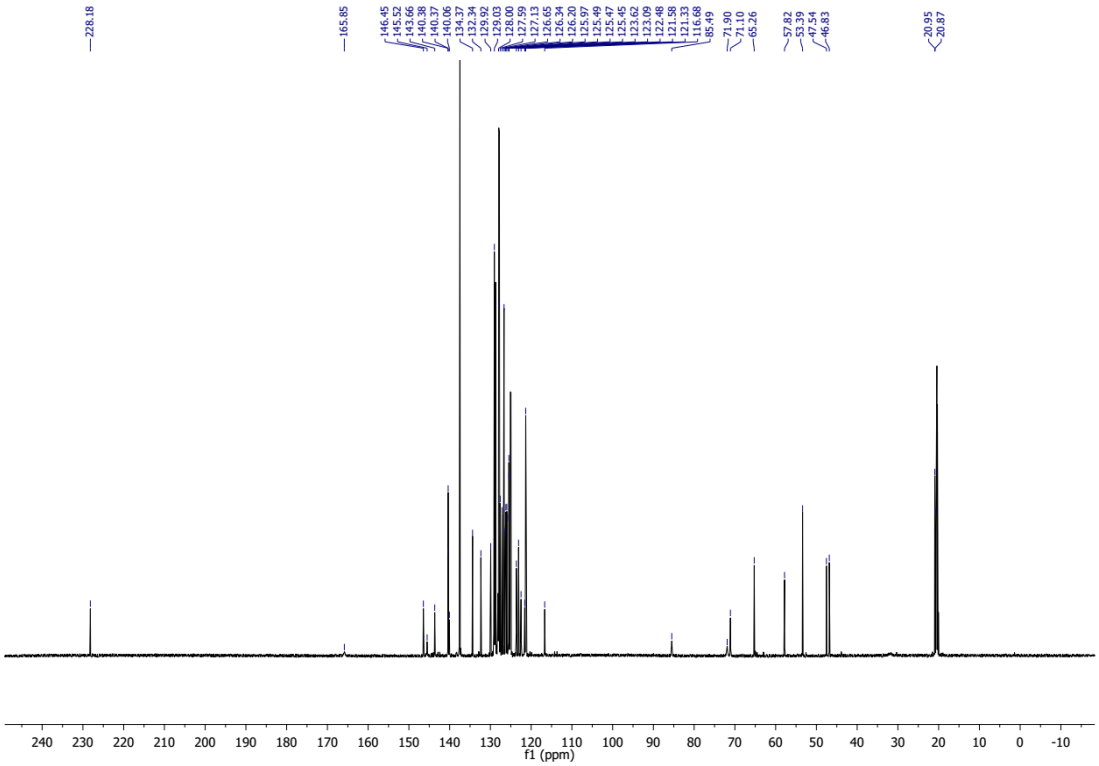

gCOSY:

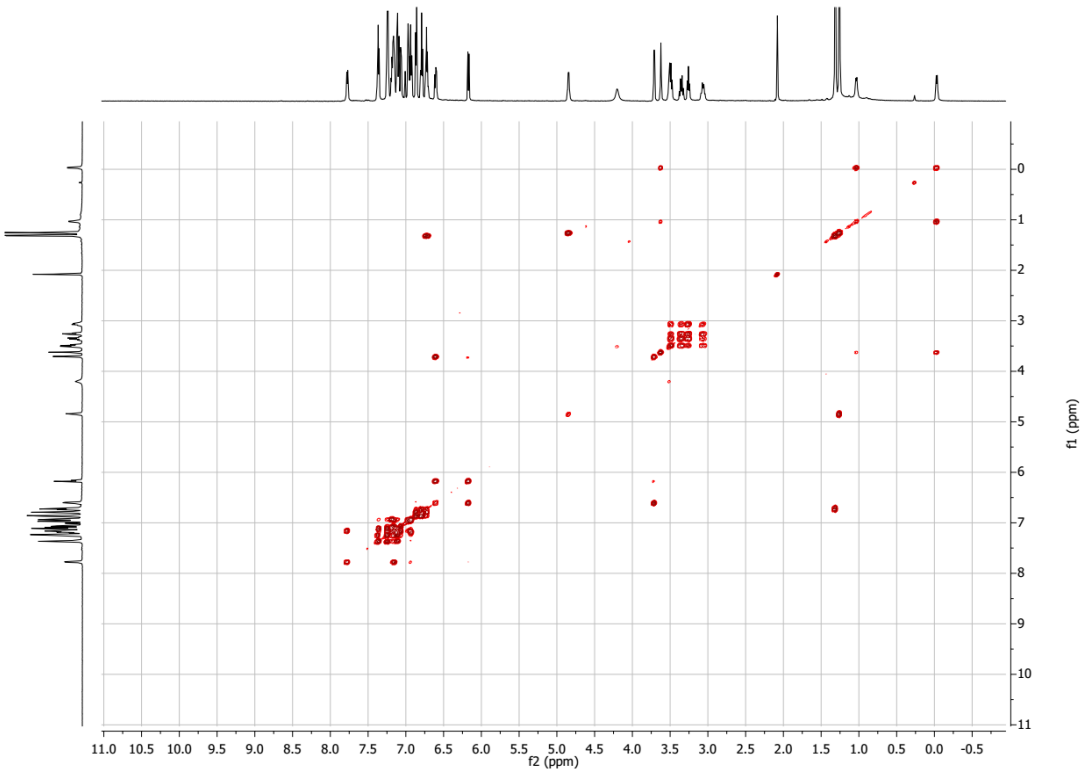

gHSQC:

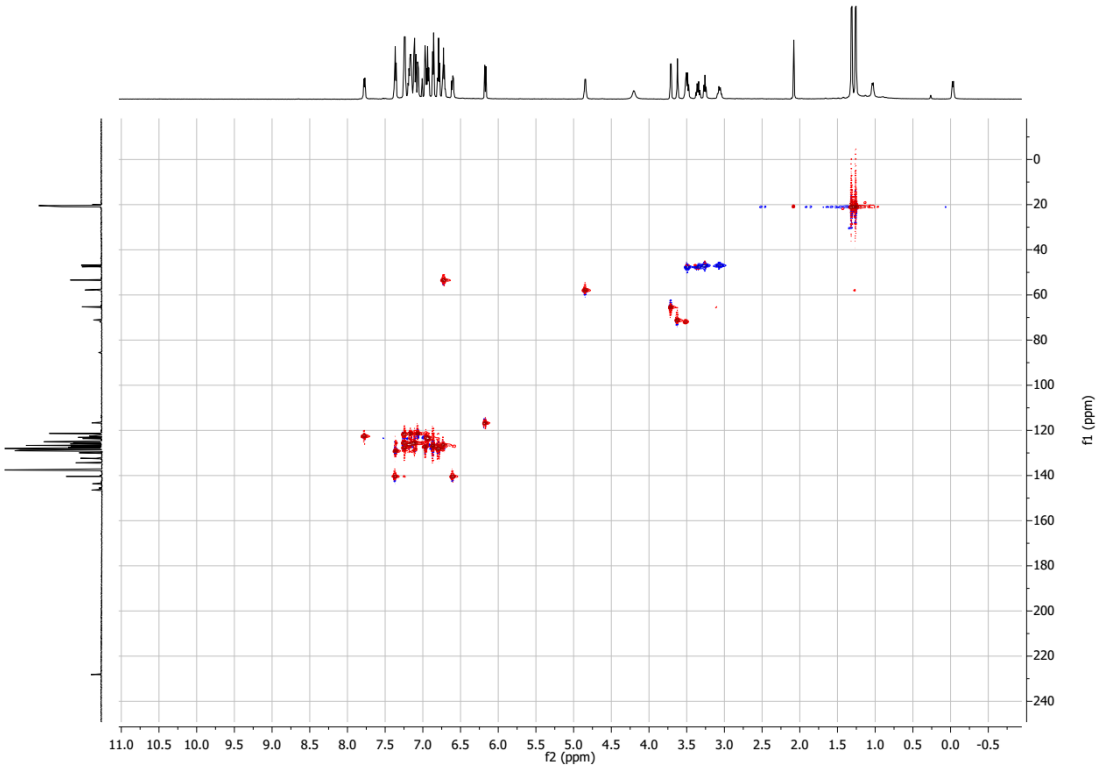

gHMBC:

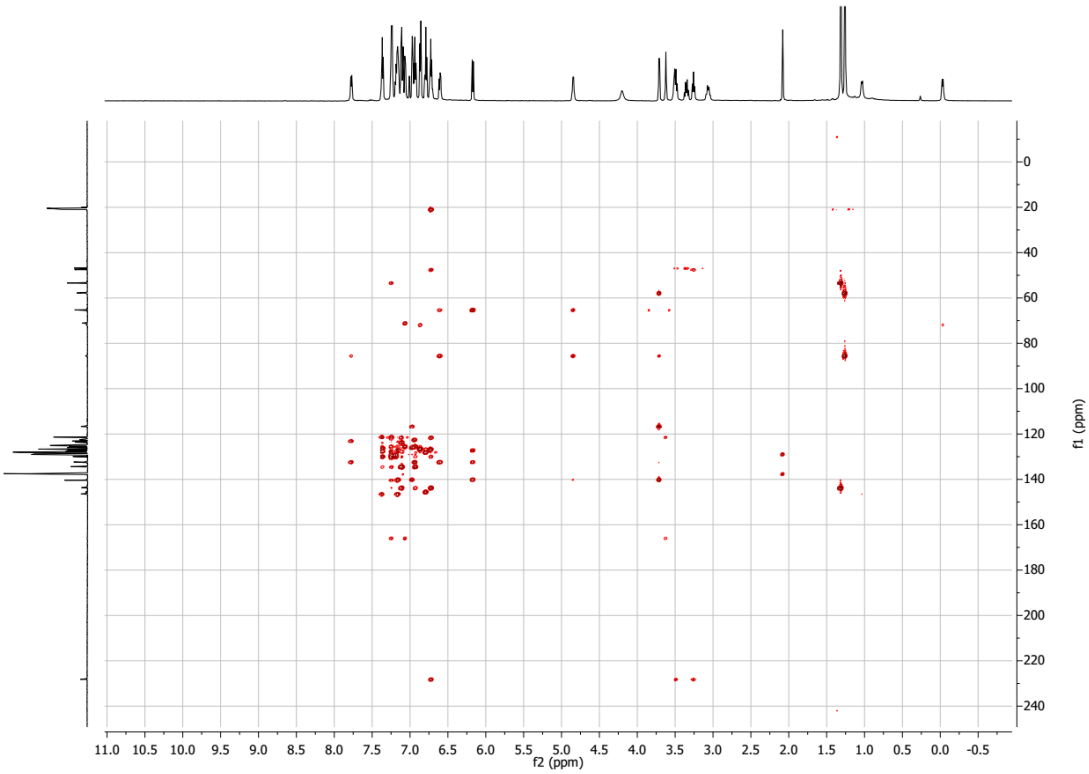

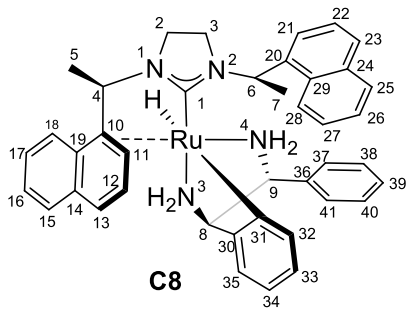

^{1}H NMR (600 MHz, -30 ºC, Toluene-d_8, connectivities were confirmed by gCOSY, gHSQC, gHMBC, 1D-NOESY and 1D-TOCSY experiments) δ 8.54 (d, *J* = 6.2 Hz, 1H, *H*C32), 8.39 (d, *J* = 7.9 Hz, 1H, *H*C18), 7.58 (t, *J* = 7.0 Hz, 1H, *H*C33), 7.43 (t, *J* = 7.3 Hz, 1H, *H*C34), 7.39 – 7.33 (m, 2H, *H*C25, *H*C17), 7.33 – 7.28 (m, 2H, *H*C21, *H*C35), 7.28 – 7.24 (m, 1H, *H*C27), 7.24 – 7.20 (m, 1H, *H*C23), 7.20 – 7.00 (m, 5H, *H*C37, *H*C41, *H*C22, *H*C26, *H*C28), 6.97 – 6.89 (m, 2H, *H*C16, *H*C15), 6.88 – 6.79 (m, 1H, *H*C6), 6.79 – 6.72 (m, 1H, *H*C12), 6.69 – 6.56 (m, 3H, *H*C38, *H*C40, *H*C39), 6.05 (d, *J* = 9.1 Hz, 1H, *H*C13), 4.87 (q, *J* = 6.4 Hz, 1H, *H*C4), 3.31 (d, *J* = 5.7 Hz, 1H, *H*C11), 3.26 – 2.98 (m, 4H, H_2C3, H_2C2, *H*C8), 2.90 (t, *J* = 9.8 Hz, 1H, *H*C2), 2.81 (t, *J* = 9.5 Hz, 1H, *H*C9), 2.62 (d, *J* = 10.2 Hz, 1H, H_2N4), 2.26 (d, *J* = 11.1 Hz, 1H, H_2N4), 1.42 (d, *J* = 6.9 Hz, 3H, H_3C7), 1.25 (d, *J* = 6.4 Hz, 3H, H_3C5), 0.98 (d, *J* = 9.3 Hz, 1H, H_2N3), 0.56 (d, *J* = 9.3 Hz, 1H, H_2N3), -2.08 (s, 1H, *H*Ru). **^{13}C NMR** (151 MHz, -30 ºC, Toluene-d_8, connectivities were confirmed by gHSQC and gHMBC experiments) δ 231.0 (C1), 190.6 (C31), 148.2 (C30), 147.0 (C19), 142.0 (C20), 141.2 (C12), 140.8 (C32), 139.7 (C36), 134.0 (C24), 131.8 (C14), 130.0 (C30), 129.4 (C25), 128.6 (C38, C40), 128.2 (C28), 127.6 (C23), 127.6 (C39), 127.0 (C15, C27), 125.9 (C17), 125.8 (C18), 125.7 (C22), 125.7 (C26), 125.4 (C37, C41), 125.0 (C33), 122.8 (C16), 122.7 (C35, C21), 122.0 (C34), 117.4 (C13), 68.3 (C10), 66.0 (C8), 61.8 (C4), 61.0 (C9), 53.6 (C6), 50.6 (C11), 46.7 (C2), 46.41 (C3), 20.8 (C7), 19.9 (C5). ESI-MS: calculated $[C_{41}H_{42}N_4Ru - H^-]^+$: 691.2369, found: 691.2377.

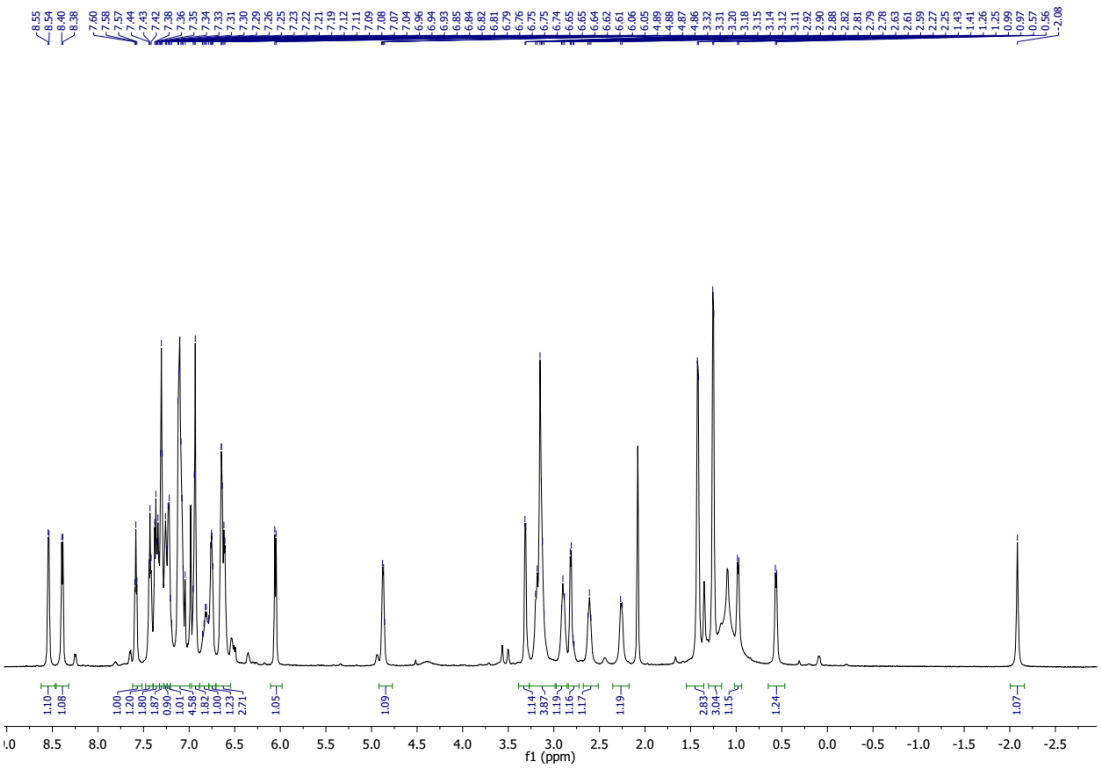
f1 (ppm)

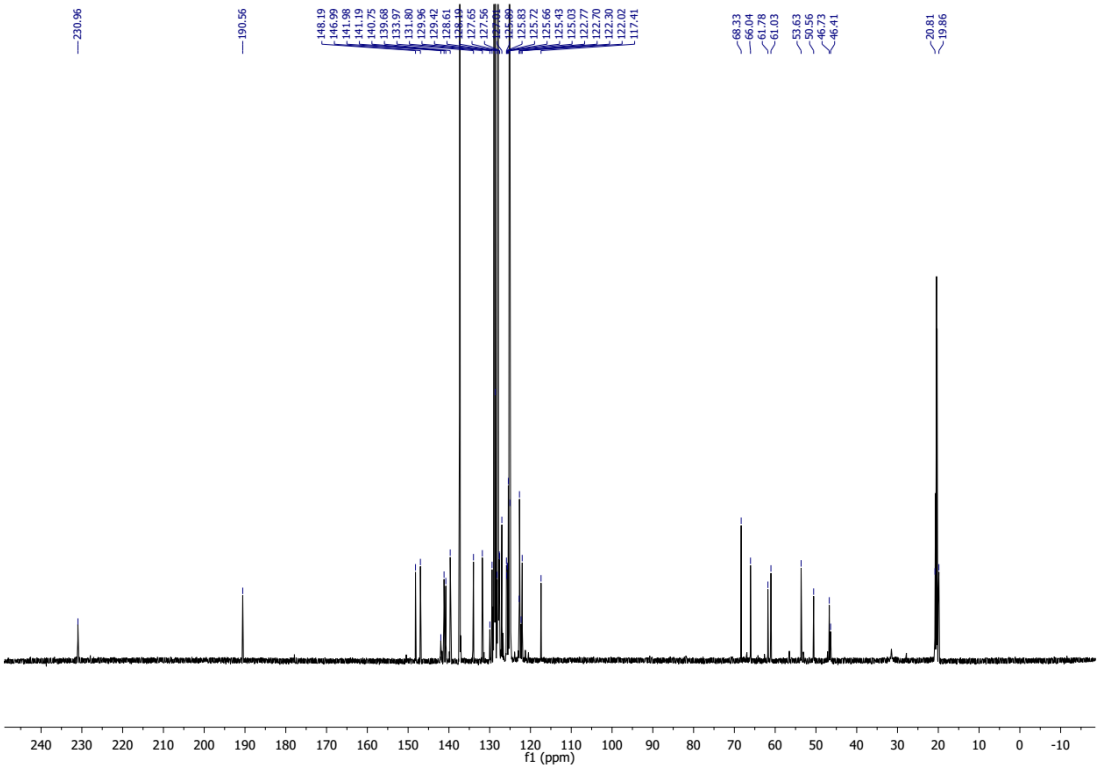
f1 (ppm)

gCOSY:

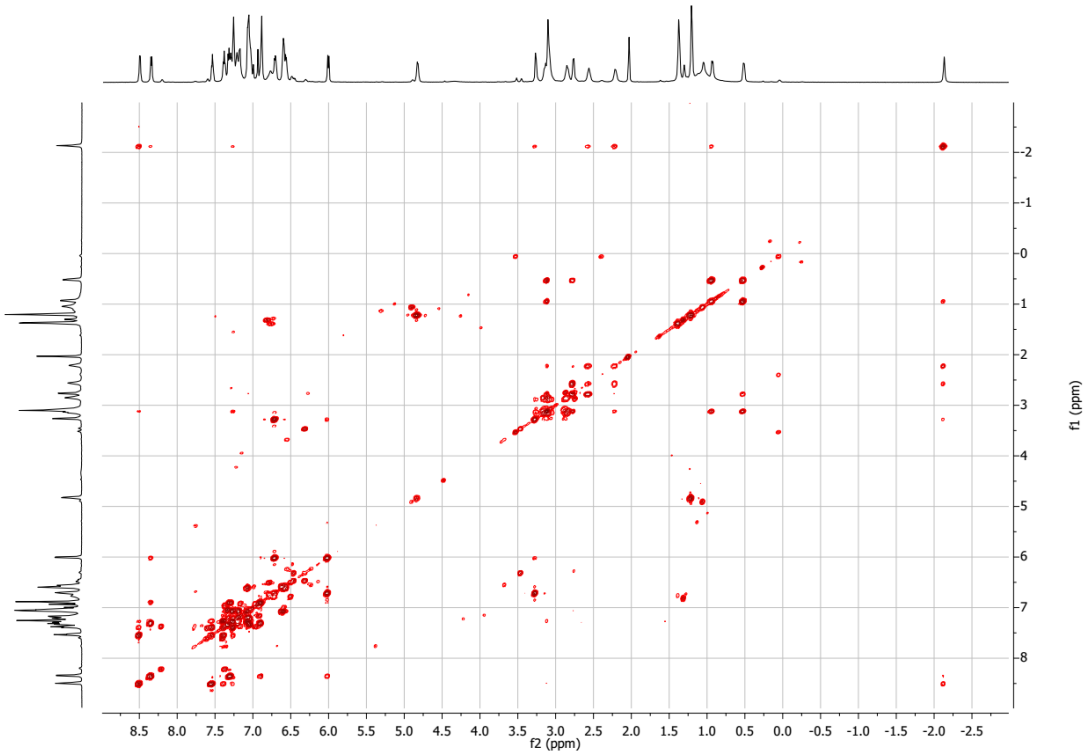

gHSQC:

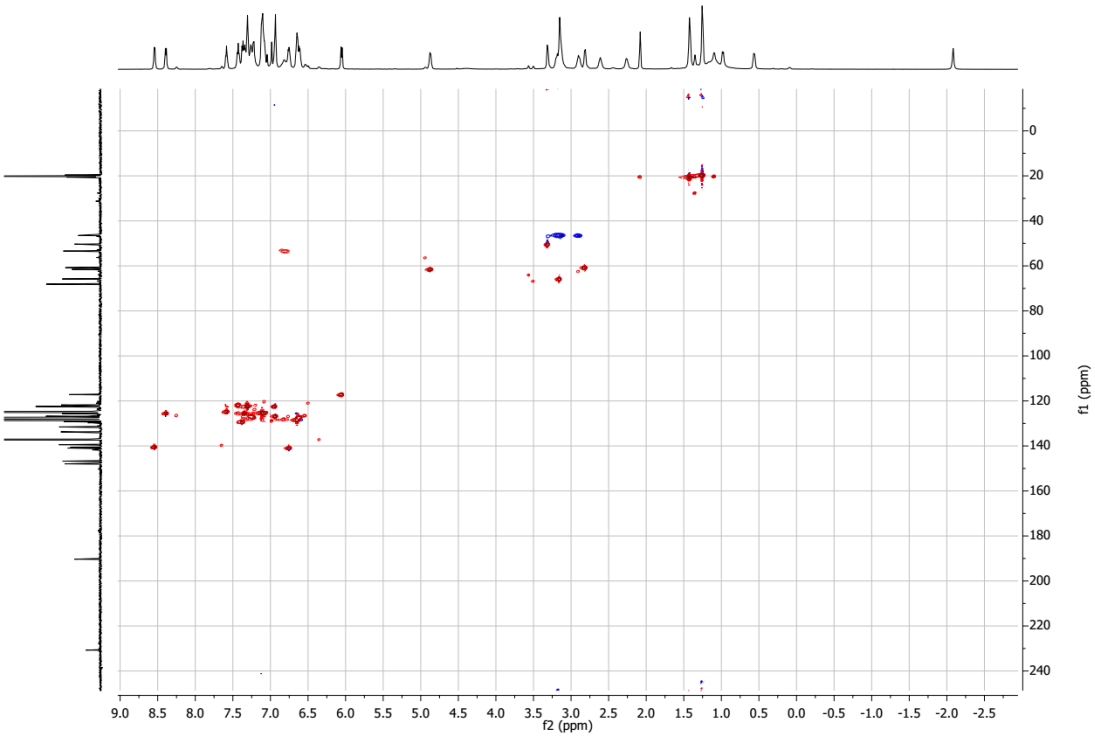

gHMBC:

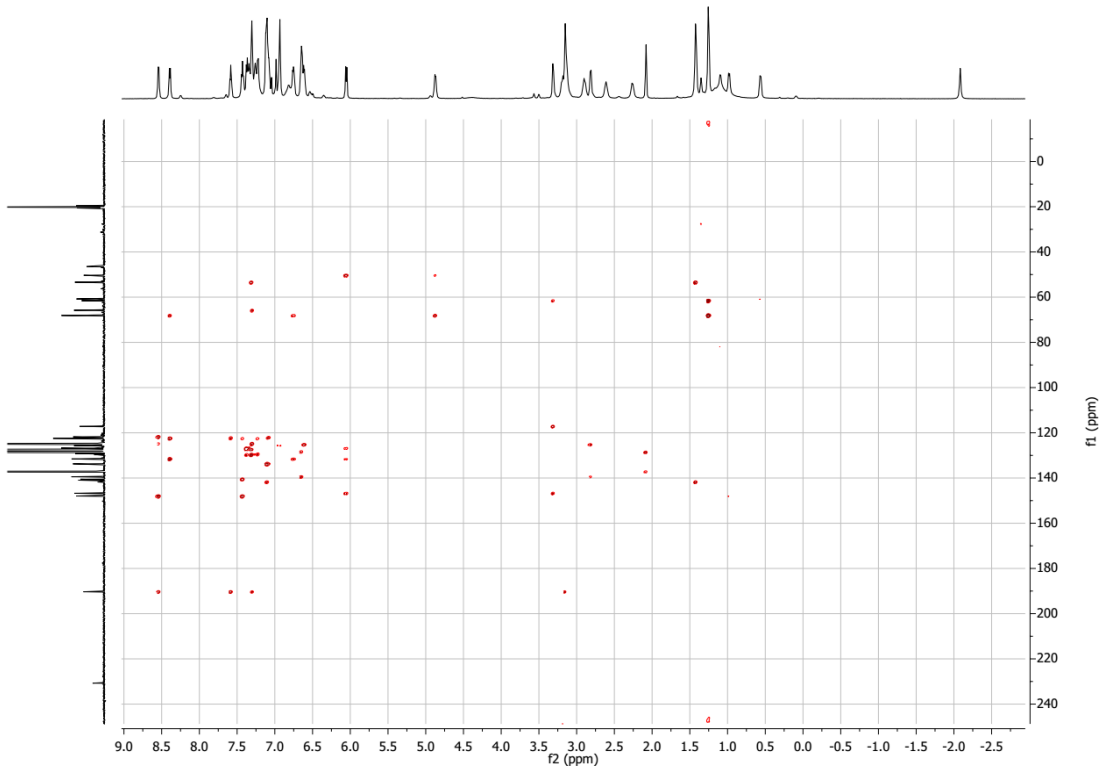

(F) Quantum chemical investigation of the reaction mechanism

1. Computational Details

All calculations for this work have been performed with the Turbomole v7.2.1 program package[6] using DFT with the PBE0 hybrid functional.[7] In addition, the D3 dispersion correction[8] with Becke-Johnson damping[9] is applied to ensure a robust description of dispersive interactions. The solvent effects of toluene have been taken into account using the COSMO implicit solvent model.[10] For the numerical integration, the Turbomole m4 grid was used. SCF convergence was assumed after energy changes of less than 1E-7 a.u., while geometry convergence thresholds were set to 1E-6 a.u. for energy changes and 1E-3 a.u. for the norm of the SCF-energy gradient. Frequency analyses have been performed for all optimized structures to confirm minima and transition states and to calculate Gibbs free energies. For the latter, a correction for small vibrational frequencies[11] was applied. For geometry optimizations, transition state search and frequency analysis, the def2-SVP basis set was employed.[12]

2. Validation: Comparison of Structures

To confirm that the chosen method is suitable to describe the given systems, the crystal structure of the catalyst is geometrically optimized and the obtained bond lengths and angles are compared to the experimentally determined values. A selection of the obtained results is given in Table S1 for the bond lengths and Table S2 for the bond angles. The data show that both the angles and the bond lengths are in overall good agreement.

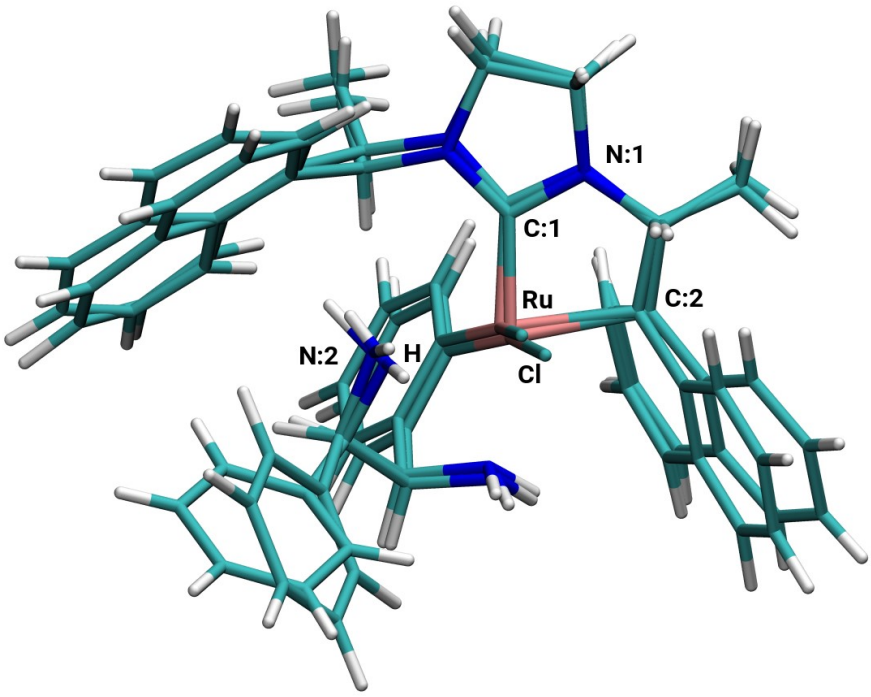

Figure S4. Overlay of the crystal structure and the computationally optimized structure (PBE0/ def2-SVP).

In Figure S4 the results are visualized by overlaying the computationally relaxed structure and the experimental crystal structure. It can be seen that they are in good general agreement. The only exception is the phenyl group, which is not coordinated to Ru and thus can rotate without significant barrier. In conclusion it can be assumed that the chosen method is sufficient to describe the systems investigated.

Table S1. Comparison of bond lengths between the crystal structure and the calculated geometry.

Bond Length (Å)		
	Crystal Structure	DFT (PBE0/def2-SVP)
(Ru)-(Cl)	2.53	2.51
(Ru)-(N:2)	2.16	2.16
(N:2)-(H)	0.92	1.03
(Ru)-(C:1)	1.94	1.95
(Ru)-(C:2)	2.21	2.16
(C:1)-(N:1)	1.38	1.36

Table S2. Comparison of bond angles between the crystal structure and the calculated geometry.

Bond Angle (deg)		
	Crystal Structure	DFT (PBE0/def2-SVP)
(N:2)-(Ru)-(Cl)	78.05	76.82
(H)-(N:2)-(Ru)	98.21	96.43
(N:2)-(Ru)-(C:1)	97.77	101.48
(Ru)-(C:1)-(N:1)	135.10	135.51

3. Conceivable Mechanisms

For the adsorption of the substrate to the catalyst and the transfer of the hydride and the proton to the substrate several reaction pathways and configurations have to be considered. Fortunately, the stoichiometric NMR-experiment conducted allows to identify one of the amino-groups as the proton donor, thus restricting the number of possible mechanisms. In the first set of the remaining possible reaction pathways (Scheme S1) the hydrogen atom bonded to the nitrogen of the catalyst forms a hydrogen-bond to the oxygen on the substrate, and the hydride attacks in β-position of the sulfone group. Second, the proton is transferred to the α-position relative to the same sulfone group. It is conceivable that this pathway can proceed in three different ways: First, a concerted mechanism is possible (1a), where proton and hydride are transferred

at the same time. Then, a stepwise mechanism is possible where the hydride is transferred first, followed by a direct hydrogen transfer (1b). The third possibility (1c) for this mechanism to happen is that after the hydride attacked in β-position (as in 1b) the hydrogen is transferred to the oxygen it was hydrogen-bonded to. The final product is then generated through tautomerization.

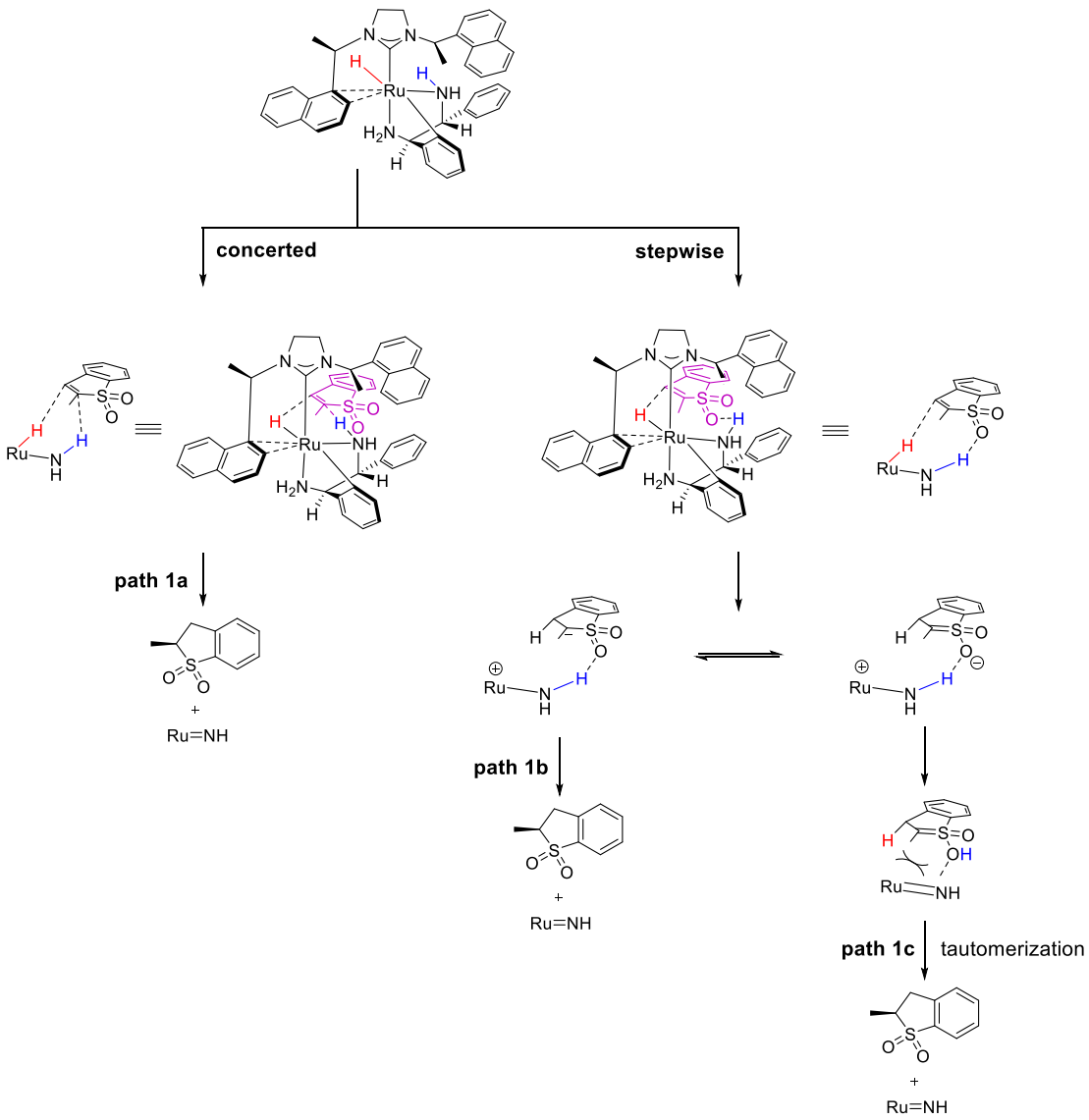

Scheme S1. Proposed mechanisms for the hydrogenation in β-position.

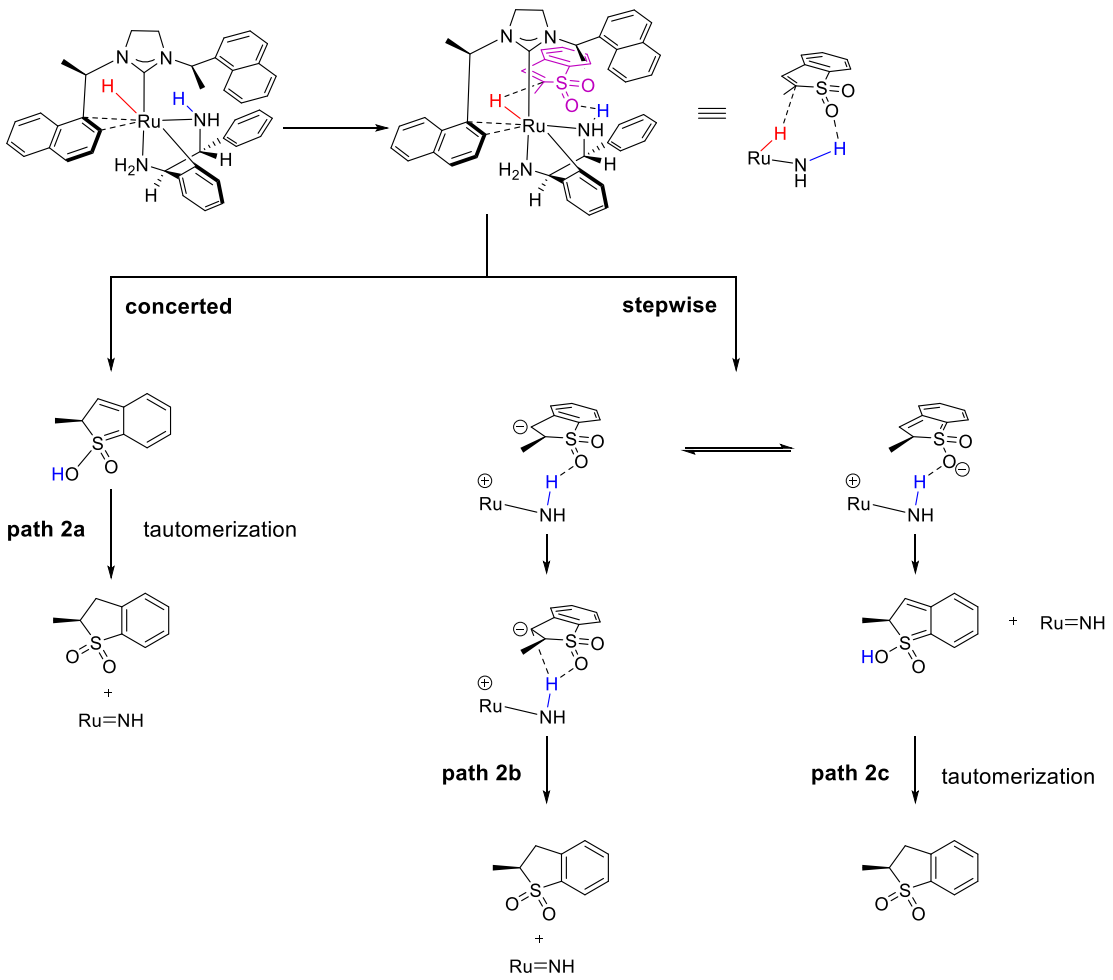

Scheme S2. Proposed mechanisms for the hydrogenation in α-position.

The second set of possible reaction pathways (Scheme S2) is characterized by the transfer of the hydride to the α-position of the sulfone group on the substrate. As for the first pathway, three different mechanisms are conceivable: A concerted mechanism (2a), the formation of a hydrogen bond with subsequent transfer of the hydrogen to the β-position (2b) and the transfer of the hydrogen to the oxygen of the substrate followed by tautomerization to yield the final product (2c). For all possible pathways both the attack to the Re- and to the Si-face of the substrate are explored and compared.

4. Results

4.1. Optimized Structures

All reaction pathways discussed in the following sections have some common structures, whose optimized geometries are presented in this section. First, the general structure of the catalyst is shown, both for the hydrogenated and the dehydrogenated from. Then the substrate and one enantiomer of the product are presented, followed by the precatalysts for both enantiomers. Finally, the product associated to the dehydrogenated catalyst is given for both enantiomers.

The Hydrogenated Catalyst

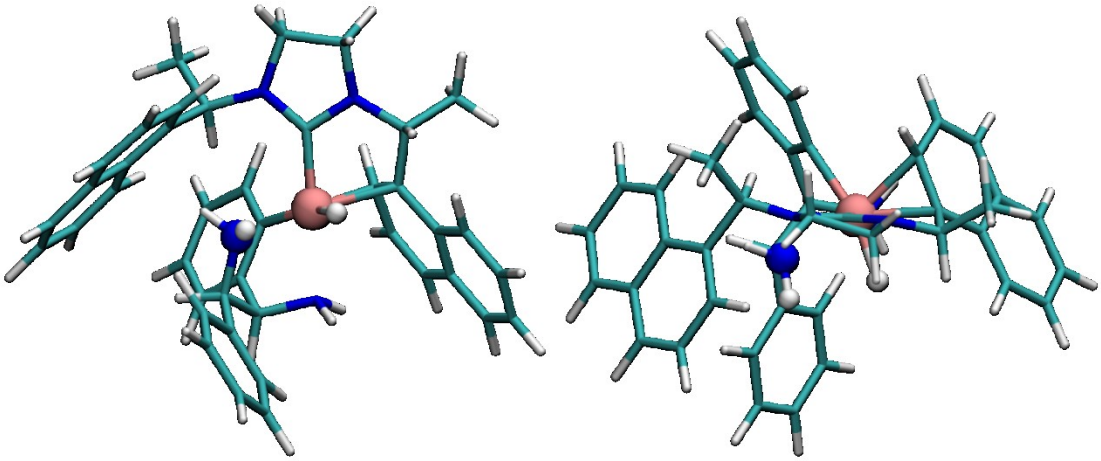

Figure S5. Front view (left) and top view (right) of the structure of the hydrogenated catalyst optimized using PBE0/def2-SVP.

The Dehydrogenated Catalyst

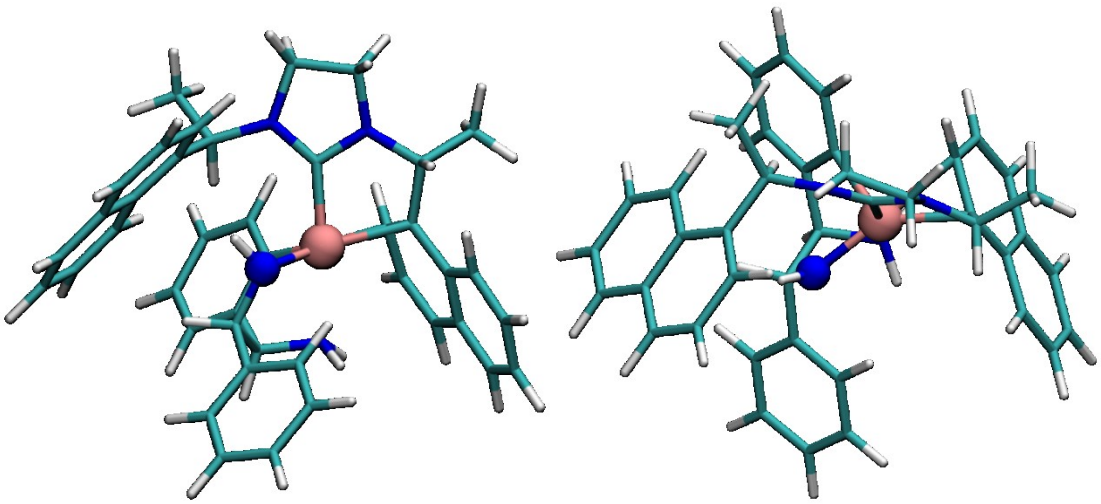

Figure S6. Front view (left) and top view (right) of the structure of the dehydrogenated catalyst optimized using PBE0/def2-SVP.

Starting Material / Substrate

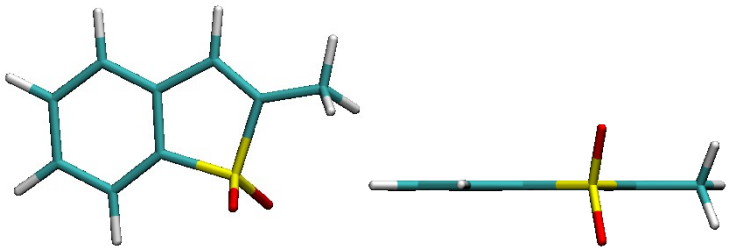

Figure S7. Front view (left) and top view (right) of the structure of the substrate to be hydrogenated in the reaction optimized using PBE0/def2-SVP.

Product [(*S*)-Enantiomer]

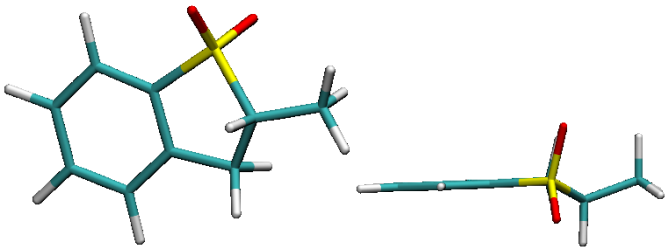

Figure S8. Front view (left) and top view (right) of the structure of the product of the hydrogenation [(*S*)-enantiomer] optimized using PBE0/def2-SVP.

Precatalyst [(*R*)-Product]

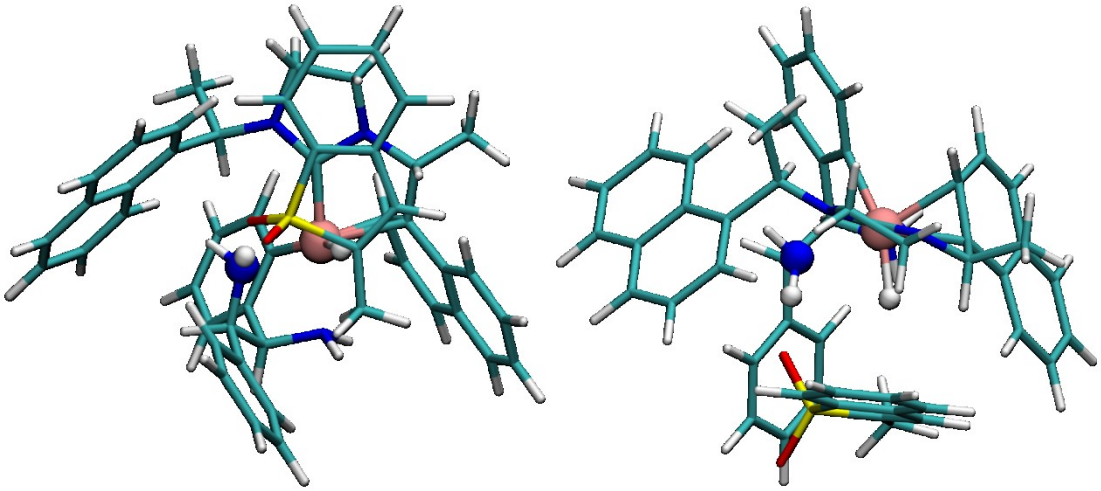

Figure S9. Front view (left) and top view (right) of the structure of the precatalyst formed leading to (*R*)-product optimized using PBE0/def2-SVP.

Precatalyst [(*S*)-Product]

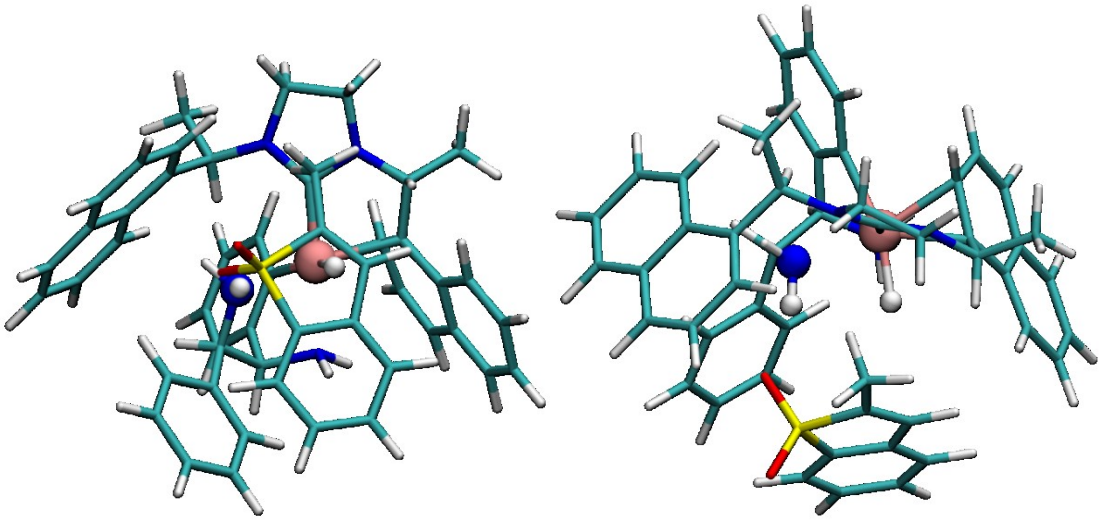

Figure S10. Front view (left) and top view (right) of the structure of the precatalyst formed leading to (*S*)-product optimized using PBE0/def2-SVP.

Product-Catalyst Complex [(*R*)-Product]

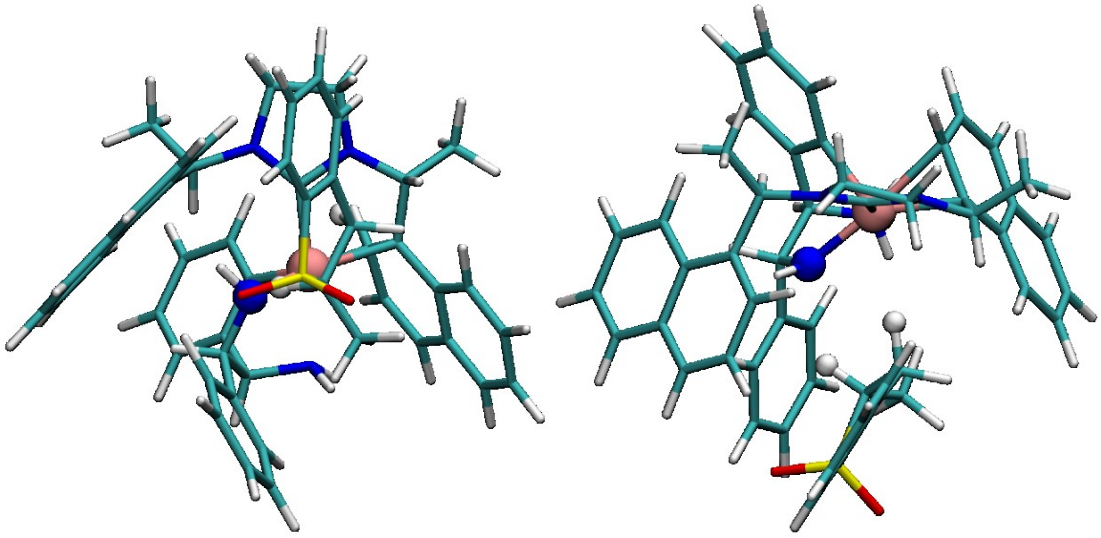

Figure S11. Front view (left) and top view (right) of the structure of the complex between the newly formed product and the dehydrogenated catalyst leading to the (*R*)-product optimized using PBE0/def2-SVP.

Product-Catalyst Complex [(*S*)-Product]

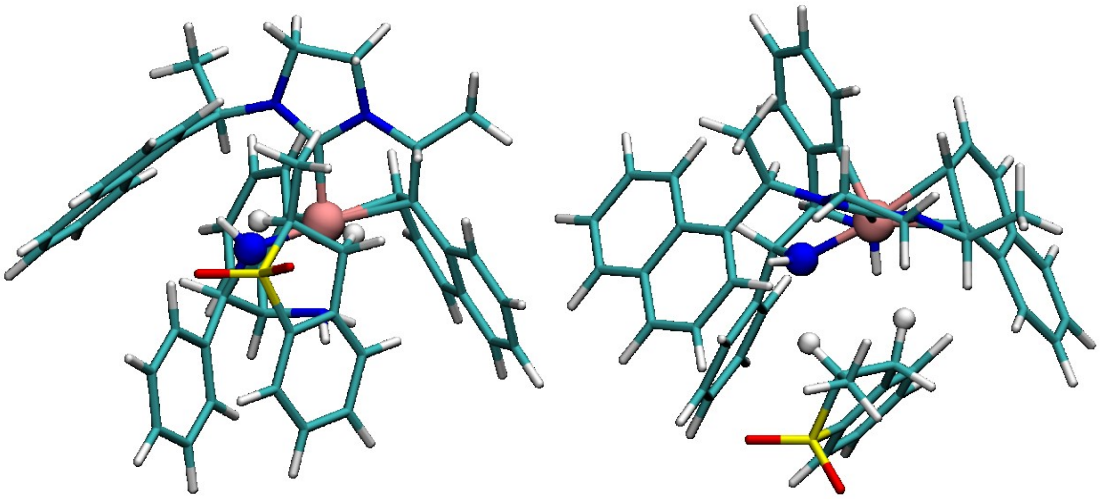

Figure S12. Front view (left) and top view (right) of the structure of the complex between the newly formed product and the dehydrogenated catalyst leading to the (*S*)-product optimized using PBE0/def2-SVP.

4.2. Proton Transfer to the Sulfone Group (Pathways 1c, 2a and 2c)

The reaction pathways 1c, 2a and 2c all have in common that the proton is transferred to the oxygen of the sulfone group and then the final product is formed *via* tautomerization. However, during the exploration of these mechanisms it turned out, that intermediates with the proton transferred to the sulfone group are thermodynamically unstable. Since it was not possible to optimize minimum structures for these intermediates, the general thermodynamics of the reaction was investigated by calculating the Gibbs free energy of the optimized isolated molecules (as shown in Scheme S3). As a result of this study it turned out that the isolated products of the proton transfer to the sulfone group are destabilized by 66.4 kcal/mol, ruling out all mechanisms including this step (Pathways 1c, 2a and 2c).

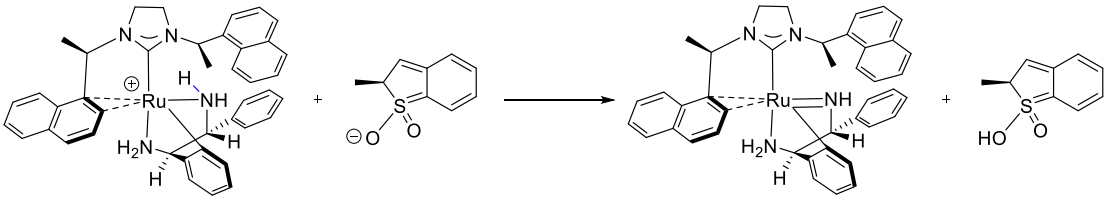

Scheme S3. Model reaction to explore the general thermodynamics of a proton transfer to the oxygen of the sulfone group at the substrate.

4.3. Pathway 1a

Reaction pathway 1a corresponds to a concerted mechanism where the hydride is transferred to the β-position of the sulfone group and at the same time the proton is transferred to the α-position (Scheme S4). For this pathway a mechanism leading to the (*S*)-product and one leading to the (*R*)-product have been optimized and the calculated Gibbs free energy for each optimized structure is given in Table S3 and Figure S13. For both pathways, first a pre-complex (PC / C8⋯3a) is formed from the starting materials (SMs / C8+3a). Then via a single transition state (TS) the products (P⋯Cat / C7⋯4a) are formed, which then dissociate (P+Cat / C7+4a). One can see that the precatalyst leading to the (*R*)-product is 2.4 kcal/mol more stable than that leading to the (*S*)-product. However, the transition state is 3.2 kcal/mol more stable for the (*S*)-product. This leads to an overall barrier of 9.0 kcal/mol for the formation of the (*R*)-product and a barrier of 3.4 kcal/mol to generate the (*S*)-product.

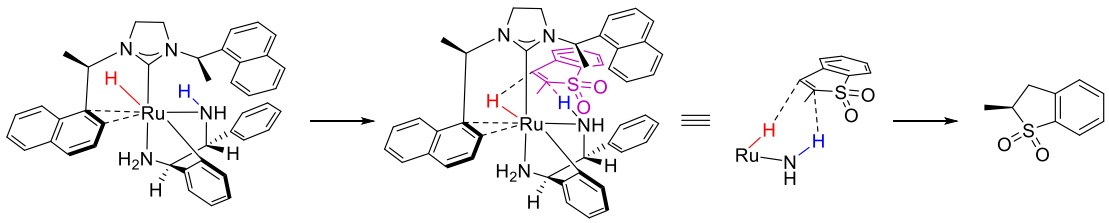

Scheme S4. Schematic mechanism for the reaction pathway 1a leading to the (*S*)-product.

Table S3. Relative Gibbs free energies for pathway 1a leading to the (*R*)- and (*S*)-product. All values are given in kcal/mol (PBE0/def2-SVP).

	SM	**PC**	**TS**	**P⋯Cat**	**P+Cat**
(*S*)-Product	0.0	–0.8	2.6	–20.9	–21.0
(*R*)-Product	0.0	–3.2	5.8	–21.0	–21.0

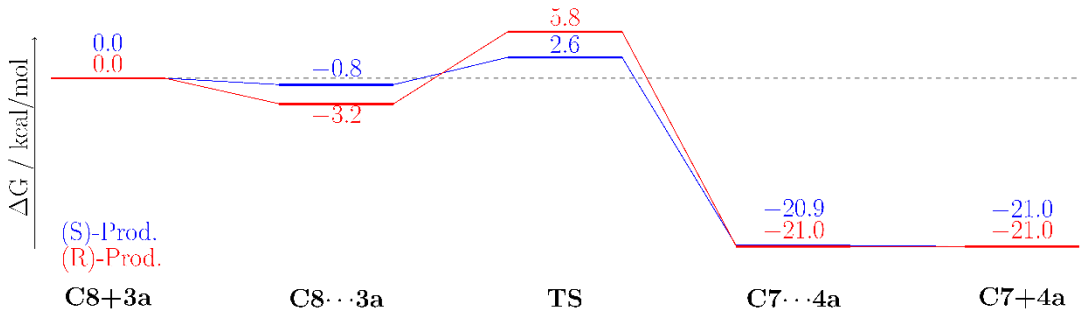

Figure S13. Relative Gibbs free energies for pathway 1a leading to the (*R*)- and (*S*)-product (PBE0/def2-SVP).

Transition-State [(*R*)-Product]

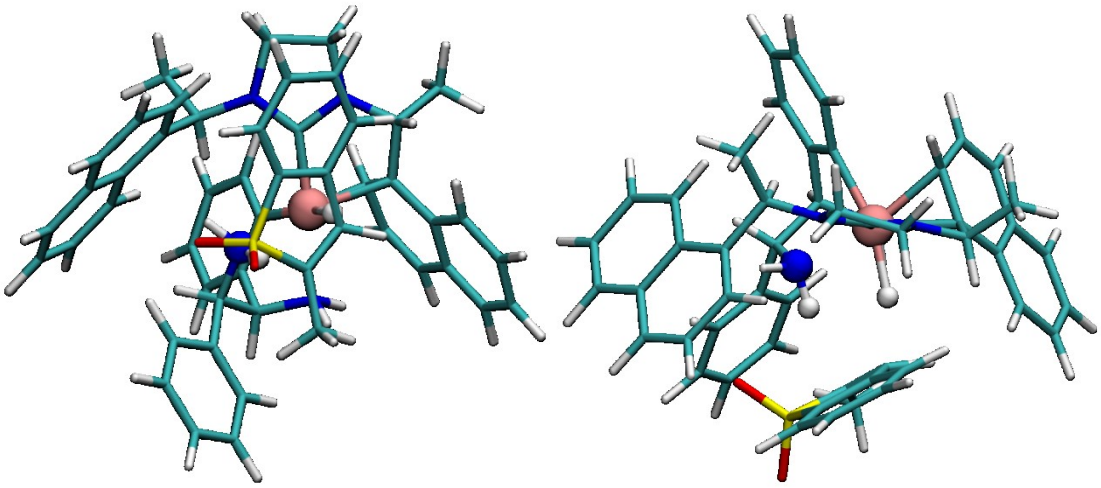

Figure S14. Front view (left) and top view (right) of the transition state in a concerted mechanism with the hydride transferred to β-position leading to the (*R*)-product optimized using PBE0/def2-SVP.

Transition-State [(*S*)-Product]

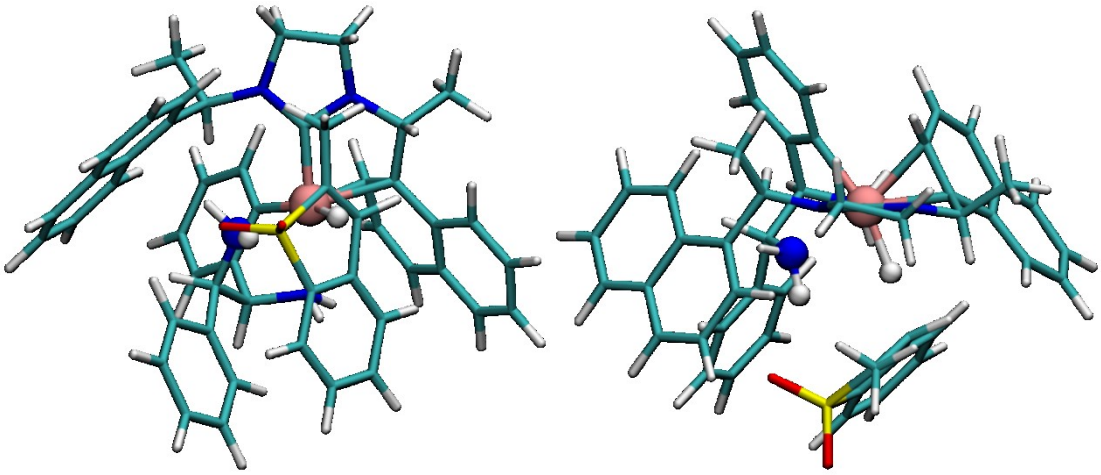

Figure S15. Front view (left) and top view (right) of the transition state in a concerted mechanism with the hydride transferred to β-position leading to the (*S*)-product optimized using PBE0/def2-SVP.

4.4. Pathway 1b

Reaction pathway 1b corresponds to a stepwise mechanism in which the hydride is transferred to the β-position relative to the sulfone group. Then, in a second step the proton is transferred to the α-position (see Scheme S5). The Gibbs free energies for all optimized structures are given in Table S4 and Figure S16. For both, the pathways leading to the (*R*)- and (*S*)-product, the starting materials form a pre-catalyst. Afterwards, the hydride is transferred to the β-position *via* a first transition-state (TS1) yielding the intermediate (IN). For the mechanism leading to the (*S*)-product this barrier is 3.4 kcal/mol. However, the barrier for the mechanism leading to the (*R*)-product is 39.4 kcal/mol, thus ruling out his pathway. For that reason only the pathway leading to the (*S*)-product was further investigated. As a next step in this pathway the proton is transferred *via* a second transition state (TS2) to the α-position with a barrier of 2.8 kcal/mol yielding the (*S*)-product.

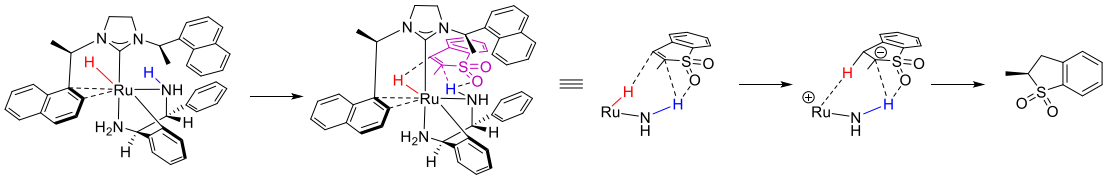

Scheme S5. Schematic mechanism for the reaction pathway 1b leading to the (*S*)-product.

Table S4. Relative Gibbs free energies for pathway 1b leading to the (*R*)- and (*S*)-product. All values are given in kcal/mol (PBE0/def2-SVP).

	SM	PC	TS1	IN	TS2	P···Cat	P+Cat
(*S*)-Product	0.0	–0.8	2.9	–9.6	–6.8	–20.9	–21.0
(*R*)-Product	0.0	–3.2	36.2	–10.3	—	–21.0	–21.0

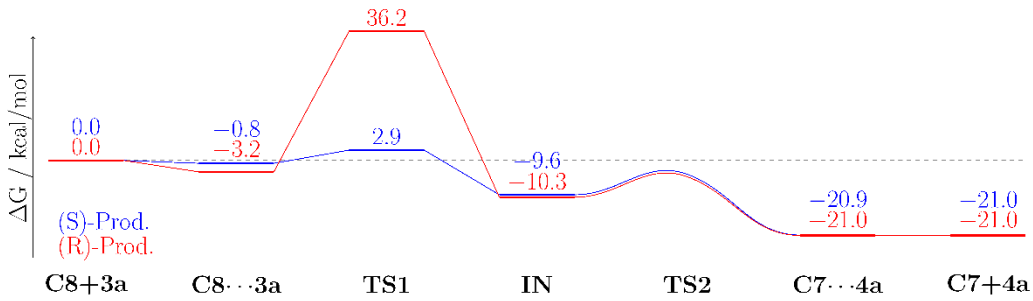

Figure S16. Relative Gibbs free energies for pathway 1b leading to the (*R*)- and (*S*)-product (PBE0/def2-SVP).

Transition-State [(*R*)-Product]

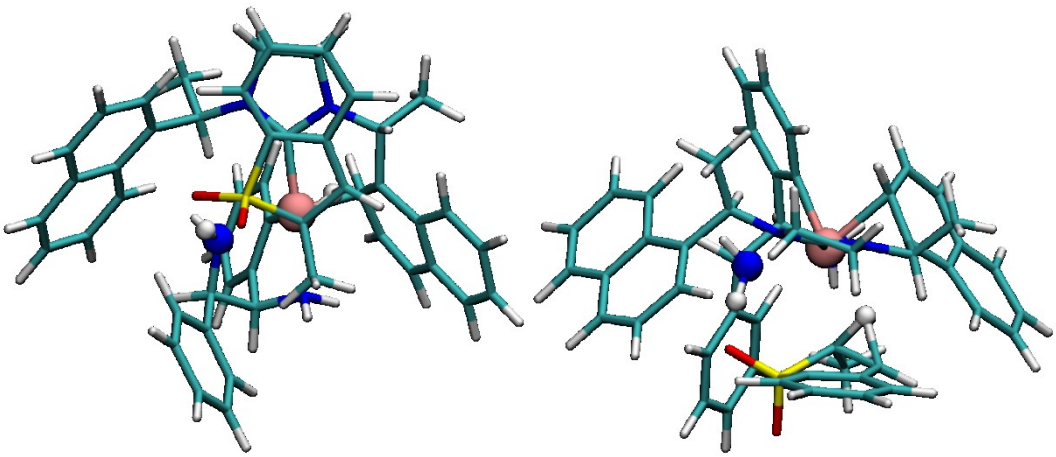

Figure S17. Front view (left) and top view (right) of the transition state for the hydride transfer to β-position in a configuration leading to the (*R*)-product optimized using PBE0/def2-SVP.

Transition-State [(*S*)-Product]

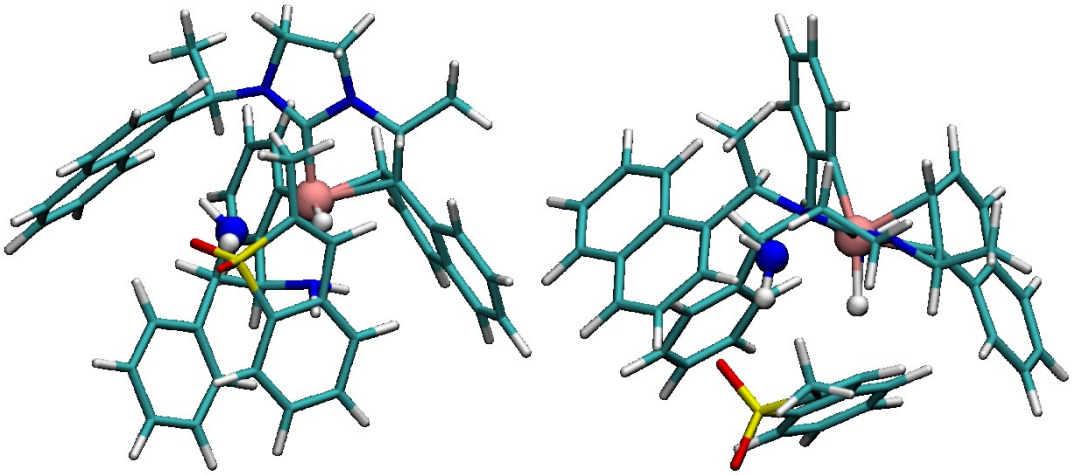

Figure S18. Front view (left) and top view (right) of the transition state for the hydride transfer to β-position in a configuration leading to the (*S*)-product optimized using PBE0/def2-SVP.

Intermediate [(*R*)-Product]

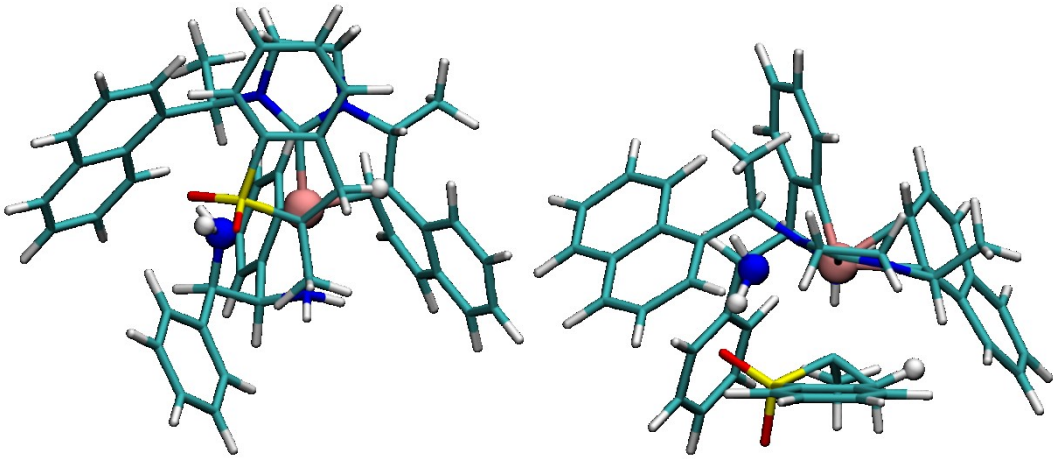

Figure S19. Front view (left) and top view (right) of the intermediate where the hydride is transferred to β-position in a configuration leading to the (*R*)-product optimized using PBE0/def2-SVP.

Intermediate [(*S*)-Product]

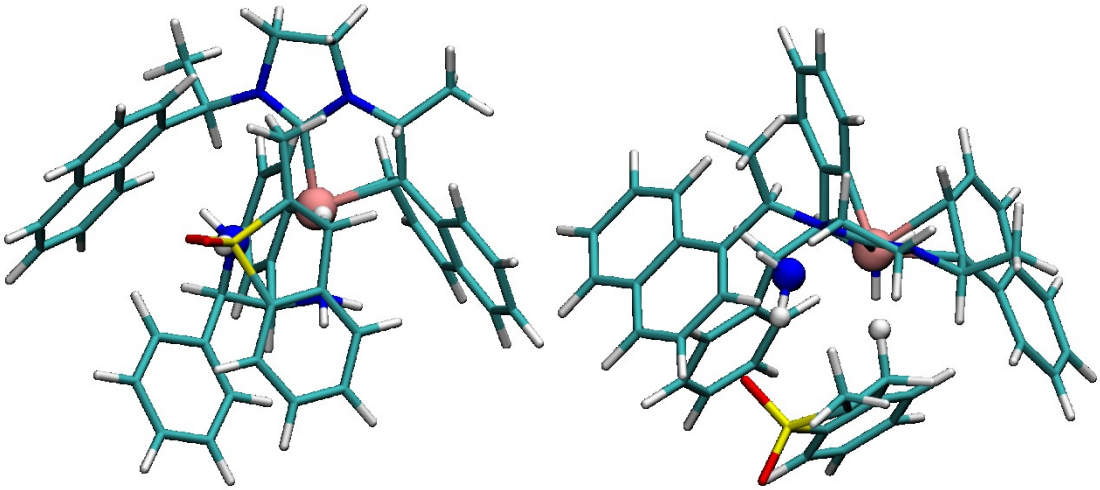

Figure S20. Front view (left) and top view (right) of the intermediate where the hydride is transferred to β-position in a configuration leading to the (*S*)-product optimized using PBE0/def2-SVP.

4.5. Pathway 2b

Reaction pathway 2b corresponds to a stepwise mechanism in which in a first step the hydride is transferred to the α-position relative to the sulfone group. Afterwards the proton is transferred to the corresponding β-position (Scheme S6). Both mechanisms [yielding the (*R*)- and (*S*)-product, respectively] were calculated and the Gibbs free energies are given in Table S5 and Figure S21. First, the starting materials form a pre-catalyst from which the hydride is transferred to the α-position relative to the sulfone group *via* a first transition-state. With a barrier of 10.8 kcal/mol for the mechanism leading to the (*S*)-product and 7.1 kcal/mol for the mechanism leading to the (*R*)-product, the reaction barriers of both pathways are higher than the corresponding barriers found for pathway 1b and 2b. As a result, the transition states for the second step, i.e., the transfer of the proton to the β-position, have not been investigated any further.

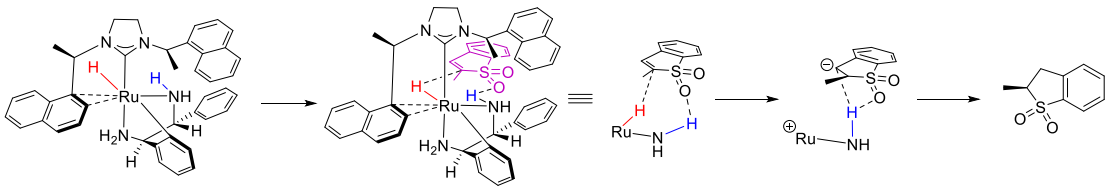

Scheme S6. Schematic mechanism for the reaction pathway 2b leading to the (*S*)-product.

Table S5. Relative Gibbs free energies for pathway 2b leading to the (*R*)- and (*S*)-product. All values are given in kcal/mol (PBE0/def2-SVP).

	SM	PC	TS1	IN	TS2	P···Cat	P+Cat
(*S*)-Product	0.0	–0.8	10.0	–27.7	—	–20.9	–21.0
(*R*)-Product	0.0	–3.2	3.9	–18.5	—	–21.0	–21.0

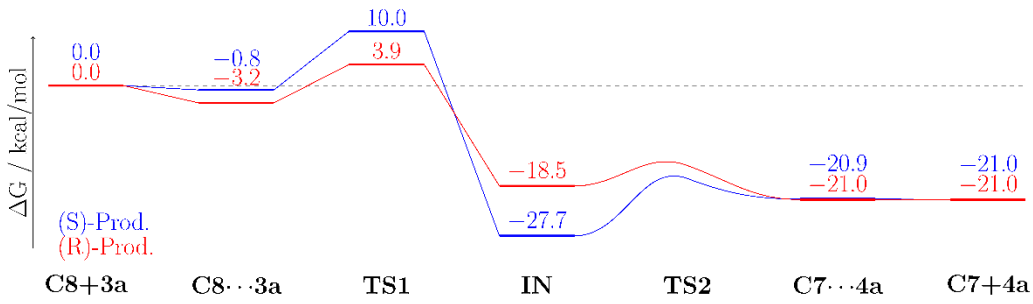

Figure S21. Relative Gibbs free energies for pathway 2b leading to the (*R*)- and (*S*)-product (PBE0/def2-SVP).

Transition-State [(*R*)-Product]

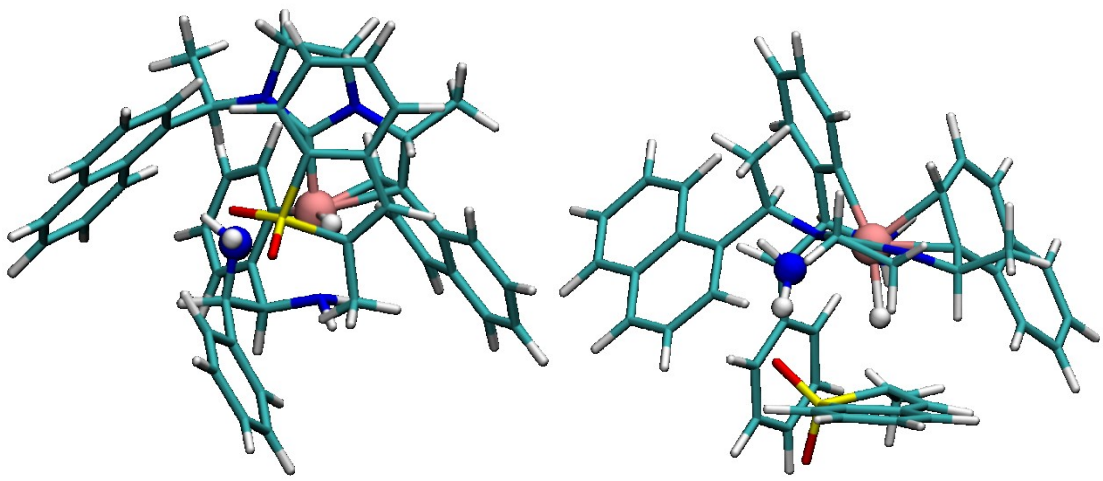

Figure S22. Front view (left) and top view (right) of the transition state for the hydride transfer to α-position in a configuration leading to the (*R*)-product optimized using PBE0/def2-SVP.

Transition-State [(*S*)-Product]

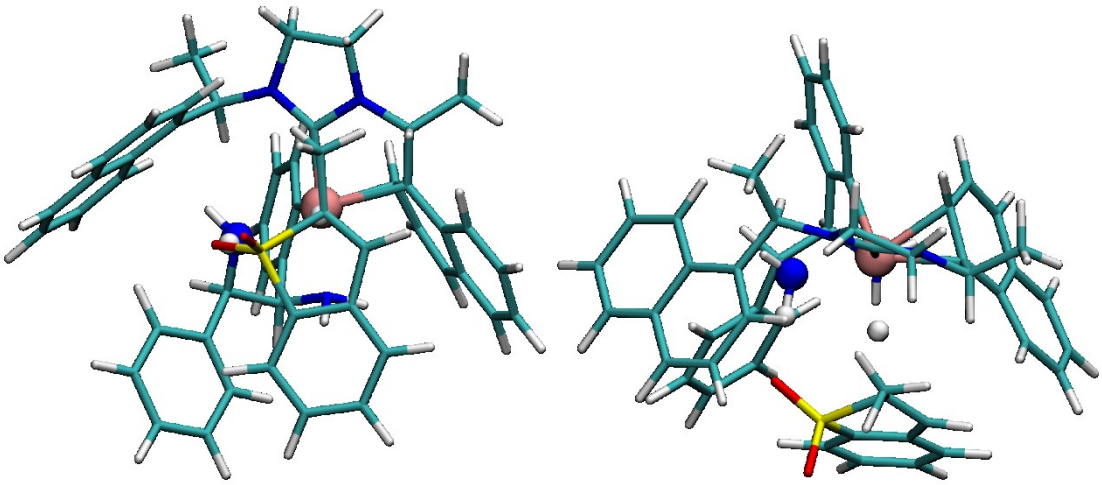

Figure S23. Front view (left) and top view (right) of the transition state for the hydride transfer to α-position in a configuration leading to the (*S*)-product optimized using PBE0/def2-SVP.

Intermediate [(*R*)-Product]

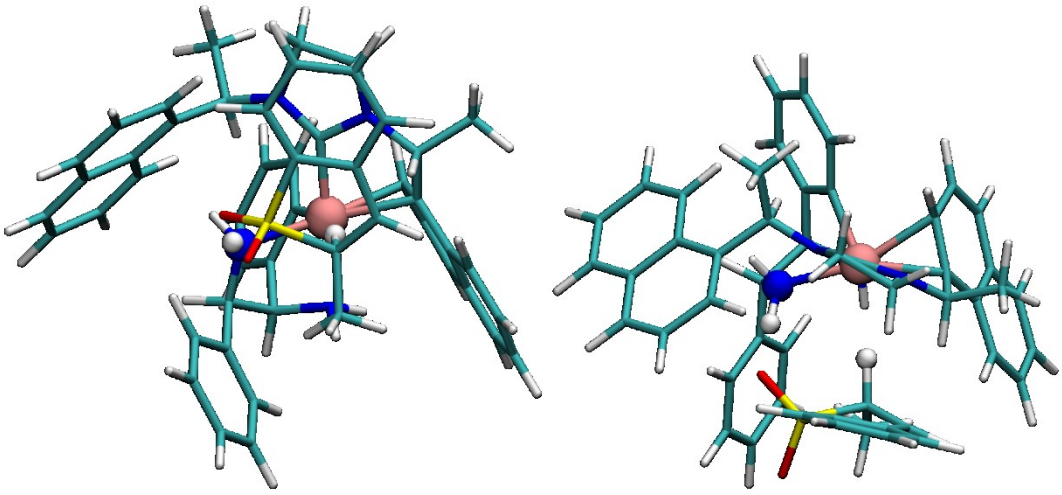

Figure S24. Front view (left) and top view (right) of the intermediate where the hydride is transferred to α-position in a configuration leading to the (*R*)-product optimized using PBE0/def2-SVP.

Intermediate [(*S*)-Product]

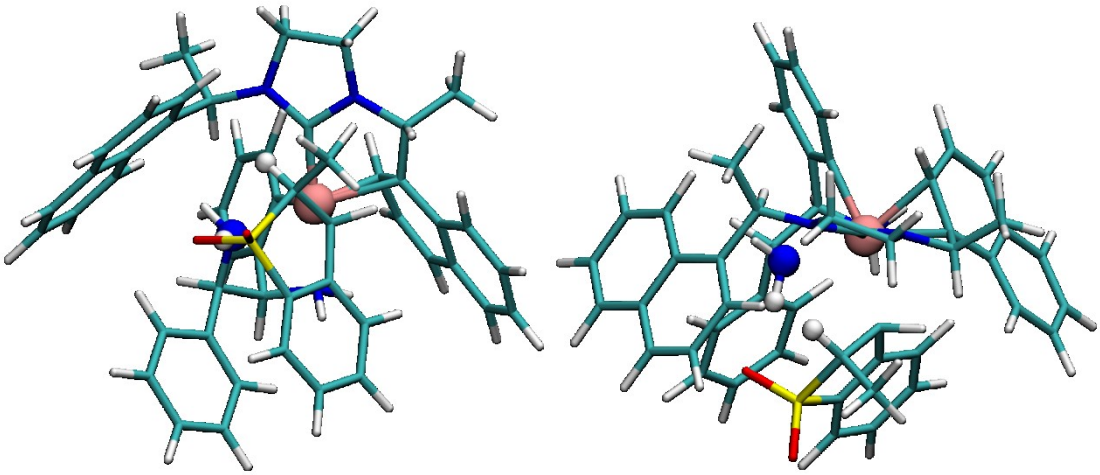

Figure S25. Front view (left) and top view (right) of the intermediate where the hydride is transferred to α-position in a configuration leading to the (*S*)-product optimized using PBE0/def2-SVP.

5. Discussion

As shown in Section 3 there are 6 conceivable mechanisms which can yield the (*S*)- and the (*R*)-product. In Section 4.2 the pathways including a proton transfer to the oxygen of the sulfone group on the substrate (pathways 1c, 2a and 2c) have been further investigated for their general thermodynamics and on that basis could be ruled out. During the exploration of the remaining mechanisms it became evident that the reaction barriers for the hydride transfer tend to be higher than the barriers for the proton transfer. For this reason, only the transition states for the hydride transfer of mechanism 1a, 1b and 2b yielding the (*S*)- and the (*R*)-product have been optimized in a first step. The activation energies resulting from these transition states are summarized in Table S6. The two mechanisms with the lowest activation energy for the first reaction step both lead to the (*S*)-product and transfer the hydride to the β-position of the substrate. Moreover, both mechanisms are very similar with the only difference being that pathway 1a corresponds to a concerted mechanism with an activation energy of 3.4

kcal/mol, while pathway 1b happens in a stepwise fashion with the highest activation energy being the hydride transfer with 3.7 kcal/mol. Due to the similarity of the mechanism and the similar reaction barriers the transition states have been compared in detail. We found that they are identical except for rotations of side groups. In order to clarify to which reaction pathway the transition state actually belongs, an intrinsic reaction coordinate exploration has been performed. It showed that the reaction coordinate from the transition state belongs to the stepwise mechanism 1b. The remaining transition state for the proton transfer in step two of pathway 1b was calculated with a Gibbs free energy of –6.8 kcal/mol, and the associated activation energy is 3.2 kcal/mol. The full reaction pathway is shown in Figure S26. It can be seen that the activation energy for the proton transfer is lower than that for the hydride transfer and consequently, pathway 1b provides the most favorable mechanism for this reaction.

Table S6. Summary of the activation energies for the hydride transfer (PBE0/def2-SVP).

Mechanism	**Enantiomer**	**Barrier**
1a	(*R*)	9.0 kcal/mol
	(*S*)	3.4 kcal/mol
1b	(*R*)	39.4 kcal/mol
	(*S*)	3.7 kcal/mol
1c	(*R*)	Excluded due to unfavorable proton transfer
	(*S*)	
2a	(*R*)	Excluded due to unfavorable proton transfer

	(*S*)	
2b	(*R*)	7.1 kcal/mol
	(*S*)	10.8 kcal/mol
2c	(*R*)	Excluded due to unfavorable proton transfer
	(*S*)	

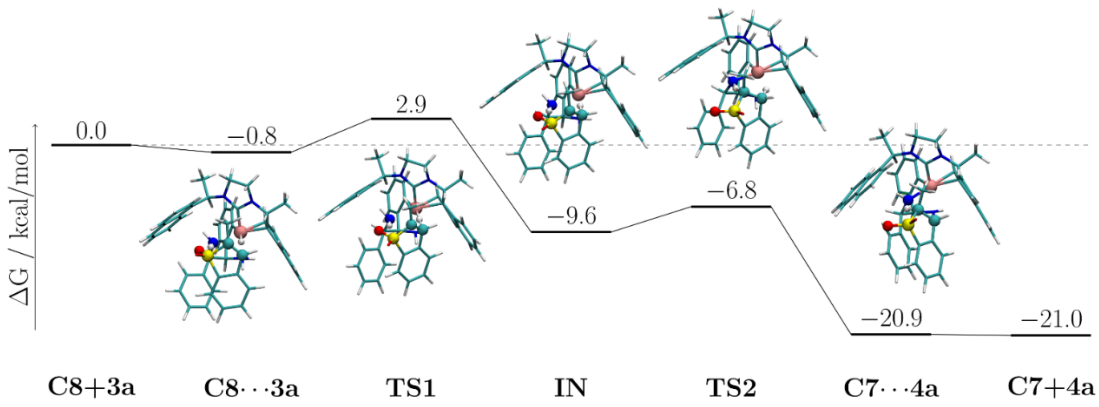

Figure S26. Final reaction pathway (1b) with the overall lowest activation energies (PBE0/def2-SVP).

(G) References

(1) Urban, S.; Ortega, N.; Glorius, F. *Angew. Chem., Int. Ed.* **2011**, *50*, 3803.

(2) Sun, X.; Wang, S.; Sun, S.; Zhu, J.; Deng, J. *Synlett* **2005**, 2776.

(3) Li, W.; Wiesenfeldt. M. P.; Glorius, F. *J. Am. Chem. Soc.* **2017**, *139*, 2585.

(4) (a) Tosatti, P.; Pfaltz, A. *Angew. Chem., Int. Ed.* **2017**, *56*, 4579. (b) Luyksaar, S. I.; Migulin, V. A.; Nabatov, B. V.; Krayushkin, M. M. *Russ. Chem. Bull., Int. Ed.* **2010**, *59*, 446.

(5) Winn, C. L.; Guillen, F.; Pytkowicz, J.; Roland, S.; Mangeney, P.; Alexakis, A. *J. Organomet. Chem.* **2005**, *690*, 5672.

(6) TURBOMOLE V7.2.1 2017, a development of University of Karlsruhe and Forschungszentrum Karlsruhe GmbH, 1989-2007, TURBOMOLE GmbH, since 2007; available from http://www.turbomole.com.

(7) Perdew, J. P.; Ernzerhof, M.; Burke, K. *J. Chem. Phys.* **1996**, *105*, 9982–9985.

(8) Grimme, S.; Antony, J.; Ehrlich, S.; Krieg, H. *J. Chem. Phys.* **2010**, *132*, 154104.

(9) Grimme, S.; Ehrlich, S.; Goerigk, L. *J. Comp. Chem.* **2011**, *32*, 1456–1465.

(10) Klamt, A.; Schürmann, G. *J. Chem. Soc., Perkin Trans. 2* **1993**, 799–805.

(11) Grimme, S. *Chem. Eur. J.* **2012**, *18*, 9955–9964.

(12) Weigend, F.; Ahlrichs, R. *Phys. Chem. Chem. Phys.* **2005**, *7*, 3297–3305.

(H) Copies of NMR spectra

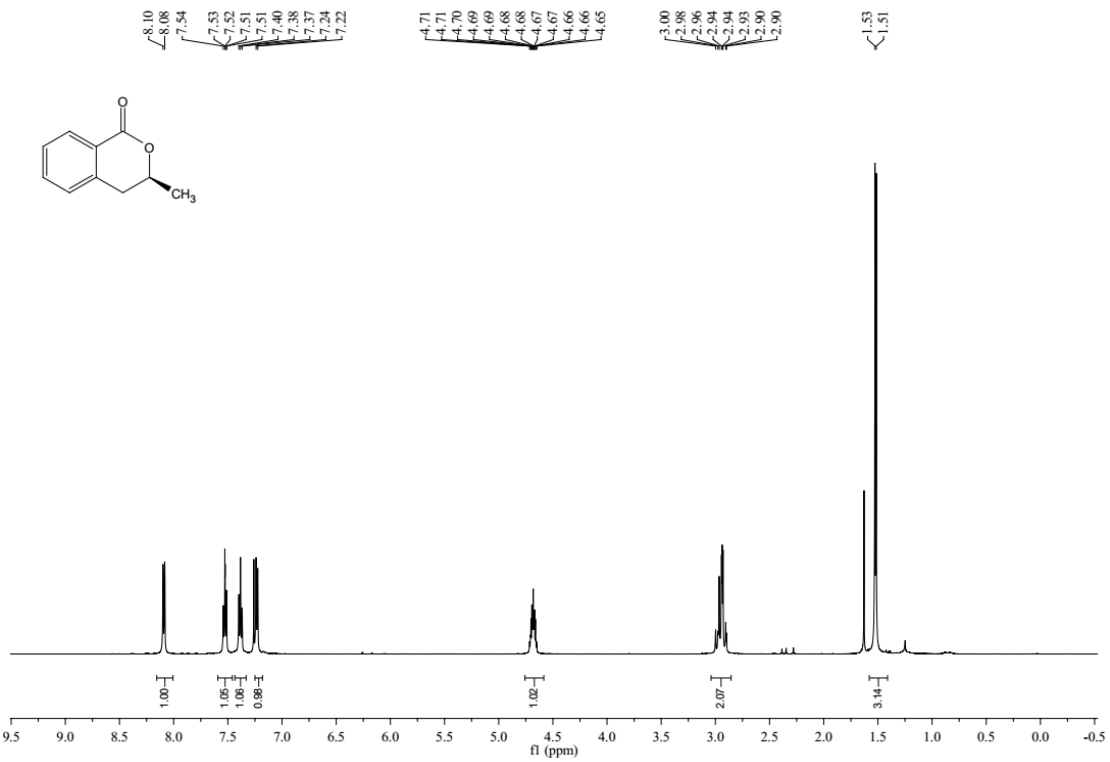
8.10
8.08
7.54
7.53
7.52
7.51
7.51
7.40
7.38
7.37
7.24
7.22
4.71
4.71
4.70
4.69
4.69
4.68
4.68
4.67
4.67
4.66
4.66
4.65
3.00
2.98
2.96
2.94
2.94
2.93
2.90
2.90
1.53
1.51
O
O
CH3
1.00
1.05
1.00
0.98
1.02
2.07
3.14
9.5 9.0 8.5 8.0 7.5 7.0 6.5 6.0 5.5 5.0 4.5 4.0 3.5 3.0 2.5 2.0 1.5 1.0 0.5 0.0 -0.5
f1 (ppm)

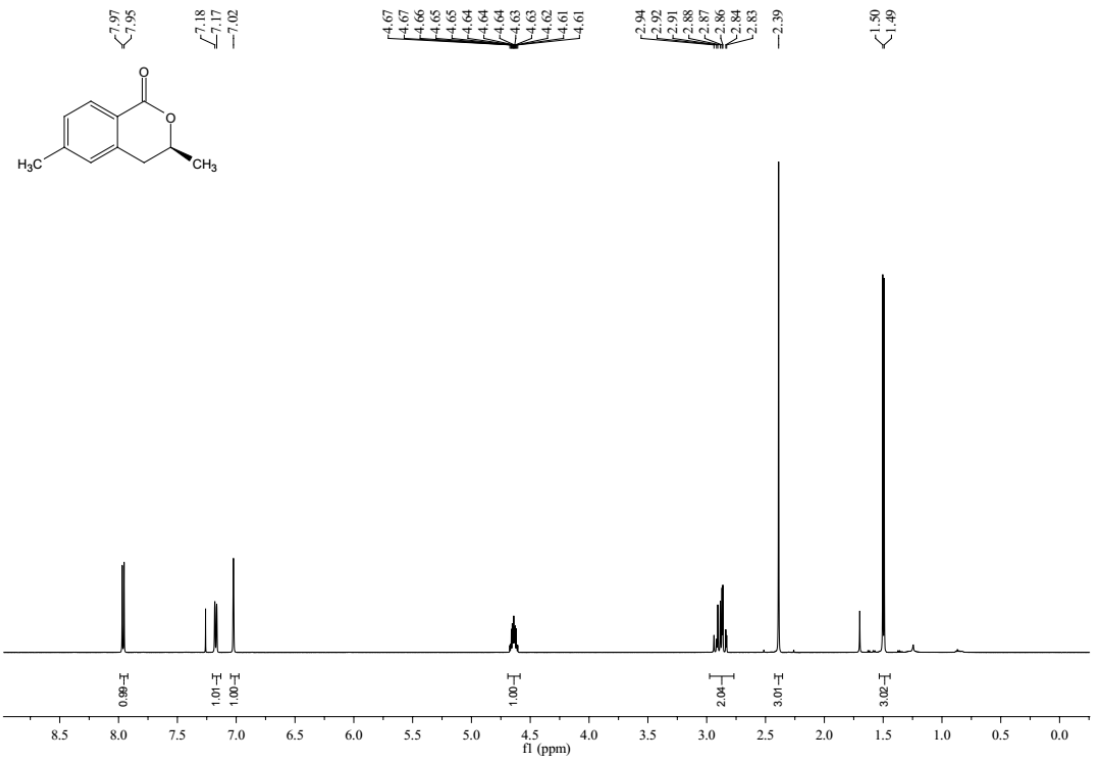
7.97
7.95
7.18
7.17
7.02
4.67
4.67
4.66
4.65
4.65
4.64
4.64
4.64
4.63
4.63
4.62
4.61
4.61
2.94
2.92
2.91
2.88
2.87
2.86
2.84
2.83
2.39
1.50
1.49
O
O
H3C
CH3
0.99
1.01
1.00
1.00
2.04
3.01
3.02
8.5 8.0 7.5 7.0 6.5 6.0 5.5 5.0 4.5 4.0 3.5 3.0 2.5 2.0 1.5 1.0 0.5 0.0
f1 (ppm)

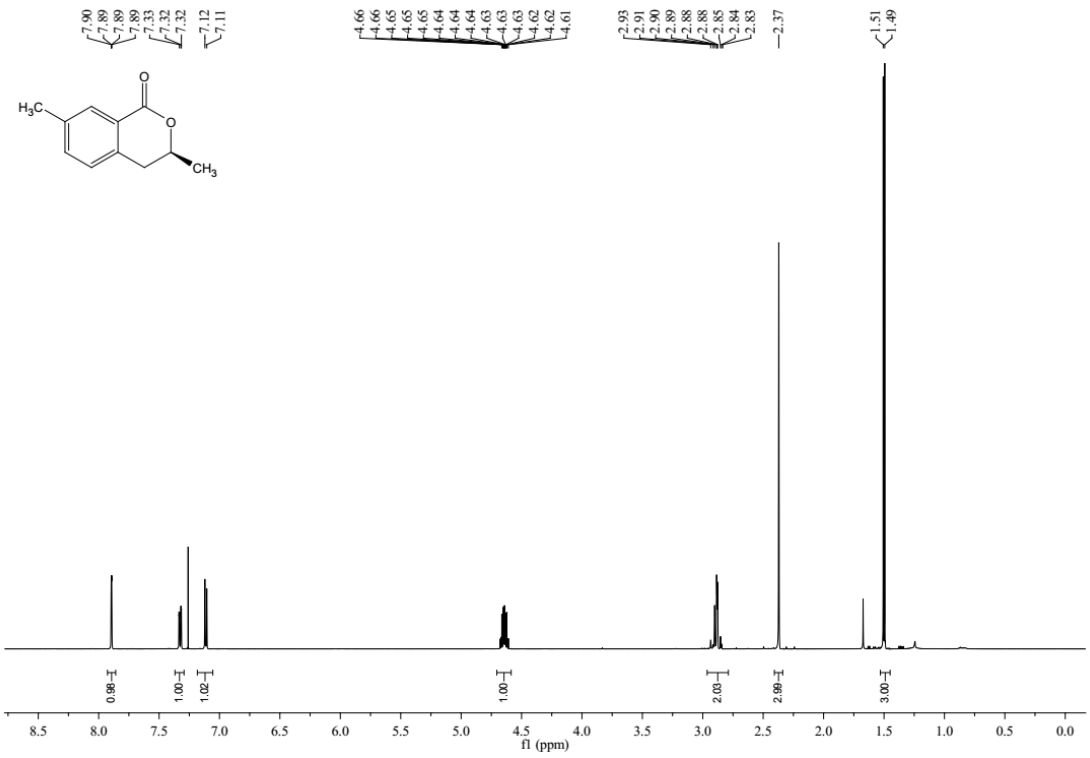
7.90
7.89
7.89
7.89
7.33
7.32
7.32
7.12
7.11
4.66
4.66
4.65
4.65
4.65
4.64
4.64
4.64
4.63
4.63
4.63
4.62
4.62
4.61
2.93
2.91
2.90
2.89
2.88
2.88
2.85
2.84
2.83
2.37
1.51
1.49
O
H3C
O
CH3
0.98
1.00
1.02
1.00
2.03
2.99
3.00
8.5
8.0
7.5
7.0
6.5
6.0
5.5
5.0
4.5
4.0
3.5
3.0
2.5
2.0
1.5
1.0
0.5
0.0
f1 (ppm)

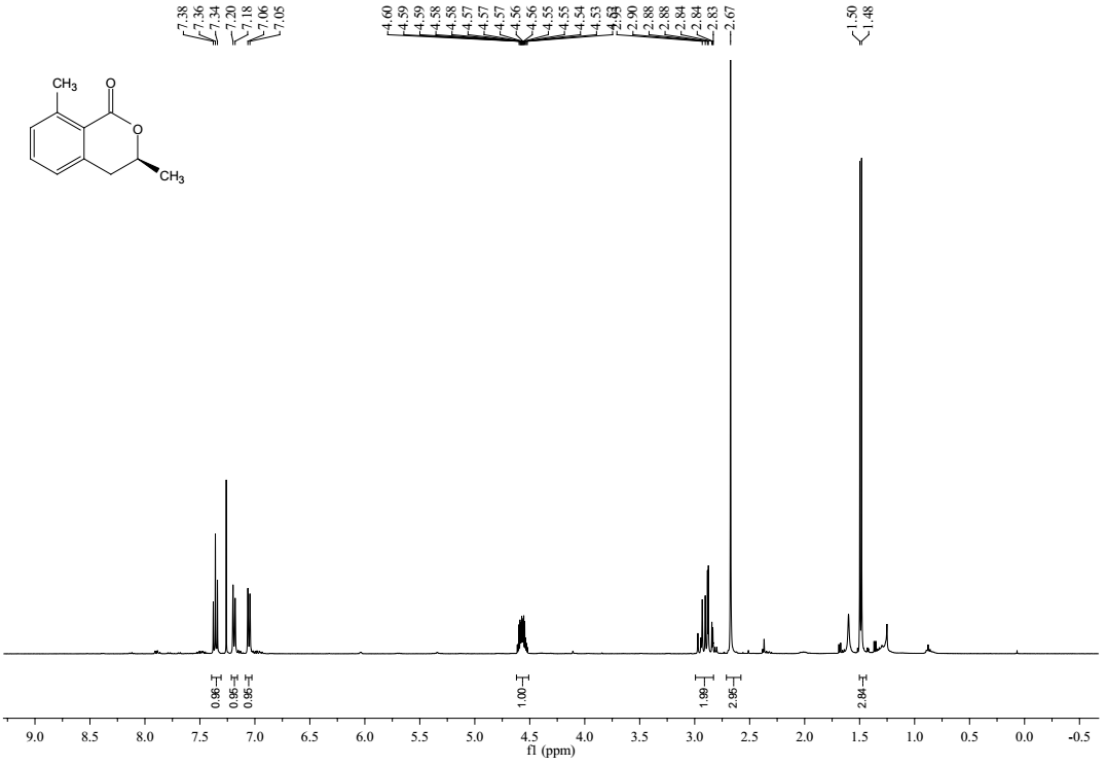
7.38
7.36
7.34
7.20
7.18
7.06
7.05
4.60
4.59
4.59
4.58
4.58
4.57
4.57
4.57
4.56
4.56
4.55
4.55
4.54
4.53
2.90
2.88
2.88
2.84
2.84
2.83
2.67
1.50
1.48
CH3
O
O
CH3
0.98
0.95
0.95
1.00
1.99
2.95
2.84
9.0
8.5
8.0
7.5
7.0
6.5
6.0
5.5
5.0
4.5
4.0
3.5
3.0
2.5
2.0
1.5
1.0
0.5
0.0
-0.5
f1 (ppm)

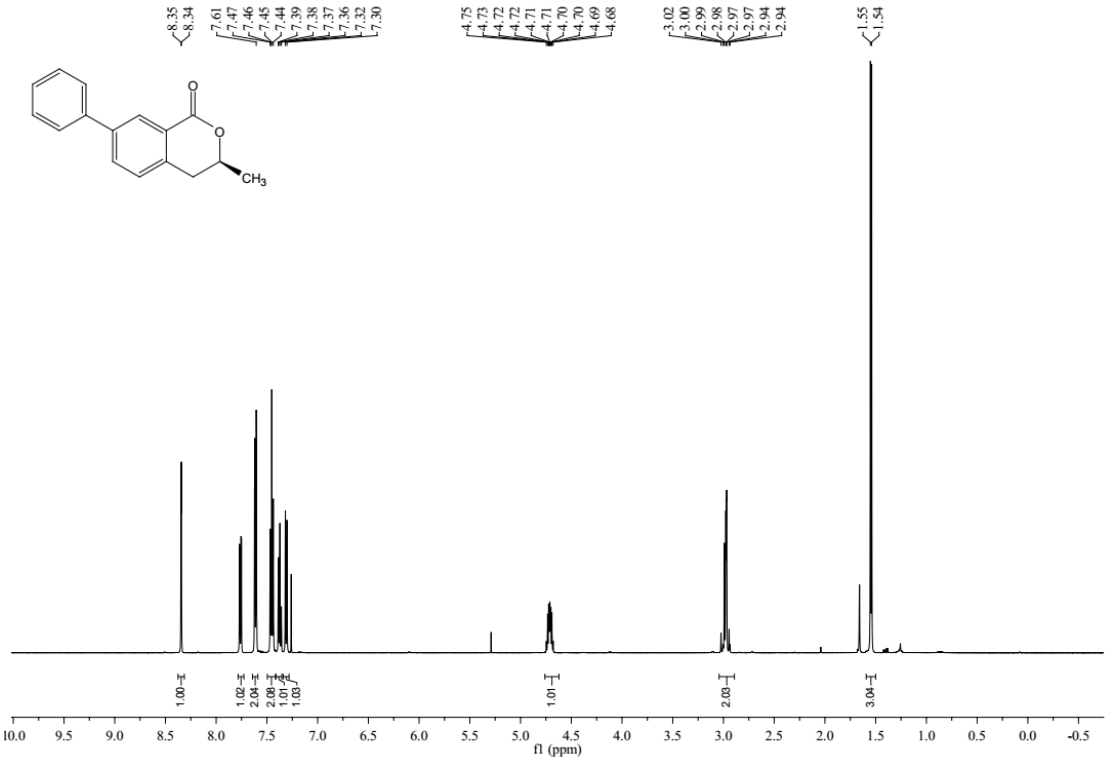
8.35
8.34
7.61
7.47
7.46
7.45
7.44
7.39
7.38
7.37
7.36
7.32
7.30
4.75
4.73
4.72
4.72
4.71
4.71
4.70
4.70
4.69
4.68
3.02
3.00
2.99
2.98
2.97
2.97
2.94
2.94
1.55
1.54
O
O
CH3
1.00
1.02
2.04
2.08
1.01
1.03
1.01
2.03
3.04
10.0 9.5 9.0 8.5 8.0 7.5 7.0 6.5 6.0 5.5 5.0 4.5 4.0 3.5 3.0 2.5 2.0 1.5 1.0 0.5 0.0 -0.5
f1 (ppm)

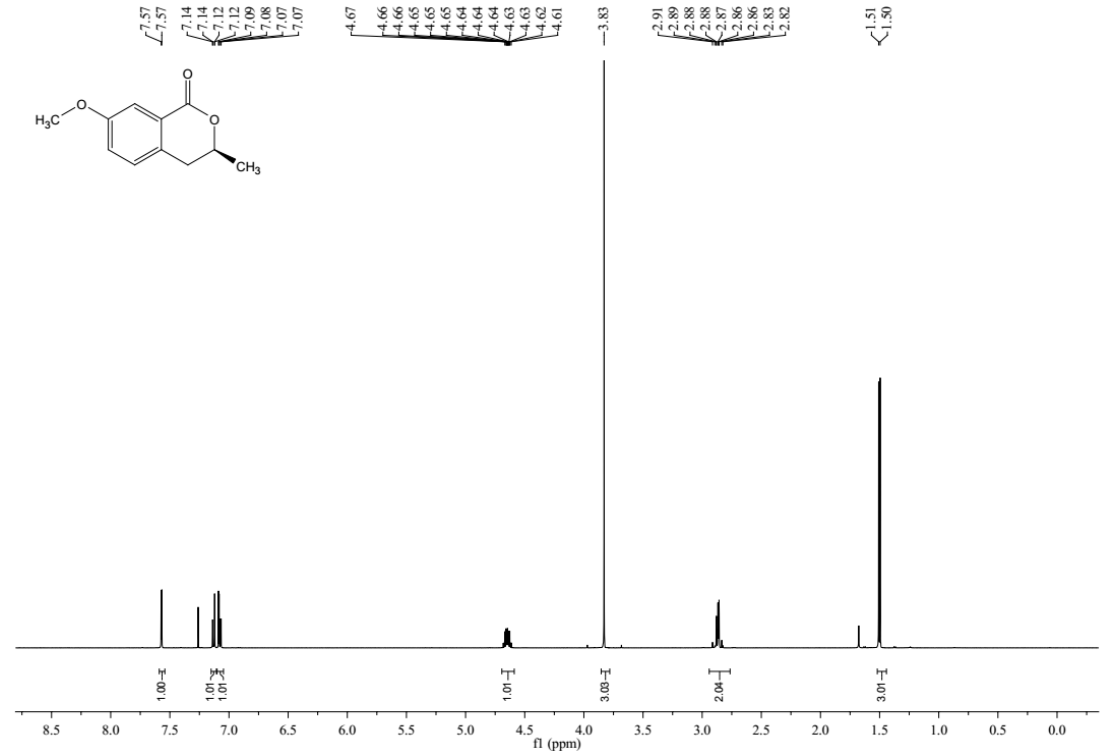
7.57
7.57
7.14
7.14
7.12
7.12
7.09
7.08
7.07
7.07
4.67
4.66
4.66
4.65
4.65
4.65
4.64
4.64
4.64
4.63
4.63
4.62
4.61
3.83
2.91
2.89
2.88
2.88
2.87
2.86
2.86
2.83
2.82
1.51
1.50
O
H3C
O
O
CH3
1.00
1.01
1.01
1.01
3.03
2.04
3.01
8.5 8.0 7.5 7.0 6.5 6.0 5.5 5.0 4.5 4.0 3.5 3.0 2.5 2.0 1.5 1.0 0.5 0.0
f1 (ppm)

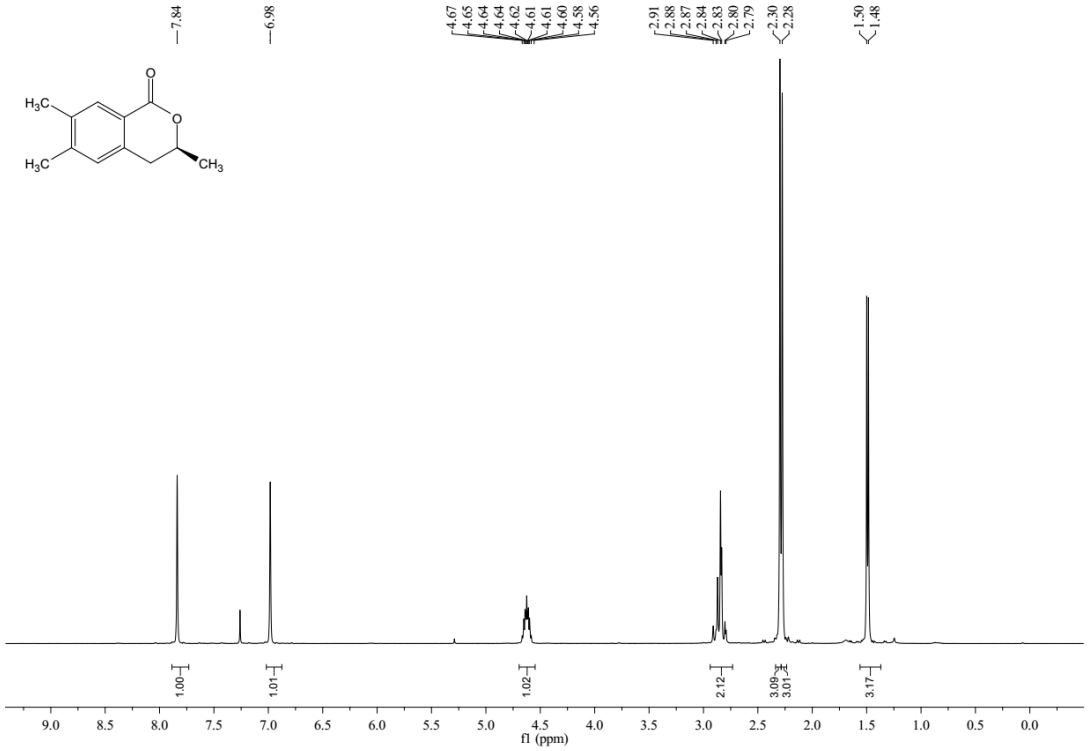
7.84
6.98
4.67
4.65
4.64
4.64
4.62
4.61
4.61
4.60
4.58
4.56
2.91
2.88
2.87
2.84
2.83
2.80
2.79
2.30
2.28
1.50
1.48
H3C
H3C
O
O
CH3
1.00
1.01
1.02
2.12
3.09
3.01
3.17
9.0 8.5 8.0 7.5 7.0 6.5 6.0 5.5 5.0 4.5 4.0 3.5 3.0 2.5 2.0 1.5 1.0 0.5 0.0
f1 (ppm)

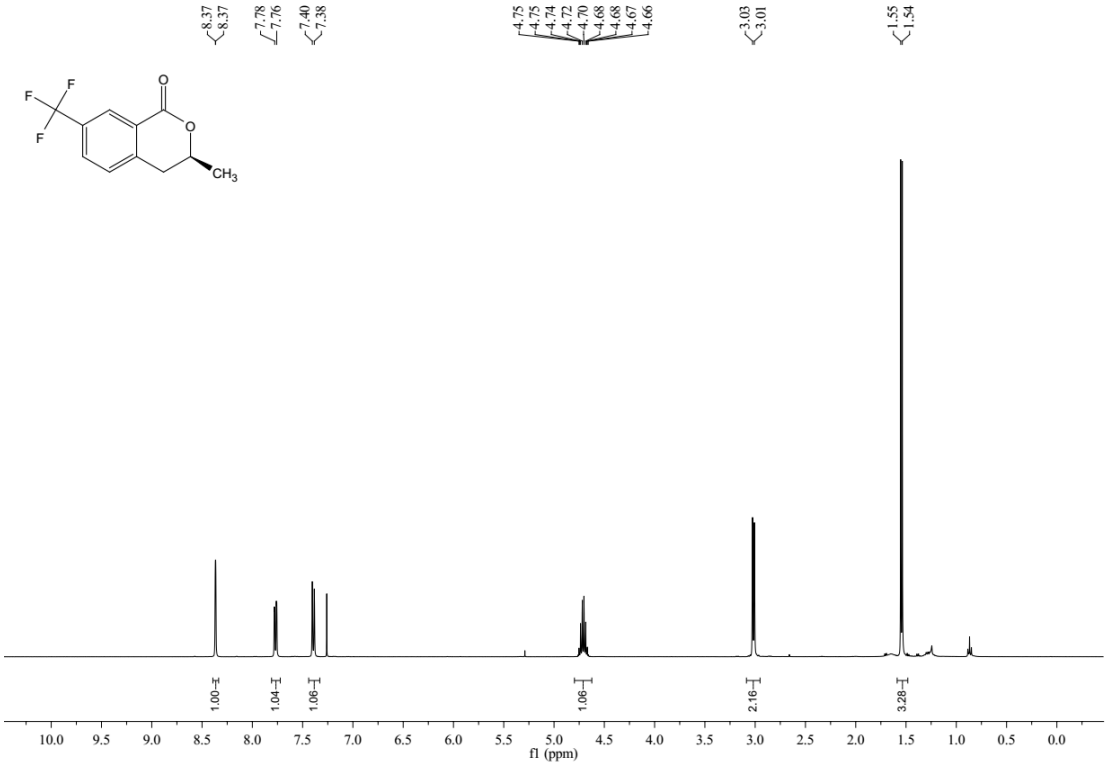
8.37
8.37
7.78
7.76
7.40
7.38
4.75
4.75
4.74
4.72
4.70
4.68
4.68
4.67
4.66
3.03
3.01
1.55
1.54
F
F
F
O
O
CH3
1.00
1.04
1.06
1.06
2.16
3.28
10.0 9.5 9.0 8.5 8.0 7.5 7.0 6.5 6.0 5.5 5.0 4.5 4.0 3.5 3.0 2.5 2.0 1.5 1.0 0.5 0.0
f1 (ppm)

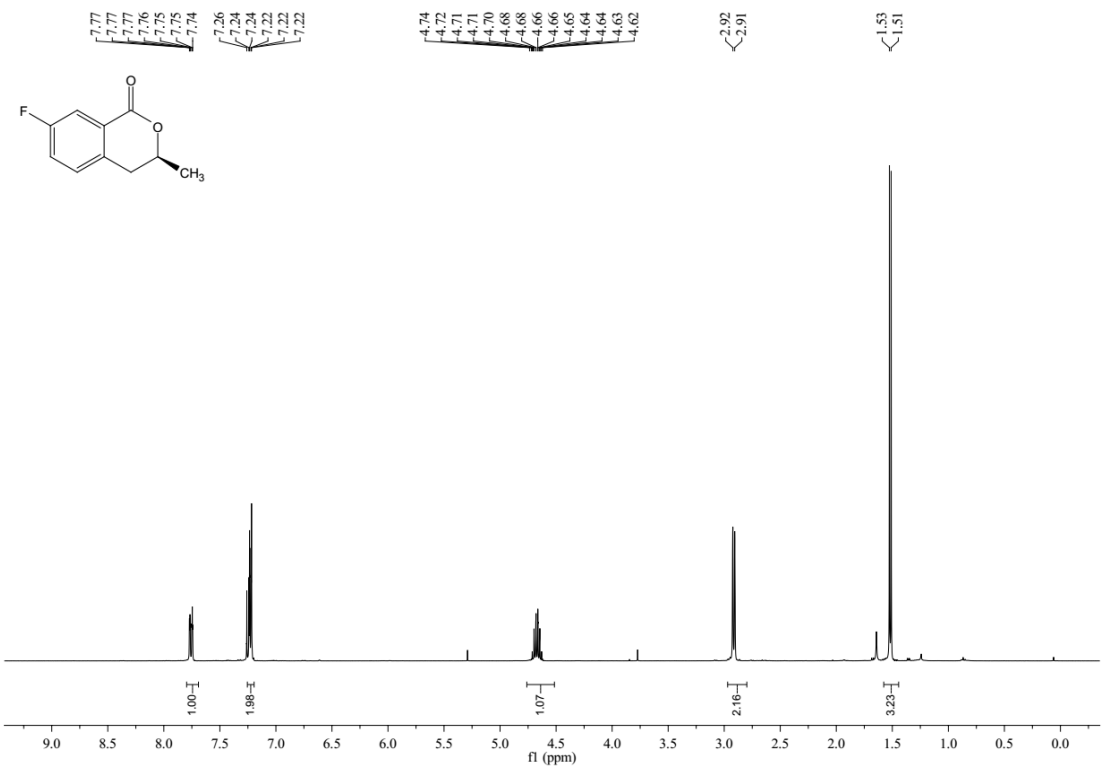
7.77
7.77
7.77
7.76
7.75
7.75
7.74
7.26
7.24
7.24
7.22
7.22
7.22
4.74
4.72
4.71
4.71
4.70
4.68
4.68
4.66
4.66
4.65
4.64
4.64
4.63
4.62
2.92
2.91
1.53
1.51
F
O
O
CH3
1.00
1.98
1.07
2.16
3.23
9.0 8.5 8.0 7.5 7.0 6.5 6.0 5.5 5.0 4.5 4.0 3.5 3.0 2.5 2.0 1.5 1.0 0.5 0.0
f1 (ppm)

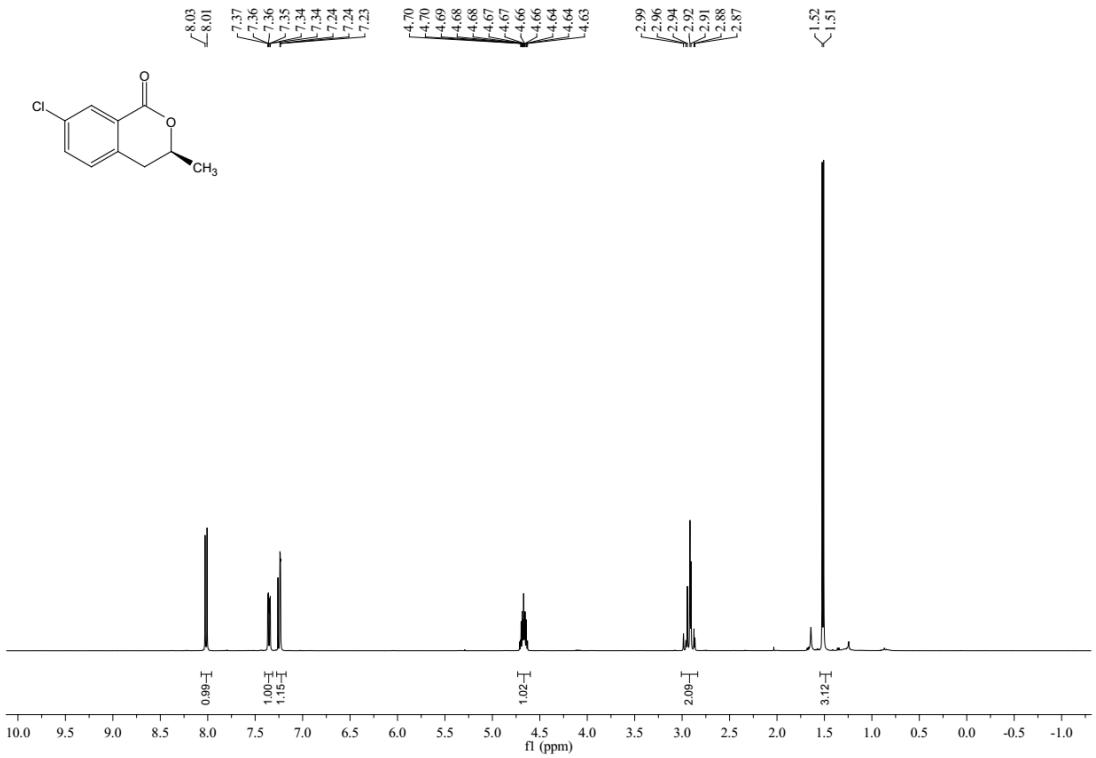
8.03
8.01
7.37
7.36
7.36
7.35
7.34
7.34
7.24
7.24
7.23
4.70
4.70
4.69
4.68
4.68
4.67
4.67
4.66
4.66
4.64
4.64
4.63
2.99
2.96
2.94
2.92
2.91
2.88
2.87
1.52
1.51
Cl
O
O
CH3
0.99
1.00
1.15
1.02
2.09
3.12
10.0 9.5 9.0 8.5 8.0 7.5 7.0 6.5 6.0 5.5 5.0 4.5 4.0 3.5 3.0 2.5 2.0 1.5 1.0 0.5 0.0 -0.5 -1.0
f1 (ppm)

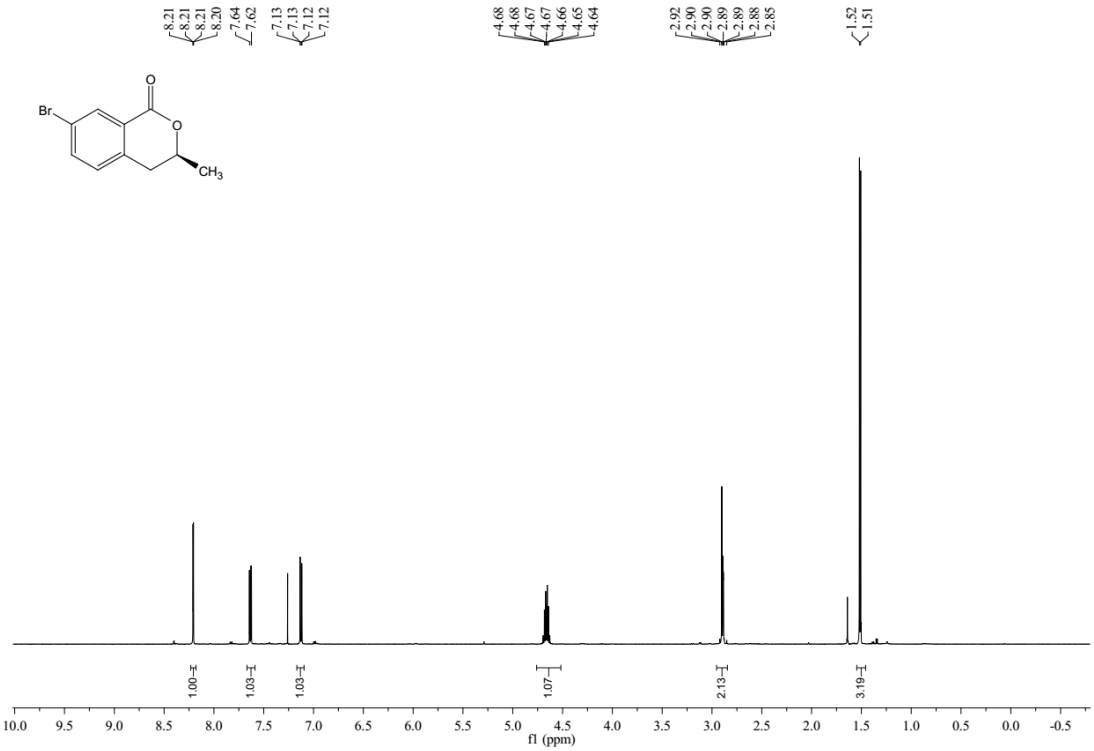
8.21
8.21
8.21
8.20
7.64
7.62
7.13
7.13
7.12
7.12
4.68
4.68
4.67
4.67
4.66
4.65
4.64
2.92
2.90
2.90
2.89
2.89
2.88
2.85
1.52
1.51
Br
O
O
CH3
1.00
1.03
1.03
1.07
2.13
3.19
10.0 9.5 9.0 8.5 8.0 7.5 7.0 6.5 6.0 5.5 5.0 4.5 4.0 3.5 3.0 2.5 2.0 1.5 1.0 0.5 0.0 -0.5
f1 (ppm)

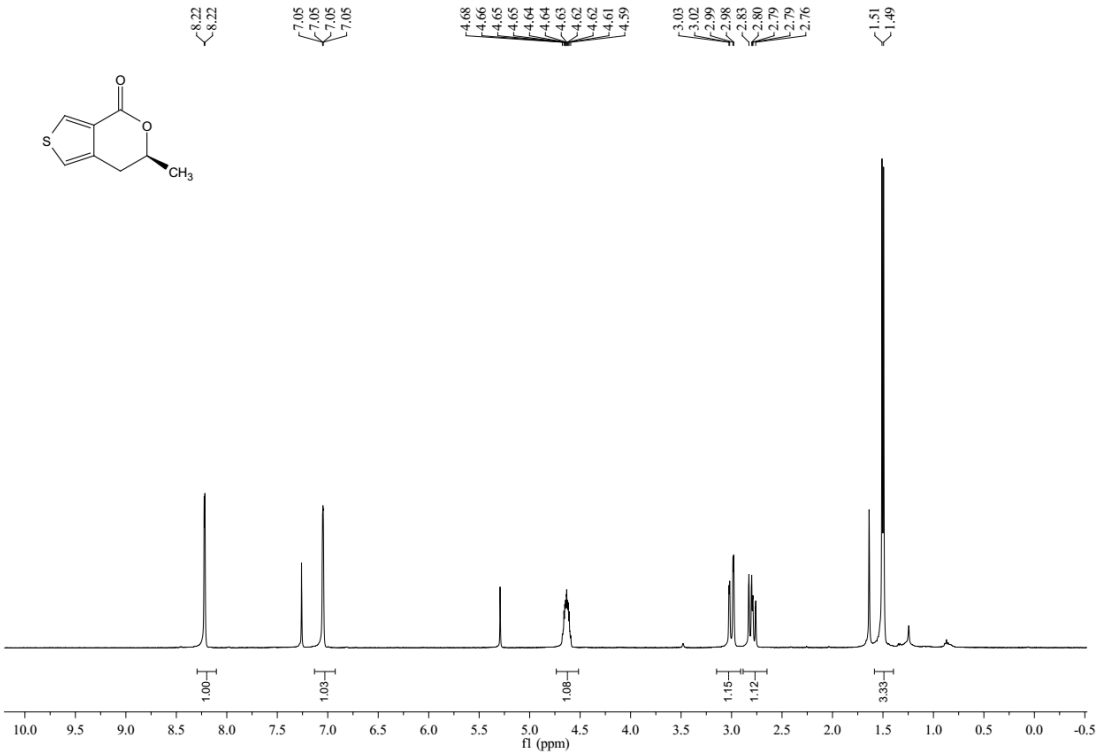
8.22
8.22
7.05
7.05
7.05
7.05
4.68
4.66
4.65
4.65
4.64
4.64
4.63
4.62
4.62
4.61
4.59
3.03
3.02
2.99
2.98
2.83
2.80
2.79
2.79
2.76
1.51
1.49
O
O
S
CH3
1.00
1.03
1.08
1.15
1.12
3.33
10.0 9.5 9.0 8.5 8.0 7.5 7.0 6.5 6.0 5.5 5.0 4.5 4.0 3.5 3.0 2.5 2.0 1.5 1.0 0.5 0.0 -0.5
f1 (ppm)

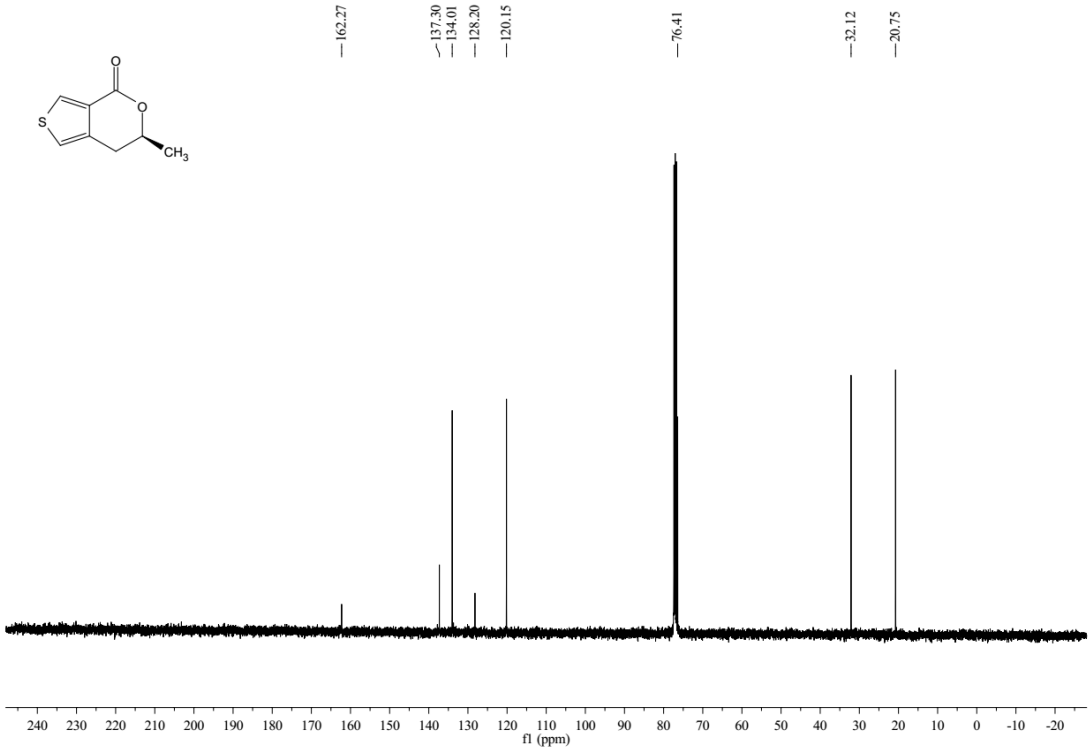
162.27
137.30
134.01
128.20
120.15
76.41
32.12
20.75
S
O
O
CH3
240 230 220 210 200 190 180 170 160 150 140 130 120 110 100 90 80 70 60 50 40 30 20 10 0 -10 -20
f1 (ppm)

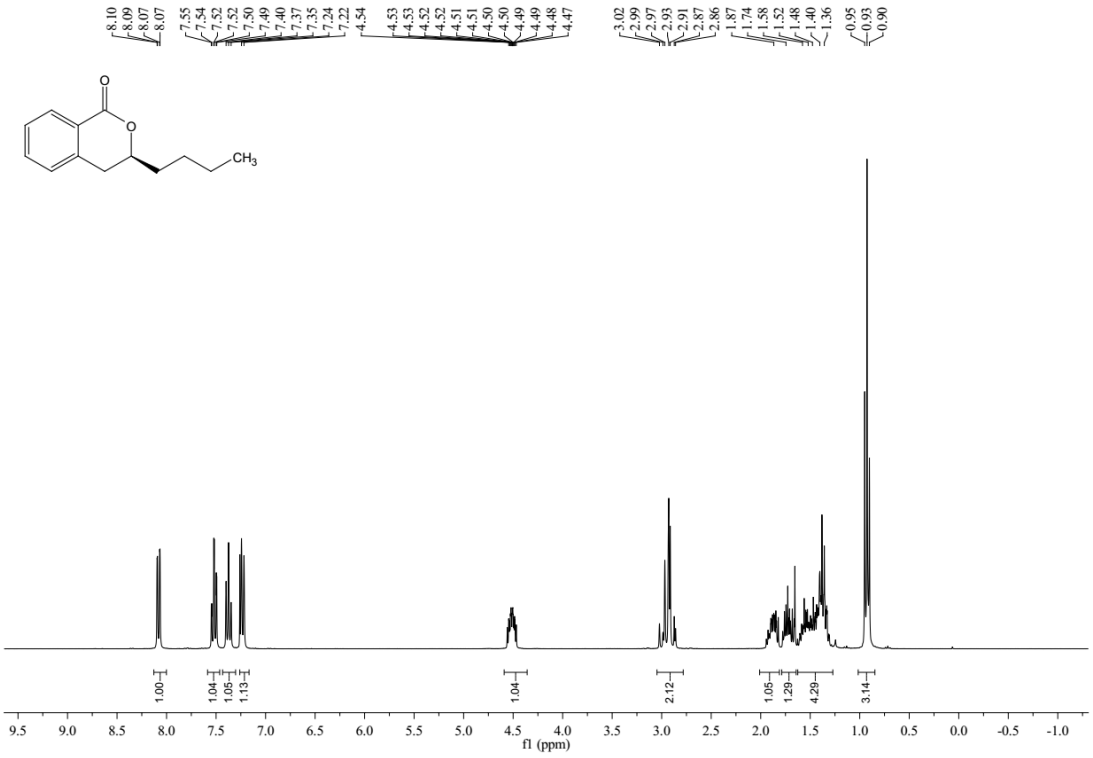
8.10
8.09
8.07
8.07
7.55
7.54
7.52
7.52
7.50
7.49
7.40
7.37
7.35
7.24
7.22
4.54
4.53
4.53
4.52
4.52
4.51
4.51
4.50
4.50
4.49
4.49
4.48
4.47
3.02
2.99
2.97
2.93
2.91
2.87
2.86
1.87
1.74
1.58
1.52
1.48
1.40
1.36
0.95
0.93
0.90
O
O
CH3
1.00
1.04
1.05
1.13
1.04
2.12
1.05
1.29
4.29
3.14
9.5 9.0 8.5 8.0 7.5 7.0 6.5 6.0 5.5 5.0 4.5 4.0 3.5 3.0 2.5 2.0 1.5 1.0 0.5 0.0 -0.5 -1.0
f1 (ppm)

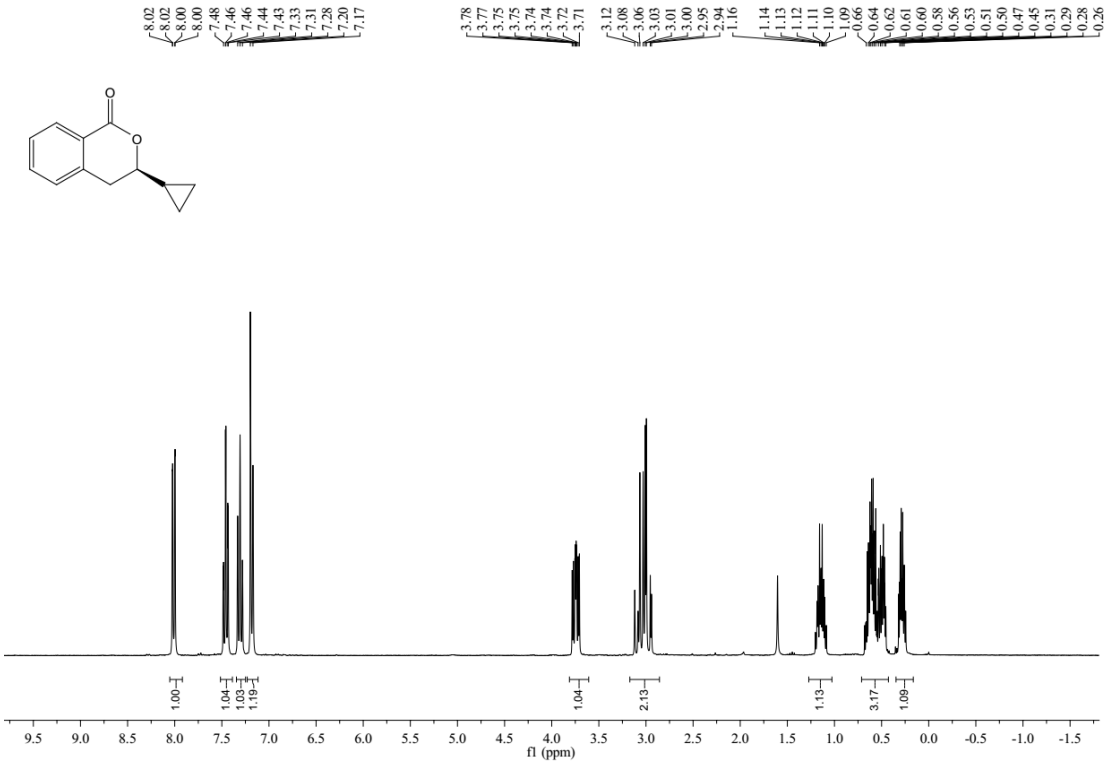
8.02 8.02 8.00 8.00 7.48 7.46 7.46 7.44 7.43 7.33 7.31 7.28 7.20 7.17
3.78 3.77 3.75 3.75 3.74 3.74 3.72 3.71
3.12 3.08 3.06 3.03 3.01 3.00 2.95 2.94
1.16
1.14 1.13 1.12 1.11 1.10 1.09
0.66 0.64 0.62 0.61 0.60 0.58 0.56 0.53 0.51 0.50 0.47 0.45 0.31 0.29 0.28 0.26
O
O
1.00 1.04 1.03 1.19 1.04 2.13 1.13 3.17 1.09
9.5 9.0 8.5 8.0 7.5 7.0 6.5 6.0 5.5 5.0 4.5 4.0 3.5 3.0 2.5 2.0 1.5 1.0 0.5 0.0 -0.5 -1.0 -1.5
f1 (ppm)

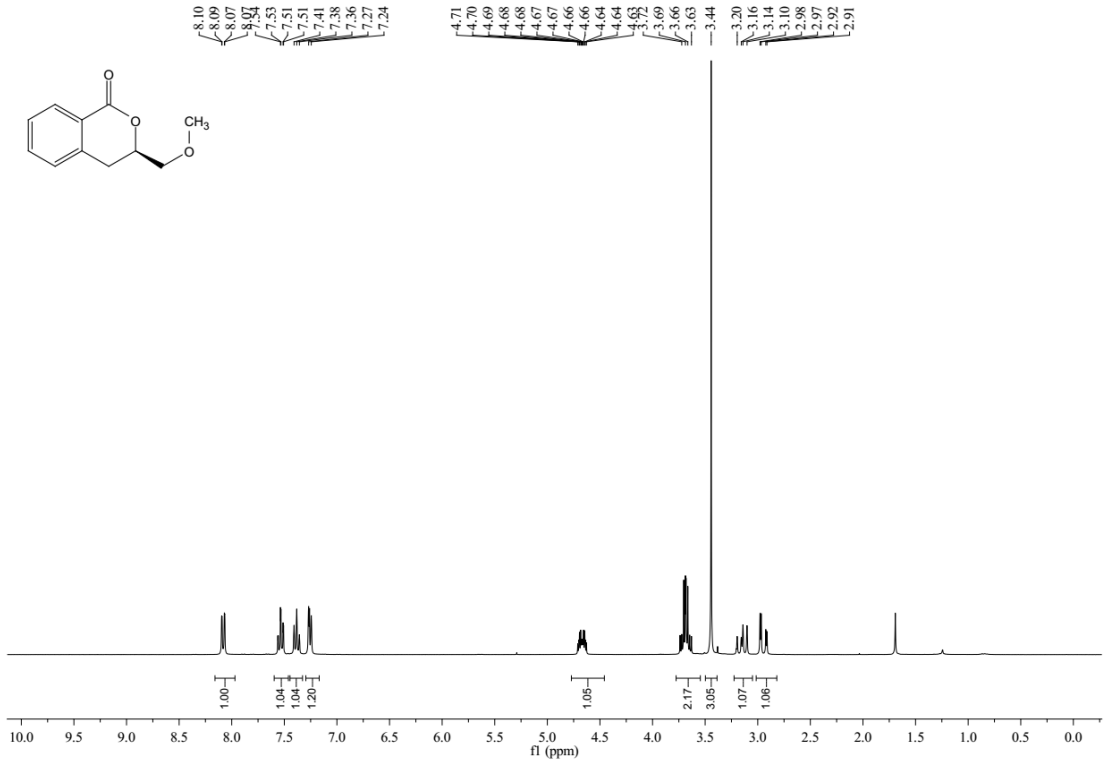
8.10 8.09 8.07 8.07 7.54 7.53 7.51 7.51 7.41 7.38 7.36 7.27 7.24
4.71 4.70 4.69 4.68 4.68 4.67 4.67 4.66 4.66 4.64 4.64 4.63 4.62
3.69 3.66 3.63
3.44
3.20 3.16 3.14 3.10 2.98 2.97 2.92 2.91
O
O
CH3
O
1.00 1.04 1.04 1.20 1.05 2.17 3.05 1.07 1.06
10.0 9.5 9.0 8.5 8.0 7.5 7.0 6.5 6.0 5.5 5.0 4.5 4.0 3.5 3.0 2.5 2.0 1.5 1.0 0.5 0.0
f1 (ppm)

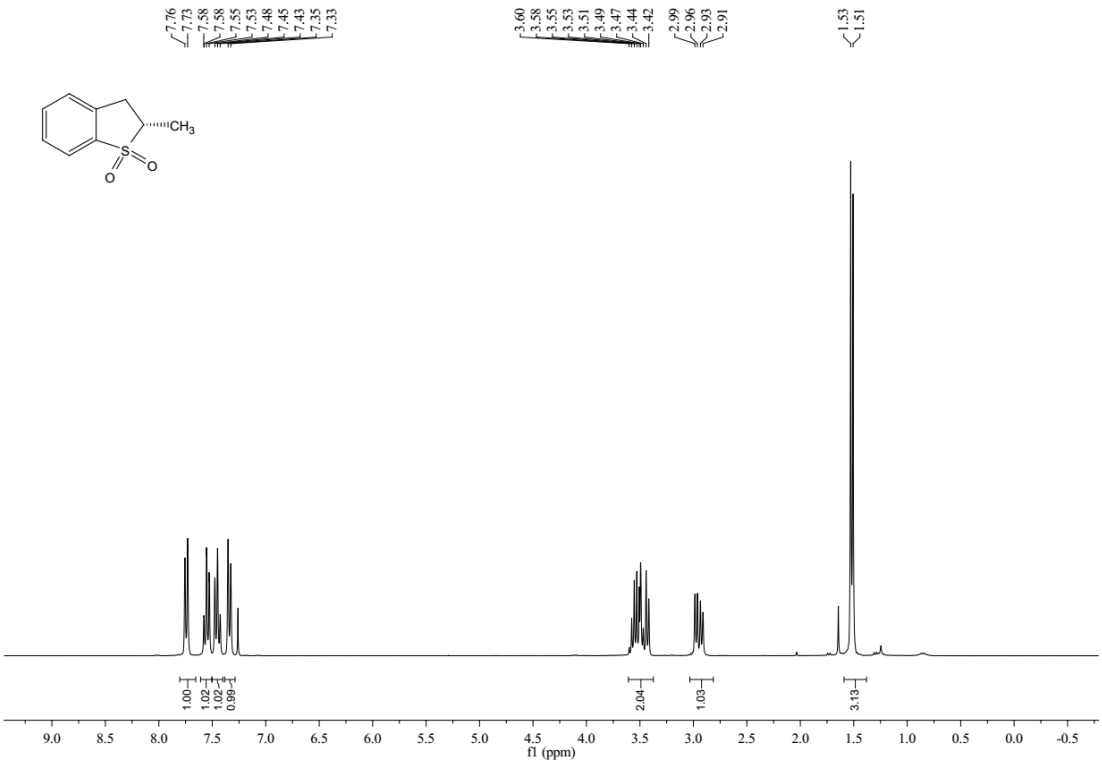
7.76
7.73
7.58
7.58
7.55
7.53
7.48
7.45
7.43
7.35
7.33
3.60
3.58
3.55
3.53
3.51
3.49
3.47
3.44
3.42
2.99
2.96
2.93
2.91
1.53
1.51
CH3
S
O
O
1.00
1.02
1.02
0.99
2.04
1.03
3.13
9.0 8.5 8.0 7.5 7.0 6.5 6.0 5.5 5.0 4.5 4.0 3.5 3.0 2.5 2.0 1.5 1.0 0.5 0.0 -0.5
f1 (ppm)

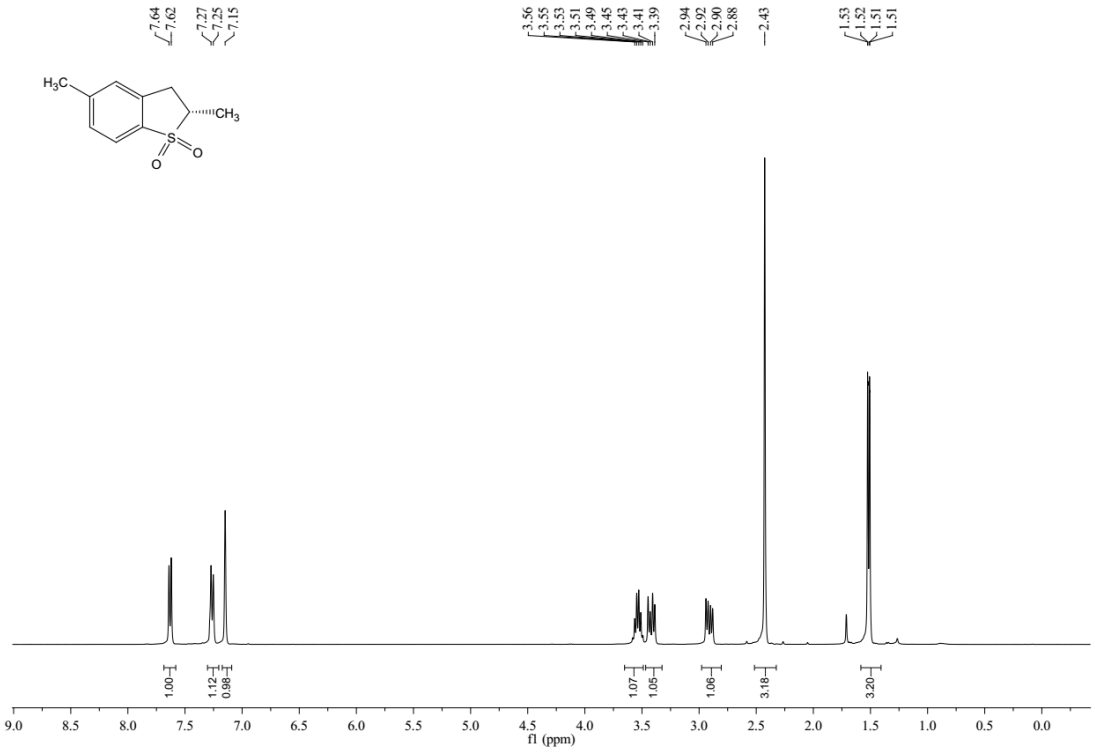
7.64
7.62
7.27
7.25
7.15
3.56
3.55
3.53
3.51
3.49
3.45
3.43
3.41
3.39
2.94
2.92
2.90
2.88
2.43
1.53
1.52
1.51
1.51
H3C
CH3
S
O
O
1.00
1.12
0.98
1.07
1.05
1.08
3.18
3.20
9.0 8.5 8.0 7.5 7.0 6.5 6.0 5.5 5.0 4.5 4.0 3.5 3.0 2.5 2.0 1.5 1.0 0.5 0.0
f1 (ppm)

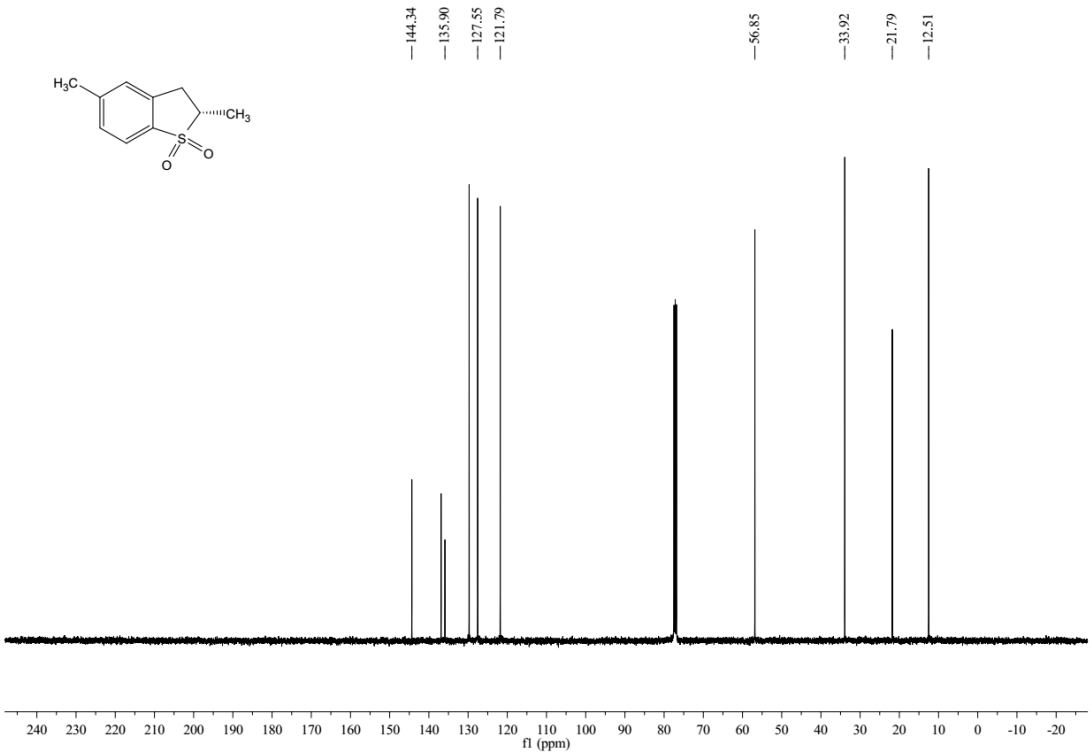
144.34
135.90
127.55
121.79
56.85
33.92
21.79
12.51
H3C
CH3
S
O
O
240 230 220 210 200 190 180 170 160 150 140 130 120 110 100 90 80 70 60 50 40 30 20 10 0 -10 -20
f1 (ppm)

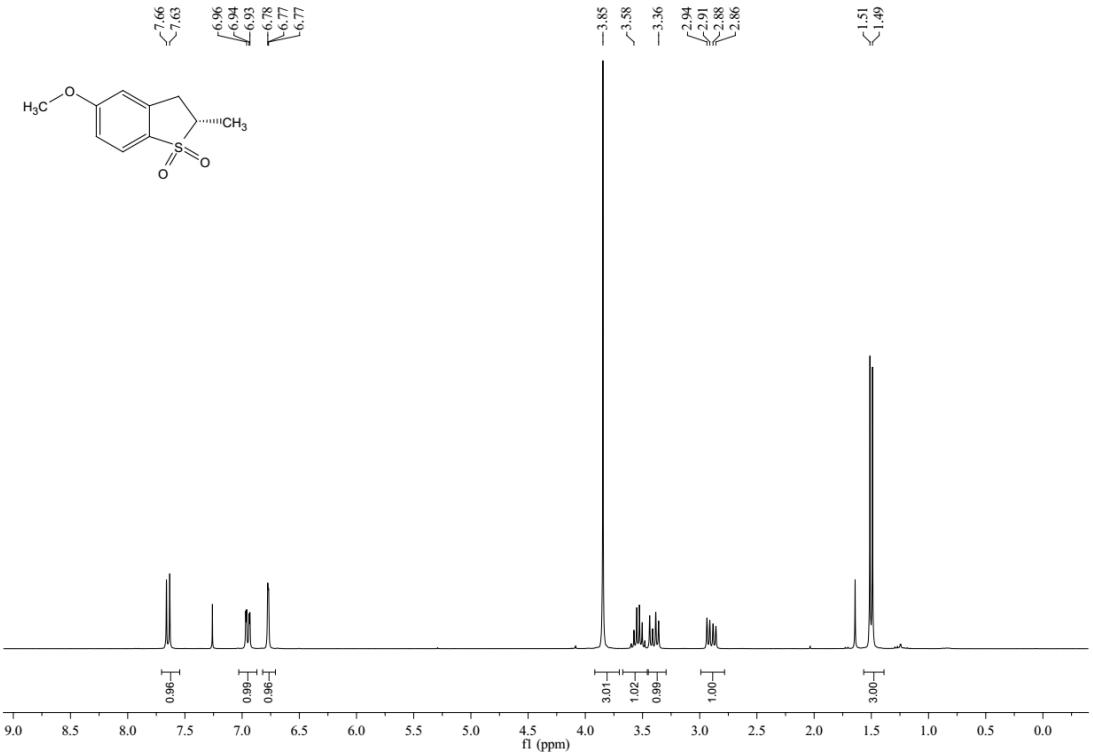
7.66
7.63
6.96
6.94
6.93
6.78
6.77
6.77
3.85
3.58
3.36
2.94
2.91
2.88
2.86
1.51
1.49
H3C
O
CH3
S
O
O
0.96
0.99
0.96
3.01
1.02
0.99
1.00
3.00
9.0 8.5 8.0 7.5 7.0 6.5 6.0 5.5 5.0 4.5 4.0 3.5 3.0 2.5 2.0 1.5 1.0 0.5 0.0
f1 (ppm)

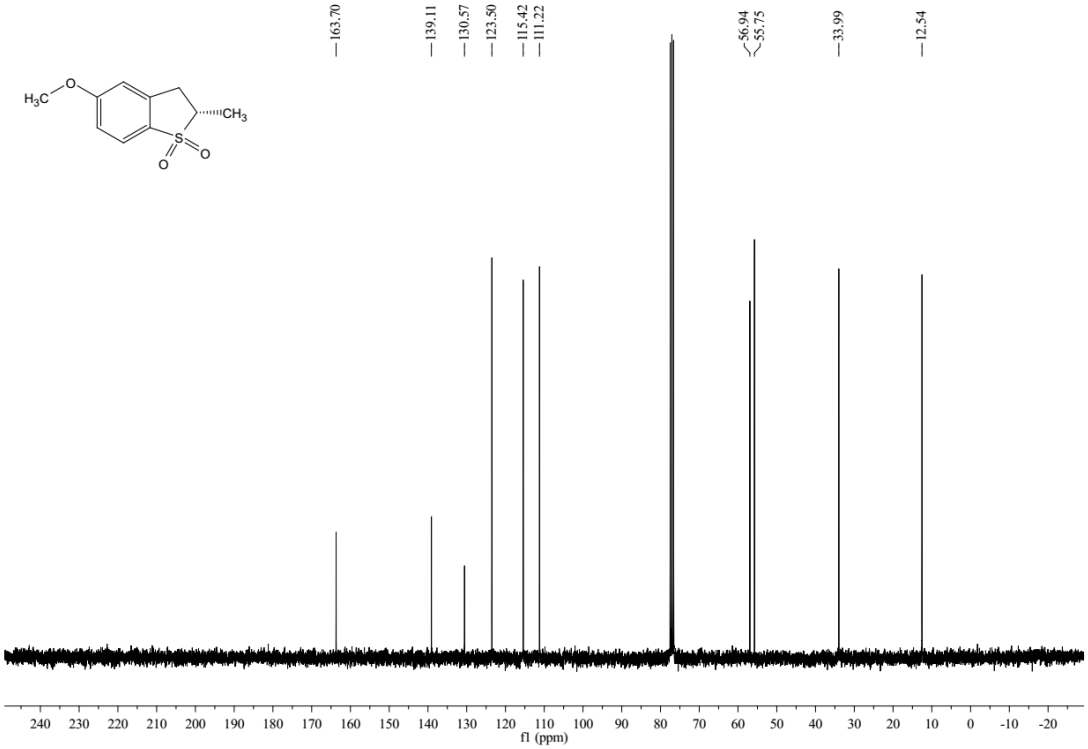
163.70
139.11
130.57
123.50
115.42
111.22
56.94
55.75
33.99
12.54
H3C
O
CH3
S
O
O
240 230 220 210 200 190 180 170 160 150 140 130 120 110 100 90 80 70 60 50 40 30 20 10 0 -10 -20
f1 (ppm)

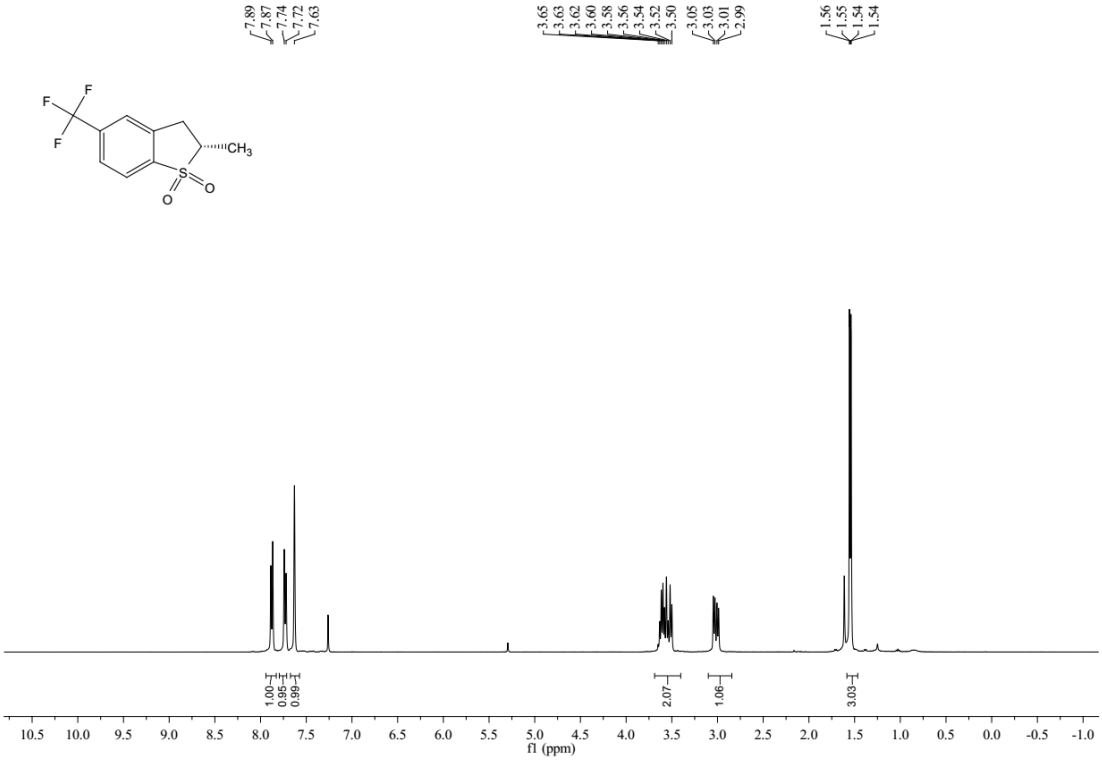
7.89
7.87
7.74
7.72
7.63
3.65
3.63
3.62
3.60
3.58
3.56
3.54
3.52
3.50
3.05
3.03
3.01
2.99
1.56
1.55
1.54
1.54
F
F
F
CH3
S
O
O
1.00
0.95
0.99
2.07
1.06
3.03
10.5 10.0 9.5 9.0 8.5 8.0 7.5 7.0 6.5 6.0 5.5 5.0 4.5 4.0 3.5 3.0 2.5 2.0 1.5 1.0 0.5 0.0 -0.5 -1.0
f1 (ppm)

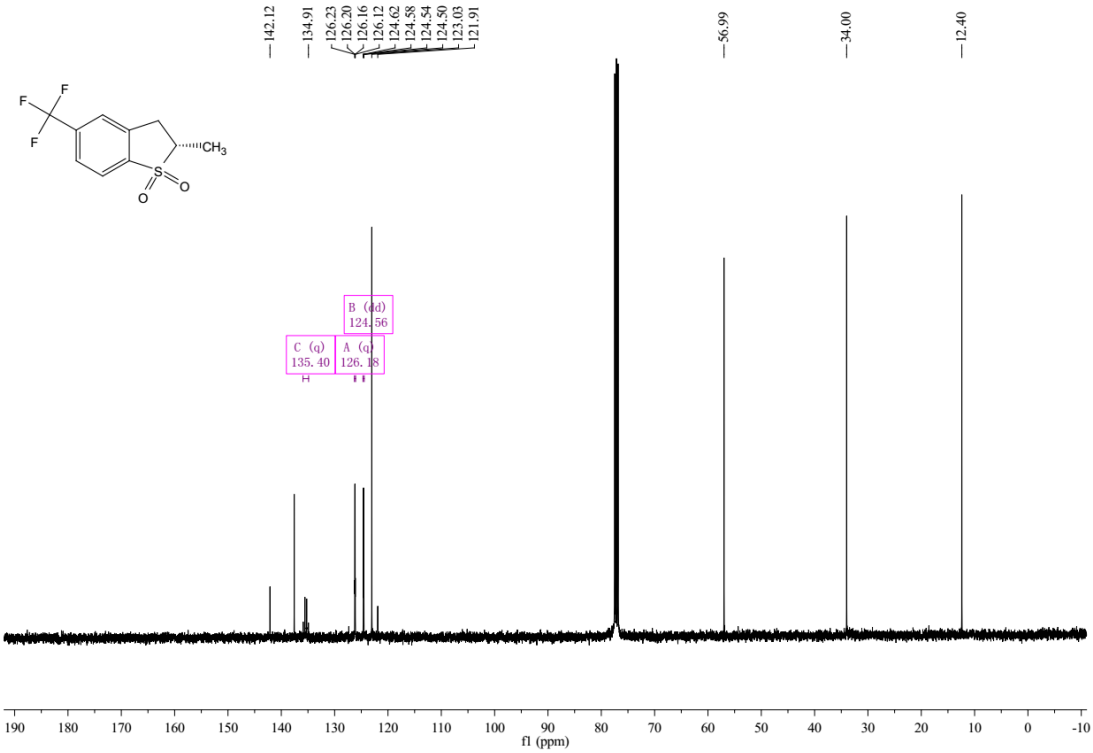
142.12
134.91
126.23
126.20
126.16
126.12
124.62
124.58
124.54
124.50
123.03
121.91
56.99
34.00
12.40
B (dd)
124.56
C (q)
135.40
A (q)
126.18
F
F
F
CH3
S
O
O
190 180 170 160 150 140 130 120 110 100 90 80 70 60 50 40 30 20 10 0 -10
f1 (ppm)

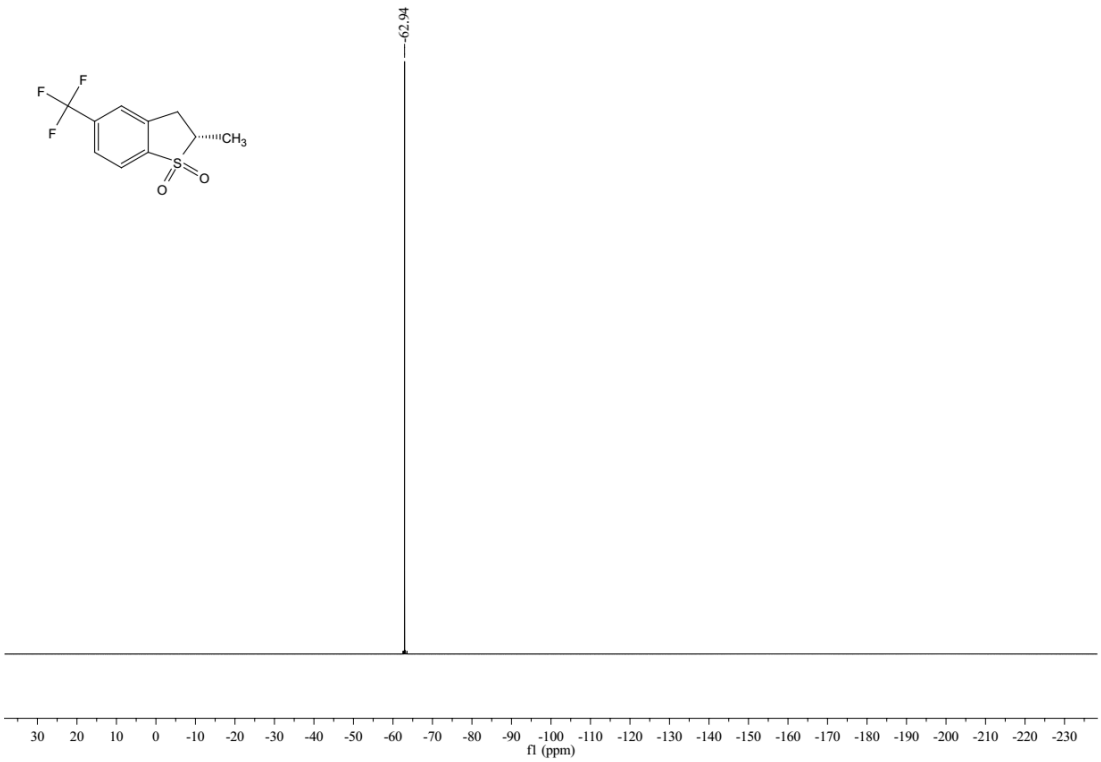
62.94
F
F
F
CH3
S
O
O
30 20 10 0 -10 -20 -30 -40 -50 -60 -70 -80 -90 -100 -110 -120 -130 -140 -150 -160 -170 -180 -190 -200 -210 -220 -230
f1 (ppm)

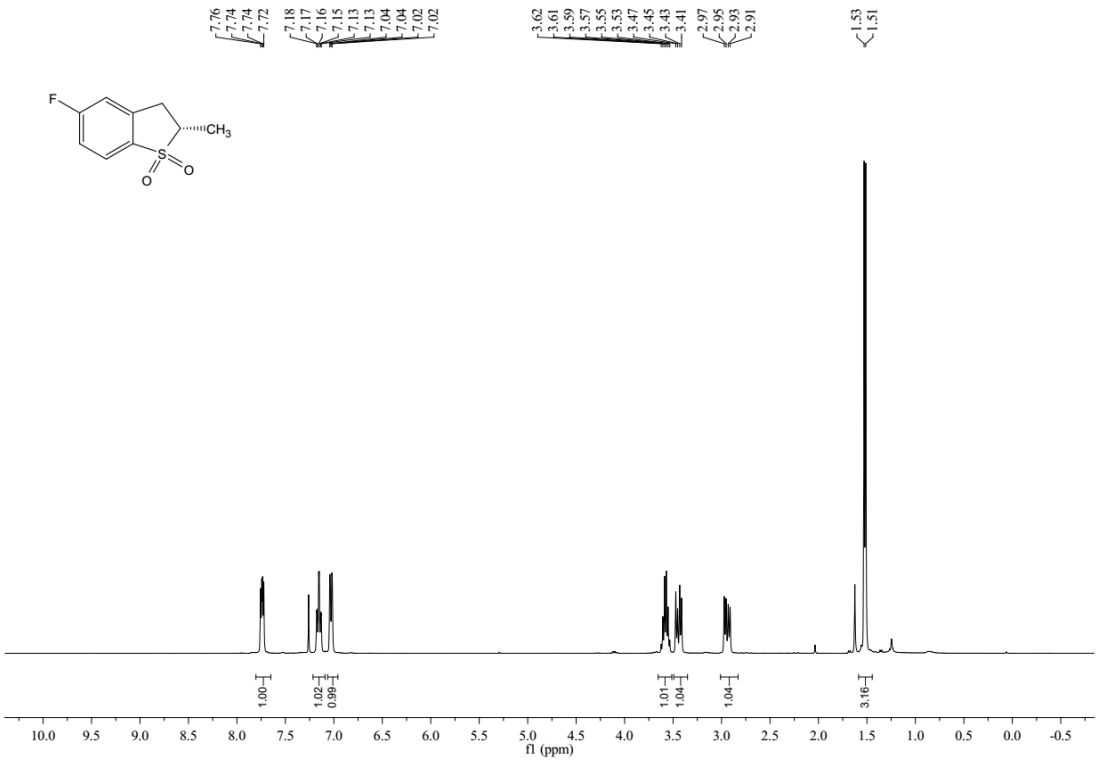
7.76
7.74
7.74
7.72
7.18
7.17
7.16
7.15
7.13
7.13
7.04
7.04
7.02
7.02
3.62
3.61
3.59
3.57
3.55
3.53
3.47
3.45
3.43
3.41
2.97
2.95
2.93
2.91
1.53
1.51
F
CH3
S
O
O
1.00
1.02
0.99
1.01
1.04
1.04
3.16
10.0 9.5 9.0 8.5 8.0 7.5 7.0 6.5 6.0 5.5 5.0 4.5 4.0 3.5 3.0 2.5 2.0 1.5 1.0 0.5 0.0 -0.5
f1 (ppm)

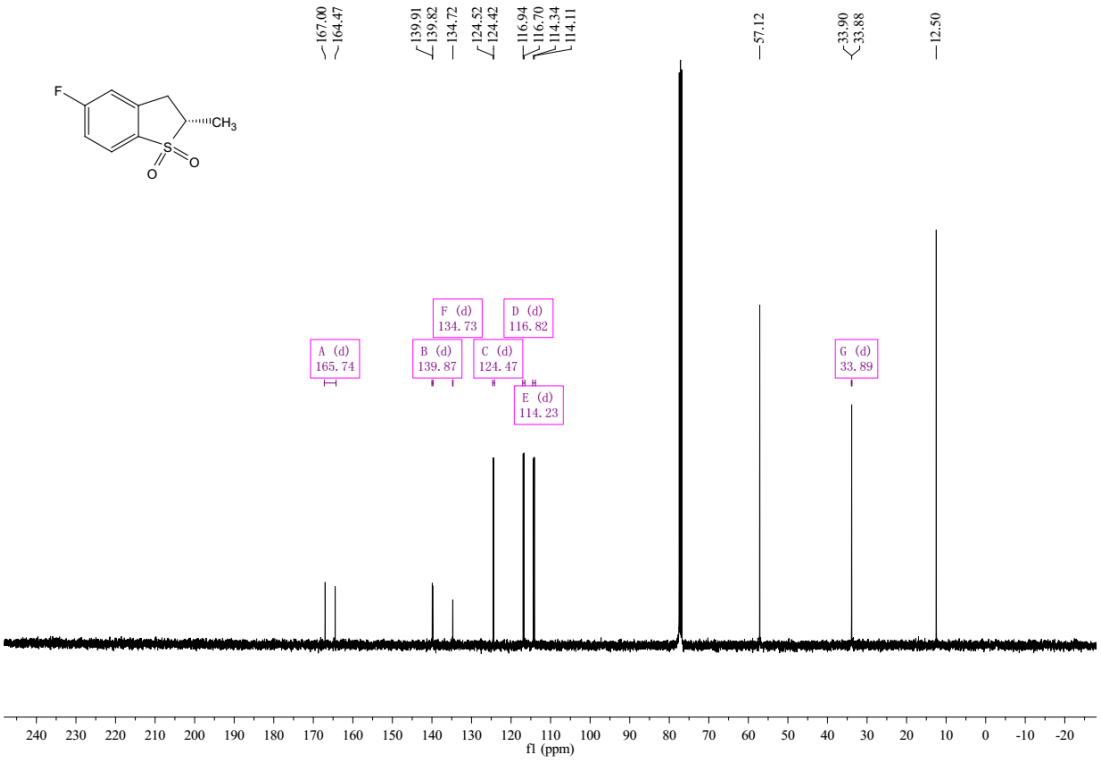
167.00
164.47
139.91
139.82
134.72
124.52
124.42
116.94
116.70
114.34
114.11
57.12
33.90
33.88
12.50
F
CH3
S
O
O
A (d)
165.74
B (d)
139.87
F (d)
134.73
C (d)
124.47
D (d)
116.82
E (d)
114.23
G (d)
33.89
240 230 220 210 200 190 180 170 160 150 140 130 120 110 100 90 80 70 60 50 40 30 20 10 0 -10 -20
f1 (ppm)

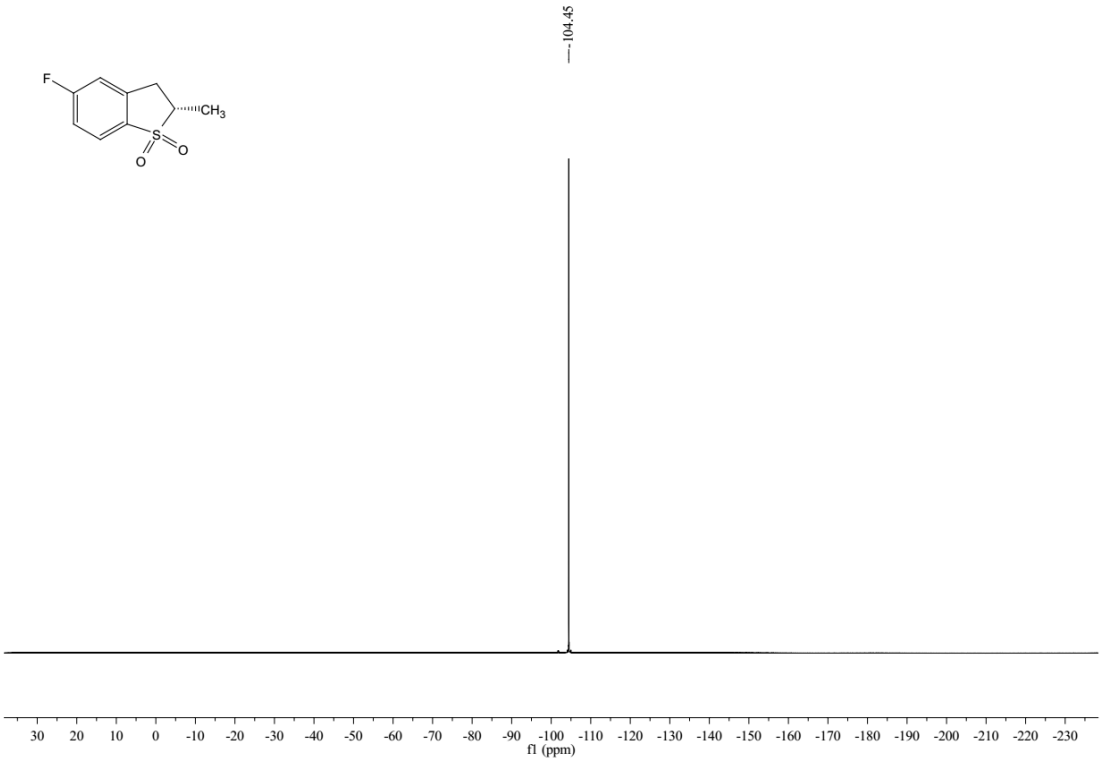
-104.45
F
CH3
S
O
O
30 20 10 0 -10 -20 -30 -40 -50 -60 -70 -80 -90 -100 -110 -120 -130 -140 -150 -160 -170 -180 -190 -200 -210 -220 -230
f1 (ppm)

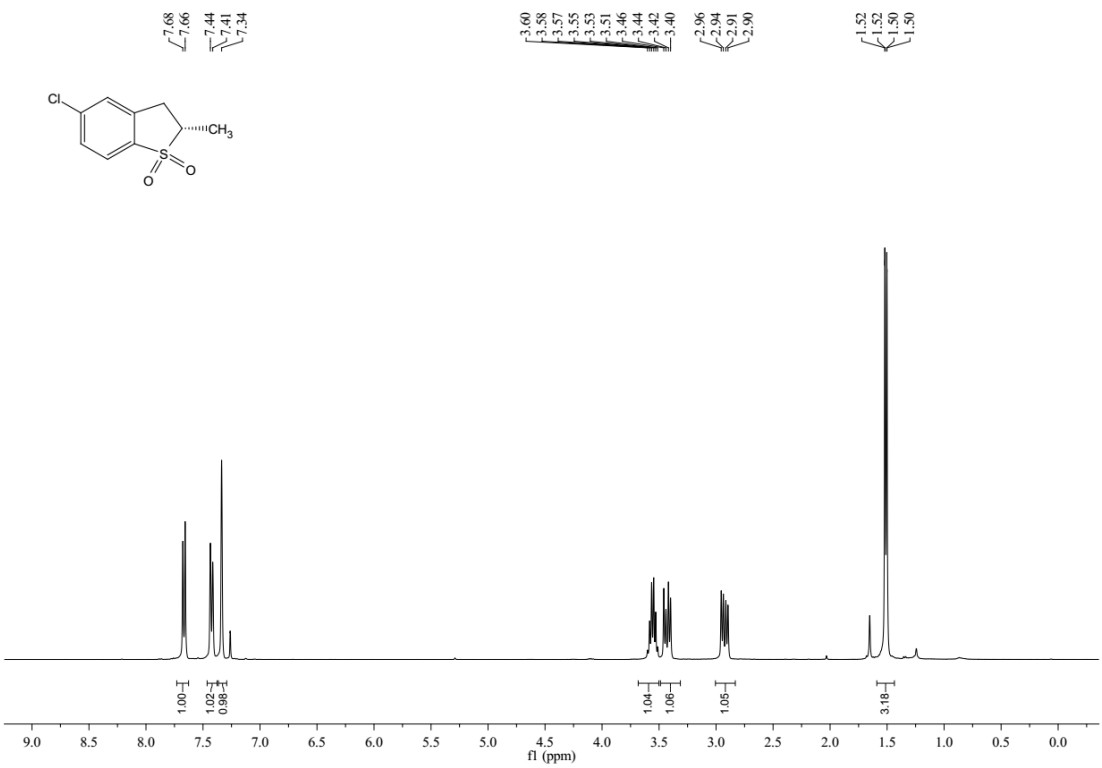
7.68
7.66
7.44
7.41
7.34
3.60
3.58
3.57
3.55
3.53
3.51
3.46
3.44
3.42
3.40
2.96
2.94
2.91
2.90
1.52
1.52
1.50
1.50
Cl
CH3
S
O
O
1.00
1.02
0.98
1.04
1.06
1.05
3.18
9.0 8.5 8.0 7.5 7.0 6.5 6.0 5.5 5.0 4.5 4.0 3.5 3.0 2.5 2.0 1.5 1.0 0.5 0.0
f1 (ppm)

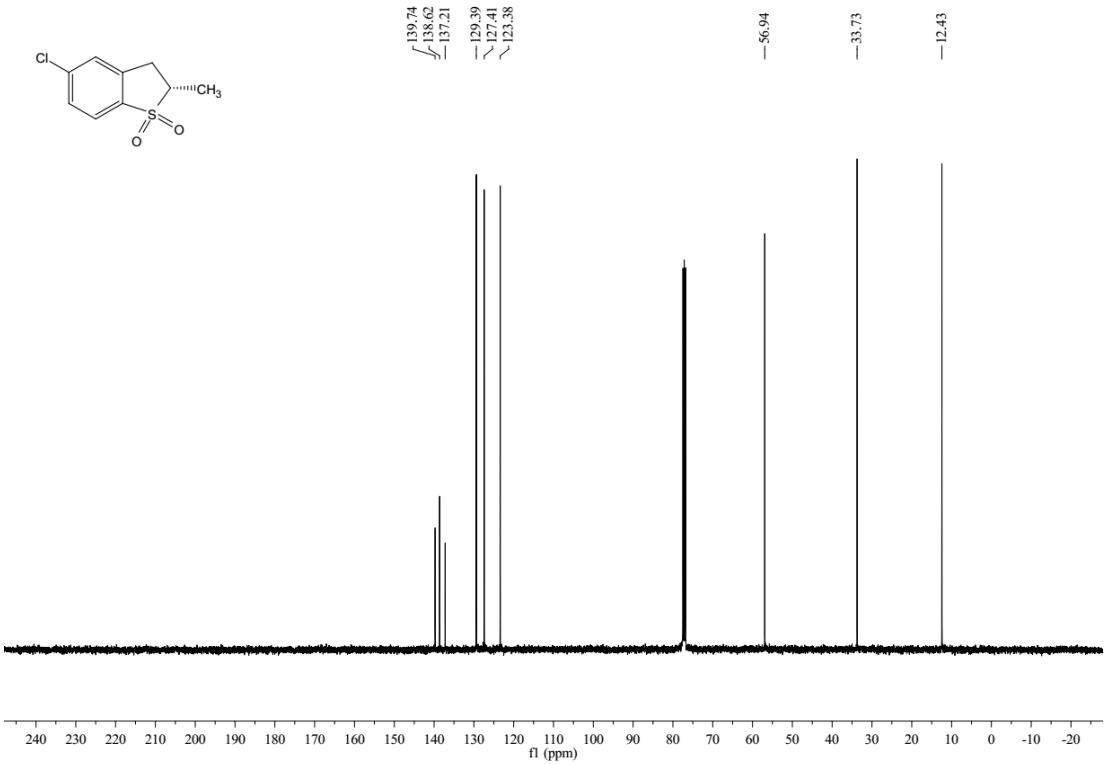
139.74
138.62
137.21
129.39
127.41
123.38
56.94
33.73
12.43
Cl
CH3
S
O
O
240 230 220 210 200 190 180 170 160 150 140 130 120 110 100 90 80 70 60 50 40 30 20 10 0 -10 -20
f1 (ppm)

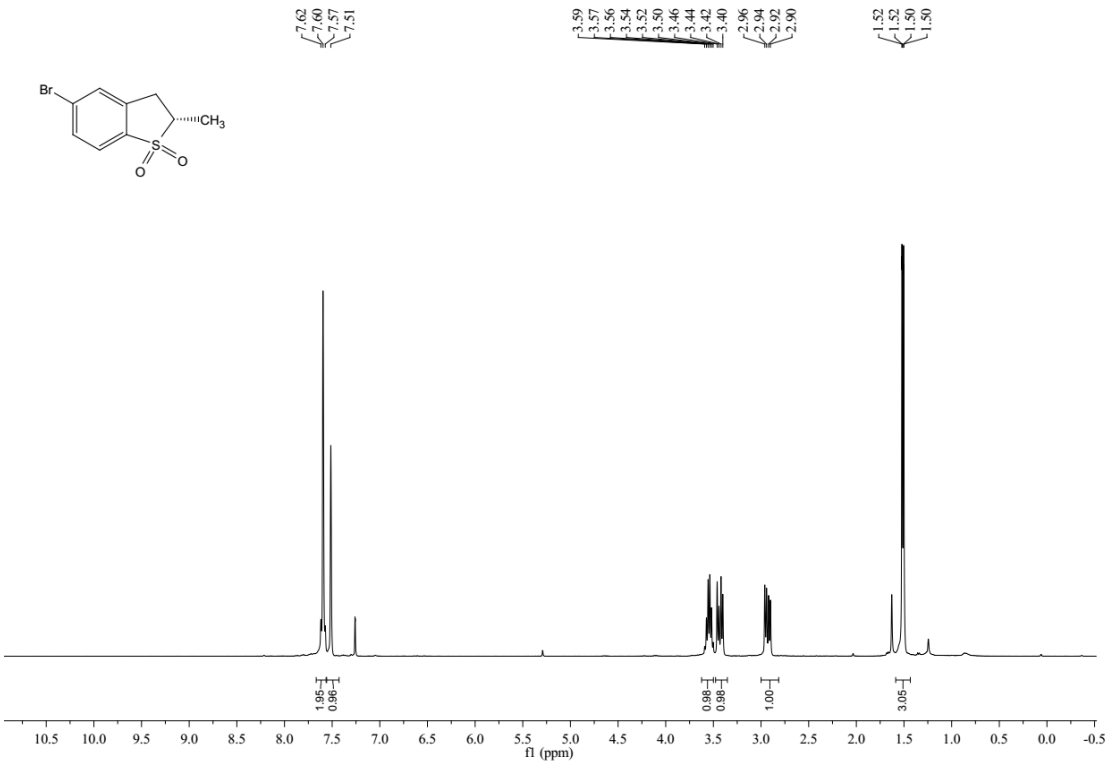
7.62
7.60
7.57
7.51
3.59
3.57
3.56
3.54
3.52
3.50
3.46
3.44
3.42
3.40
2.96
2.94
2.92
2.90
1.52
1.52
1.50
1.50
Br
CH3
S
O
O
1.95
0.98
0.98
0.98
1.00
3.05
10.5 10.0 9.5 9.0 8.5 8.0 7.5 7.0 6.5 6.0 5.5 5.0 4.5 4.0 3.5 3.0 2.5 2.0 1.5 1.0 0.5 0.0 -0.5
f1 (ppm)

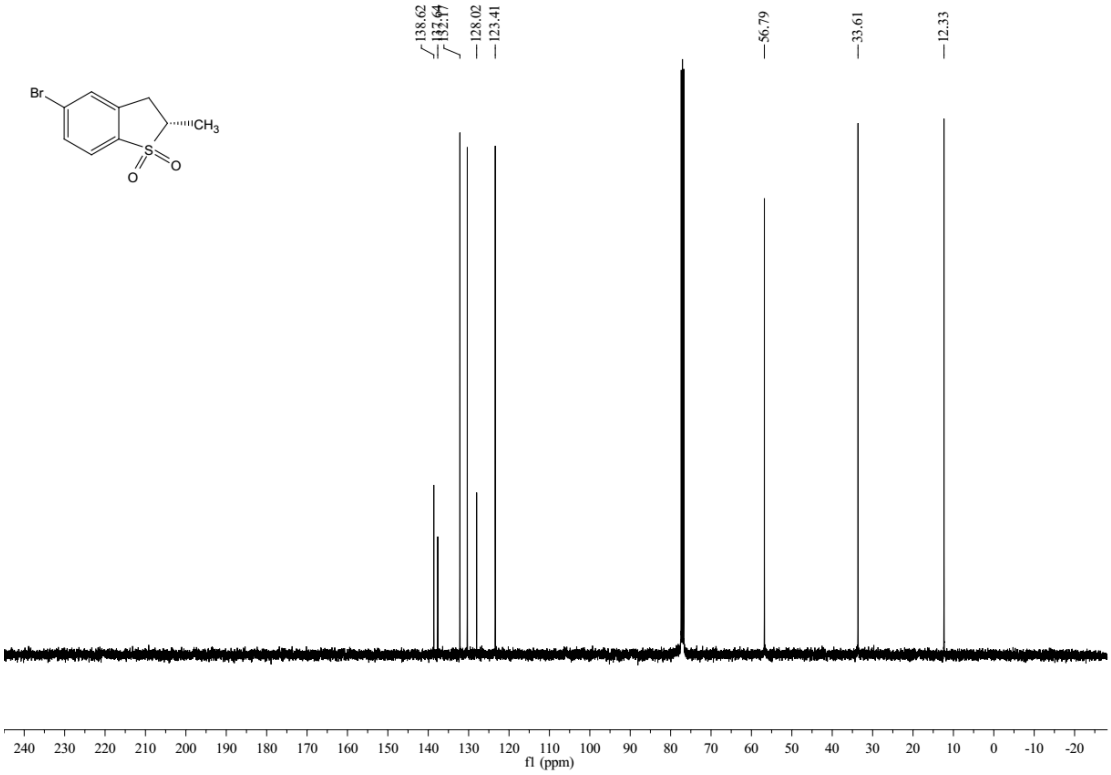
138.62
133.64
132.47
128.02
123.41
56.79
33.61
12.33
Br
CH3
S
O
O
240 230 220 210 200 190 180 170 160 150 140 130 120 110 100 90 80 70 60 50 40 30 20 10 0 -10 -20
f1 (ppm)

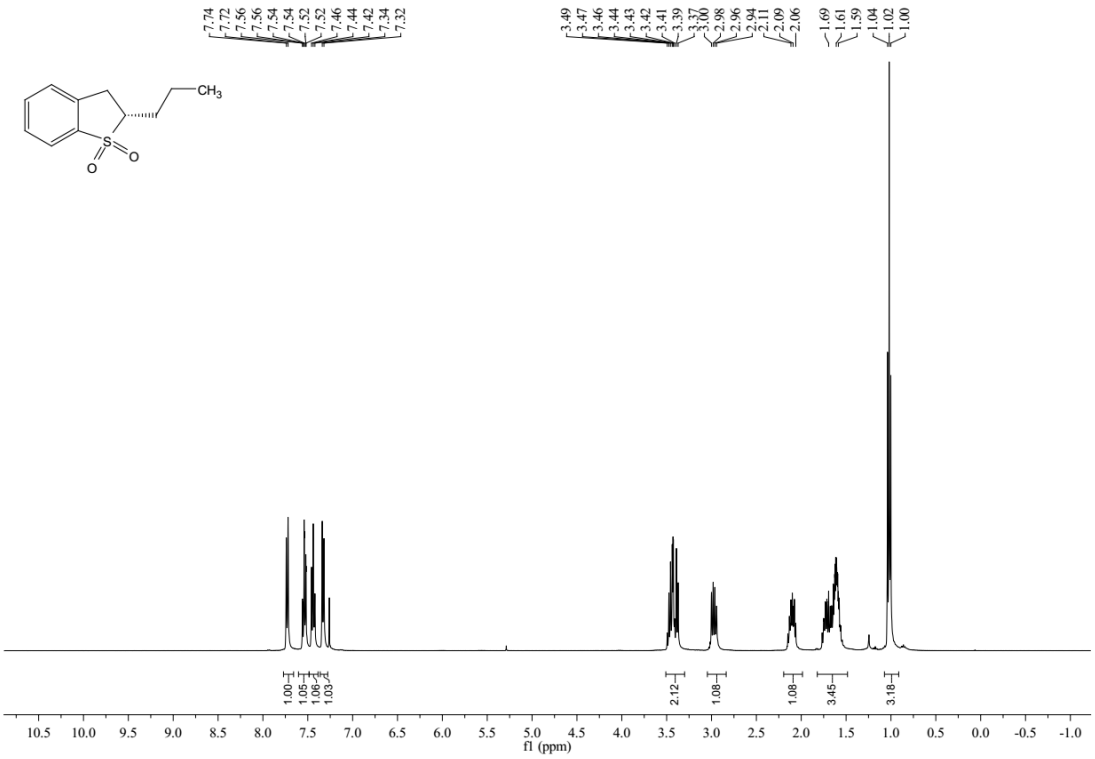
7.74
7.72
7.56
7.56
7.54
7.54
7.52
7.52
7.46
7.44
7.42
7.34
7.32
3.49
3.47
3.46
3.44
3.43
3.42
3.41
3.39
3.37
3.00
2.98
2.96
2.94
2.11
2.09
2.06
1.69
1.61
1.59
1.04
1.02
1.00
CH3
S
O
O
1.00
1.05
1.06
1.03
2.12
1.08
1.08
3.45
3.18
10.5 10.0 9.5 9.0 8.5 8.0 7.5 7.0 6.5 6.0 5.5 5.0 4.5 4.0 3.5 3.0 2.5 2.0 1.5 1.0 0.5 0.0 -0.5 -1.0
f1 (ppm)

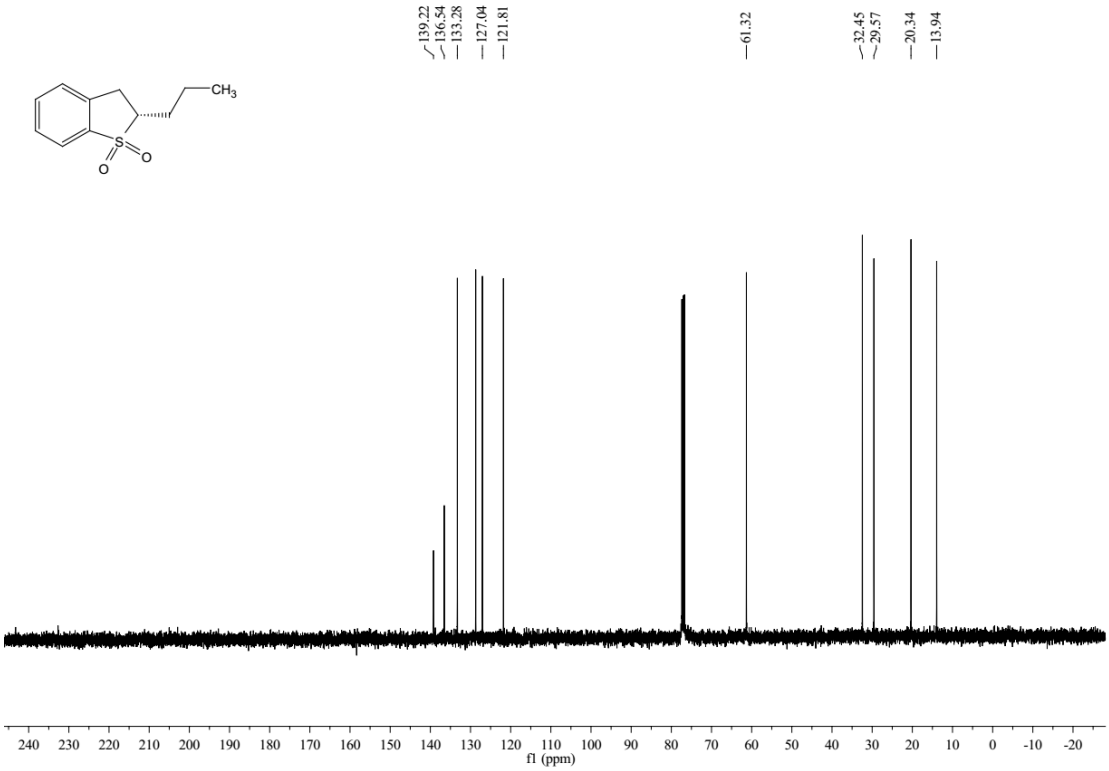
139.22
136.54
133.28
127.04
121.81
61.32
32.45
29.57
20.34
13.94
CH3
S
O
O
240 230 220 210 200 190 180 170 160 150 140 130 120 110 100 90 80 70 60 50 40 30 20 10 0 -10 -20
f1 (ppm)

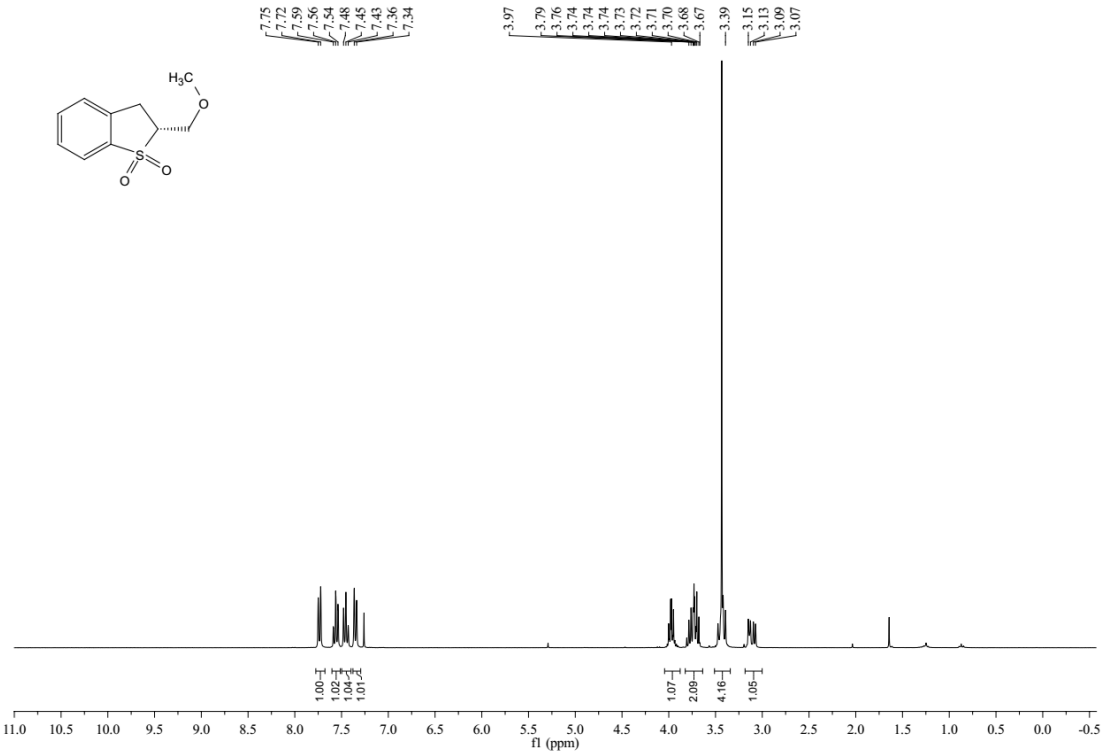
7.75
7.72
7.59
7.56
7.54
7.48
7.45
7.43
7.36
7.34
3.97
3.79
3.76
3.74
3.74
3.74
3.73
3.72
3.71
3.70
3.68
3.67
3.39
3.15
3.13
3.09
3.07
H3C
O
S
O
O
1.00
1.02
1.04
1.01
1.07
2.09
4.16
1.05
11.0 10.5 10.0 9.5 9.0 8.5 8.0 7.5 7.0 6.5 6.0 5.5 5.0 4.5 4.0 3.5 3.0 2.5 2.0 1.5 1.0 0.5 0.0 -0.5
f1 (ppm)

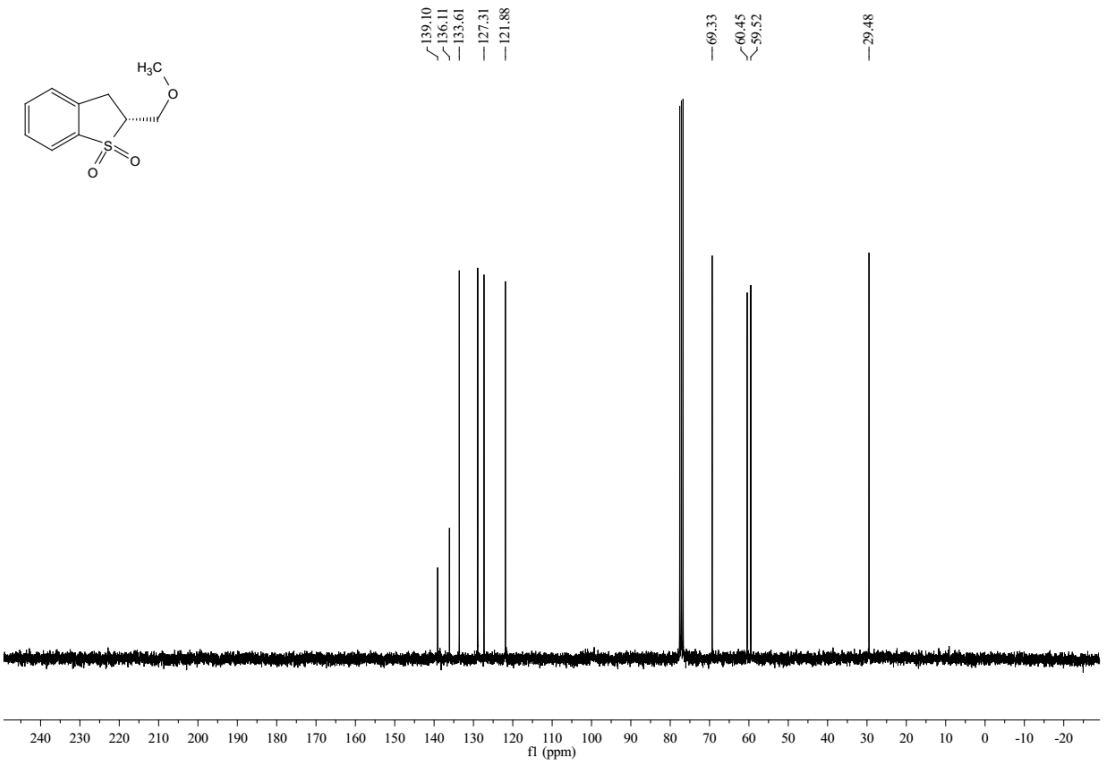
139.10
136.11
133.61
127.31
121.88
69.33
60.45
59.52
29.48
H3C
O
S
O
O
240 230 220 210 200 190 180 170 160 150 140 130 120 110 100 90 80 70 60 50 40 30 20 10 0 -10 -20
f1 (ppm)

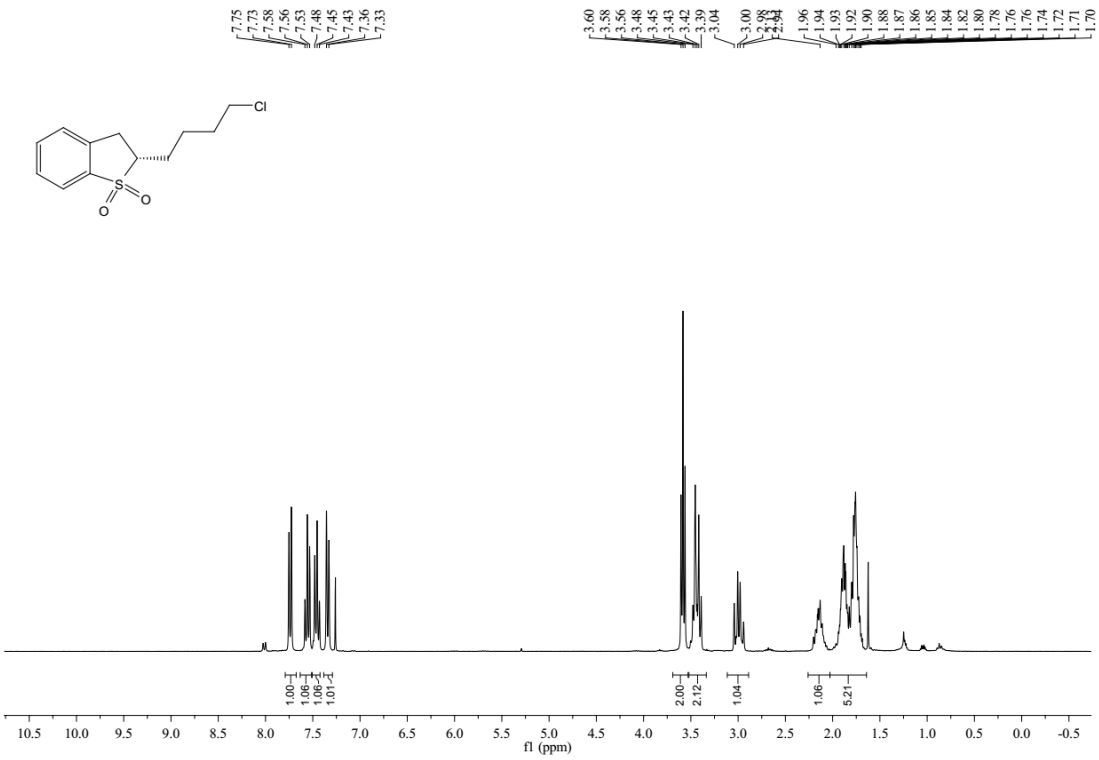
7.75
7.73
7.58
7.56
7.53
7.48
7.45
7.43
7.36
7.33
3.60
3.58
3.56
3.48
3.45
3.43
3.42
3.39
3.04
3.00
2.98
2.94
1.96
1.94
1.93
1.92
1.90
1.88
1.87
1.86
1.85
1.84
1.82
1.80
1.78
1.76
1.76
1.74
1.72
1.71
1.70
Cl
S
O
O
1.00
1.06
1.06
1.01
2.00
2.12
1.04
1.06
5.21
10.5 10.0 9.5 9.0 8.5 8.0 7.5 7.0 6.5 6.0 5.5 5.0 4.5 4.0 3.5 3.0 2.5 2.0 1.5 1.0 0.5 0.0 -0.5
f1 (ppm)

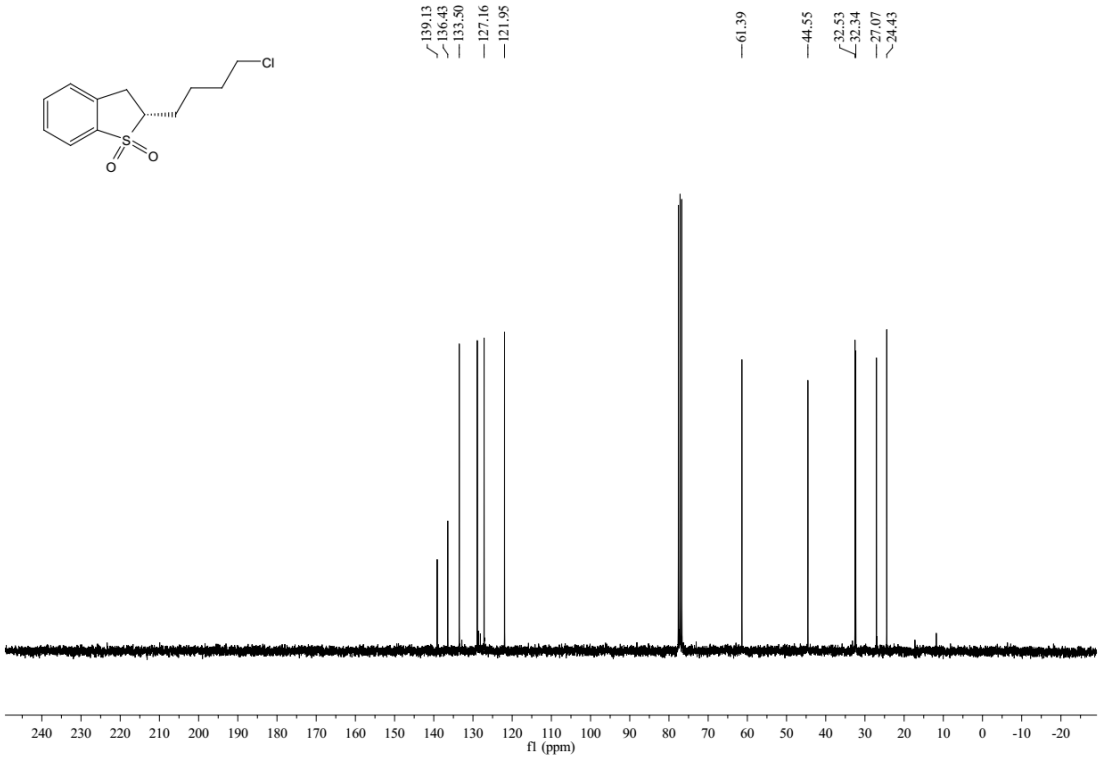
139.13
136.43
133.50
127.16
121.95
61.39
44.55
32.53
32.34
27.07
24.43
Cl
S
O
O
240 230 220 210 200 190 180 170 160 150 140 130 120 110 100 90 80 70 60 50 40 30 20 10 0 -10 -20
f1 (ppm)

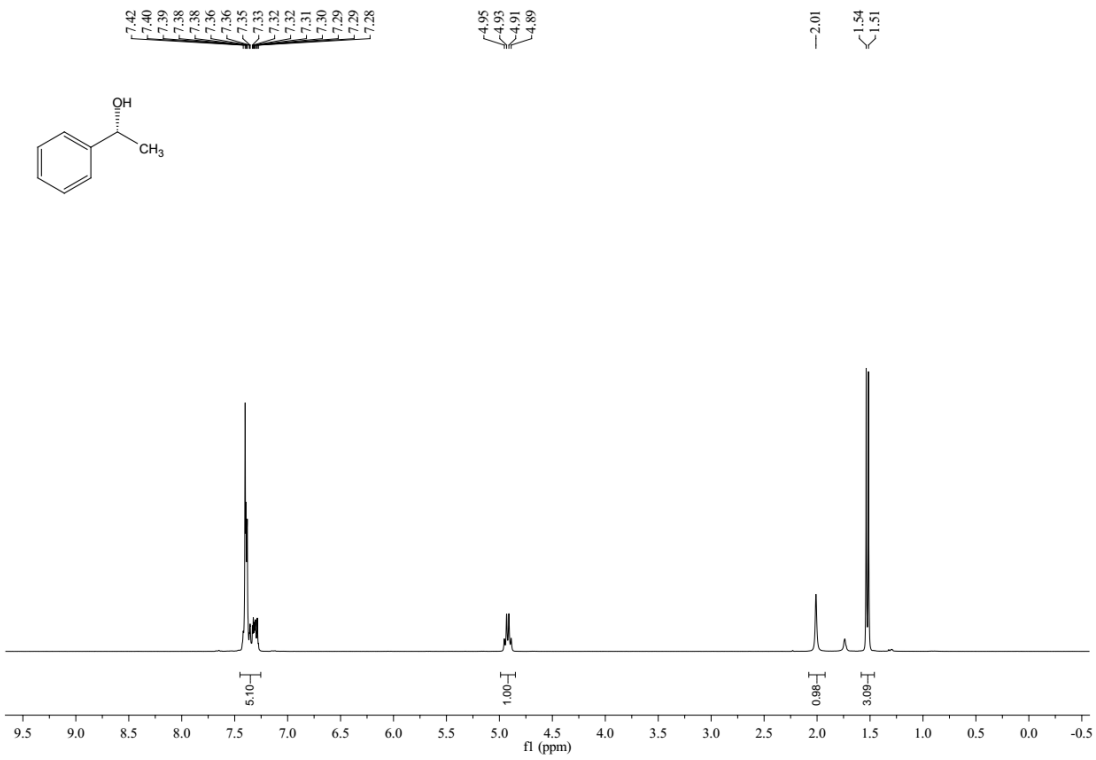
7.42
7.40
7.39
7.38
7.38
7.36
7.36
7.35
7.33
7.32
7.32
7.31
7.30
7.29
7.29
7.28
4.95
4.93
4.91
4.89
2.01
1.54
1.51
OH
CH3
5.10
1.00
0.98
3.09
9.5 9.0 8.5 8.0 7.5 7.0 6.5 6.0 5.5 5.0 4.5 4.0 3.5 3.0 2.5 2.0 1.5 1.0 0.5 0.0 -0.5
f1 (ppm)

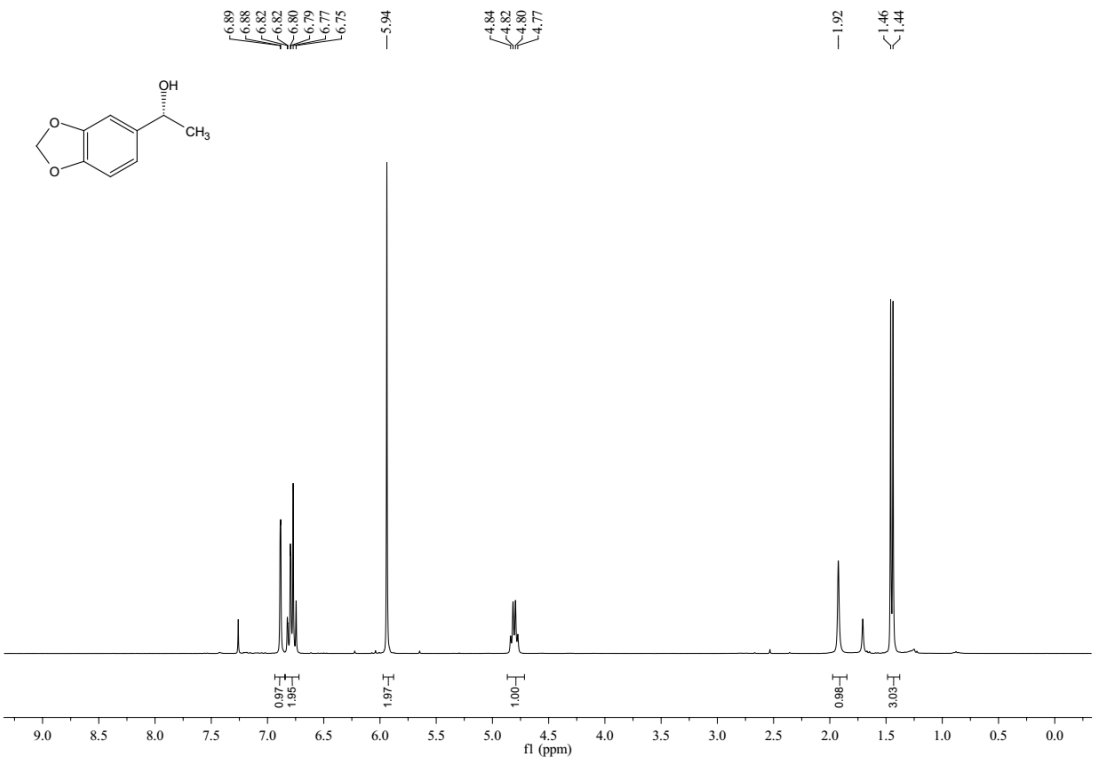
6.89
6.88
6.82
6.82
6.80
6.79
6.77
6.75
5.94
4.84
4.82
4.80
4.77
1.92
1.46
1.44
OH
CH3
O
O
0.97
1.95
1.97
1.00
0.98
3.03
9.0 8.5 8.0 7.5 7.0 6.5 6.0 5.5 5.0 4.5 4.0 3.5 3.0 2.5 2.0 1.5 1.0 0.5 0.0
f1 (ppm)

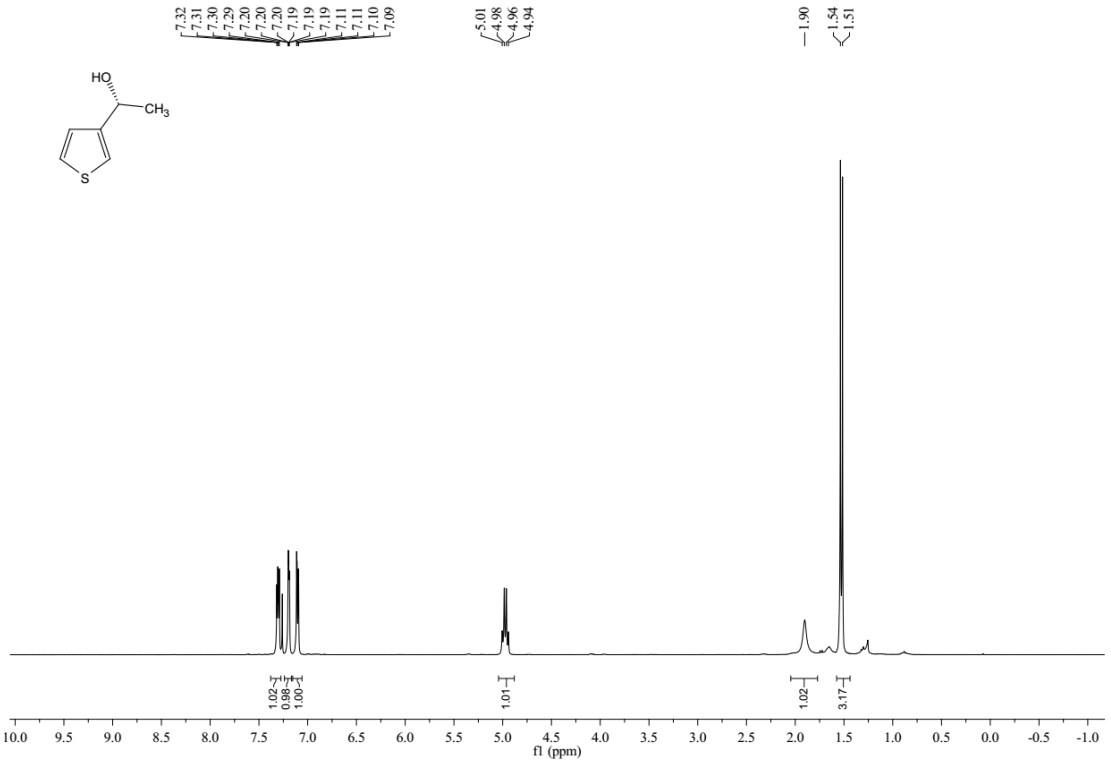
7.32
7.31
7.30
7.29
7.20
7.20
7.20
7.19
7.19
7.19
7.11
7.11
7.10
7.09
5.01
4.98
4.96
4.94
1.90
1.54
1.51
HO
CH3
S
1.02
0.98
1.00
1.01
1.02
3.17
10.0 9.5 9.0 8.5 8.0 7.5 7.0 6.5 6.0 5.5 5.0 4.5 4.0 3.5 3.0 2.5 2.0 1.5 1.0 0.5 0.0 -0.5 -1.0
f1 (ppm)

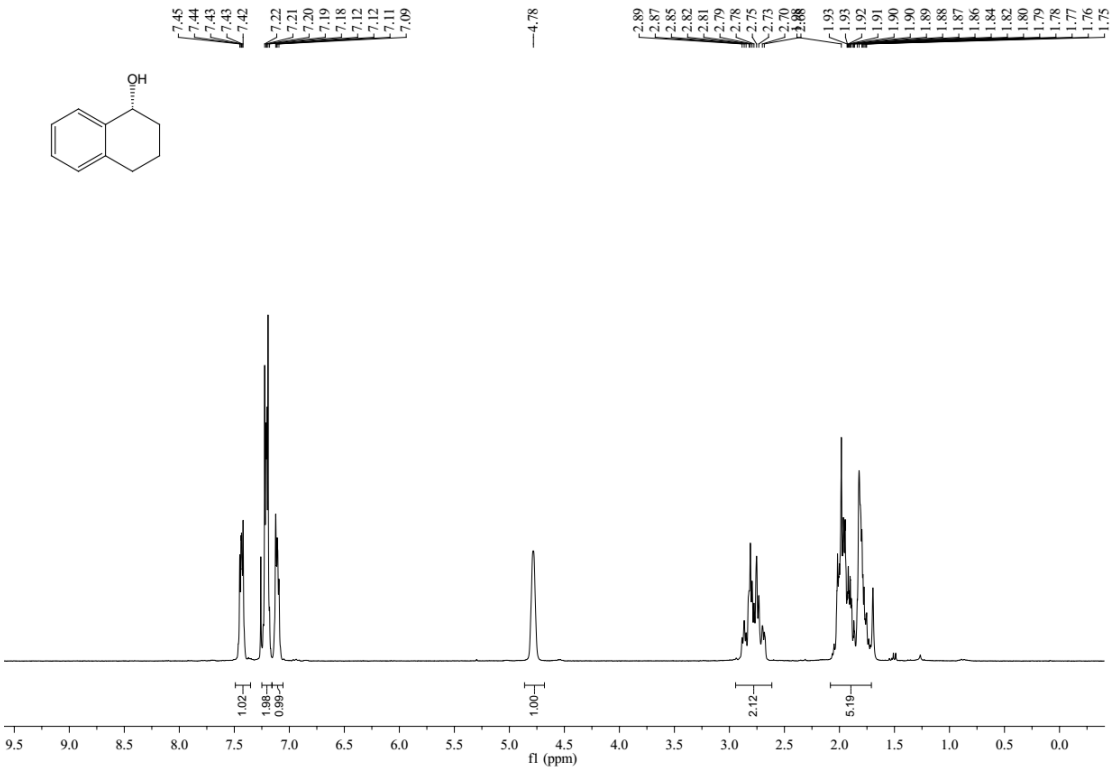
OH
7.45
7.44
7.43
7.43
7.42
7.22
7.21
7.20
7.19
7.18
7.12
7.12
7.11
7.09
4.78
2.89
2.87
2.85
2.82
2.81
2.79
2.78
2.75
2.73
2.70
1.93
1.93
1.92
1.91
1.90
1.90
1.89
1.88
1.87
1.86
1.84
1.82
1.80
1.79
1.78
1.77
1.76
1.75
1.02
1.98
0.99
1.00
2.12
5.19
9.5 9.0 8.5 8.0 7.5 7.0 6.5 6.0 5.5 5.0 4.5 4.0 3.5 3.0 2.5 2.0 1.5 1.0 0.5 0.0
f1 (ppm)

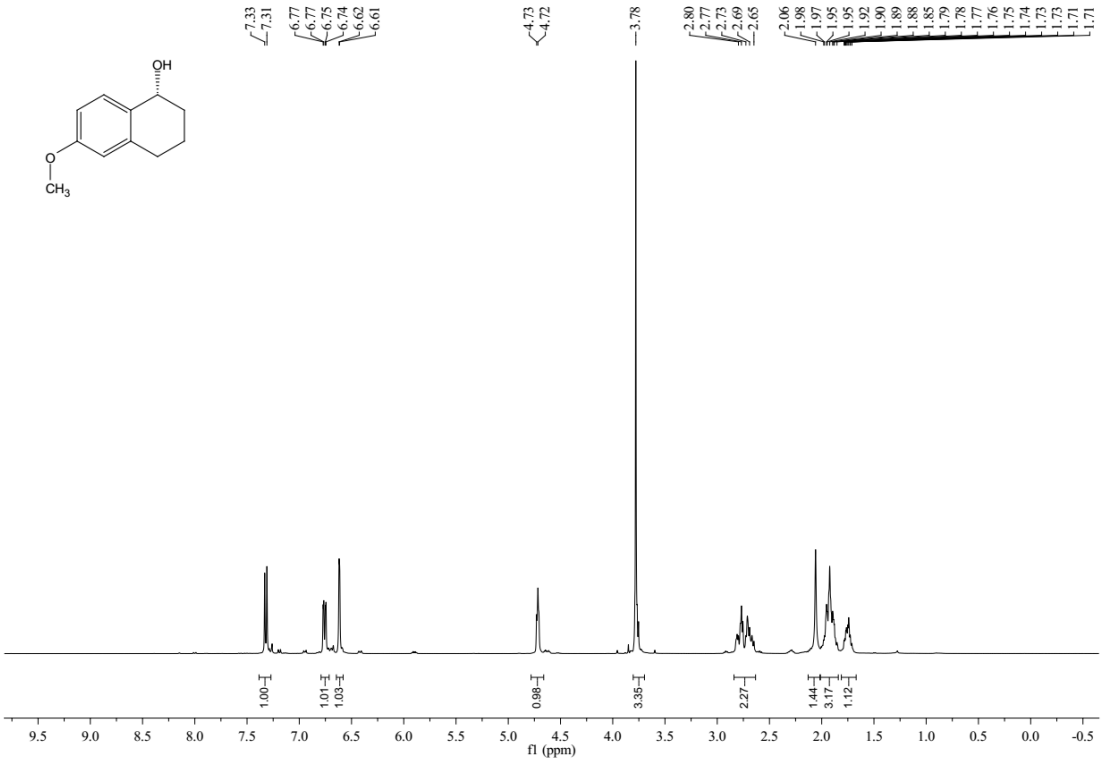
OH
O
CH3
7.33
7.31
6.77
6.77
6.75
6.74
6.62
6.61
4.73
4.72
3.78
2.80
2.77
2.73
2.69
2.65
2.06
1.98
1.97
1.95
1.95
1.92
1.90
1.89
1.88
1.85
1.79
1.78
1.77
1.76
1.75
1.74
1.73
1.73
1.71
1.71
1.00
1.01
1.03
0.98
3.35
2.27
1.44
3.17
1.12
9.5 9.0 8.5 8.0 7.5 7.0 6.5 6.0 5.5 5.0 4.5 4.0 3.5 3.0 2.5 2.0 1.5 1.0 0.5 0.0 -0.5
f1 (ppm)

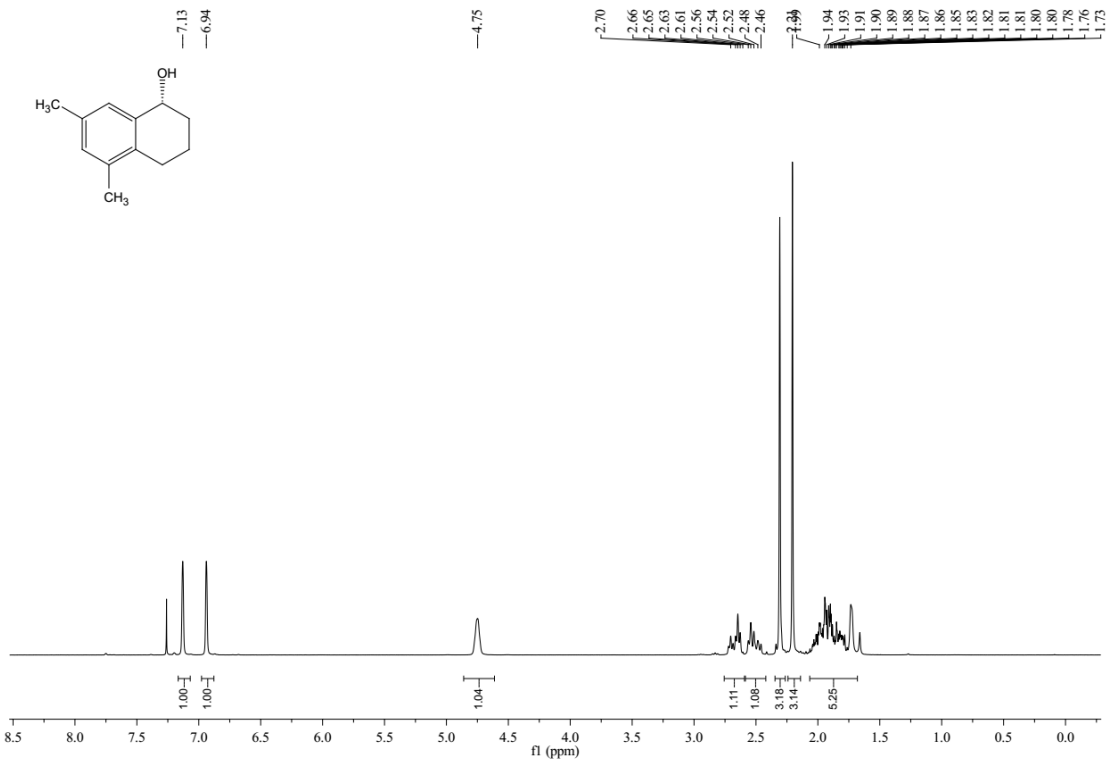
OH
H3C
CH3
7.13
6.94
4.75
2.70
2.66
2.65
2.63
2.61
2.56
2.54
2.52
2.48
2.46
1.94
1.93
1.91
1.90
1.89
1.88
1.87
1.86
1.85
1.83
1.82
1.81
1.81
1.80
1.80
1.78
1.76
1.73
1.00
1.00
1.04
1.11
1.08
3.18
3.14
5.25
8.5
8.0
7.5
7.0
6.5
6.0
5.5
5.0
4.5
4.0
3.5
3.0
2.5
2.0
1.5
1.0
0.5
0.0
f1 (ppm)

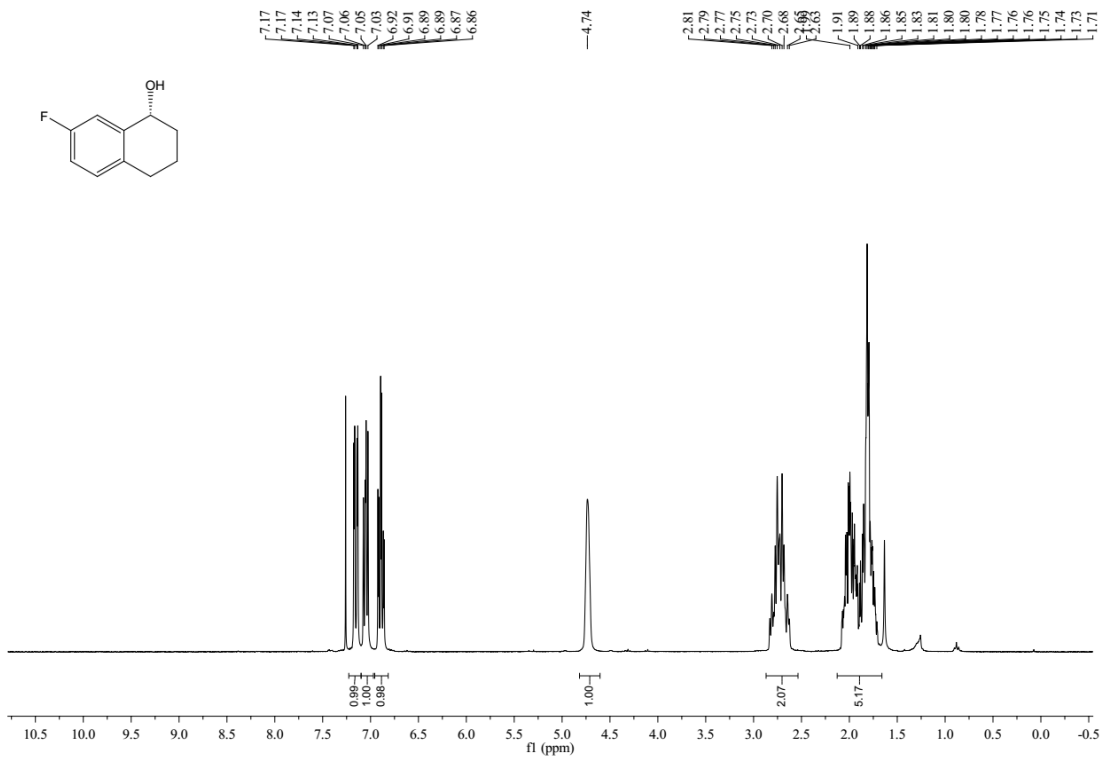
OH
F
7.17
7.17
7.14
7.13
7.07
7.06
7.05
7.03
6.92
6.91
6.89
6.89
6.87
6.86
4.74
2.81
2.79
2.77
2.75
2.73
2.70
2.68
2.63
1.91
1.89
1.88
1.86
1.85
1.83
1.81
1.80
1.80
1.78
1.77
1.76
1.76
1.75
1.74
1.73
1.71
0.99
1.00
0.98
1.00
2.07
5.17
10.5
10.0
9.5
9.0
8.5
8.0
7.5
7.0
6.5
6.0
5.5
5.0
4.5
4.0
3.5
3.0
2.5
2.0
1.5
1.0
0.5
0.0
-0.5
f1 (ppm)

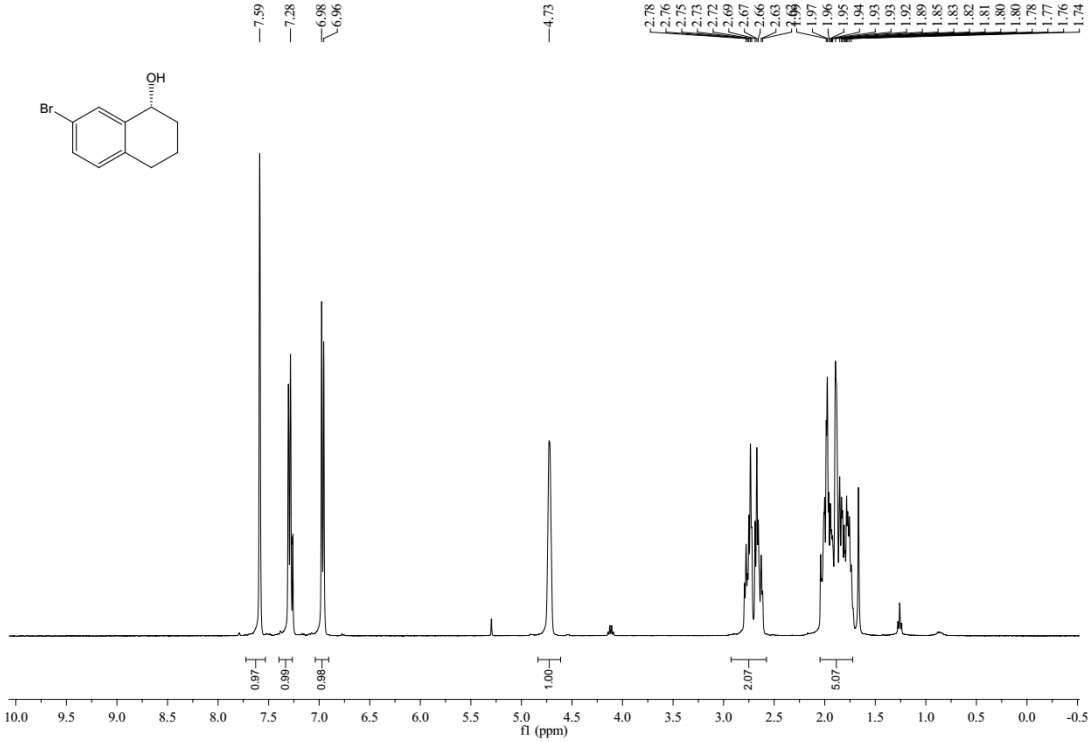
OH
Br
7.59
7.28
6.98
6.96
4.73
0.97
0.99
0.98
1.00
2.07
5.07
f1 (ppm)

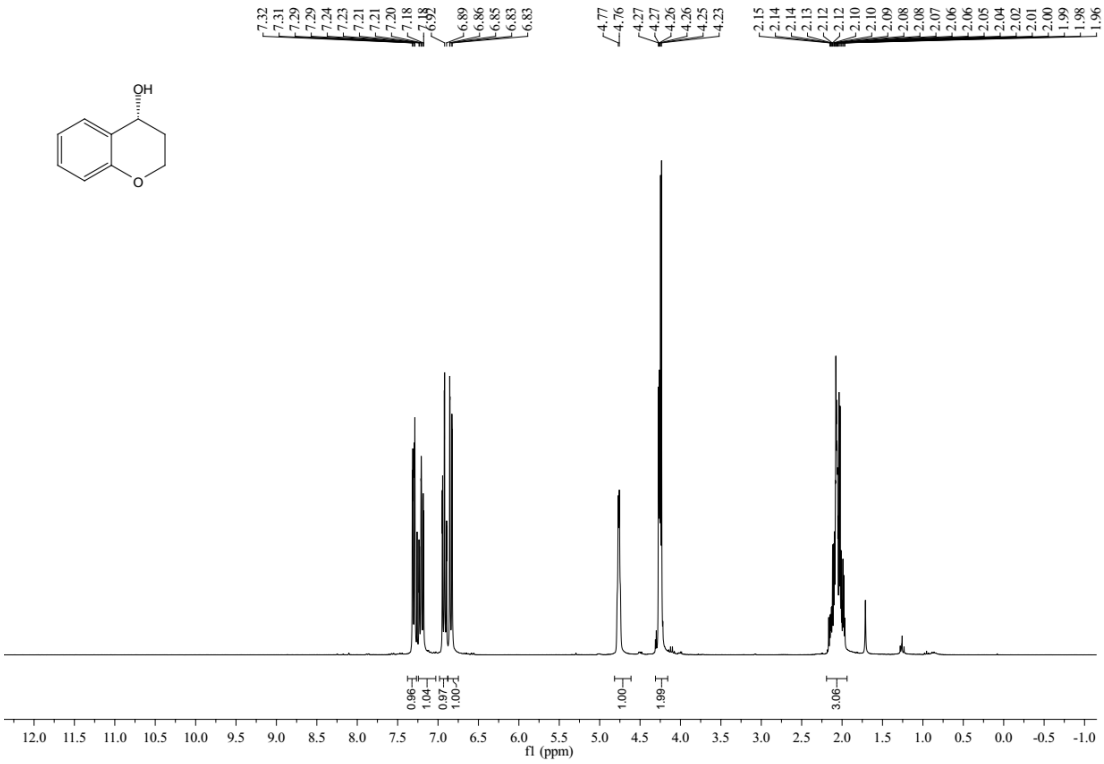
OH
O
0.96
1.04
0.97
1.00
1.00
1.99
3.06
f1 (ppm)

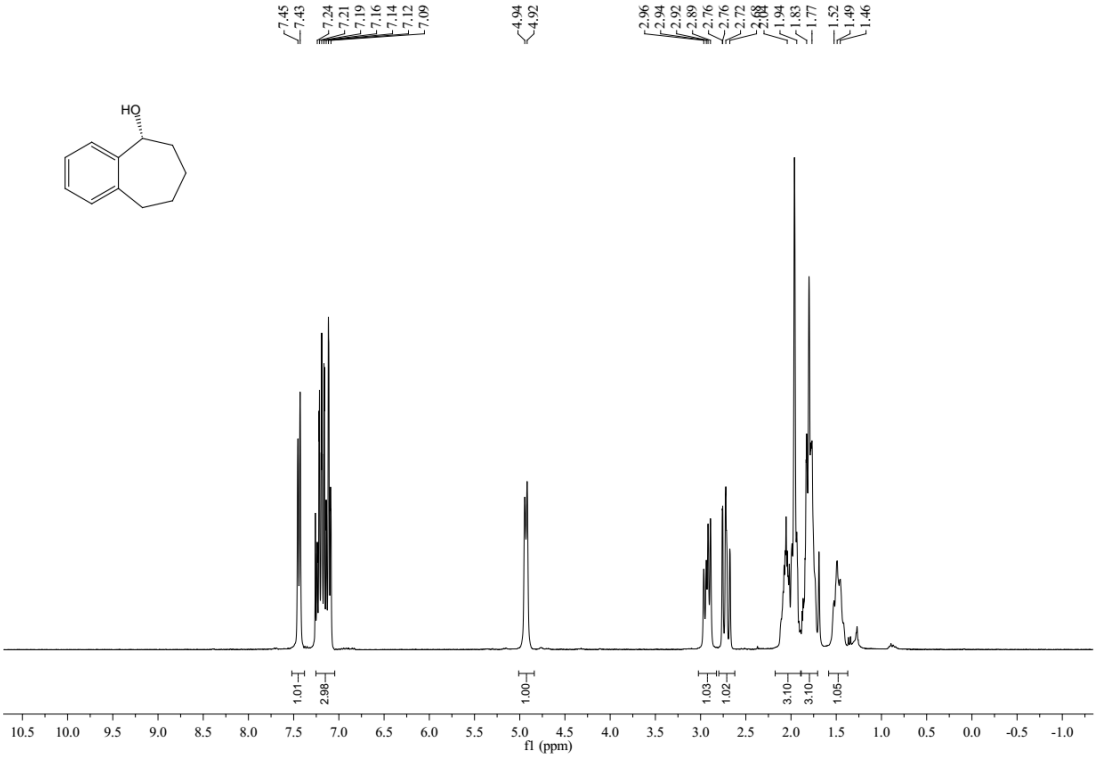
HO
7.45
7.43
7.24
7.21
7.19
7.16
7.14
7.12
7.09
4.94
4.92
2.96
2.94
2.92
2.89
2.76
2.76
2.72
2.68
2.64
1.94
1.83
1.77
1.52
1.49
1.46
1.01
2.98
1.00
1.03
1.02
3.10
3.10
1.05
10.5 10.0 9.5 9.0 8.5 8.0 7.5 7.0 6.5 6.0 5.5 5.0 4.5 4.0 3.5 3.0 2.5 2.0 1.5 1.0 0.5 0.0 -0.5 -1.0
f1 (ppm)